Structure and Function Analysis of the Mammalian ATP-Binding Cassette Transporters, ABCB1 and ABCB4

Michael Nicolaou

A Thesis presented for the degree of
Doctor of Philosophy

September 2012

Membrane Transport Biology Group

Centre for Cutaneous Research

The Blizard Institute

Queen Mary University of London

"He bound devious Prometheus with inescapable harsh bonds, fastened through the middle of a column, and he inflicted on him a long-winged eagle, which ate his immortal liver, but it grew as much in all at night as the long-winged bird would eat all day."

Hesiod "Theogony, v. 521-525"

«Τον Προμηθέα με τις πολλές ιδέες, τον έδεσε με άλυτα και βασανιστικά δεσμά τυλίγοντας κολώνα στη μέση και ξεσηκώνοντας εναντίον του αετό με μακρυά φτερά. Κι αυτός του έτρωγε το αθάνατο συκώτι, αλλ' αυτό ξαναγινόταν το ίδιο τη νύχτα, όσο είχε φάει τη μέρα το όρνιο με τα μακρυά φτερά».

Βλ. Ἡσίοδου «Θεογονία, σ. 521-525»

Declaration

I declare that the work presented in this thesis is my own and has not been submitted in any form for another degree or diploma at any university or other institute of tertiary education. Information derived from the published or unpublished work of others has been acknowledged in the text and a list of references is given.

Michael Nicolaou

PhD Student

Abstract

Mammalian ABC (ATP-binding cassette) transporters are integral membrane proteins that translocate allocrites across biological membranes using ATP as a substrate.

ABCB1 is a polyspecific efflux pump which can confer multidrug resistance in cancer. ABCB1 is also expressed in a variety of normal tissues where it functions to prevent the accumulation of toxic allocrites. Direct inhibition of ABCB1 can therefore have detrimental effects on patients. Identification of ABCB1-interacting partners that influence trafficking or function would therefore provide alternative targets for therapy which may be cell- or tissue-type specific. The "split-ubiquitin" yeast two-hybrid system, that can detect protein:protein interactions at the plasma membrane, was used to screen for ABCB1-interactors in a human liver library. All candidates isolated from the screen interacted with ABCB1 in a non-specific manner when subjected to strict testing.

ABCB4, a close relative of ABCB1, is expressed primarily at the hepatocyte canalicular membrane where it flops phosphatidylcholine (PC) into the outer leaflet for extraction by bile salts. Many ABCB4 non-synonymous mutations have been linked to cholestatic liver diseases in humans, but data confirming an impact on ABCB4 function is lacking. Transient expression of wild-type (WT) ABCB4 in tissue culture has proved difficult because the protein is toxic to HEK293T cells. However, co-expression of the phosphatidylserine flippase ATP8B1 (FIC1) and its accessory protein CDC50A allowed the cells to tolerate ABCB4. To investigate the impact of SNPs on ABCB4 function, equivalent changes were introduced into the ABCB4 cDNA for transient expression in the presence or absence of ATP8B1/CDC50A. ABCB4 expression and targeting to the plasma membrane were monitored by western analysis and confocal microscopy, respectively, and, by "feeding" the transfected cells [*methyl*-^{3}H]choline, PC efflux to added bile salt acceptor was measured. By thus mimicking the situation at the canalicular membrane I report the preliminary characterisation of nine variants of ABCB4 that have been linked to cholestatic liver disease.

Acknowledgements

I would like to thank my supervisor Prof. Kenny Linton for providing me with the opportunity to be part of the Membrane Transport Biology Group, for his invaluable support through the course of my degree and for his continued guidance over the last years. Somehow, he always finds a way to push you through and keep you going even during the most difficult of times. Thank you Kenny.

I would also like to express my gratitude to Johnny and Eddie for being there whenever I needed them, for passing their knowledge to me and for helping me cope with those "tricky" problems whenever they would arise (they do come up more often than you would think)!

A big "thank you" also goes out to everyone else in the laboratory for providing me with help and advice and for making it such a pleasant environment to work in. Cheers guys!

Last, but definitely not least, I would like to thank my parents, Kalliniko and Eleni Nicolaou. Without them, none of this would have been possible. They provided me with endless support, understanding and encouragement throughout the years. I will be eternally grateful.

This thesis is dedicated to them.

Σ'ευχαριστώ μαμά, σ'ευχαριστώ μπαμπά.

Nomenclature

3-AT	3-amino-1,2,4-riazole
4-PBA	sodium 4-phenylbutyrate
Å	Ångstrom
Ab	antibody
ABC	ATP-binding cassette
AD	activation domain
Ade	adenine
AIR	5'-phosphoribosyl-5-aminoimidazole
Ala	alanine
ALT	alanine transaminase
AML	acute myeloid leukaemia
ANOVA	analysis of variance
Arg	arginine
ARL6IP5	ADP-ribosylation-like factor interacting protein 5
ASBT	apical sodium-dependent bile salt transporter or IBAT
ASGR2	asialoglycoprotein receptor 2 (transcript variant 1)
Asn	asparagine
Asp	aspartic acid
ATP	adenosine triphosphate
ATP6V0B	ATPase H^+-transporting lysosomal 21 kDa V0 subunit b
BBB	blood-brain barrier
BC	biliary cirrhosis
BCRP	breast cancer resistance protein
BD	DNA-binding domain

BRIC	benign recurrent intrahepatic cholestasis
BS	bile salts
BSEP	bile salt-export protein
CA	cholic acid
CAIR	5'-phosphoribosyl-4-carboxy-5-aminoimidazole
Cav1	caveolin 1 (VIP21)
CCK	cholecystokinin
CDCA	chenodeoxycholic acid
cDNA	complementary DNA
CDP	cytidine diphosphate
CF	cystic fibrosis
CFTR	cystic fibrosis transmembrane conductance regulator
CHO	Chinese hamster ovary cells
Ci	Curie = 3.7×10^{10} Bq (Becquerel)
CIC	contraceptive-induced cholestasis
cLPM	canalicular liver plasma membrane
CLSM	confocal laser scanning microscopy
cMOAT	ABCC2/MRP2
CMV	cytomegalovirus
co-IP	co-immunoprecipitation
CRP	C-reactive protein
CsA	cyclosporin A
CTP	cytidine triphosphate
C_{ub}	ubiquitin C-terminus
CYB5A	cytochrome b5 type A
CYP7A1	cytochrome P450 cholesterol 7α-hydroxylase

Cys	cysteine
DAG	diacylglycerol
DCA	deoxycholic acid
DIC	drug-induced cholestasis
DMEM	Dulbecco's Modified Eagle Medium
DMSO	dimethyl sulfoxide
DPBS	Dulbecco's phosphate buffered saline
DTT	dithiothreitol
E. coli	*Escherichia coli*
$E_2$17βG	estradiol-17β-glucuronide
EBP	emopamil-binding protein
ECL	extracellular loop
EDTA	ethylenediaminetetraacetic acid
ER	endoplasmic reticulum
ERAD	ER-associated degradation
Ergic32	ER-Golgi intermediate compartment protein 32
FATP4	fatty acid transport protein 4
FBS	fetal bovine serum
FIC1	ATP8B1
FXDY5	FXYD domain-containing ion transport regulator 5
FXR	farnesoid-X receptor
Gly	glycine
GS	glycosphingolipids
GST	glutathione *S*-transferase
GTPase	guanosine triphosphatase
HAX-1	HCLS1-associated protein X-1

HC	hepatocellular carcinoma
HDAC6	histone de-acetylase 6
HEK293	human embryonic kidney 293 cells
HeLa	human cervical cancer cells
HepG2	human liver hepatocellular carcinoma cells
His	histidine
HRP	horseradish peroxidase
IBABP	ileal bile acid binding protein
IBAT	ileal bile acid transporter
ICP	intrahepatic cholestasis of pregnancy
IFITM3	interferon-induced transmembrane protein 3
ILe	isoleucine
iMYTH	integrated split-ubiquitin membrane yeast two hybrid
IPTG	isopropyl 1-thio-β-D galactopyranoside
LASS2	ceramide synthase 2
LB	Lysogeny broth
LCA	lithocholic acid
LDH	lactate dehydrogenase
Leu	leucine
LiAc	lithium acetate dehydrate
LLC-PK1	pig kidney epithelial cells
LPAC	low phospholipid-associated cholelithiasis
LPL	lipoprotein lipase
LRH-1	liver receptor homologue-1
LXR	liver-X receptor
MDCK	Madin-Darby canine kidney epithelial cells

MDH2	malate dehydrogenase 2
MDR	multidrug resistance
MDR1	multidrug resistance protein 1
MDR3	multidrug resistance protein 3
Met	methionine
MHC	major histocompatibility complex
M-MLV	Moloney Murine Leukemia Virus
mRNA	messenger RNA
MRP	multidrug resistance-associated protein
MSH	membrane-spanning helix
MXR	mitoxantrone resistance protein
NBD	nucleotide-binding domain
NTCP	Na^+-dependent taurocholate co-transporting polypeptide
N_{ub}	ubiquitin N-terminus
O/N	overnight
OATP	organic anion transporting polypeptide
OD	optical density
Orf3a	ORF3a cucumber mosaic virus
OST	organic solute transporter
PA	phosphatidic acid
PAF	platelet-activating factor (1-*O*-alkyl-2-acetyl-*sn*-glycero-3-phosphocholine)
PAGE	polyacrylamide gel electrophoresis
PBC	primary biliary cirrhosis
PBS-T	phosphate buffered saline + 1.0 (v/v) Tween 20
PC	phosphatidylcholine
PCR	polymerase chain reaction

PE	phosphatidylethanolamine
PEG	poly[ethylene glycol])
PEI	Polyethyleneimine
PEMT	phosphatidylethanolamine *N*-methyltransferase
PET	positron emission tomography
PFIC1	progressive familial intrahepatic cholestasis type 1
PFIC2	progressive familial intrahepatic cholestasis type 2
PFIC3	progressive familial intrahepatic cholestasis type 3
P-gp	P-glycoprotein
Phe	phenylalanine
PI	phosphatidylinositol
PKC	protein kinase C
PLP2	proteolipid protein 2
PM4-S	5α-pregnan-3α-ol-20-one sulphate
PM5-S	5α-pregnan-3β-ol-20-one sulphate
PMSF	phenylmethylsulfonyl fluoride
pre-mRNA	precursor mRNA
PS	phosphatidylserine
PSC	primary sclerosing cholangitis
PVDF	polyvinylidene fluoride
RACK1	receptor for activated C-kinase 1
Ras	rat sarcoma
Rh123	rhodamine123
RT	room temperature
RXR	retinoid-X receptor
S.O.C.	Super Optimal broth with Catabolite repression

SD	selective, defined media
SDS	sodium dodecyl sulphate
Ser	serine
SERP1	stress-associated endoplasmic reticulum protein 1
SERPINA1	serpin peptidase inhibitor member 1
SHP	small heterodimer partner
siRNA	small interfering RNA
SM	shingomyelin
SMC	structural maintenance of chromosomes
SNP	single-nucleotide polymorphism
SOX4	sex-determining region box 4
SPGP	sister of P-gp
SSR3	signal sequence receptor gamma
STAT6	signal transducer and activator of transcription 6
SUR	sulfonylurea receptor
SU-YTH	spli-ubiquitin yeast two-hybrid system
TAE	Tris base, acetic acid and EDTA buffer
TAP	transporter associated with antigen processing
TC	taurocholate
TCA	trichloroacetic acid
TE	Tris-EDTA
TF	transcription factor
Thr	threonine
TM9SF4	transmembrane 9 superfamily protein member 4
TMBIM4	transmembrane BAX inhibitor motif containing 4
TMD	transmembrane domain

TMEM85	transmembrane protein 85
TNFSF13B	tumour necrosis factor superfamily member 13
Trp	tryptophan
Ub	ubiquitin
UBP	ubiquitin-specific protease
UDCA	ursodeoxycholic acid
UT	untransfected
Val	valine
VAPB	vesicle-associated membrane protein-associated protein B
VIP21	vesicular integral-membrane protein of 21 kDa (Cav1)
VKORC1	vitamin K epoxide reductase complex (subunit 1)
WA	Walker A motif
WB	Walker B motif
WT	wild-type
X. laevis	*Xenopus laevis*
X-Gal	5-bromo-4-chloro-3-indolyl-beta-D-galactopyranoside
YIF1A	Yip1 interacting factor homolog A
YIP1B	Yip1-interacting factor homolog B
YTH	yeast two-hybrid
α	alpha
β	beta
γ	gamma
γ-GT	γ-glutamyl transferase
δ	delta
ε	epsilon
ζ	zeta

η	eta
θ	theta
μ	mu
Λ	lambda

Contents

List of Figures

List of Tables

Chapter One

1 Introduction

1.1 The ABCs of ABCs

The ATP-binding cassette (ABC) is a superfamily of integral membrane proteins, members of which have been found in all organisms studied to date (eukaryotic, eubacteria or archaebacteria) (Higgins, 1992). ABC proteins use energy derived from ATP binding and/or hydrolysis to drive an array of cellular processes. These range from mRNA export, as exemplified by Elf1p in *Schizosaccharomyces pombe* (Kozak et al., 2002) to double strand break repair involving Rad50 (Hopfner et al., 2000) and chromatin remodelling typified by SMC (structural maintenance of chromosomes) proteins such as BsSMC in *Bacillus subtilis* and MukB in *Escherichia coli* (*E. coli*) (Graumann et al., 1998, Melby et al., 1998). However, the vast majority of ABC proteins translocate allocrites[1] across a biological membrane (Linton and Holland, 2011).

1.2 Mammalian ABC proteins

The human complement of ABC transporters comprises 48 genes encoding proteins primarily involved in the translocation of allocrites across cellular membranes (Linton and Holland, 2011). Phylogenetic analysis of the amino acid sequences of the human ABC proteins shows that they form seven distinct subfamilies, A to G (Dean et al., 2001). Many of the human ABC transporters have important roles in normal physiology and consequently their dysregulation or malfunction underlies a number of important diseases. This thesis focuses on two related mammalian exporters, ABCB1 and ABCB4, involved in drug efflux and lipid flopping into the bile, respectively. In the first chapter, a general overview of the structural features of the human ABC proteins is provided with particular focus on ABCB1 and ABCB4. In addition, the physiological role of several human ABC

[1] The term **allocrite** was coined by Blight and Holland (Blight and Holland, 1990) to describe a compound which is translocated by a transporter protein but is not changed chemically (i.e. a transport substrate). This was done to distinguish the transported solute from the "true" ABC substrate which is ATP.

proteins is considered to outline the importance of these proteins in human health and disease and to highlight the significance of understanding how they function at the molecular level.

1.2.1 Preface to Project 1: ABCB1 and multidrug resistance

ABCB1 (MDR1/P-glycoprotein) is one of the major proteins involved in the development of multidrug resistance (MDR) in cancer patients and poses an obstacle in their chemotherapeutic treatment (Gottesman et al., 2002, Higgins, 2007). In normal physiology, ABCB1 is responsible for preventing the accumulation of toxic allocrites in the variety of tissues in which it is expressed. Therefore direct inhibition of ABCB1 can have detrimental effects on patients. In Chapter 3, the use of a modified version of the yeast two-hybrid system to screen for ABCB1-interactors is described. The aim of the experimental research was to identify ABCB1-interacting partners which influence its trafficking and/or function and provide alternative targets for therapy. Unfortunately, all candidates isolated from the screen interacted with ABCB1 in a non-specific manner when subjected to strict testing.

1.2.2 Preface to Project 2: ABCB4 and cholestatic liver disease

ABCB4 (MDR3 in humans, Mdr2 in mice) has 78% sequence identity (at the amino acid level) with ABCB1 (Lincke et al., 1991) but despite the high level of identity, ABCB4 does not exhibit broad allocrite specificity [although transport of a small subset of ABCB1 allocrites has been demonstrated for ABCB4 (Smith et al., 2000)]. ABCB4 is primarily a phosphatidylcholine (PC) floppase which is highly expressed in the hepatocyte where it acts as one of the key players in bile formation (Smit et al., 1993, Smith et al., 1994). A large number of mutations have been reported which implicate ABCB4 in a spectrum of cholestatic disease. This ranges from the most severe phenotype, progressive familial intrahepatic cholestasis type 3 (PFIC3), to the milder, intermittent forms of cholestasis, e.g. benign recurrent intrahepatic cholestasis (BRIC), drug-induced cholestasis (DIC) or

intrahepatic cholestasis of pregnancy (ICP). It is important, therefore, to understand the effect of such mutations on ABCB4 in order to elucidate the molecular basis of cholestatic liver disease. The approach to investigate the effect of ABCB4 mutations on the level of expression, trafficking and functionality of the protein in a mammalian expression system is described in Chapters 4 and 5.

1.3 The ABCB subfamily of proteins

The human ABCB (MDR/TAP) subfamily of proteins is the third largest of the ABC subfamilies and comprises 11 members (ABCB1 – ABCB11). *ABCB1* is expressed in a variety of tissues including the brain, liver, testes, heart, kidneys and intestines (Cordon-Cardo et al., 1990, Cordon-Cardo et al., 1989, Fojo et al., 1987, Thiebaut et al., 1987, Thiebaut et al., 1989) where it acts as a drug efflux pump protecting the organism against xenobiotics. *ABCB11* is expressed in the liver (Gerloff et al., 1998) and it is the main bile salt export pump in humans (Strautnieks et al., 1998). *ABCB4* is also expressed in the liver (Buschman et al., 1992) where it functions as a phosphatidylcholine floppase (van Helvoort et al., 1996). The transporter associated with antigen processing (TAP) heterodimer TAP1/2 (ABCB2/ABCB3) functions at the endoplasmic reticulum (ER) where it is involved in the cellular immune response via antigen presentation to MHC Class I molecules which can then be recognised by cytotoxic T lymphocytes (Lankat-Buttgereit and Tampe, 2002). *ABCB5* is mainly expressed in pigmented cells (Chen et al., 2005) and it is thought to be involved in the development of chemoresistance in human melanomas (Frank et al., 2005). *ABCB9*, the closest homologue of the TAP proteins (Yamaguchi et al., 1999b), is most highly expressed in the testes where it localises in the lysosomal compartments but its function has not yet been elucidated (Zhang et al., 2000). Finally, ABCB6, ABCB7, ABCB8 and ABCB10 all localise to the mitochondria where they act as

homodimers involved in iron–sulphur (Fe–S) cluster biogenesis and cellular iron metabolism (Zutz et al., 2009).

Evidently, the members of the ABCB subfamily cover a diverse spectrum of biological functions and are expressed in a variety of tissues in the human body. ABCB1 and ABCB4 are amongst the largest proteins of the ABCB subfamily (1280 amino acids in length). Although they display a high degree of similarity, each protein performs a different biological function and displays a distinct tissue expression pattern. As ABCB1 and ABCB4 are the most pertinent transporters in the context of this report, they are considered in more detail in the following sections along with relevant examples drawn from the other ABC subfamilies where appropriate.

1.4 Structural organisation of the ABCB1 and ABCB4 proteins

ABC transporters are ubiquitous and likely to be found in any organism. They have a vast variety of allocrites ranging from small inorganic ions and essential amino acids to oligopeptides and even whole proteins. Although they can be very different in their physiological roles, all ABC transporters share a common basic structure. This is composed, minimally, of four domains (Figure 1-1). Two transmembrane domains (TMDs) which span the membrane several times and form the translocation pathway across the lipid bilayer, and two nucleotide-binding domains (NBDs) which contain the ABC and bind and hydrolyse ATP acting as engines for the conformational changes induced during the transport process (Higgins et al., 1986).

ABCB1 and ABCB4 are encoded as a single polypeptide with four domains (2×TMDs with 2×NBDs) and they both localise to apical membrane of polarised cells (Buschman et al.,

1992, Hammerle et al., 2000, Petriz et al., 2004). Most of our knowledge on ABCB4 topology and predicted structure is based on studies of the best characterised member of the ABC family, ABCB1. Because of the high sequence homology between ABCB1 and ABCB4 (Van der Bliek et al., 1987) , it is reasonable to assume that both proteins adopt a

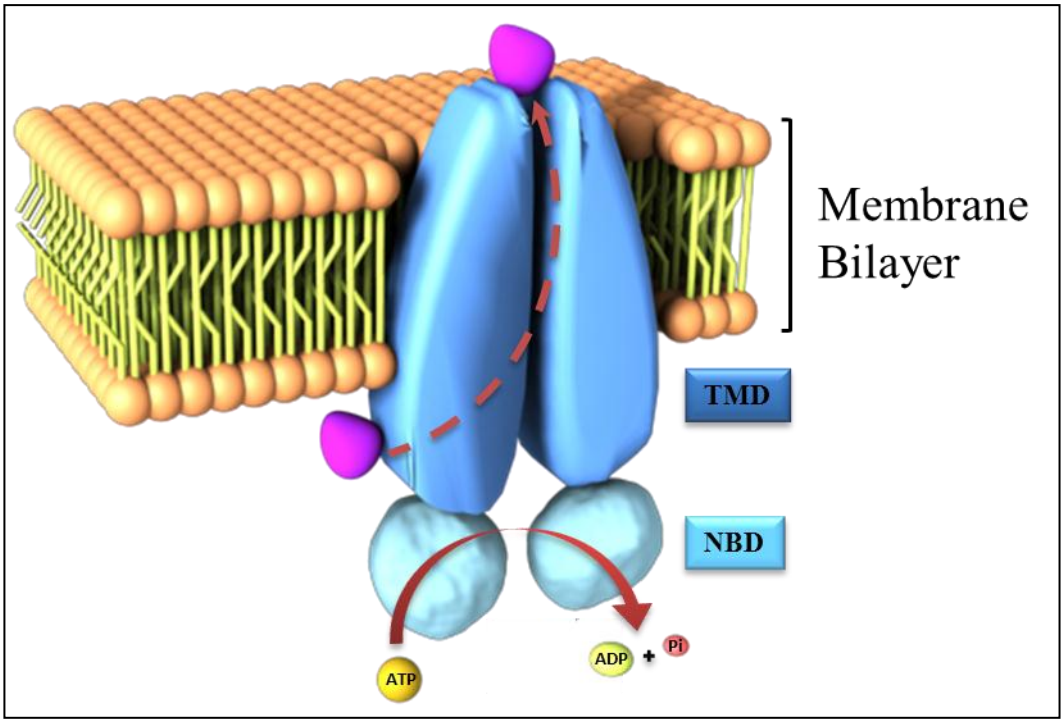

Figure 1-1. ***The core architecture of an ABC transporter*****.**

The minimal functional unit of an ABC transporter comprises two transmembrane domains (TMDs) and two nucleotide binding domains (NBDs). TMDs form the allocrite translocation pathway across the membrane and are not conserved across the ABC family. NBDs are the engines of the transporter which provide energy via ATP hydrolysis and are highly homologous amongst members of the ABC family. The process represented here is for an ABC exporter. Image created using the 3ds Max software from Autodesk.

similar conformation and that ABCB4 translocates its allocrite(s) in a manner analogous to xenotoxin translocation fulfilled by ABCB1. In fact, as already mentioned, ABCB4 can transport drugs albeit with low efficiency (Smith et al., 2000) and ABCB1 has been reported to transport several phospholipids (Bosch et al., 1997, Eckford and Sharom, 2005, Romsicki and Sharom, 2001). Structure determination of ABC exporters has provided insights into the mechanisms of energy and signal transduction between the NBDs and

TMDs, which when interpreted in conjunction with biochemical and biophysical data, has led to an understanding of the mechanism of allocrite efflux.

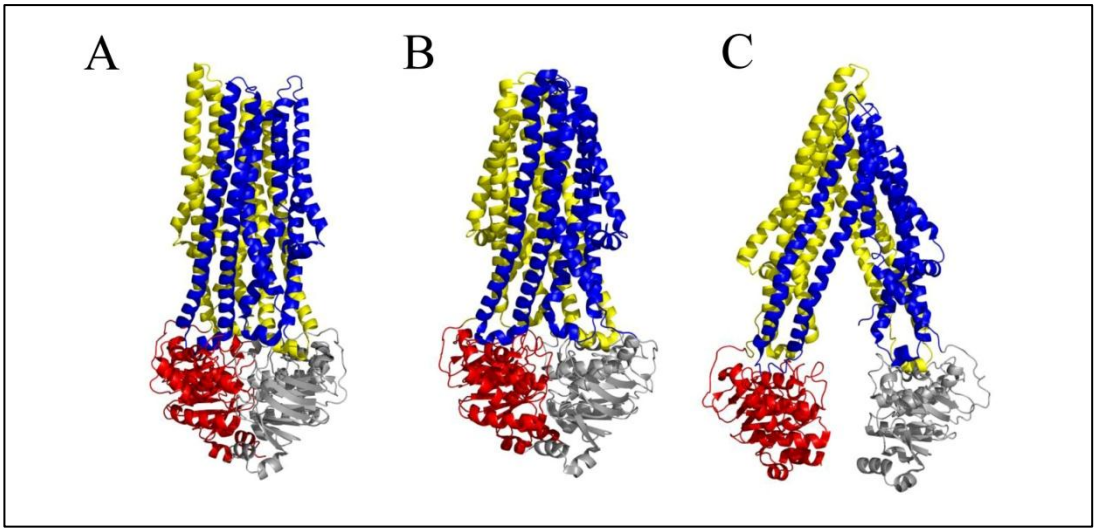

Figure 1-2. *Structures of ABC exporters.*

All structures are shown cartoon format, with TMDs coloured in yellow and blue and NBDs coloured in red and grey. (A) Sav1866 (PDB: 2HYD), (B) MsbA (PDB: 3B60) and (C) Abcb1a (PDB: 3G5U). Modified from (Zolnerciks et al., 2011).

A number of NBD crystal structures now available have revealed the true nature of the NBD-NBD dimer which forms the catalytic site for ATP hydrolysis (Chen et al., 2003, Hopfner et al., 2000, Karpowich et al., 2001, Obmolova et al., 2000, Schmitt et al., 2003, Smith et al., 2002, Verdon et al., 2003, Zaitseva et al., 2006) and is described in Section 1.4.1. Complementary to these data, are the crystal structures for 3 complete ABC exporters (Figure 1-2): the bacterial exporter Sav1866 from *Staphylococcus aureus* (Dawson and Locher, 2006), the lipid floppase MsbA from *Salmonella typhimurium*, *E. coli* and *Vibrio Cholerae* (Ward et al., 2007) and the ABCB1 homologue, Abcb1a, from *Mus musculus* (Aller et al., 2009). Abcb1a crystallised in a different conformation in which the NBDs do not share an interface. This may represent a different conformation of the transporter adopted during the transport cycle, but the physiological relevance remains untested. These

structures, notwithstanding their limited number and medium resolution, have revealed a TMD structure unique to exporters whose main features are summarised in Section 1.4.2.

1.4.1 The nucleotide-binding domains (NBDs)

The NBDs share a high degree of identity throughout the entire ABC family and all contain seven conserved motifs (Figure 1-3) (Kerr, 2002). Each NBD has an L-shaped topology with two subdomains. The F1-type "core" subdomain contains the Walker A (GxxGxGKS[S/T]) and Walker B (φφφφDE) motifs (where X is any amino acid; φ is a hydrophobic residue) together with the A-, Q-, D- and H-loops. The α-helical subdomain contains the ABC signature (LSGGQ) motif. In a full ABC transporter, the NBDs align in

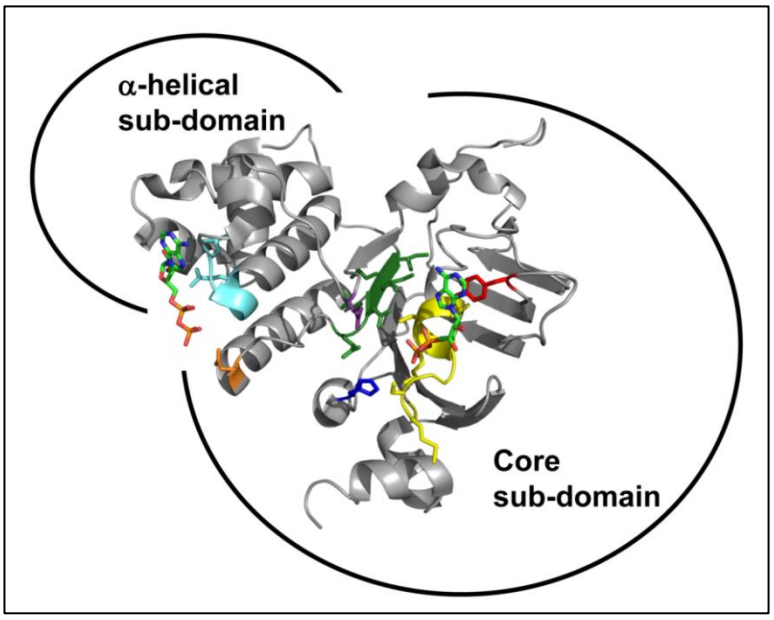

Figure 1-3. ***Structure of an ABC transporter NBD.***

This view shows one NBD from the perspective of its partner NBD across the NBD-NBD interface. The side chains of key amino acids and nucleotide (ADP) are shown in stick format. ADP molecules are coloured by atomic element (carbon, green; nitrogen, blue; oxygen, red; phosphorus, orange). The seven conserved motifs in each NBD are also highlighted. The core F_1-ATPase-like ATP-binding subdomain contains: the Walker A (yellow) and Walker B (green) motifs, the A-loop (red) and the Q- (purple), D- (orange) and H- (dark blue) loops. The α-helical subdomain contains the ABC signature (light blue) motif. Adapted from (Zolnerciks et al., 2011).

a "head-to-tail" arrangement such that the Walker A motif (essential for ATP binding and hydrolysis) of one NBD is in close association with the ABC signature motif [also known

as the C-motif which is unique to the ABC superfamily (Hyde et al., 1990)] of the apposing NBD, allowing two ATP molecules to be trapped at the interface (Jones et al., 2009, Rees et al., 2009, Zolnerciks et al., 2011).

1.4.2 The transmembrane domains (TMDs)

Each of the aforementioned crystal structures obtained for ABC exporters (Figure 1-2) comprises six membrane-spanning helices (MSHs) per TMD followed by an NBD. In each TMD the MSHs extend significantly (~25 Å) into the cytosolic space. What is most notable in the conformation adopted by the bacterial Sav1866 is a phenomenon described as *domain-swapping* (Dawson and Locher, 2006), which was also observed later in the crystal structure of the mouse Abcb1a (Aller et al., 2009). In this arrangement, a number of the MSHs from one TMD are in close association with a number of MSHs from the other TMD. In the case of Sav1866, MSH1-2 from one TMD associate with MSH3-6 from the other TMD (Dawson and Locher, 2006). For Abcb1a, the composition of the two helix bundles is different but still occurs in a domain-swapped arrangement (MSH4-5 of the first TMD associate with MSH1-3 and 6 of the second TMD) (Aller et al., 2009). Domain swapping allows each TMD to contact both NBDs via specific architecturally conserved α-helical loops known as the *coupling helices* (Locher et al., 2002). The coupling helices form non-covalent interactions with the NBDs at their shared interface. This causes the MSHs to be tilted significantly in respect to the plane of the membrane so that the TMDs are always closed to one side of the membrane and prevent the passive diffusion of allocrites. Such arrangement allows the two intracellular loops of each TMD to contact both NBDs which may be what allows the inwardly-open conformation observed in a Abcb1a crystal to form and be stage of the efflux cycle. Consequently, the TMDs are mechanistically coupled to the NBDs in a way that structural rearrangements caused by allocrite binding at the

TMDs, is transduced into the NBDs to stimulate ATP binding and hydrolysis, to drive translocation of the allocrite, and to reset the transporter (Zolnerciks et al., 2011).

1.5 ABCB1 and ABCB4 topology

The original topology model of ABCB1 predicted 6 hydrophobic transmembrane α-helices per TMD each followed by a hydrophilic NBD on the cytoplasmic face of the plasma membrane (Chen et al., 1986) (Figure 1-4). Such topology was later confirmed by Loo and Clarke in a mutant form of human ABCB1 whereby specific cysteine residues were introduced into the predicted extracellular or cytosolic loops of an otherwise cysteine-less protein and assaying for their ability to be biotinylated (Loo and Clarke, 1995a). In addition, the crystal structure of the murine ABCB1 homologue, albeit at a medium resolution, demonstrates two bundles of 6 MSHs per TMD each followed by a lobular NBD (Aller et al., 2009).

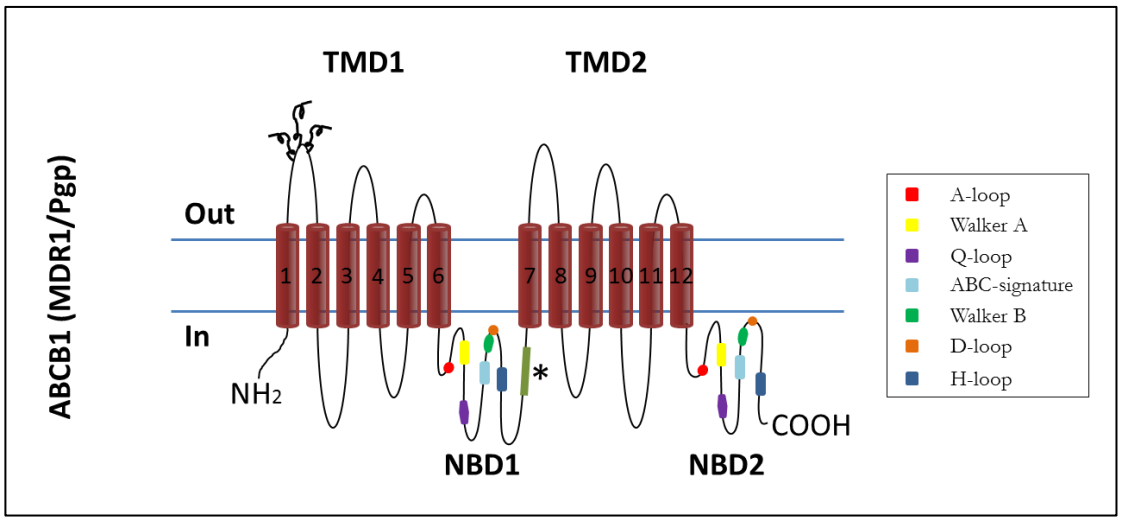

Figure 1-4. *Domain organisation of ABCB1*.

The topology of ABCB1 is illustrated highlighting the arrangement of the transmembrane domains (TMDs) and the nucleotide-binding domains (NBDs). The numbered cylinders within the TMDs represent the membrane-spanning α-helices. The seven conserved motifs within the NBDs are also demonstrated. The linker region, a cytoplasmic stretch of 75 amino acids joining the two TMDs is indicated with an asterisk (*). The glycosylation sites (N91, N94 and N99) in the first extracellular loop are indicated by the helical lines.

Comparison of the primary sequence of *ABCB4* with that of *ABCB1* reveals an almost identical topology for the two proteins (Van der Bliek et al., 1987). Such observation is in agreement with the outcome of a prediction algorithm which, based on the incorporation of experimental data, calculates that ABCB4 should have a similar topology to ABCB1 (Tusnady et al., 2006). It is therefore expected that the crystal structure of ABCB4 would closely resemble that obtained by Stephen Aller and colleagues for the murine homologue of ABCB1 (Aller et al., 2009).

1.6 The role of the "linker region" in ABCB1 and ABCB4

The first NBD is joined to the second TMD of ABCB1 by a stretch of 75 amino acids (residues 633–709 as predicted by computer-assisted algorithms), commonly known as the linker region (Figure 1-4) (Chen et al., 1986, Germann et al., 1996, Hrycyna et al., 1998). This region has been shown to be phosphorylated *in vivo* by protein kinase C alpha (PKCα) (Chambers et al., 1990, Ma et al., 1991, Orr et al., 1993). The role of the linker region in ABCB1 is yet to be defined but mutagenesis of the residues which are phosphorylated by PKCα has no effect on the localisation and function of the transporter (Germann et al., 1996, Goodfellow et al., 1996) [for a more detailed account of the interaction between ABCB1 and PKCα and its role in the development of MDR see Section 1.11.2.1].

In contrast, a role for the linker region (residues 623-699) on the localisation, function and rate of maturation of ABCB4 has been suggested. In a yeast two-hybrid screen using the linker region of ABCB4 as bait against a human liver cDNA library, *RACK1* (receptor for activated C-kinase 1) was identified as a novel binding partner of *ABCB4* and confirmed by GST (glutathione *S*-transferase)-pulldown of purified recombinant domains (Ikebuchi et al., 2009). RACK1 is a scaffold protein identified through its ability to bind activated PKC and this interaction is thought to stabilise activated PKC and facilitate the regulation of the

phosphorylation state of target proteins (Mochly-Rosen et al., 1991). In fact, the apical localisation of the cystic fibrosis transmembrane conductance regulator (CFTR/ABCC7) has been shown to be regulated by RACK1 (Auerbach and Liedtke, 2007, Liedtke et al., 2002) suggesting that trafficking of ABC proteins can be modulated by RACK1. Suppression of endogenous *RACK1* by siRNA in HepG2 cells (polarised cells derived from human hepatoma), resulted in intracellular retention of ABCB4 as opposed to the expected localisation at the bile canalicular membrane of the polarised cells but the localisation of ABCB1 was not affected (Ikebuchi et al., 2009). In a HeLa cell line in which *RACK1* had been stably knocked down, it was shown that the absence of *RACK1* expression affected the rate of maturation of exogenous ABCB4 (Ikebuchi et al., 2009). Finally, the level of activity of ABCB4 both in the presence and in the absence of *RACK1* expression was assayed in HeLa cells by measuring the amount of [^{14}C]PC effluxed by ABCB4 into the cell medium (Ikebuchi et al., 2009). In this assay, the ABCB4-mediated [^{14}C]PC efflux was reduced by the suppression of *RACK1* expression (Ikebuchi et al., 2009).

Collectively, the above data suggest that ABCB1 and ABCB4, despite their high degree of identity, can be regulated by different mechanisms.

1.7 Glycosylation

ABCB1 is a 170 kDa membrane protein featuring *N*-linked glycosylation with oligosaccharides of the "complex" type (Richert et al., 1988, Schinkel et al., 1993). In eukaryotes, the consensus site for *N*-linked glycosylation has the amino acid sequence of Asn (asparagine)-X-Thr (threonine)/Ser (serine), where X can be any amino acid except proline (Kornfeld and Kornfeld, 1985). Although sequence analysis of ABCB1 predicts 10

possible sites for *N*-linked glycosylation (Chen et al., 1986), only three are exposed to the lumen of the endoplasmic reticulum and thus glycosylated (Gribar et al., 2000, Richert et al., 1988, Schinkel et al., 1993). All three consensus sites cluster on the first extracellular loop of ABCB1 at the amino acid residues Asn91, Asn94 and Asn99 (Figure 1-4) (Schinkel et al., 1993). Glycosylation-deficient ABCB1 retains its drug-transport function and substrate specificity (Gribar et al., 2000, Schinkel et al., 1993) however, it is expressed at a lower level than WT ABCB1 because a greater fraction of the mutant protein misfolds and is degraded by the proteasome (Gribar et al., 2000).

ABCB4 has two consensus *N*-glycosylation sites. However, the effects of glycosylation on ABCB4 trafficking and/or function have not been studied extensively. Although glycosylation does not appear to have a strong effect on ABCB1 (Gribar et al., 2000, Schinkel et al., 1993), disruption of *N*-linked glycosylation of another ABC protein, ABCG2, has been shown to modulate trafficking to the cell membrane, reduce stability and enhance proteasomal degradation (Nakagawa et al., 2009).

1.8 The discovery of ABCB1 and its implications in MDR

In 1973, Dano presented evidence of the active export of daunomycin from a drug resistant Ehrlich ascites tumour cell line (Dano, 1973). Shortly after, work done on colchicine resistant Chinese hamster ovary (CHO) cells revealed a 170 kDa cell membrane glycoprotein, termed P-glycoprotein (P-gp, also known as MDR1), which could alter the permeability of the cells to amphiphilic drugs and could not be detected in wild type (WT) cells (Juliano and Ling, 1976). Resistance to daunorubicin was also noted in Ehrlich ascites tumour cells (Skovsgaard, 1978). Several lines of evidence correlated the level of resistance with the amount of the 170 kDa protein at the membrane (Juliano and Ling, 1976, Kartner

et al., 1983, Riordan and Ling, 1979) and in most of the MDR cell lines studied (human, hamster or mouse) an overexpression of P-gp could be observed (Gerlach et al., 1986b, Kartner et al., 1983). Successful cloning and isolation of the complete mouse and human cDNAs for the *MDR1* gene revealed the internal homology of the two halves of the protein. Sequence analysis showed homology with conserved bacterial counterparts and so P-gp (ABCB1) was assigned to the ATP binding cassette (ABC) family of proteins and it was predicted to function as a drug efflux pump (Chen et al., 1986, Gerlach et al., 1986a, Gros et al., 1986b, Gros and Shustik, 1991, Ueda et al., 1987). To confirm this theory, overexpression of the cDNA encoding ABCB1 was shown to convert drug sensitive cells into resistant ones (Gros et al., 1986a, Ueda et al., 1987).

Early photoaffinity labelling experiments carried out in membrane vesicles derived from multidrug-resistant KB carcinoma cells, demonstrated that ABCB1 is indeed a drug- and ATP-binding protein (Cornwell et al., 1987a, Cornwell et al., 1986, Cornwell et al., 1987b). In addition, drug-transport assays performed in plasma membrane vesicles from the same KB cell line, showed that ATP hydrolysis was essential for allocrite transport by ABCB1 and that drug-resistance reversing agents could inhibit ABCB1-dependent efflux (Horio et al., 1988). Collectively, these studies established the basic mechanism by which ABCB1 transports its allocrites.

Further studies using purified ABCB1, from drug-resistant cell lines, which had been functionally reconstituted in proteoliposomes, showed that ABCB1 displayed drug-stimulated ATPase activity and that it could transport drugs across a lipid bilayer against their concentration gradient (Ambudkar, 1995, Ambudkar et al., 1992, Shapiro and Ling, 1994, Sharom et al., 1993).

Taken together, these early experiments confirmed that ABCB1 is an ATP-dependent drug-efflux pump responsible for multidrug resistance.

1.9 Association of other ABC proteins with MDR

ABCB1 is not the only protein affecting drug pharmacokinetics. A human small cell lung cancer cell line (H69AR) which did not overexpress ABCB1, could develop cross-resistance to a variety of anti-cancer agents (Cole, 1990, Mirski et al., 1987). The cDNA of the gene responsible for this phenotype was cloned from these cells and, based on primary sequence analysis, it was concluded that it coded for another protein belonging to the ABC family: the multidrug resistance-associated protein 1 (MRP1/ABCC1) (Cole et al., 1992). In 1998, a third xenobiotic transporter involved in MDR was identified from human breast cancer cells (MCF-7/AdrVp) that did not overexpress ABCB1 or ABCC1, but were resistant to anthracycline anticancer drugs. When overxpressed in MCF-7 cells, the protein was able to confer resistance to mitoxantrone, doxorubicin, and daunorubicin. The protein was named breast cancer resistance protein (BCRP). It is also known as mitoxantrone resistance protein (MXR) and it is another member of the ABC family of transporters designated as ABCG2 (Allikmets et al., 1996, Doyle et al., 1998, Miyake et al., 1999).

1.10 ABCB1 in normal physiology

ABCB1 is expressed in a variety of normal human tissues including the brain, liver, testes, heart, kidneys and intestines (Cordon-Cardo et al., 1990, Cordon-Cardo et al., 1989, Fojo et al., 1987, Thiebaut et al., 1987, Thiebaut et al., 1989). Its primary function appears to be to pump xenotoxins out of cells against their concentration gradient. This function is best exemplified in the *Abcb1a*/*Abcb1b* (formerly known as *Mdr1a* and *Mdr1b*, the two

functional equivalents of ABCB1 in the rodent) knock-out mice. Disruption of either (*Abcb1a* or *Abcb1b*) or both of the genes generated mice with a normal physiology and fertility which displayed a marked alteration in drug sensitivity (Schinkel et al., 1997, Schinkel et al., 1994). Absence of the transporter(s), which are highly expressed in capillary endothelial cells that form the blood-brain barrier (Cordon-Cardo et al., 1989, Thiebaut et al., 1989), resulted in the toxic accumulation of ivermectin, vinblastine and digoxin in the brain of *Abcb1a/b* null mice, ultimately resulting in death (Schinkel et al., 1997, Schinkel et al., 1994). In the liver, ABCB1 is involved in the efflux of toxic substrates into the bile as demonstrated by the accumulation of vinblastine in the liver of *Abcb1*$^{-/-}$ mice (Schinkel et al., 1997, Schinkel et al., 1994). ABCB1 also functions in the intestine limiting the re-uptake of drugs such as paclitaxel (Taxol) into the blood stream. These data are also corroborated by studies in humans, in which inhibition of ABCB1 has been shown by PET studies, to dramatically alter the distribution of tracer drugs (Gottesman et al., 2002).

Experiments carried out in human haematopoietic stem cells negative for rhodamine 123 staining (Rh123; a fluorescent dye that accumulates in the mitochondria) revealed high levels of ABCB1 expression (Chaudhary and Roninson, 1991). The decreased accumulation of Rh123 was attributed to ABCB1-mediated efflux which has led to the suggestion that ABCB1 may, physiologically, be involved in the efflux of toxic substrates from progenitor cells or, of factors that would otherwise drive their differentiation (Chaudhary and Roninson, 1991).

The function of ABCB1 and Abcb1a as floppases of short-chain analogues of endogenous membrane lipids has also been described (Bosch et al., 1997, van Helvoort et al., 1996) but neither functional Abcb1a nor Abcb1b could compensate for Abcb4 function in *Abcb4* null mice (Smit et al., 1993). The physiological role of such floppase function for ABCB1 is

unclear but there is evidence to support a role in the secretion of short-chain phosphocholine signalling molecules. Platelet-activating factor (PAF; 1-*O*-alkyl-2-acetyl-*sn*-glycero-3-phosphocholine) is one such naturally occurring short-chain phosphocholine. It is a potent bioactive lipid and is involved in various pathological conditions, such as angiogenesis in breast cancers, metastasis and multiple organ failure (Anderson et al., 1991, Montrucchio et al., 1998). One of the best characterised roles for PAF is as a mediator of cell-cell interactions in the inflammatory response (Prescott et al., 2000). PAF is secreted by a variety of cells (e.g. epithelial and endothelial cells) and exerts its function by binding to a G-coupled receptor on the extracellular surface of the target cell (Prescott et al., 2000). In order for PAF to perform its function, it has to be transported from its site of synthesis in the cytosol to the extracellular leaflet of the plasma membrane. It has been demonstrated that ABCB1 can translocate PAF from the inner to the outer leaflet of the plasma membrane suggesting a role for the glycoprotein in intercellular signalling (Raggers et al., 2001).

1.11 Why study the ABCB1 interactome?

ABCB1 presents a major impediment to chemotherapeutic treatments for cancer patients. As highlighted in the examples above (Section 1.10), it also has an important physiological role in the protection of several pharmacological sanctuaries, such as the brain, testes, liver and intestines; from which it effluxes xenotoxins. It may also be involved in intercellular signalling. Direct inhibition of ABCB1 can therefore have detrimental effects on cancer patients. Consequently, identification of ABCB1-interacting partners that influence trafficking or function could provide alternative targets for therapy.

ABCB1 has been shown to retain function when purified from insect cells (*Tricoplusia ni*) and reconstituted in proteoliposomes (Sharom et al., 1999). While this indicates that ABCB1 can work in isolation it is also known to interact with other proteins during folding/trafficking and at the plasma membrane. These interactions are not well characterised, and it is likely that the whole ABCB1-interactome has not yet been discovered. A number of proteins that have previously been shown to interact with ABCB1 are described below.

1.11.1 ABCB1 interactors involved in intracellular trafficking

The nascent ABCB1 protein has three potential glycosylation sites (residues 91, 94 and 99, Figure 1-4) on the first extracellular loop (ECL) (Chen et al., 1986, Schinkel et al., 1993) and is synthesised in the ER as a 150 kDa core-glycosylated intermediate. In the ER, ABCB1 interacts specifically with four molecular chaperones (calnexin, calreticulin, ERp57 and Hsc70) which modulate the folding of *N*-glycosylated polypeptides (High et al., 2000, Loo and Clarke, 1994, Loo and Clarke, 1995b). Misfolded ABCB1 is retained in the ER and rapidly degraded (Loo and Clarke, 1997) via the 26S proteasome (Goldberg, 2003) whereas the correctly folded form translocates to the Golgi where it is further modified to a 170 kDa mature glycoprotein (Molinari et al., 1998, Molinari et al., 1994) before transport to the plasma membrane. Trafficking of ABCB1 from the Golgi to the apical domain or the plasma membrane of polarised and non-polarised cells, respectively, occurs via intracellular endosomes (Fu and Roufogalis, 2007, Kipp and Arias, 2000, Wakabayashi et al., 2005) and it is thought to involve interactions with actin cytoskeleton (actin disruption leads to intracellular accumulation of fluorescently-labelled ABCB1 (Fu and Roufogalis, 2007).

1.11.2 Function-related ABCB1 interactors

The mature, fully glycosylated form of ABCB1 localises to the apical membrane of polarised cells and the plasma membrane of non-polarised cells as shown by confocal microscopy (Hammerle et al., 2000, Petriz et al., 2004). Here, ABCB1 has been shown to interact with a number of other proteins, such as protein kinase C alpha and caveolin-1, both of which are thought to modulate its function.

1.11.2.1 ABCB1 and protein kinase C

Protein kinase C (PKC) is a key enzyme in signal transduction and modulation of cell growth, cell proliferation, apoptosis and malignant transformation. To date, 11 subspecies of PKC have been reported (alpha [α], beta-I [β-I], beta-II [β-II], gamma [γ], delta [δ], epsilon [ε], zeta [ζ], eta [η], theta [θ], lambda [Λ] and mu [μ]) which differ in their expression profiles, biochemical properties, activator requirements and substrate specificity; suggesting distinct roles in different signalling pathways (Hug and Sarre, 1993). The common PKC isoenzyme alpha (PKCα) is calcium (Ca^{2+})-dependent and is activated by the phospholipid derivative diacylglycerol (DAG) in response to extracellular signals such as growth factors and cytokines (Nishizuka, 1995). Activation of PKC can also occur via the tumour-promoting phorbol esters (Castagna et al., 1982) and such activation can induce an MDR phenotype in a breast cancer cell line (MCF7) (Fine et al., 1988). Detailed studies of the PKC isoenzymes involved in MDR revealed that there was a ten-fold increase in PKCα expression in drug-resistant MCF7 cells compared to the parental line (Blobe et al., 1993). Furthermore, transfection of MCF7 cells with a vector coding for antisense cDNA against PKCα increased the drug sensitivity of the cells by three-fold (Ahmad and Glazer, 1993) while overexpression of PKCα in BC-19 cells resulted in decreased drug accumulation (Yu et al., 1991).

The phospholipid-dependent PKC family of serine/threonine kinases has been implicated in MDR (Rumsby et al., 1998). In many of the MDR cell-lines studied to date, there is an elevated level of both expression and activity of PKC and in most cases the isoenzyme involved is PKCα (Fine et al., 1996). Activation of PKC in MDR cells correlates with increased ABCB1 phosphorylation and decreased drug accumulation (Bates et al., 1993, Blobe et al., 1993, Chambers et al., 1990, Chambers et al., 1992, Hamada et al., 1987). Co-immunoprecipitation (co-IP) studies revealed a close association PKCα and ABCB1 in membrane vesicles from Sf9 insect cells (Ahmad et al., 1994) and in human carcinoma cell lines (Yang et al., 1996). All of the above evidence points towards a role for PKCα in the regulation of ABCB1 through phosphorylation of its serine residues. Analysis of the phosphorylation sites of ABCB1 both *in vivo* and *in vitro* showed that ABCB1 is phosphorylated on the "linker" region (a highly charged region connecting the two homologous halves of the protein) (Chambers et al., 1990, Ma et al., 1991, Orr et al., 1993). The major phosphorylation sites comprise a cluster of three serine residues (Ser661, Ser667 and Ser671) all of which appear to be phosphorylated *in vivo* (Chambers et al., 1994, Chambers et al., 1993) but this phosphorylation appears to have no effect on the localisation or the efflux function of the transporter (Germann et al., 1996, Goodfellow et al., 1996).

It is not yet clear what effect the association of ABCB1 with PKCα has on ABCB1 function but there is evidence to suggest a role for PKCα in the transcriptional activation of the *ABCB1* gene through the Ras (Rat sarcoma) small GTPase (guanosine triphosphatase) which is under the positive influence of PKCs (Grunicke et al., 1994). In addition, phosphorylation of the "linker" region was shown to affect the interaction of ABCB1 with a number of substrates without affecting its ATPase activity (Szabo et al., 1997). Moreover, a role for PKC-mediated phosphorylation of ABCB1 in the regulation of

volume activated chloride channels has been described which implicates ABCB1 in the modulation of cell volume (Hardy et al., 1995, Idriss et al., 2000, Vanoye et al., 1999). Finally, it has been proposed that ABCB1 affects the trafficking of PKCα (Sardini A., personal communication). Activation of PKCα by a phorbol ester resulted in the transport of the protein from the cytoplasm to the cell membrane. In the absence of ABCB1, PKCα was re-internalised and localised to a perinuclear compartment within 30 minutes of exposure of the cells to phorbol ester. When the same experiment was performed in cells expressing ABCB1, no re-internalisation was evident even after 120 minutes of exposure (Sardini A., personal communication).

1.11.2.2 ABCB1 and caveolin-1

"Liquid-ordered" microdomains within the lipid bilayer of the cell membrane are known as lipid rafts (Rietveld and Simons, 1998). Such microdomains deviate from the classical "liquid crystalline state" of the cellular membrane (Singer and Nicolson, 1972) in that they are enriched in cholesterol and sphingolipids as opposed to phospholipids (Simons and Ikonen, 1997); a feature that makes them resistant to solubilisation with Triton-X 100 at low temperature (4°C) (Moldovan et al., 1995). Lipid rafts are thought to be important in transmembrane signal transduction by recruiting receptors to a microenvironment to allow faster communication between ligands and effector proteins (Brown and London, 1998, Rietveld and Simons, 1998, Simons and Ikonen, 1997, Simons and Toomre, 2000).

Structural protein components can be integrated in lipid rafts changing the morphology and function of the microdomains. One such structural component is caveolin-1 (CAV1/VIP21) (Rothberg et al., 1992, Kurzchalia et al., 1992, Glenney, 1992). CAV1 is a 22 kDa hairpin-like, palmitoylated (Dietzen et al., 1995) and cholesterol-binding (Murata et al., 1995) integral membrane protein with cytoplasmic amino and carboxy termini (Dupree

et al., 1993, Monier et al., 1995). Polymerisation of CAV1 monomers results in the invagination of lipid rafts and the formation of caveolae: 50- to 100-nm flask-shaped plasma membrane invaginations. Caveolae are found in most differentiated cell types with a notable abundance in adipocytes, endothelial cells, fibroblasts, muscle cells and type I pneumocytes (Cohen et al., 2004, Razani et al., 1999) and complete absence from lymphocytes and neurons of the central nervous system (Cameron et al., 1997, Fra et al., 1994). The main roles of caveolae include vesicular transport (transcytosis/endocytosis), cholesterol homeostasis and signal transduction (Cohen et al., 2004, Razani et al., 2002).

CAV1 is upregulated in human MDR cancer cells (Belanger et al., 2003, Lavie et al., 1998, Yang et al., 1998). One of the most uniform associations between MDR and the expression of ABCB1 is found in patients with acute myelogenous leukaemia (AML) (Leith et al., 1999) where the *CAV1* and *ABCB1* genes have been shown by real-time quantitative polymerase chain reaction to be coordinately regulated (Pang et al., 2004). This suggests an interaction between ABCB1 and CAV1 but it remains to be elucidated whether *CAV1* expression affects ABCB1 function in AML patients.

A number of investigations have demonstrated a physical interaction between Cav1 and Abcb1 in isolated brain capillaries or in drug-resistant cancer cell lines (Barakat et al., 2007, Demeule et al., 2000, Hawkins et al., 2010, Jodoin et al., 2003). Immunogold cytochemistry at the electron microscope level on human and rat brain tissue detected a fraction of ABCB1/Abcb1 in plasma membrane invaginations (caveolae) in all cells that constitute the blood-brain barrier (BBB), i.e., capillary endothelial cells, pericytes and astrocytes (Bendayan et al., 2006). Experiments performed in COS7 cells, have shown that Abcb1 is negatively regulated by Cav1 (Jodoin et al., 2003) and siRNA work in RBE4 cells demonstrated that Cav1 downregulation stimulates Abcb1 efflux function (Barakat et al.,

2007). Evidence for a negative regulation of Abcb1 by Cav1 *in vivo* has also been obtained from *in situ* rat brain perfusion experiments (Hawkins et al., 2010).

In drug-resistant human colon and breast adenocarcinoma cell lines ABCB1 was shown to localise in at least two distinct membrane compartments (Lavie et al., 1998). One compartment had the physical characteristics of caveolae whereas the other compartment was detergent-soluble and it was demonstrated that the expression of *CAV1* was not a prerequisite of ABCB1 localisation to the caveolae fraction (Lavie et al., 1998). These data are in agreement with the results obtained by Jodoin *et al.* (2003) in an *in vitro* model for the BBB where a large fraction of Abcb1 molecules was found to localise in caveolar fractions and to interact with Caveolin-1 in both caveolar and non-caveolar fractions. ABCB1 is highly expressed in endothelial cells at the BBB where it plays a protective role against brain toxicity (Beaulieu et al., 1997, Demeule et al., 2001, Schinkel, 1999, Schinkel et al., 1994). Understanding the significance of ABCB1/CAV1 interaction in the caveolar compartments will provide alternative means of overcoming ABCB1 drug-efflux function and to increase drug passage through the BBB.

1.12 The "split-ubiquitin" yeast two-hybrid system as a means of studying the ABCB1 interactome

The identification of proteins that interact with ABCB1 should enhance our understanding of the function of this efflux transporter and its mechanism of action. In an attempt to enrich the pool of known ABCB1 interactors, the "split-ubiquitin" yeast two-hybrid (SU-YTH) system was employed (Stagljar and Fields, 2002) and is described in Chapter 3. The system allows for the identification and characterisation of interactions between an integral membrane protein of interest, in this case ABCB1, and other integral membrane proteins

or membrane-associated proteins or cytosolic proteins. Compared to the conventional yeast two-hybrid system (Fields and Song, 1989), the SU-YTH offers the advantage of detecting protein:protein interactions between full-length proteins at the cell membrane whilst allowing for the preservation of post-translational modifications such as glycosylation (Stagljar et al., 1998, Thaminy et al., 2003).

Identification of novel interactors of ABCB1 was achieved through screening of an adult human liver cDNA library (Section 3.2.4). Prior to doing so, the expression of ABCB1:Cub bait was confirmed by the "NubI/NubG" test (Section 3.2.1.2) and the level of self-activation of the ABCB1:Cub bait was assayed (Section 3.2.3). A total of 29 putative interactors were isolated from the library screen but following strict testing using the appropriate controls, none of the candidate proteins was shown to specifically interact with ABCB1 (Section 3.2.5) and the underlying reasons for this unsuccessful attempt are considered in Section 3.3.

1.13 Canalicular ABC transporters and liver disease

Many of the human ABC transporters have important roles in normal physiology and morbidity (Borst and Elferink, 2002, Linton and Holland, 2011); a number of which are involved in the formation of bile. Bile is a complex mixture of bile salts, phospholipids, cholesterol, bile pigments, electrolytes and proteins. Bile salts are required for the solubilisation of dietary fats and lipophilic vitamins. They are synthesised in the hepatocyte and secreted across the canalicular membrane into the biliary tree where they are eventually expelled into the small intestine in response to food intake to fulfil their primary role. Bile salts are then reabsorbed very efficiently by enterocytes, and secreted into the portal vein for return to the liver to complete the *enterohepatic cycle*.

Both the synthesis and enterohepatic cycling of bile salts is under tight control at the protein and genetic level to limit their intrahepatic and serum concentrations. Disruption of the mechanisms which control bile salt synthesis and circulation, and the mechanisms that protect the membranes of the biliary tree can lead to serious disease due to the inherently toxic nature of bile salts. In the biliary tree, where high concentrations of bile salts exist, phospholipids are secreted to form a mixed micelle with the bile salts and reduce their detergent activity. The anabolic enzymes, the transporters, receptors and transcription factors involved in bile salt homeostasis are now largely identified and are described in detail below. In particular, the role of three transporters responsible for the majority of bile flow; ABCB11, ABCB4 and ATP8B1, are highlighted.

1.13.1 The liver and biliary tract

The liver, the largest of the internal organs, is involved in a wide range of processes. These include bile synthesis and secretion, excretion of bilirubin, amino acid and lipid metabolism as well as the elimination of toxins (Aspinall and Taylor-Robinson, 2002). Due to its complicated and highly specified functions, the liver has a complex architecture and a double blood supply system (Figure 1-6). Oxygenated blood (20%) is provided by the hepatic artery branching out from the aorta, while venous blood (80%) from the intestines and spleen arrives through the hepatic portal vein (Stevens and Lowe, 2005). Approximately 70% of the cells in the liver are hepatocytes (parenchymal cells); whereas the remaining 30% are non-parenchymal cells such as the phagocytic Küpffer cells, stellate cells (also known as Ito or fat-storing cells), endothelial cells, epithelial cells and lymphocytes (Figure 1-6) (Ishibashi et al., 2009).

Secretion of bile by the liver and recycling through the biliary tree (Figure 1-5) is physiologically important as this is the main driving force for solute and water movement

within the enterohepatic circulation. The liver produces 400 – 600 ml of bile per day (Arias et al., 1994) and its secretion depends on the function of membrane transporters on the surface of hepatocytes and cholangiocytes (Esteller, 2008). Hepatocytes are responsible for the secretion of "primary" bile (bile salts, cholesterol, bilirubin, drug metabolites and heavy metals), into the bile canaliculus, or bile ductules that are formed between adjacent hepatocyte plates and lined with cholangiocytes. Through secretory and reabsorptive processes, cholangiocytes are responsible for the fluidity and pH of bile and account for 40% of the total bile volume (Strazzabosco, 1997).

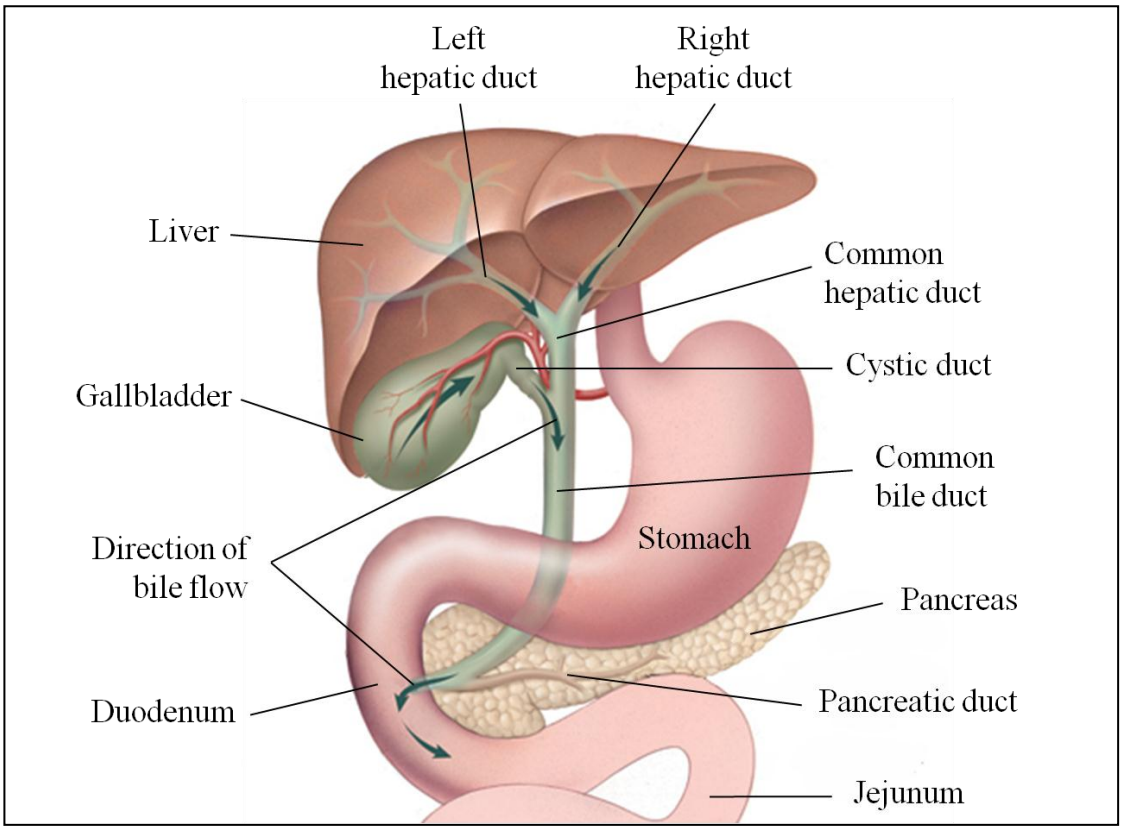

Figure 1-5. ***The liver and biliary tract*****.**

The main organs involved in the synthesis and secretion of bile into the small intestine. Image modified from: http://healthbasictips.com/wp-content/uploads/2011/09/Gallbladder1.jpg

Studies on the finer structure of intrahepatic bile ducts of various sizes (large, intermediate and small) have shown that they are lined by cholangiocytes that differ both in shape and

size. Specifically, they are cuboidal or flattened in small ducts (or ductules) and columnar in large ducts (Steiner and Carruthers, 1961). The intrahepatic bile ductules emerging from the hepatocytes gradually merge to establish larger ducts and eventually coalesce to form the left and right hepatic ducts which join to form the common hepatic duct (Figure 1-5). The gallbladder is responsible for concentrating the bile (5- to 10-fold) by the net reabsorption of sodium, calcium, chloride and bicarbonate ions followed by the passive movement of water (Dietschy, 1966). It is joined to the biliary tree via the cystic duct where it merges with the common hepatic duct to form the common bile duct (coledochus; Figure 1-5). Following the ingestion of food, the gallbladder contracts and empties its contents into the common bile duct in response to the hormone cholecystokinin (CCK) (Spellman et al., 1979). The common bile duct merges with the pancreatic duct at the ampulla of Vater (Figure 1-5) where the release of digestive enzymes into the duodenum is controlled by the sphincter of Oddi under the influence of CCK (Wiley et al., 1988). The release of bile into the duodenum marks the beginning of the solubilisation of dietary fats.

1.13.2 The hepatocyte

The main functional cell of the liver is the hepatocyte which displays a high level of metabolic activity in three broad categories: 1. lipid metabolism, 2. carbohydrate metabolism and 3. protein metabolism (Mitra and Metcalf, 2009). As a consequence of these metabolic activities, the hepatocyte performs both an excretory (e.g. bilirubin, drug metabolites, antibiotics) and a secretory (e.g. bile acids, phospholipids, cholesterol) function (Campbell, 2006).

Although the hepatocytes appear homogenous using light microscopy, they can have different metabolic profiles (Katz, 1992) and such differences are dictated by the relative

position of a hepatocyte within the functional unit of the liver, i.e. the liver acinus (Figure 1-6) (Rappaport et al., 1954). Morphologically, the hepatocytes are organised in a hexagonal

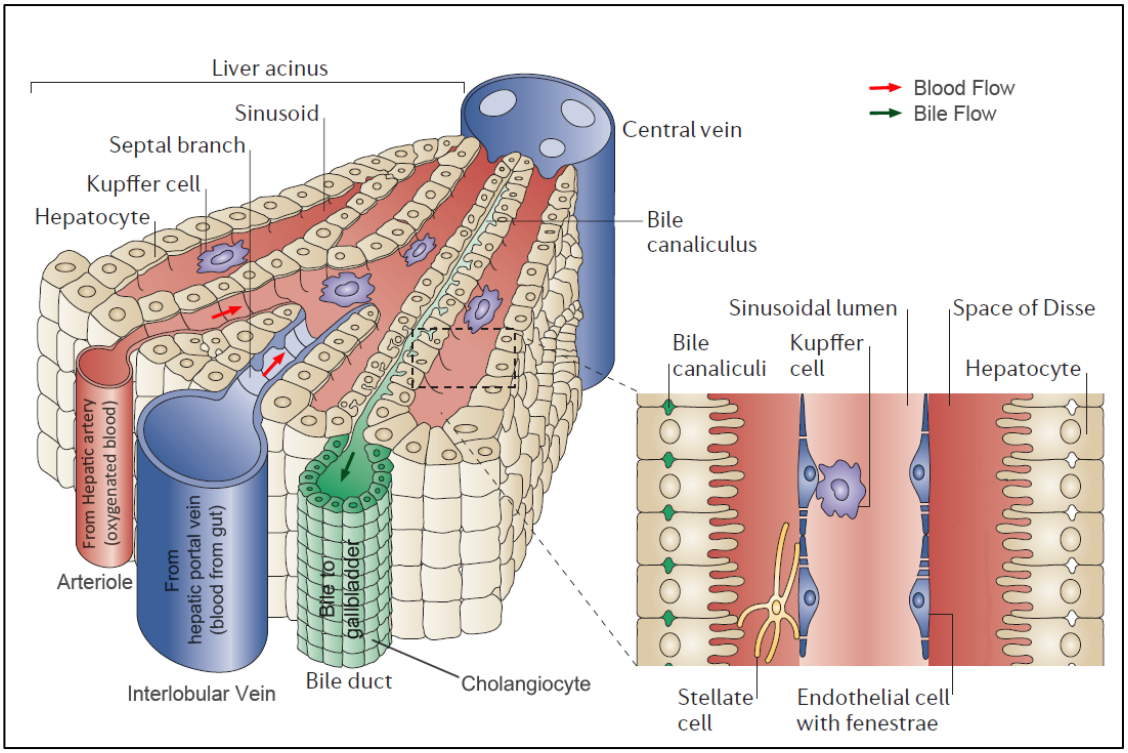

Figure 1-6. *The liver lobule*.

Blood supply to the liver is provided through branches of the hepatic portal vein (from the gut) and the hepatic artery (oxygenated blood from the aorta). Image modified from (Adams and Eksteen, 2006).

manner forming the liver lobule (Kaplowitz, 1992). In this arrangement, the portal tract (made of the terminal portal venule, terminal hepatic arteriole and bile duct) is at each corner with the central vein in the middle of the lobule (Ishibashi et al., 2009). Within the lobule, the hepatocytes are arranged in one-cell thick plates of 15 – 25 cells which run from the central vein to the periphery of the lobule. Blood flowing from the portal tract to the central vein fills the space between the liver-cell plates and forms the hepatic sinusoids which are lined with fenestrated endothelial cells (Figure 1-6). The space between the sinusoidal endothelium and the microvillar surface of the hepatocytes is known as the

space of Disse and allows for the exchange of solutes between the blood and the hepatocytes (Figure 1-6).

The surface of the hepatocyte comprises distinct domains which differ in functionality and molecular composition (Arias et al., 1994). Consequently the polarised hepatocyte plasma membrane has three types of cell surface: 1. the basal (or sinusoidal) surface, which is covered by microvilli, faces the sinusoids and is involved in the exchange of metabolites with the blood, 2. the lateral surface which is formed between adjacent hepatocytes joined by epithelial cell junctions (e.g. tight junctions, gap junctions, desmosomes and adherens junctions) and 3. the apical (bile canalicular) surface which is formed by invaginations of the apical membrane of apposing hepatocytes and delimited by junctional complexes (Figure 1-6). A number of membrane transporters are known to be expressed at the sinusoidal and canalicular surface of the hepatocyte (Table 1-1) where they are involved in the transport of substrates from the blood to the hepatocyte or from the hepatocyte to the bile, respectively.

Membrane transporter	Function	Reference
Apical membrane (canalicular)		
ABCB4 (MDR3)	PC floppase	(van Helvoort et al., 1996)
ABCB11 (BSEP/SPGP)	Bile salt export	(Gerloff et al., 1998)
ATP8B1 (FIC1)	PS flippase/microvillus formation	(Paulusma et al., 2006); (Paulusma et al., 2008); (Verhulst et al., 2010)
ABCG5/ABCG8	Efflux of plant and animal sterols	(Berge et al., 2000)
ABCC2 (MRP2/cMOAT)	Efflux of conjugated bilirubin and organic anions	(Paulusma et al., 1997)
ABCB1 (MDR1/PGP)	Efflux of xenobiotics	(van Asperen et al., 2000)
ABCG2 (BCRP/MXR)	Efflux of xenobiotics	(Ando et al., 2007)
Basolateral membrane (sinusoidal)		
NTCP (SLC10A1)	Uptake of conjugated and unconjugated bile salts from the sinusoids	(Hagenbuch and Dawson, 2004)
OATPs (SLC21)	Uptake of unconjugated bile salts, organic cations	(Hagenbuch and Meier, 2003)

Table 1-1. ***Membrane transporters expressed on the canalicular and sinusoidal membranes of the hepatocyte.***

The canalicular surface is of particular importance as it plays an integral role in the formation and enterohepatic circulation of bile. From the perspective of human cholestatic morbidity, three of the hepatocyte canalicular transporters are key. The bile salt export pump (ABCB11) and the phosphatidylcholine (PC) floppase (ABCB4), efflux the two main components of bile (bile salts and PC). The third protein necessary for bile flow from the hepatocyte is a P-type ATPase, ATP8B1 (FIC1). ATP8B1 appears to flip a different lipid, phosphatidylserine (PS), in the opposite direction to PC flop by ABCB4 (i.e. it flips PS inwardly). The flux of bile salts across the canalicular membrane is what drives bile flow, and mutations in any of the three aforementioned transporters lead to cholestatic liver disease. It is therefore important to understand the molecular basis for such diseases in order to facilitate therapeutic intervention tailored to each individual. Chapters four and five in this thesis focus on the characterisation of ABCB4 single-nucleotide polymorphisms (SNPs) in an attempt to understand the physiological significance of ABCB4 activity in cholestatic liver disease.

1.13.3 Bile salt synthesis

The movement of bile acids and bile alcohols from the hepatocytes (their site of synthesis in the liver) to the portal circulation, through the biliary tree and the small intestine, is known as the *enterohepatic circulation*. This is a very efficient recycling system in which approximately 95% of the bile salts are re-absorbed; the remaining 5% that is lost is replaced by *de novo* synthesis in the liver. Such process allows for the re-utilisation of these detergent-like molecules and forms the major route of cholesterol catabolism in mammals.

The bile salt pool comprises a mixture of primary bile salts that are synthesised *de novo* in the hepatocyte and secondary and tertiary bile salts, which result from bacterial catabolism

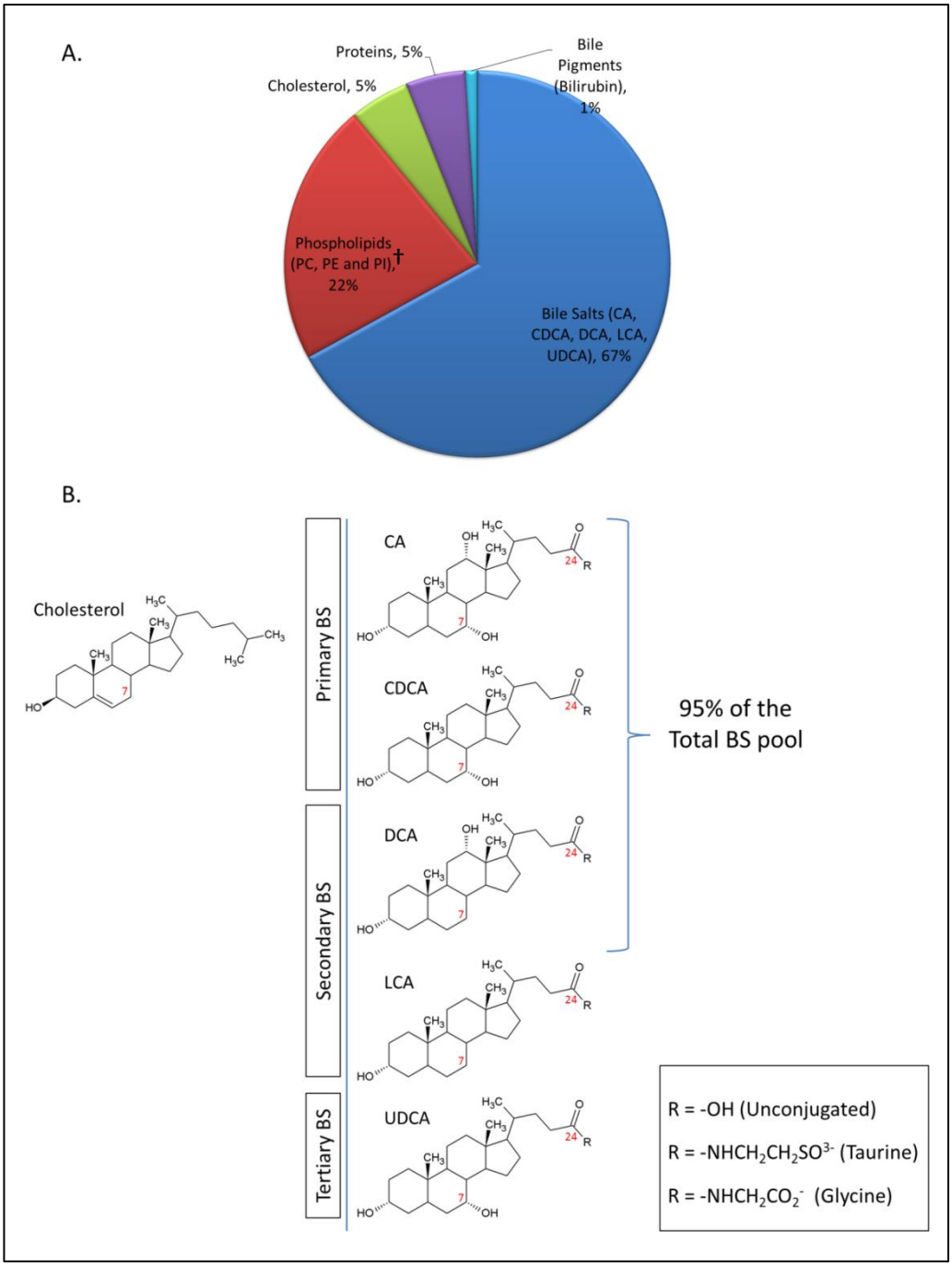

Figure 1-7. ***Solute composition of bile and chemical structure of the major bile salts in healthy humans.***

(A). Organic composition (as weight percentage) of bile in healthy adult humans [modified from (Esteller, 2008)]. † The predominant phospholipid is PC. (B). Chemical structure of the major bile salts (BS) comprising the human BS pool. The 24-carbon *primary* bile acids CA and CDCA are synthesised in the liver from cholesterol. The rate-limiting step is the C_7-hydroxylation of cholesterol, catalysed by the microsomal CYP7A1. *Secondary* bile acids (DCA and LCA) are formed in the gut through the 7 α-dehydroxylation of primary bile acids by bacterial enzymes. Together, CA, CDCA and DCA form 95% of the total BS pool. Epimerisation of the C_7 hydroxyl of CDCA results in the formation of 7-oxolithocholic acid, which is further modified in the liver to form the more polar and hydrophilic *tertiary* bile acid UDCA. The carboxyl group (C_{24}) of 99% of BS is amidated with either glycine or taurine [adopted from (Nicolaou et al., 2012)]. CA, cholic acid; CDCA, chenodeoxycholic acid; DCA, deoxycholic acid; LCA, lithocholic acid; UDCA, ursodeoxycholic acid; R, functional group; PC, phosphatidylcholine; PI, phosphatidylinositol; PE, phosphatidylethanolamine.

of the primary bile salts in the gut (Figure 1-7A). Cholates, deoxycholates, lithocholates, chenodeoxycholates, and ursodeoxycholates are the most common bile salts found in healthy adult humans and comprise 92% - 99% of the total biliary bile salts (Stellaard et al., 1985). In humans two *primary* bile salts termed cholic acid (CA) and chenodeoxycholic acid (CDCA) are synthesised in the hepatocytes using cholesterol as a starting material (Hofmann and Hagey, 2008). This process involves at least 14 different enzyme activities and it begins with a key hydroxylation event catalysed by the cytochrome P450 enzyme, CYP7A1 (cytochrome P450 cholesterol 7α-hydroxylase). The expression of *CYP7A1* is induced by cholesterol (and oxy-sterol metabolites) and repressed by bile salts, providing tight control of bile salt synthesis at this rate-limiting step (Russell, 2003). By the action of the symbiotic gut microflora, *secondary* bile salts are formed from primary bile salts. The major reaction of physiological significance is 7 α-dehydroxylation of primary bile salts to give deoxycholic acid (DCA) and lithocholic acid (LCA) from CA and CDCA, respectively. CA, CDCA and DCA comprise about 95% of the total bile salt pool in humans. The remainder is mostly LCA and the *tertiary* bile salt ursodeoxycholic acid (UDCA; which is formed by the reduction of 7-oxolithocholic acid by intestinal bacteria and is further modified in the liver) (Arias et al., 1994). Bile salts exist mostly in their soluble form in the biliary tree as glycine and taurine conjugates; unconjugated bile salts comprise only 0.1% to 0.4% of the total biliary bile salts (Matoba et al., 1986). Amidation with glycine or taurine at carbon-24 (C_{24}; Figure 1-7B) reduces the pKa such that most bile salts ionised at the low pH present in the biliary tree (Russell and Setchell, 1992). Amidation thus increases their hydrophilicity, making them more effective emulsifying agents, and decreases their toxicity (Hofmann, 2009). It also significantly reduces their ability to diffuse passively across cell membranes, and influx and efflux systems have evolved to ensure sufficient trancellular flux through enterocytes and hepatocytes (Nicolaou et al., 2012).

1.13.4 Regulation of bile salt homeostasis in the hepatocyte

Control of bile salt homeostasis at the genetic level is achieved through a set of nuclear hormone receptors: the farnesoid-X receptor (FXR), the retinoid-X receptor (RXR), the liver receptor homologue-1 (LRH-1), the small heterodimer partner (SHP) and the liver-X receptor (LXR) (Chawla et al., 2000, Russell, 2003). Oxysterols in the liver bind RXR:LXRα heterodimers which in turn up-regulate CYP7A1 expression resulting in an increase in bile salt synthesis (Peet et al., 1998). Increased bile salts in the hepatocyte bind FXR:RXR heterodimers, activating FXR (Makishima et al., 1999), which subsequently induces the transcription of SHP (Goodwin et al., 2000, Lu et al., 2000). SHP downregulates the expression of CYP7A1 and its own expression by binding and inactivating LRH-1 (Goodwin et al., 2000, Lu et al., 2000). ABCB4 and ABCB11 are also targeted by FXR and their induction leads to increased export of bile salts and PC from the hepatocyte (Ananthanarayanan et al., 2001, Huang et al., 2003).

1.13.5 The enterohepatic circulation

The enterohepatic cycle (Figure 1-8), as mentioned above (Section 1.13.3), is very efficient at recovering bile salts. The cycle begins at the canalicular membrane of the hepatocyte where newly synthesised bile salts are effluxed into the canaliculus by the bile salt export pump ABCB11. ABCB11, and its cognate transporters ABCB4 and ATP8B1 that are necessary for bile flow are described in detail below. The bile collects in the gall bladder which, following the ingestion of food contracts and empties its contents into the common bile duct in response to CCK secreted by the mucosal epithelium of the small intestine. To exit the gastrointestinal tract and return to the hepatocyte the bile salts must cross three membranes; the apical and basolateral of the ileocyte, and the basolateral of the hepatocyte (Kullak-Ublick et al., 2004, Meier and Stieger, 2002, Trauner and Boyer, 2003).

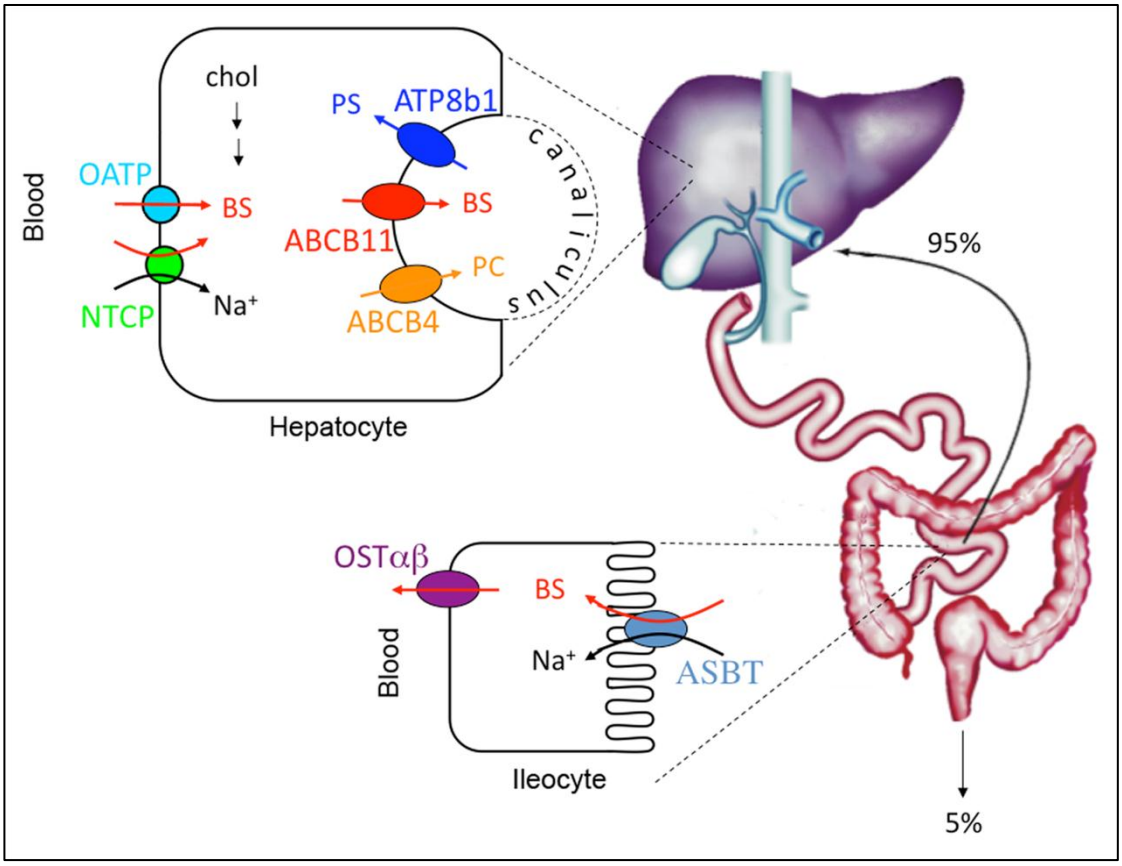

Figure 1-8. ***The enterohepatic recycling of bile salts (BSs).***

Approximately 95% of the secreted BSs are re-absorbed in the enterohepatic cycle. *De novo* synthesis from cholesterol (chol) in the liver replaces the 5% that is lost in the faeces. Newly synthesised BSs are effluxed into the bile canaliculus by the bile salt export pump ABCB11, where they form micelles with phosphatidylcholine (PC) flopped to the outer leaflet of the canalicular membrane by ABCB4. The action of the phosphatidylserine (PS)-flippase ATP8B1 is thought be involved in the maintenance of lipid asymmetry at the canalicular membrane. Once they are secreted into the canaliculus, BSs collect in the gall bladder and are episodically released into the small intestine in response to hormonal signals. In the distal ileum, apical sodium-dependent bile salt transporter (ASBT) imports BSs into the ileocyte in a Na^+-dependent manner. At the basolateral membrane of the ileocyte, BSs are exported by the heterodimeric organic solute transporter OSTα/β into the portal vein and thence to the liver. At the basolateral membrane of the hepatocyte, BSs are imported mainly via the Na^+-dependent taurocholate co-transporting polypeptide (NTCP). Members of the organic anion transporting polypeptides (OATPs) also import BSs via either facilitated diffusion or an antiport mechanism in exchange for bicarbonate or reduced glutathione [adopted from (Nicolaou et al., 2012)].

1.13.5.1 Trans-ileocyte transport of bile salts

Trans-ileocyte transport of BSs (Figure 1-8) involves the apical sodium-dependent bile salt transporter [ASBT; also known as the ileal bile acid transporter (IBAT)]; the cytosolic ileal bile acid binding protein (IBABP); and the basolateral organic solute transporter (a

heterodimer of alpha and beta subunits; OSTα/β) (Dawson et al., 2005, Gong et al., 1994, Hagenbuch and Meier, 2004, Soroka et al., 2010).

ASBT (SLC10A2) is a member of the SLC10 family of solute carriers (Hagenbuch and Dawson, 2004). It is expressed on the apical membrane of the ileocytes lining the distal ileum (Coppola et al., 1998, Hagenbuch and Meier, 2004). ASBT concentrates bile salts in the ileocyte by a symport mechanism driven by the sodium gradient across the apical membrane. Sodium is thus cotransported with the bile salt (the intra-ileocyte sodium concentration is kept low by the Na^+K^+ATPase on the basolateral membrane). Translocation of bile salts through the ileocyte to the basolateral membrane is thought to involve IBABP, which can bind to the intracellular face of ASBT (Gong et al., 1994, Kramer et al., 1995). At the basolateral membrane, OSTα/β exports the bile salts into the portal vein. OSTα/β was first described in the skate *Leucoraja erinacea* (Dawson et al., 2005) before the human homologue was cloned in 2003 (Seward et al., 2003). In humans it is expressed at high levels in a variety of tissues including liver and small intestine and is the primary exporter of bile salts into the systemic circulation (Seward et al., 2003, Soroka et al., 2010). OSTα/β works by facilitated diffusion, transporting bile salts (and other organic solutes and steroids) down their concentration gradients. After secretion into the portal blood, BSs reach the liver where they diffuse into the perisinusoidal space of Disse (Figure 1-6) and come into contact with the basolateral membrane of the hepatocyte.

1.13.5.2 Trans-hepatocyte transport of bile salts

BSs in the portal blood are efficiently taken up from the space of Disse by the hepatocyte's basolateral membrane transporters (Figure 1-8) (Hagenbuch and Meier, 1996). In the basolateral membrane there are both Na^+-dependent and Na^+-independent systems for the uptake of bile salts (Dawson et al., 2009, Kullak-Ublick et al., 2000, Meier and Stieger,

2002, Trauner and Boyer, 2003). The Na^+-dependent taurocholate co-transporting polypeptide [NTCP (SLC10A1), another SLC10 family transporter] is the most important, contributing 80% of the transport capacity and it is only expressed in the basolateral membrane (Hagenbuch and Meier, 1994). NCTP transports both conjugated and unconjugated bile salts (bile salts are commonly deamidated in the intestine by bacteria) into the hepatocyte (Boyer et al., 1994, Hagenbuch and Meier, 1994, Hagenbuch and Meier, 2004, Hata et al., 2003, Kramer et al., 1999, Platte et al., 1996) by symport with sodium ions [with a stoichiometry of 2 × Na^+ ions per bile salt (Schroeder et al., 1998)]. The Na^+-independent system is mediated by the organic anion transporting polypeptides (OATPs) which belong to the SLCO (SLC21) family of solute carriers (Hagenbuch and Dawson, 2004, Kullak-Ublick et al., 2000, Meier, 1995, Trauner and Boyer, 2003). The main human OATPs (OATP1A2, OATP1B1, OATP1B3 and OATP2B1) are expressed at the basolateral membrane of the hepatocyte and primarily transport unconjugated bile salts (Alrefai and Gill, 2007, Hagenbuch and Meier, 2003, Hagenbuch and Meier, 2004, Kullak-Ublick et al., 2000). OATP1A2 is unique in its substrate specificity in that it can also transport organic cations (similar to OSTα/β) (Kullak-Ublick et al., 2001).

Following uptake, the mechanism of translocation through the hepatocyte is not well understood but most likely involves carrier proteins. Several cytoplasmic proteins including glutathione S-transferases, steroid dehydrogenases and fatty acid binding proteins have been shown to have affinity for bile salts but no definitive evidence for a role in intra-hepatocyte transport has been reported (Agellon and Torchia, 2000). In the hepatocyte, the recycled bile salts are added to the pool synthesised *de novo* and delivered to ABCB11 for export across the canalicular membrane.

1.13.5.3 Transport across the canalicular membrane

Our current understanding of this key activity in the intrahepatic cycle stems from 1969, when a rare progressive familial intrahepatic cholestatic (PFIC) disease was first described by Clayton *et al.*, (Clayton et al., 1969) (the condition is still referred to as Byler disease after the eponymous Amish kindred in which it was described). It is now clear that there are at least three primary active transport proteins that are necessary for bile flow across the canalicular membrane, and each gives rise to a different type of autosomal recessive PFIC. All three present similarly as cholestasis early in life, often within the first year (Table 1-2) (Clayton et al., 1969).

	ATP8B1 (OMIM_602397)	ABCB11 (OMIM_603201)	ABCB4 (OMIM_171060)
Alternative names	FIC1	BSEP, SPGP	MDR3
Function	PS-flippase microvillus formation	Bile salt export	PC-floppase
Associated PFIC	Type 1	Type 2	Type 3
Cholestatic onset	1st year – adolescence	1st year – adolescence	1st year- early childhood
Biliary bile acid	Very low, PS present	Absent	Normal but devoid of PC
Serum Bile salts γ-GT ALT Cholesterol	 High Normal Mild Elevation Sometimes elevated	 High Normal Five times normal levels Often elevated	 Normal Raised Five times normal levels Normal
Liver histology	Canalicular cholestasis Granular bile	Giant cell hepatitis	Bile duct proliferation and fibrosis
Pruritus	Severe	Severe	Moderate
Extrahepatic symptoms	Diarrhoea, pancreatitis, hearing loss	None	None
Conditions associated with partial function	BRIC1, ICP	BRIC2, ICP, DIC, CIC, HC	(BRIC3?), ICP, DIC, LPAC, CIC

Table 1-2. ***Diseases associated with mutations in ATP8B1, ABCB11 and ABCB4.***

PFIC, progressive familial intrahepatic cholestasis; PS, phosphatidylserine; PC, phosphatidylcholine; γ-GT, γ-glutamyl transferase; ALT, alanine transaminase; BRIC1/2/3, benign recurrent intrahepatic cholestasis type 1/2/3; ICP, intrahepatic cholestasis of pregnancy; LPAC, low phospholipid-associated cholelithiasis; DIC, drug-induced cholestasis; CIC, contraceptive-induced cholestasis; HC, hepatocellular carcinoma.

Affected individuals absorb dietary fats and fat-soluble vitamins inefficiently, which leads to growth restriction and progressive liver damage caused by increased hepatic and serum levels of bile salts. Affected individuals also commonly have jaundice and intractable pruritus. The condition progresses to end-stage liver disease in the first or second decade.

Characterisation of these patients has allowed the genetic aetiology of PFIC to be determined and the three transporters that are key to bile flow across the canalicular membrane to be identified and characterised. PFIC types 2 and 3 are caused by mutations to the transporters that efflux the two major components of bile; bile salts via ABCB11, and the lipid PC via ABCB4. PFIC1 (Byler Disease) is caused by mutation of ATP8B1, which transports PS in the opposite direction (from the outer to the inner leaflet of the membrane). While PFIC3 patients may be differentially diagnosed by raised serum γ-glutamyl transferase (γ-GT), and immunohistochemistry can be invaluable to establish whether specific transporters are implicated in disease aetiology (Knisely and Gissen, 2010), definitive clinical diagnosis generally requires genetic testing. It is becoming increasingly apparent that there is a spectrum of cholestatic disease caused by mutations in *ABCB11*, *ABCB4* and *ATP8B1*. This ranges from the severe phenotype of PFIC to milder, intermittent forms of cholestasis, e.g. benign recurrent intrahepatic cholestasis (BRIC), drug-induced cholestasis (DIC) or intrahepatic cholestasis of pregnancy (ICP) (Table 1-2).

1.13.5.3.1 ABCB11: the bile salt exporter and the etiological root of PFIC2

In 1991, Nishida *et al.*, described an ATP-dependent system for the transport of taurocholate in canalicular membrane vesicles derived from rat liver (Nishida et al., 1991). This observation was soon confirmed by three other groups (Adachi et al., 1991, Muller et al., 1991, Stieger et al., 1992) and a low stringency hybridisation screen on pig liver cDNA identified a novel gene with high sequence identity to the human drug efflux pump ABCB1 (described in more detail above). This new gene was eventually renamed *Abcb11* [earlier names include sister of Pgp (*spgp*), and bile salt export pump (*Bsep*)] (Childs et al., 1995). Successful cloning of the full-length rat homologue showed that *Abcb11* could function *in vitro* as a bile salt efflux transporter in the presence of ATP, and northern blot analysis revealed that it was primarily expressed in the liver (Gerloff et al., 1998). Positional cloning

of the human orthologue was then correlated with a set of mutations linked to PFIC2 (Strautnieks et al., 1998). This established ABCB11 as the main bile salt export pump in the human liver and mapped the *ABCB11* gene to chromosome 2q24. Expression of the 140-150 kDa human ABCB11 in insect cells confirmed its ability to transport bile salts in an ATP-dependent manner, with an apparent affinity for different bile salts that reflects the composition of the bile salt pool in humans (Byrne et al., 2002, Noe et al., 2002). Knock-out mice deficient for *Abcb11*, develop intrahepatic cholestasis, but the phenotype is less severe than in PFIC2 patients (Wang et al., 2001). This is considered to be due to the less toxic nature of the murine bile salt pool and the compensatory up-regulation of other ABC transporters. In *Abcb11*$^{-/-}$ mice there is a dramatic decrease in the export of cholic acid but the total output of bile salts is only slightly reduced (Wang et al., 2001). This unexpected observation was later shown to be due to the up-regulation of *Abcb1a*, which could apparently function as bile salt transporter in the absence of *Abcb11* (Lam et al., 2005). However, no compensatory increase in *ABCB1* mRNA has been observed in PFIC2 patients (Keitel et al., 2005).

ABCB11 mutations have been reported in patients with PFIC2 and benign recurrent intrahepatic cholestasis type 2 or BRIC2 (Byrne et al., 2009, Byrne et al., 2002, Chen et al., 2002, Goto et al., 2003, Jansen et al., 1999, van Mil et al., 2004). Biochemically, PFIC2 is characterised by normal γ-GT and normal cholesterol levels in the serum but very low biliary bile salts (Davit-Spraul et al., 2009, Morotti et al., 2011). BRIC2 develops usually after the first decade and can progress into PFIC2 although it is normally episodic and benign (Lam et al., 2006, Noe et al., 2005, van Mil et al., 2004). Mutations in *ABCB11* have also been linked to ICP (Dixon et al., 2009), DIC (Keitel et al., 2006, Lang et al., 2006, Pauli-Magnus et al., 2004b, Pauli-Magnus et al., 2005) and contraceptive-induced cholestasis (CIC) (Meier et al., 2008). The association of genetic variation in *ABCB11* with

ICP and CIC prompted research into the mechanisms by which reproductive hormones can impair ABCB11 function. Two sulphated progesterone metabolites have been demonstrated to trans-inhibit efflux of bile acids by ABCB11 in an oocyte model system (Vallejo et al., 2006). Furthermore, oestrogen 17β-glucuronide has also been demonstrated to trans-inhibit ABCB11 in an SF9 cell vesicle system (Stieger et al., 2000). Many of the *ABCB11* SNPs described have since been shown to affect mRNA splicing, protein stability and/or protein function *in vitro* (Byrne et al., 2009). *ABCB11* deficiency is also associated with hepatocellular carcinoma in young children (Knisely et al., 2006).

1.13.5.3.2 ABCB4: The PC flopper and the etiological root of PFIC3

ABCB4 was first cloned in 1987 by Van der Bliek *et al.* from a human liver cDNA library and named *MDR3*, due to its high degree of similarity with the third hamster "multidrug resistance" (*Mdr*) gene (Van der Bliek et al., 1987). The *ABCB4* gene locus spans 74kb on chromosome 7q21.1 and gives four alternatively spliced transcripts (Lincke et al., 1991). The high level of expression in the canalicular membrane suggested an important role for *ABCB4* in the liver (Buschman et al., 1992), which was later confirmed by the generation of *Abcb4*$^{-/-}$ mice (Smit et al., 1993). Mice deficient in *Abcb4* developed severe liver disease characterised by a complete absence of PC from the bile. Analysis of fibroblasts from transgenic mice showed that Abcb4 flops PC from the inner to the outer leaflet of the plasma membrane (Smith et al., 1994). The human orthologue was cloned and also shown to translocate PC specifically, across the plasma membrane (van Helvoort et al., 1996) and, when knocked-in to *Abcb4*$^{-/-}$ mice, human *ABCB4* rescued PC excretion into the bile (Smith et al., 1998). In the absence of ABCB4, the detergent activity of bile salts transported into the bile by ABCB11 can solubilise cell membranes resulting in biliary toxicity (Donovan et al., 1991). Homozygous mutation of *ABCB4* causes PFIC3, which presents within the first few years of age with pruritus, jaundice and growth restriction

(Oude Elferink and Groen, 2002, Pauli-Magnus et al., 2005). Liver histology reveals portal fibrosis, which can progress to cirrhosis and ductular proliferation that eventually leads to end-stage liver disease (Davit-Spraul et al., 2009, Morotti et al., 2011). Biochemically, PFIC3 can be distinguished from PFIC1 and 2 by high levels of γ-GT in the serum and complete absence of PC from the bile (Jacquemin et al., 2001).

It is becoming increasingly apparent that mutations of *ABCB4* are associated with a spectrum of cholestatic diseases. These overlap with *ABCB11* phenotypes and include ICP (Mullenbach et al., 2003), DIC (Oude Elferink and Paulusma, 2007), CIC and low phospholipid associated cholelithiasis [(LPAC), a form of cholesterol gallstone disease (Rosmorduc et al., 2001)]. Recently, missense mutations in *ABCB4* have also been reported in two heterozygous patients with cholangiocarcinoma (a malignant tumour in the biliary tract) in two unrelated families (Tougeron et al., 2012). Together, these conditions suggest that *ABCB4*-dependent hepatobiliary disease is common. ICP (also known as obstetric cholestasis) presents in the third trimester of pregnancy when oestrogen levels reach their peak (Dixon et al., 2009, Eloranta et al., 2002, Gendrot et al., 2003, Jacquemin et al., 1999, Mullenbach et al., 2003). Symptoms include severe pruritus and abnormal bile flow in the mother, which resolve rapidly after delivery. ICP carries a significant increased risk of adverse pregnancy outcome and intrauterine death, and affects 0.6% of births in the British Caucasian population. In LPAC, female gender and parity (in agreement with the influence of oestrogens in bile flow, as suggested for ICP) are among the major risk factors. LPAC patients often also present with raised serum γ-GT, further implicating ABCB4.

In 2004, 18 mutations in *ABCB4* had been associated with PFIC3 and 30 mutations were linked to induced cholestatic disease, but often only in single or few families (Pauli-Magnus et al., 2004b). These include 11 and 16 SNPs, respectively, which encode non-synonymous

changes in the protein sequence. The effects of these SNPs on protein trafficking, function and response to inducing agents, have not been characterised, so the causal conjunction between *ABCB4* SNPs remains to be definitively proved for some hepatobiliary diseases (particularly the induced forms with a complex aetiology).

Some insights into the functional consequences of *ABCB4* mutation have been obtained by two groups which have used the closest homologue of ABCB4, ABCB1, to express and characterise the effect of mutations identified in patients (Delaunay et al., 2009, Dixon et al., 2000). This was achieved by mimicking clinically-relevant mutations in the multidrug resistance *ABCB1* and measuring the effect on ABCB1 expression and drug efflux. However, this approach is limited and only relevant if the particular amino acid is conserved in both proteins and performs the same function. This rules out the study of amino acid changes that directly influence PC binding or efflux, or responses to hormones of pregnancy, contraceptives or other drugs. Biochemical characterisation of *ABCB4* SNPs directly has, hitherto, been difficult for two reasons: the technical difficulty of measuring the flux of PC from the inner to the outer leaflet of the plasma membrane; and because expression of functional PC floppase, transiently *in vitro*, appears to be deleterious to cells and leads to cell death. These difficulties have now been overcome and this new data has coincidentally shed some light on why ATP8B1 is needed in the canalicular membrane [see below (Groen et al., 2011)].

1.13.5.3.3 ATP8B1 (FIC1): The PS flipper and the etiological root of PFIC1

Surprisingly, mutation of neither *ABCB11* nor *ABCB4*, which transport the two major components in bile, could explain the original Byler family PFIC pedigree. The third transport protein that appears to be necessary for bile flow across the canalicular membrane was not discovered until 1998, when Laura Bull identified the *ATP8B1* gene on

chromosome 18q21 by positional cloning (Bull et al., 1998). ATP8B1 (also known as FIC1) is a P-type ATPase which functions in complex with the accessory protein CDC50A (Paulusma et al., 2008). ATP8B1 moves a different membrane phospholipid, PS, in the opposite direction to the transport of PC by ABCB4. PS is generally restricted to the inner leaflet of the plasma membrane and so is not normally exposed at the cell surface. There are three lines of evidence in support of PS-flippase activity for ATP8B1: (a) loss of ATP8B1 activity reduces bile flow but causes the appearance of PS in the residual flow; this is also true of *Atp8b1*-deficient mice following taurocholate infusion (Paulusma et al., 2006); (b) fluorescently-labelled PS analogues are internalised by UPS-1 cells following transient expression of ATP8B1 (Paulusma et al., 2008, Ujhazy et al., 2001); and (c) the same cells show reduced binding of annexin-V when added extracellularly (annexin-V has a high affinity for native PS when the PS headgroup is exposed on the cell surface).

ATP8B1-deficiency is linked to several cholestatic liver diseases, PFIC1 and BRIC1 (Bull et al., 1998), and ICP (Mullenbach et al., 2005, Painter et al., 2005). PFIC1 is by far the most severe (Klomp et al., 2004). Scanning electron micrographs of bile from patients reveals coarse granules [sometimes called "Byler bile" (Clayton et al., 1969)]. Histological examination of early liver biopsies revealed relatively mild liver damage, compared to PFIC2 and PFIC3, with lobular architecture largely preserved and an absence of giant cells (Clayton et al., 1969). Signs of cholestasis are, in fact, largely confined to the canaliculi (Clayton et al., 1969). In keeping with these observations, serum levels of hepatic enzymes γ-GT and ALT, are only mildly elevated in patients with PFIC1. Nevertheless, the common outcome is cirrhosis and end-stage liver disease within the second decade. The presence of ATP8B1 at apical membranes of pancreatic acinar cells, enterocytes of the ileum and jejunum, and cochlear hair cells of the inner ear means that PFIC1 is a pleiotropic condition. Extrahepatic symptoms include intractable diarrhoea (Lykavieris et al., 2003),

sensorineural hearing loss (Stapelbroek et al., 2009) and, in a few cases, pancreatitis (Tygstrup et al., 1999).

BRIC1 is also associated with *ATP8B1* (Klomp et al., 2004). Affected individuals present with episodic bouts of cholestasis, pruritus and extrahepatic symptoms such as diarrhoea, which may last days, weeks or months but is not progressive. It is considered benign because no lasting liver damage occurs and, during remission, patients are biochemically normal. However, as is the case with PFIC1, pruritus can be very severe during cholestatic episodes and some patients have elected for liver transplantation in order to improve quality of life (EASL, 2009). Initial onset of BRIC1 generally occurs early in childhood and episodes can occur multiple times within a single year, although there is considerable variation and some patients remain in remission for a decade or more (Tygstrup et al., 1999). Triggers of cholestatic episodes are not well defined but there is anecdotal correlation with viral infection and use of the contraceptive pill (de Pagter et al., 1976, Tygstrup et al., 1999). BRIC1 is less severe than PFIC1 and it is presumed that the mutations associated with BRIC1 have a milder impact on protein function, although this has not been demonstrated definitively.

1.13.6 Are the functions of ABCB4 and ATP8B1 complementary?

It is well established that the phospholipids in the plasma membrane are arranged asymmetrically. For example, the sphingolipids and PC are enriched in the outer leaflet, while phosphatidylethanolamine (PE), phosphatidylinositol (PI) and PS are enriched in the inner leaflet (Figure 1-9). This lipid asymmetry and the high concentration of sphingolipids and cholesterol in the outer leaflet is thought to influence the lipid packing, fluidity and barrier function (Elliott et al., 2005, van Meer et al., 2008), and is particularly important at the canalicular membrane which is essentially under attack from bile salts that are effluxed

into the canaliculus by ABCB11. ABCB4 flops excess PC into the outer leaflet, which might be expected to destabilise the bilayer but is extracted into the bile by the detergent activity of the bile salts. ABCG5 and ABCG8 also efflux cholesterol into the bile, presumably for the same purpose: to form a bile salt/lipid mixed micelle and reduce the detergent nature of the bile salt. If a PS flippase is important for bile flow one must expect PS to appear in the outer leaflet. The lipid and bile salt traffic at the canalicular membrane means that it is in a continuous state of flux and the ensuing instability may allow PS to flop spontaneously into the outer leaflet. Alternatively, it is possible that PS is flopped by ABCB4 directly, although there is no evidence for this because analogues of PS were not tested in the most comprehensive study of ABCB4 substrate specificity (van Helvoort et al., 1996). Whichever the explanation, the presence of PS in the outer leaflet will, along with the excess of PC flopped by ABCB4, dilute the relative concentration of sphingolipids and cholesterol, thus prevent the leaflet from forming a liquid crystalline phase. This would render the canalicular membrane more sensitive to detergent solubilisation. This has led to the suggestion that ATP8B1 is required to re-internalise the flopped PS to maintain the liquid crystalline order of the canalicular membrane. In the *ATP8B1*-deficient state this does not happen and the membrane is progressively damaged by the liver's own metabolites.

Is there any evidence to support this theory? Data from our own lab and from the lab of our collaborator Ronald Oude Elferink strongly suggests that ATP8B1 is critically important to cell survival when ABCB4 is present.

It was observed that transient expression of ABCB4 in HEK293T (human embryonic kidney 293T) cells was deleterious to the integrity of the membrane and cell survival [cells became leaky and released the cytoplasmic enzyme lactate dehydrogenase (LDH) into the

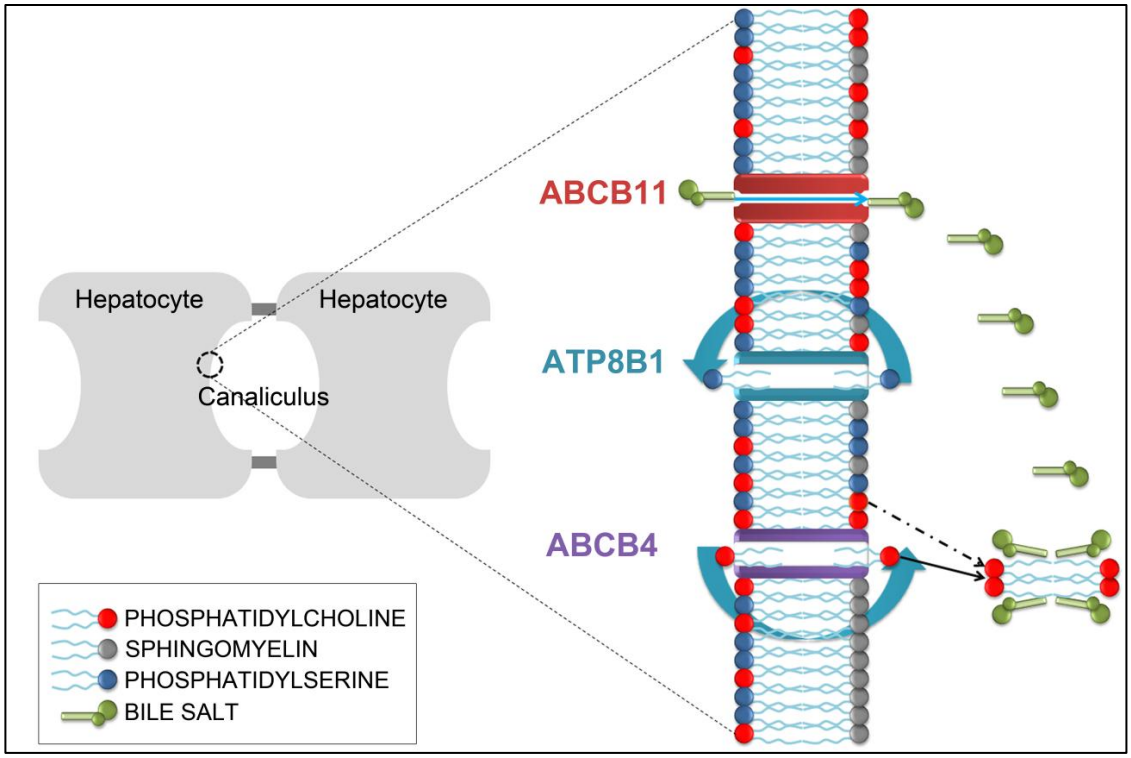

Figure 1-9. ***Maintenance and role of lipid asymmetry at the canalicular membrane.***

Lipid asymmetry at the plasma membrane is known to be important for barrier function. Bile salts are exported into the bile canaliculus by ABCB11. The PC floppase ABCB4 flops PC into the outer leaflet of the canalicular membrane, where it is extracted into the bile by bile salts. Flopping of excess PC destabilises the canalicular membrane, causing PS to flop spontaneously into the outer leaflet (alternatively, ABCB4 may flop PS directly). The dilution of sphingomyelin in the outer leaflet induces a liquid disordered phase and renders the canalicular membrane more sensitive to detergent solubilisation. The PS flippase ATP8B1 is therefore required to flip PS back into the inner leaflet of the canalicular membrane to maintain its liquid crystalline order (adapted from Nicolaou et al., 2012).

culture medium; (Figure 1-9A)] (Groen et al., 2011). ABCB4 protein level in the transiently-transfected cells was therefore low (Figure 1-9B). However, LDH release could be attenuated and ABCB4 expression rescued when ATP8B1 (and its cofactor CDC50A) was co-expressed. These cells co-expressing the PC floppase and the PS flippase were able to secrete PC in a bile salt-dependent manner (Figure 1-9C). Consistent with this observation, double knock-out mice that lacked expression of *Abcb4* and *Atp8b1* had a milder phenotype than *Atp8b1*-deficient mice suggesting that the phenotype of the latter was at least in part due to the cytotoxic effect of unchecked Abcb4 activity on the integrity of the canalicular membrane (Groen et al., 2011).

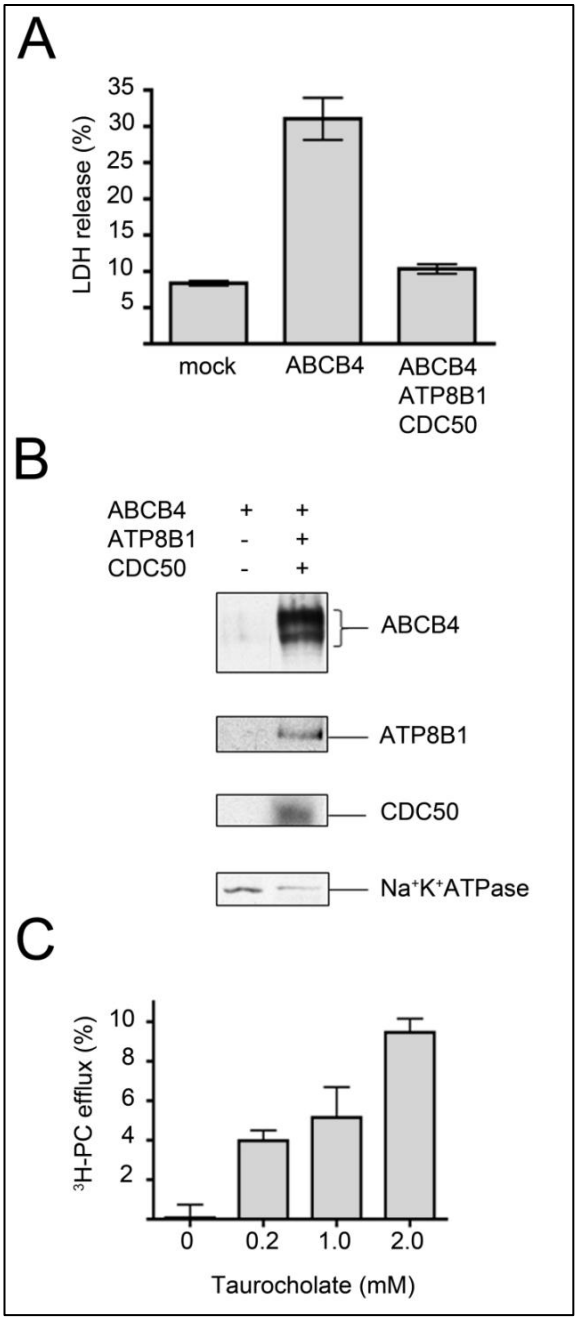

Figure 1-10. ***ATP8B1 is necessary for functional expression of ABCB4.***

(A). ABCB4 expression alone in HEK293T cells is cytotoxic causing lactate dehydrogenase (LDH) to be released from the cells. This is rescued by co-expression of ATP8B1 and CDC50A. (B). Western analysis showing that transient expression of the ABCB4 PC floppase is only tolerated when the ATP8B1/CDC50A PS flippase is co-expressed. (C). Cells co-expressing the PC floppase and PS flippase can efflux PC to added taurocholate [adapted from (Groen et al., 2011)].

1.13.7 Functional studies of ABCB4 *in vitro*

As described in Section 1.13.5.3.2, many mutations have been reported which implicate ABCB4 malfunction in a spectrum of cholestatic disease. This ranges from the most severe

phenotype, PFIC3, to the milder, intermittent forms of cholestasis, e.g. BRIC, DIC or ICP (Table 1-2). Although in PFIC3 the link between mutation and disease is clear, in the majority of liver diseases the underlying causes are complex and include diet, physiological conditions such as pregnancy or therapeutic drug use, as well as genetics. In these cases, association with particular mutations in ABCB4 is suspected but not proved. To investigate the aetiology of cholestatic liver disease, I have introduced suspected disease-causing mutations into the recombinant transporter for transient expression in HEK293T cells (in the presence and absence of the ATP8B1/CDC50A PS flippase). ABCB4 expression and trafficking was monitored by western analysis and confocal microscopy, and function was measured by ^{3}H- PC efflux to bile salts added to the culture medium. By mimicking the situation at the canalicular membrane, an initial characterisation of mutant ABCB4 that are associated with cholestatic liver disease has been achieved and reported in chapters 4 and 5 of this thesis.

1.14 Aims

The aims of the two projects described in this report are listed below.

1.14.1 Project 1 (ABCB1)

The overall aim of Project 1 was to employ the SU-YTH system in yeast to identify proteins that interact with ABCB1 and, ultimately, to study their effects on its localisation or its ability to efflux drugs.

1.14.2 Project 2 (ABCB4)

The aim of Project 2 was to use a transient expression system in which ABCB4 is co-expressed with the ATP8B1/CDC50A PS flippase in HEK293T cells to investigate the aetiology of cholestatic liver disease at the molecular level.

Chapter Two

2 Materials and Methods

2.1 Cell strains

The yeast (NMY51), bacterial (XL10-Gold®) and mammalian (HEK293T) cell strains used in this investigation are outlined below.

2.1.1 NMY51 yeast reporter strain

MATa his3Δ200 trp1-901 leu2-3, 112 ade2 LYS2::$(lexAop)_4$-HIS3 ura3::$(lexAop)_8$-lacZ ade2::$(lexAop)_8$-ADE2 GAL4

2.1.2 XL10-Gold® Ultracompetent *E. coli* cells

Tet^r Δ (mcrA)183 Δ(mcrCB-hsdSMR-mrr)173 endA1 supE44 thi-1 recA1 gyrA96 relA1 lac Hte [F´ proAB $lacI^qZ\Delta M15$ Tn10 (Tet^r) Amy Cam^r]

2.1.3 HEK293T mammalian cells

Human embryonic kidney 293 cells (Graham et al., 1977) stably and constitutively expressing the SV40 large T antigen (HEK293T) allowing for the expression of transfected plasmids containing the SV40 origin of replication were obtained from the Imperial Cancer Research Fund, cell production unit.

2.2 Plasmids

The vectors used for the transformation of yeast and bacteria as well as the transfection of mammalian cells are described in Table 2-1.

Vector	Auxotrophic Marker (Yeast)	Resistance Marker (*E. Coli*)	Source
SU-YTH Bait Vectors			
pBT3-N	*LEU2*	Kanamycin	Dualsystems Biotech
pBT3-N:CD36	*LEU2*	Kanamycin	J. Wharton, London
pBT3-N:FATP4	*LEU2*	Kanamycin	J. Wharton, London

Table 2-1. ***List of vectors used in the investigation.***

Vector	Auxotrophic Marker (Yeast)	Resistance Marker (*E. Coli*)	Source
SU-YTH Library Vectors			
pPR3-STE	*TRP1*	Ampicillin	Dualsystems Biotech
pPR3-N (NubG-X)	*TRP1*	Ampicillin	Dualsystems Biotech
pDL2xN-SUC (X-NubG)	*TRP1*	Ampicillin	Dualsystems Biotech
pDL2xN-STE (X-NubG)	*TRP1*	Ampicillin	Dualsystems Biotech
SU-YTH Control Prey Vectors			
pCCW-Alg5p	*LEU2*	Kanamycin	Dualsystems Biotech
pAI-Alg5 (NubI)	*TRP1*	Ampicillin	Dualsystems Biotech
pDL2-Alg5 (NubG)	*TRP1*	Ampicillin	Dualsystems Biotech
pPR3-STE:Caveolin	*TRP1*	Ampicillin	J. Wharton, London
pPR3-STE:PKCα	*TRP1*	Ampicillin	This study
Cloning Vectors			
pGEM3®-3Zf(-)		Ampicillin	Promega
pGEM3®-3Zf(-):PKCα Vector			
pGEM3®-3Zf(-):PKCα		Ampicillin	This study
PKCα-GFP Vector			
EGFP-PKCα(cDNA)			A. Sardini, London
ABCB4			
pcDNA3.1-ABCB4wt		Ampicillin	Groen *et al.* (2011)
pcDNA3.1-G535D		Ampicillin	This study
pcDNA3.1-M301T		Ampicillin	This study
pcDNA3.1-E528D		Ampicillin	This study
pcDNA3.1-L591Q		Ampicillin	This study
pcDNA3.1-P1161S		Ampicillin	This study
pcDNA3.1-R545C		Ampicillin	This study
pcDNA3.1-A286V		Ampicillin	This study
pcDNA3.1-S320F		Ampicillin	M. Rodriguez-Romero, London
pcDNA3.1-A546D		Ampicillin	M. Rodriguez-Romero, London
pcDNA3.1-E558Q		Ampicillin	Groen *et al.* (2011)
ATP8B1			
pCI-neo-ATP8B1		Ampicillin	Groen *et al.* (2011)
CDC50A			
pCI-neo-CDC50		Ampicillin	Groen *et al.* (2011)
CFP/GFP/YFP			
pECFP-C1		Kanamycin	Clontech
pEGFP-C1		Kanamycin	Clontech
pEGFP-C1		Kanamycin	Clontech

Table 2-1. ***(continued) List of vectors used in the investigation.***

2.3 Primer list

A list of the oligonucleotides used in this investigation is provided in Table 2-2.

Name	Sequence (5' – 3')	Source
Mutagenic Primers		
pGEM3®-3Zf(-):PKCα		
***Pci*I-F:PKCα**	CGGGTGCTGGTGACATGTCTGACGTTTTCCC	Sigma-Aldrich
***Age*I-R:PKCα**	CGCTGGTGAGTTTCAACCGGTACTCTGTAAGAT	Sigma-Aldrich
pcDNA3.1-ABCB4		
G535D	GCCCAGCTGAGTG**A**TGGGCAGAAGCAG	Sigma-Aldrich
M301T	AAAAAGCTATTTCAGCAAACATTTCCA**C**GGGTATTGCCTTCC	Sigma-Aldrich
E528D	GACACCCTGGTTGGAGA**C**AGAGGGGCC	Sigma-Aldrich
L591Q	CCACCATTGTGATAGCACACCGAC**A**ATCTACGG TCCGAAATGCAG ATGTC	Sigma-Aldrich
P1161S	GCCAACATACATCCTTTCATCGAGACGTTG**T**CCCACAAATATGAAA	Sigma-Aldrich
R545C	GGATCGCCATTGCA**T**GTGCCCTGGTTCGC	Sigma-Aldrich
A286V	GAAAGGTATCAGAAACATTTAGAAAATG**T**CAAAGAGATTGGAATTAAAAA AGCTATT	Sigma-Aldrich
S320F	CTGGCCTTCTGGTATGGAT**T**CACTCTAGTCATATCAAA	Sigma-Aldrich
A546D	CGCCATTGCACGTG**A**CCTGGTTCGCAACC	Sigma-Aldrich
E558Q	GATCCTTCTGCTGGAT**C**AGGCGACGTCAGCATTGGAC	Sigma-Aldrich
Sequencing Primers		
pGEM3®-3Zf(-):PKCα		
PKCaR1	AGACGCCGTGGAGTCGTT	A. Sardini
PKCaF1	TGCACGAGGTGAAGGACC	A. Sardini
PKCaF2	GTCTGTAGAAAATCTGGG	A. Sardini
PKCaF3	GATAACGTCATGTTGGAT	A. Sardini
PKCaF4	GCTAACATAGACCAGTCT	A. Sardini
pEGFP-C1F1	TCCTGCTGGAGTTCGTGACC	A. Sardini
pUC/M13F	CGCCAGGGTTTTCCCAGTCACGAC	Promega
pUC/M13R	TCACACAGGAAACAGCTATGAC	Promega
pcDNA3.1-ABCB4		
ABCB4_389F	GATTGGGTGCTGGAGTTCTTGTTG	Sigma-Aldrich
ABCB4_918F	CATTTCCATGGGTATTGCCTTCCTG	Sigma-Aldrich
ABCB4_1440F	GGTGTGGTGAGTCAGGAGCCGGTG	Sigma-Aldrich
ABCB4_1983F	GCCCCAAATGGCTGGAAATCTCGC	Sigma-Aldrich
ABCB4_2473F	CTTGCCACAGATGCTGCCCAAGTCC	Sigma-Aldrich
ABCB4_2981F	CTCTAGGACATGCCAGTTCATTTGC	Sigma-Aldrich
ABCB4_3393F	CTGCAGC ATTGCCGAGAATATTGCC	Sigma-Aldrich
ABCB4_491R	CAGTGGTGTCATTGATGTCAAACC	Sigma-Aldrich
pPR3-N, pDL2xN-SUC, pDL2xN-STE		
pNubGx	GTCGAAAATTCAAGACAAGG	Sigma-Aldrich
pDSL-Nx	GTAAGCGTGACATAACTAATTACATG	Sigma-Aldrich

Table 2-2. ***List of primers used in the investigation.***

The underlined and emboldened letters indicate the single nucleotide change introduced to the WT ABCB4 coding sequence.

2.4 Yeast transformation solutions and reagents

All yeast transformation solutions were prepared by dissolving the reagents listed in the tables below in the appropriate volume of sterile water. Following preparation, the solutions were passed through a sterile filter (0.2 μm) and stored at room temperature. PEG (poly[ethylene glycol]) and LiAc (Lithium acetate dehydrate) were aliquoted in 50 ml Falcon tubes (SLS, UK), capped tightly and sealed with Parafilm "M" to avoid evaporation. It is crucial to avoid evaporation as the concentration of these reagents is a very critical parameter to achieve good transformation efficiency. Single-stranded (SS) carrier DNA from salmon sperm was prepared by dissolving 200 mg of salmon sperm DNA type III sodium salt (Sigma-Aldrich, UK; D1636) in 100 ml sterile water (2 mg ml^{-1} stock) into a 250 ml sterile glass beaker. Initially the large chunks of DNA were dissolved by pipetting up and down with a 25 ml sterile strippette (Corning Inc., UK) followed by continuous stirring for 2 – 3 hours at RT (room temperature) until all DNA was dissolved. Subsequently, the DNA was aliquoted into sterile 1.5 ml eppendorf test tubes (Eppendorf, UK), boiled on a hot block (DRI Block® DB.2A; Techne LTD, UK) for 5 min at 99°C and immediately chilled in an ice/water bath before being stored at -20°C. For small-scale transformations the SS DNA was thawed and used directly. For large-scale transformations the SS DNA was thawed on ice, boiled again at 99°C for 5 min, chilled immediately on an ice/water bath and kept on ice until required.

50% PEG (Poly[ethylene glycol])		
Reagent	For 100 ml	Source
PEG 4000	50 g	Sigma-Aldrich
dH_2O	80ml	

1 M LiAc (Lithium acetate dihydrate)		
Reagent	For 100 ml	Source
LiAc dihydrate	10.2 g	Sigma-Aldrich
dH_2O	to 100 ml	

10 × TE (Tris-EDTA), pH 7.5		
Reagent	For 1 L	Source
Tris-Cl pH 7.5 (1 M)	100 ml	Sigma-Aldrich
EDTA pH 7.8 (0.5 M)	20 ml	Sigma-Aldrich
dH_2O	to 1 L	

2.5 Yeast media

All selective defined (SD) media were prepared using synthetic drop-out mix lacking *Trp* (tryptophan), *Leu* (leucine), *His* (histidine) and *Ade* (adenine) and supplemented with the appropriate amino acid where appropriate. Amino acid stocks were prepared as summarised in the table below, passed through a sterile filter (0.2 μm) and kept at 4°C for up to one month. All yeast growth media, after preparation, were autoclaved for 15 min at 121°C and kept at room temperature. Yeast agar plates (90 mm) containing SD or growth (YPAD) media were prepared using aseptic techniques and stored at 4°C for up to two weeks. Prior to use, plates were dried and equilibrated at 30°C in an incubator (Sanyo, UK).

SD Plates			
Supplement	Amount/Litre	Final Concentration	Source
Yeast Nitrogen base without amino acids	6.7 g	0.7 %	ForMedium™
Dropout Mix	0.6-0.7 g	0.1 %	ForMedium™
D – (+) Glucose	20 g	2 %	Sigma-Aldrich
Bacto agar	20 g	2 %	BD Biosciences
dH_2O	to 1 L		

SD medium (liquid)			
Supplement	Amount/Litre	Final Concentration	Source
Yeast Nitrogen base without amino acids	6.7 g	0.7 %	ForMedium™
Dropout Mix	0.6-0.7 g	0.1 %	ForMedium™
D – (+) Glucose	20 g	2 %	Sigma-Aldrich
dH_2O	to 1 L		

YPAD Plates			
Supplement	Amount/Litre	Final Concentration	Source
Bacto Yeast extract	10 g	1 %	BD Biosciences
Bacto peptone	20 g	2 %	BD Biosciences
D – (+) Glucose	20 g	2 %	Sigma-Aldrich
Bacto agar	20 g	2 %	BD Biosciences
Adenine Sulphate	40 mg	0.004 %	Sigma-Aldrich
dH_2O	to 1 L		

YPAD medium (liquid)			
Supplement	Amount/Litre	Final Concentration	Source
Bacto Yeast extract	10 g	1 %	BD Biosciences
Bacto peptone	20 g	2 %	BD Biosciences
D – (+) Glucose	20 g	2 %	Sigma-Aldrich
Adenine Sulphate	40 mg	0.004 %	Sigma-Aldrich
dH_2O	to 1 L		

2× YPAD medium (liquid)			
Supplement	Amount/Litre	Final Concentration	Source
Bacto Yeast extract	20 g	2 %	BD Biosciences
Bacto peptone	40 g	4 %	BD Biosciences
D – (+) Glucose	40 g	4 %	Sigma-Aldrich
Adenine Sulphate	40 mg	0.004 %	Sigma-Aldrich
dH_2O	to 1 L		

Amino Acid stocks				
Amino Acid	Stock	Amount/Litre	Final Concentration	Source
Tryptophan	10 g/L	2 ml	0.02 g/L	Sigma-Aldrich
Histidine	10 g/L	2 ml	0.02 g/L	Sigma-Aldrich
Leucine	10 g/L	10 ml	0.1 g/L	Sigma-Aldrich
Adenine	5 g/L	8 ml	0.04 g/L	Sigma-Aldrich

2.5.1 FK506 YPAD yeast agar plates

A stock solution of 10 mg ml^{-1} FK506 (Sigma-Aldrich, UK) was prepared in ethanol (Sigma-Aldrich, UK) containing 10% (v/v) Tween 20 (Sigma-Aldrich, UK).

YPAD agar plates containing FK506 at various concentrations (0, 5, 10, 20, 25, 30, 40, 50 and 100 μg ml^{-1}) were prepared by adding the appropriate volume of FK506 from the stock solution to 15 ml of YPAD agar equilibrated to 50°C before pouring into 3 cm petri dishes (Fisher Scientific, UK). Control YPAD plates lacking FK506 were also prepared which contained ethanol supplemented with Tween 20 at the same concentrations as FK506.

2.5.2 3-AT (3-amino-1,2,4-riazole) SD yeast agar plates

Where necessary yeast cells were grown on basic selection plates (either SD-*Trp-Leu-His* or SD-*Trp-Leu-His-Ade*) supplemented with 0, 1, 2.5, 5, 7.5 and 10 mM 3-AT (a competitive inhibitor of the *HIS3* gene product).

A stock solution of 1.0 M (final concentration) 3-AT was prepared by dissolving 8.4 g of 3-AT (Sigma-Aldrich, UK) in 100 ml sterile water by vortexing (Vortex Genie 2; Scientific Industries Inc., Bohemia, NY). The 100 ml stock solution was stored at -20°C in 10 ml aliquots. SD-agar plates containing 3-AT at the stated concentrations were prepared by adding the 3-AT from the stock solution (thawed on ice) to 100 ml of either SD-*Trp-Leu-His* or SD-*Trp-Leu-His-Ade* liquid medium, equilibrated at 50°C, before pouring into the 150 mm Petri dishes (VWR, Radnor, PA).

2.6 Bacterial media

Bacterial media [LB (Lysogeny broth) liquid medium and LB agar] were prepared by suspending 20 g of LB powder, Lennox (Fisher Scientific Ltd, UK; BPE1427-500) in 1 L of sterile water and autoclaved for 15 min at 121°C. For LB-agar plates, the medium was supplemented with 1.5% (w/v) bacto agar (BD Biosciences, UK) prior to autoclaving. Where necessary, the medium was allowed to cool down to 55°C before the appropriate antibiotic (100 μg ml^{-1} ampicillin) was added. For "blue/white" screening of recombinant constructs, 80 μg ml^{-1} X-gal (5-bromo-4-chloro-3-indolyl-beta-D-galactopyranoside, Fermentas, UK) and 20 mM IPTG (Isopropyl 1-thio-β-D galactopyranoside; Fisher Scientific Ltd, UK) were also added at this stage. LB-agar plates were prepared using aseptic techniques and stored at 4°C for up to one month. Prior to use, plates were dried and equilibrated at 37°C in an incubator (Sanyo, UK).

2.6.1 S.O.C. rich medium

2% tryptone, 0.5% yeast extract, 10 mM NaCl, 2.5 mM KCl, 10 mM $MgCl_2$, 10 mM $MgSO_4$, 20 mM glucose (Invitrogen, UK; 15544-034).

2.6.2 LB (Liquid)

1% (w/v) NaCl, 1% (w/v) tryptone, 0.5% (w/v) yeast extract (Fisher Scientific Ltd, UK; BPE1427-500).

2.6.3 LB-Agar (Plates)

1% (w/v) NaCl, 1% (w/v) tryptone, 0.5% (w/v) yeast extract (Fisher Scientific Ltd, UK; BPE1427-500), 1.5% (w/v) bacto agar (BD Biosciences, UK).

2.7 Mammalian cell culture

2.7.1 Media and reagents

Dulbecco's Modified Eagle Medium (DMEM; 31053), with 4.5 mg L^{-1} glucose, but no Glutamine, no Phenol Red and no Sodium Pyruvate was purchased from Gibco. TrypLE™ Express (12604), and L-Glutamine (200 mM; 25030) were also purchased from Gibco. Fetal bovine serum (FBS; F7524) and sodium pyruvate (100 mM; S8636) were purchased from Sigma-Aldrich. The cationic branched polymer Polyethyleneimine (PEI; 408727) and D-(+)-glucose (G7528), used as a transfection reagents, were supplied by Sigma-Aldrich. Poly-L-lysine (M_w 70,000-150,000; P4707) was also purchased from Sigma-Aldrich. Dulbecco's phosphate buffered saline (DPBS) was obtained from PAA Laboratories.

2.7.2 Culture conditions

HEK293T cells were grown as monolayers on 75 cm^2 tissue culture flasks (VWR, UK) and maintained by regular passage in 15 ml "feeding" medium [phenol red-free DMEM supplemented with 10% (v/v) heat-inactivated fetal calf serum, 100 U ml^{-1} penicillin, 0.1

mg ml^{-1} streptomycin, 0.584 g/L L-glutamine and 1 mM sodium pyruvate], under 5% CO_2 at 37°C with a water vapour saturated atmosphere (Galaxy 170S; New Brunswick Scientific, Edison, NJ). All manipulations were performed in a sterile environment, with disposable plasticware and glassware reserved specifically for the purpose.

2.7.3 Transfection reagents

Cells were transfected with polyethyleneimine (PEI) – DNA complexes (Boussif et al., 1995, Ehrhardt et al., 2006). PEI was prepared by dissolving 45 mg PEI in 8 ml sterile water, corrected to pH 7.2 with dilute HCl, passed through a sterile filter (0.2 μm) and kept at RT. Glucose, 5% (w/v), was prepared by dissolving 2.5 g of glucose in sterile water, passed through a sterile filter (0.2 μm) and kept at RT.

2.8 Yeast (NMY51) transformation

Yeast transformation was carried out using the LiAc (Lithium acetate dihydrate)/SS (single-stranded) carrier DNA/PEG (Poly[ethylene glycol]) method (Gietz and Schiestl, 2007b). To ensure efficient transformation, yeast cells used to inoculate YPAD or SD media were always picked from colonies not older than 2 weeks.

2.8.1 Small-scale transformation

NMY51 yeast cells taken from a fresh YPAD plate were cultured at 30°C overnight (12 – 16 h) on a rotary shaker (Innova 4000 Benchtop Incubator Shaker; New Brunswick Scientific, Edison, NJ) at 200 rpm in 50 ml YPAD to an OD_{546} (optical density) of 0.6 – 0.8 (DU® Spectrophotometer; Beckman Coulter, UK). Cultures exceeding OD_{546} of 0.8 were diluted to an OD_{546} of 0.2 and regrown to an OD_{546} of 0.6. Prior to harvesting the cells, the transformation mix [240 μl 50% (w/v) PEG, 36 μl LiAc 1.0 M, 25 μl SS DNA 2 mg ml^{-1}, 1.5 μg plasmid DNA; per reaction] was prepared in sterile 1.5 ml eppendorf test tubes

(Eppendorf, UK), vortexed briefly (Vortex Genie 2; Scientific Industries Inc., Bohemia, NY) and kept on an ice/water bath. The 50 ml culture was harvested by centrifugation for 5 min at 2500 g (Rotanta; Hettich, DE) and resuspended in 2.5 ml sterile water. Resuspended yeast cells (100 µl for each transformation) were added to sterile 1.5 ml eppendorf test tubes containing the transformation mix, vortexed for 1 min to thoroughly mix all components and incubated in a water bath at 42°C for 45 min. Following the incubation, the cell suspensions were pelleted for 5 min at 700 g. After the supernatant was removed, the cells were resuspended in 100 µl 0.9% (w/v) NaCl and spread onto 90 mm Petri SD plates, lacking the appropriate amino acid(s) (see Section 2.5), using a sterile disposable L-shaped spreader (Fisher Scientific Ltd, UK). The plates were then sealed with Parafilm "M" and incubated for 3 – 5 days at 30°C until visible colonies were produced.

2.8.2 Large-scale transformation

NMY51 yeast cells previously transformed with the ABCB1:Cub (pBT3-N:ABCB1) bait vector (as described in Section 2.8.1) were taken from a fresh SD-*Leu* plate and cultured in 10 ml SD-*Leu* medium for 8 h at 30°C on a rotary shaker (Innova 4000 Benchtop Incubator Shaker; New Brunswick Scientific, Edison, NJ) at 200 rpm. The entire 10 ml culture was then subcultured in 100 ml SD-*Leu* and grown overnight (12 – 16 h) at 30°C with shaking at 200 rpm. On the following day, the OD_{546} of the overnight culture was determined by taking a 1 ml aliquot of the culture, centrifuging it at 2500 g for 5 min, resuspending the pellet in 1 ml sterile water and measuring the OD_{546} (DU® Spectrophotometer; Beckman Coulter, UK) against a water blank. The appropriate volume of culture required to return 22.5 OD units was calculated (as instructed by the manufacturer; Dualsystems Biotech, Zurich, CH), aliquoted into 50 ml Falcon tubes (SLS, UK) and spun down for 5 min at 700 g (Rotanta; Hettich, DE). The pellet was then resuspended in 150 ml 2×YPAD (pre-warmed to 30°C) in a sterile 1 L baffled Erlenmeyer

flask. [At this stage to ensure that the correct dilution of the culture was achieved, a 1 ml aliquot was removed from the flask and spun down at 2500 g for 5 min. The pellet was resuspended in 1 ml sterile water and the OD_{546} was measured against a water blank to ensure that it was around 0.15]. Subsequently, the culture was grown at 30°C with shaking at 200 rpm to an OD_{546} of 0.6 – 0.7 (two cell divisions, 3 – 5 h). In the meantime, the transformation mixes [LiAc/TE mastermix (528 µl LiAc 1.0 M, 528 µl 10×TE pH 7.5, 3.744 ml sterile water); PEG/LiAc mastermix (750 µl LiAc 1.0 M, 750 µl 10×TE pH 7.5, 6 ml 50% (w/v) PEG) per 150 ml cell culture] and SS DNA [1 ml aliquot of SS DNA (see Section 2.4 on how to prepare) was thawed on ice, boiled at 99°C for 5 min and immediately chilled in an ice/water bath where it was kept until required] were prepared. Once the exponentially growing 150 ml cell culture had reached the required OD_{546}, it was split in 3×50 ml Falcon tubes and centrifuged for 5 min at 700 g after which the supernatant was discarded. Each cell pellet was then resuspended in 30 ml of sterile water by vortexing (Vortex Genie 2; Scientific Industries Inc., Bohemia, NY), centrifuged at 700 g for 5 min and, after the supernatant had been removed, resuspended in 1 ml LiAc/TE master mix before transferring into a sterile 1.5 ml eppendorf test tube (Eppendorf, UK). The cells were then spun at 700 g for 5 min and, after the supernatant was removed, resuspended in 600 µl of LiAc/TE mastermix. Subsequently, each of the 600 µl cell suspensions was added to a separate 50 ml Falcon tube containing 7 µg prey vector, 100 µl SS DNA and 2.5 ml PEG/LiAc mastermix, vortexed for 1 min to thoroughly mix all the components and incubated for 45 min at 30°C with brief mixing every 15 min. At the end of the incubation, 160 µl of DMSO (dimethyl sulfoxide) were added to each Falcon tube and mixed immediately by shaking followed by a 20 min incubation at 42°C. The cells were then pelleted at 700 g for 5 min, resuspended in 3 ml 2×YPAD (pre-warmed to 30°C), pooled and allowed to recover for 90 min at 30°C with slow shaking at 150 rpm. Subsequently, the cells were pelleted for 5 min at 700g, resuspended in 3.6 ml 0.9% (w/v)

NaCl and spread onto the prepared 3-AT selection plates (see Section 2.5.2). A 300 µl aliquot of cell suspension was spread on each 150 mm plate (12 plates × 300 µl = 3.6 ml) using a sterile disposable L-shaped spreader. The remaining resuspended cells were used to prepare 1:100, 1:1000 and 1:10,000 dilutions in a final volume of 1 ml of 0.9% (w/v) NaCl and spread (100 µl form each dilution) on separate 90 mm Petri SD-*Trp-Leu* plates (see Section 2.5), using a sterile disposable L-shaped spreader; these plates were used to calculate the transformation efficiency. All plates were sealed with Parafilm "M" and incubated at 30°C for 4 days. The transformation efficiency was calculated using the following formulae:

$$Total\ number\ of\ transformants = \#\ \text{of colonies on SD} - Trp - Leu\ \text{plate} \times \text{dilution factor} \times 10 \times 3.6$$

$$\text{Transformation efficiency}\left(\frac{\text{clones}}{\mu\text{g}}\text{DNA}\right) = \frac{Total\ number\ of\ transformants}{21\ \mu\text{g}}$$

The total number of transformants should be greater than 8×10^5 as indicated by the manufacturer (Dualsystems Biotech, Zurich, CH).

2.9 Bacterial (XL10-Gold® Ultracompetent Cells) transformation

Plasmid DNA was transformed into XL10-Gold® Ultracompetent cells (Agilent Technologies, UK; 200315).

XL10-Gold® Ultracompetent cells were gently thawed on ice. For each sample reaction to be transformed, 22.5 µl of bacteria were aliquoted to a prechilled 1.5 ml eppendorf test

tube (Eppendorf, UK) followed by chemical treatment with 1 µl XL10-Gold® β-mercaptoethanol mix. After gentle mixing, the cells were kept on ice for 10 min and swirled every 2 min. Subsequently, 2 µl of plasmid DNA from each sample to be transformed were added to separate aliquots of the ultracompetent cells, mixed gently and incubated on ice for 30 min. Following heat-shock at 42°C for 30 sec, the reactions were incubated on ice for 2 min before 250 µl of preheated (42°C) S.O.C. rich medium (Invitrogen, UK) was added to each tube. The cells were then allowed to recover for 1 h at 37°C with shaking at 225 rpm (Innova 4000 Benchtop Incubator Shaker; New Brunswick Scientific, Edison, NJ) before the appropriate volume from each transformation was plated on LB-ampicillin agar plates (supplemented with X-gal and IPTG where appropriate for "blue/white" screening). Transformation plates were incubated at 37°C for >18 h.

2.10 Mammalian cell (HEK293T) transfection

2.10.1 For immunoblot analysis

HEK293T cells (3×10^5) were seeded as a monolayer on 6 round-well plates (ThermoFisher Scientific, Waltham, MA; TKT-190-050T) in 2 ml "feeding" medium (see Section 2.7.2) 24 h prior to transfection. The transfection mixture [7.5 µg total plasmid DNA in 1 µl of 5% (w/v) glucose mixed with 1.5 µl PEI and adjusted to a final volume of 10 µl with sterile water] was prepared in individual 1.5 ml eppendorf test tubes (Eppendorf, UK) on the day of transfection and incubated for 10 min at RT. For the single transfections (i.e. with plasmid DNA encoding WT or mutant ABCB4 and empty pCi-Neo vector), the transfection mixture contained 2.5 µg of ABCB4-encoding plasmid and 5 µg of empty pCi-Neo vector. For the triple transfections (i.e. with three different plasmids encoding either WT or mutant ABCB4 or ATP8B1 or CDC50A), the transfection mixture contained 2.5 µg of each plasmid. At the end of the 10 min incubation, 1 ml fresh

"feeding" medium, pre-warmed to 37°C, was added to each tube and applied to the cells. Prior to the application of the transfection mixture (during the 10 min incubation period), all the medium was aspirated from each well and replaced with 1 ml fresh "feeding" medium pre-warmed to 37°C. The cells were harvested 48 h post transfection (see Section 2.18.2).

2.10.2 For cellular efflux of ^{3}H-PC

Six round-well plates were treated with 1 ml Poly-L-lysine for 1 h at RT and washed 3× in 1 ml DPBS. Poly-L-lysine improves cell adherence to the surface of the wells and prevents cells from being washed off during the subsequent stages of the experiment.

HEK293T cells (3×10^5) were seeded the pre-treated plates 24 h prior to transfection. For this assay, only triple transfections were set up as described in Section 2.10.1. During the 10 min incubation of the transfection mixture, all the medium was aspirated from each well and replaced with 600 µl fresh "feeding" medium (see Section 2.10.1) pre-warmed to 37°C. The assay was performed as described in Section 2.22.

2.10.3 For immunocytochemistry

HEK293T cells (1.2×10^5) were seeded as a monolayer on 12 round-well plates (ThermoFisher Scientific, Waltham, MA) in 1 ml "feeding" medium (see Section 2.7.2) 24 h prior to transfection. Before seeding, sterile coverslips were placed into each well and treated with 100 µl Poly-L-Lysine for 1 h at RT followed by 3 washes in 1 ml DPBS. On the day of transfection, the same volume of transfection mixture described in Section 2.10.1 was prepared per transfection, to avoid aliquoting small volumes and run the risk of introducing pipetting errors, but only 400 µl was applied to the cells (i.e. 2.5× less than for the 6-well plate). The cells were fixed 48 h post transfection (see Section 2.23).

2.11 Isolation of plasmid DNA from yeast and *E. coli*.

Small-scale (μg-quantities) preparations of plasmid DNA were isolated from both yeast and *E. coli* using the GenElute™ Plasmid Miniprep Kit (Sigma-Aldrich, UK; PLN350) as described by the manufacturer. Slight modifications to the protocol are included within the procedures outlined below. Large-scale (mg-quantities) preparations of plasmid DNA were isolated from *E. coli* using the GenElute™ HP Plasmid Maxiprep Kit (Sigma-Aldrich, UK; NA0310) using the vacuum format as described by the manufacturer and outlined below.

2.11.1 Isolation of plasmid DNA from yeast (NMY51)

Plasmid DNA was isolated from yeast by mechanical disruption of the yeast cells using glass beads. SD-*Trp-Leu* medium (3 ml) was inoculated with yeast, incubated overnight at 30°C with shaking at 200 rpm and then harvested by gentle centrifugation for 5 min at 4000 g. The cells were then resuspended in 200 μl Resuspension Solution (supplemented with 10 μg ml^{-1} RNase A) and transferred into a tube containing ~100 μl of acid-washed glass beads (Sigma-Aldrich, UK; G8772). Following vortexing for 5 min (Vortex Genie 2; Scientific Industries Inc., Bohemia, NY), the lysate was transferred into a fresh test tube and plasmid DNA was purified using the GenElute™ Plasmid Miniprep Kit (Sigma-Aldrich, UK; PLN350) as described above (see Section 2.11.2.1) with the following modifications; the cleared lysate was applied to the pre-prepared spin columns and centrifuged for 1 min at 6000 g followed by 2× wash with nuclease removal buffer (500 μl; Optional Wash Solution) and once with Wash Solution (500 μl). The purified plasmid was eluded in 50 μl of 10 mM Tris buffer, pH 8.8, stored at -20°C and used for DNA sequencing or transformation of *E. coli*.

2.11.2 Isolation of plasmid DNA from *E. coli.* (XL10-Gold®)

2.11.2.1 Small-scale preparations

Bacterial cells (2 ml) from a 5 ml overnight culture (LB broth supplemented with the appropriate antibiotic; see Section 2.6) were harvested by centrifugation for 5 min at 12,000 g. The cell pellet was then resuspended in 200 μl Resuspension Solution. Lysis Solution was then added and the solution was mixed by inversion. The alkalinity of the Lysis Buffer causes the denaturation of nucleic acids and protein within the lysate. After 5 min incubation at room temperature, Neutralization Solution (350 μl) was added, causing the aggregation of insoluble genomic DNA and high molecular weight RNA, and the precipitation of protein-SDS (sodium dodecyl sulphate) complexes. The lysate was then centrifuged for 10 min at 12,000 g. GenElute HP Miniprep Binding Columns were prepared by adding 500 μl Column Preparation Solution and centrifuging for 1min at 12,000 g. The supernatant from the cell lysate was then added to the columns and incubated for 1 min at room temperature. Following incubation, the supernatant was passed through the columns by centrifugation at 12,000 g for 1 min. The columns were washed by adding Wash Solution (500 μl) and centrifuging for 1 min at 12,000 g. The eluted Wash Solution was discarded and the columns were centrifuged as before in order to remove any traces of Wash Solution. Plasmid DNA was eluted by adding 50 μl of 10 mM Tris buffer, pH 8.8 to the column and incubating for 5 min at room temperature, followed by centrifugation for 1 min at 12,000 g. The concentration and purity of the plasmid DNA was determined by spectrophotometric analysis as described in Section 2.14 and stored at -20°C.

2.11.2.2 Large-scale preparations

A single bacterial colony from a freshly streaked plate was used to inoculate a starter culture of 5 ml LB, containing the appropriate antibiotic (see Section 2.6), in a sterile 50 ml

Erlenmeyer flask and incubated for 8 h at 37°C with shaking at 225 rpm (Innova 4000 Benchtop Incubator Shaker; New Brunswick Scientific, Edison, NJ). The starter culture was then diluted 1:500 in a suitable volume of LB broth (200 ml), containing the appropriate antibiotic, in a sterile 2 L baffled Erlenmeyer flask and incubated at 37°C with shaking at 225 rpm for 12 – 16 h. Bacterial cells (200 ml) were harvested by centrifugation at 5,000 g for 10 min at 4°C. The cell pellet was resuspended in 12 ml Resuspension/RNase A Solution by a combination of pipetting and vortexing (Vortex Genie 2; Scientific Industries Inc., Bohemia, NY). Lysis Solution (12 ml) was then added before mixing by inversion and incubating for 5min at room temperature. Following the addition (12 ml) of ice-cold Neutralization Solution and mixing by inversion, the Binding Solution (9 ml) was added, the contents were mixed by inversion, poured into the barrel of the provided filter syringe and allowed to settle for 5 min. In the meantime, the GenElute HP Maxiprep Binding Column was prepared by placing it onto the Sigma VM20 (Sigma-Aldrich, UK; VM20) vacuum manifold, adding 12 ml of Column Preparation Solution and applying vacuum until all the liquid had passed through. Subsequently, the cleared lysate from the syringe barrel was expelled into the prepared column and allowed to pass through, followed by two successive washes; the first with 12 ml of Wash Solution 1 and the second with 12 ml Wash Solution 2. Following the wash steps, the GenElute HP Maxiprep Binding Column was placed into the 50 ml collection tube provided and spun in a swinging bucket rotor (Rotanta; Hettich, DE) for 5 min at 3,000 g to dry the column by removing any residual wash solution. The binding column was then transferred into a clean 50 ml collection tube and after 3 ml of Elution Solution were added it was centrifuged at 3,000 g for 5 min to recover the plasmid DNA. Once the DNA was recovered, it was concentrated by NaAc/isopropanol precipitation. NaAc Buffer Solution 3.0 M pH 5.2 (0.1 volumes) and isopropanol (0.7 volumes) were added to the solution, mixed well by inversion and centrifuged at 15,000 g for 30 min at 4°C. The supernatant was decanted with care not to

disturb the pellet and the pellet was washed with 1.5 ml of 70% (v/v) ethanol followed by centrifugation at 15,000 g for 10 min at 4°C. The supernatant was then discarded, the pellet was air-dried until all residual ethanol had evaporated and then resuspended in 400 µl of 10 mM Tris buffer, pH 8.8. The concentration and purity of the plasmid DNA was determined by spectrophotometric analysis as described in Section 2.14 and stored at -20°C.

2.12 Agarose gel electrophoresis of DNA

Agarose gels [0.7 – 1.5% (w/v)], were prepared by melting the required amount of powdered agarose (DNA grade; Invitrogen, UK) in TAE buffer (40 mM Tris-acetate, 1 mM EDTA), by heating in a microwave oven (Sharp, UK), until clear. The melted solution was then allowed to cool down to 55°C, before the ethidium bromide (0.5 µg ml^{-1}) was added, poured into the appropriate mould (Owl Separation Systems; Thermo Fisher Scientific, UK) and allowed to harden. DNA fragments were separated by electrophoresis through a submerged gel. Prior to loading onto the gel, the samples were mixed with the appropriate volume of 6× gel-loading buffer (2.5 % Ficoll 400, 11 mM EDTA, 3.3 mM Tris-HCl, 0.017 % SDS, 0.15 % Orange G pH 8.0; NEB, UK), loaded into sample wells, and electrophoresed at 2 – 10 V cm^{-1} until the required sesolution was achieved. The DNA was visualised using a UV transilluminator and images were recorded using the MultiImage™ Light Cabinet (Alpha Innotech Corporation, San Leandro, CA).

2.13 Isolation of DNA from agarose gels

Linearised DNA was isolated from agarose gels using the PureLink™ Quick Gel Extraction Kit (Invitrogen, UK; K2100-12) which allows rapid and efficient purification of DNA fragments from TAE (Tris-acetate-EDTA) agarose gels of various percentages.

After completion of agarose gel electrophoresis, the area of the gel containing the desired DNA fragment was excised using a scalpel with a clean, sharp blade taking care to minimise the amount of agarose surrounding the DNA fragment. The gel slice containing the DNA fragment was then weighed and put into a 1.5 ml eppendorf test tube (Eppendorf, UK); if the gel slice exceeded 400 mg, it was cut into smaller slices so that no one slice would exceed 400 mg and each slice was placed into a separate test tube. Three volumes of Gel Solubilization Buffer (L3) were then added per gel volume (e.g. 1.2 ml of L3 per 400 mg of agarose gel slice) followed by heating of the test tube containing the gel slice on a hot block (DRI Block® DB.2A; Techne LTD, UK) at 50°C for 10 min, inverting every 3 min to ensure gel dissolution. After the gel slice had dissolved, the incubation was continued for a further 5 min before 1 gel volume of isopropanol was added to the dissolved slice and mixed well. A Quick Gel Extraction Column (1 per 400 mg gel slice) was attached to the Sigma VM20 (Sigma-Aldrich, UK; VM20) vacuum manifold. The dissolved gel slice containing the DNA fragment of interest was then loaded onto the centre of the silica membrane of the Quick Gel Extraction Column and vacuum was applied until all the liquid had passed through. Wash Buffer (700 μl; W1) was then added to the centre of the Quick Gel Extraction Column and vacuum was applied until all the liquid had passed through the column, before the column was transferred into a Wash Tube and centrifuged at 14,000 g for 3 min to remove any residual W1. The Quick Gel Extraction Column was then placed into a Recovery Tube before 50 μl of Elution Buffer (E5; 10 mM Tris-HCl, pH 8.5) were added followed by 1 min incubation at RT. The purified DNA was recovered by centrifugation for 1 min at 12,000 g. The concentration and purity of the plasmid DNA was determined by spectrophotometric analysis as described in Section 2.14 and stored at -20°C.

2.14 Determination of DNA yield and quality

DNA concentration in nucleic acid preparations was determined by spectrophotometry by measuring absorbance at 260 nm using the NanoDrop ND-1000 V3.5 (ThermoFisher Scientific, Waltham, MA). The quality of DNA is indicated by the ratio between the absorbance at 260 and 280 nm. For pure DNA the A_{260}/A_{280} ratio should be ~1.8. Smaller ratios usually indicate contamination by protein or organic chemicals. As a secondary measure of nucleic acid purity, the A_{260}/A_{230} ratio was also measured which should be in the range of 1.8 – 2.2.

2.15 Site-Directed Mutagenesis

Oligonucleotide-directed mutations were introduced into pcDNA3.1-ABCB4wt (Table 2-1) using the "QuikChange II XL' site-directed mutagenesis kit (Agilent Technologies, UK) which allows site-specific mutations in double-stranded plasmids isolated from a *dam*$^+$ *E. coli* strain. Such DNA is methylated and is a suitable template for mutagenesis.

2.15.1 Mutagenic Primer Design

Mutagenic oligonucleotides were designed using the web-based QuickChange Primer Design Program available at http://www.stratagene.com/qcprimerdesign and supplied by Sigma-Aldrich.

2.15.2 Mutant Strand Synthesis

The template plasmid DNA is amplified by PCR using a pair of mutagenic primers. Each primer covers the site to mutate but is complementary to opposite strands of the template, to generate mutation-containing synthesised DNA. Following amplification, *Dpn*I endonuclease digestion (1 µl of 10 U µl^{-1} *Dpn*I per reaction; for 1 h at 37°C) of methylated and hemi-methylated DNA is carried out. Because the template plasmid DNA is generated

in a *dam*$^+$ *E. coli* strain, whereas the newly-synthesised DNA is unmethylated, the template DNA is susceptible to *Dpn*I digestion. This enables selection for the newly synthesised, mutation-containing DNA, which can then be used to transform XL10-Gold® Ultracompetent Cells as described in Section 2.9.

Thermal cycling reactions were set up in thin-walled PCR tubes (Sigma-Aldrich, UK; Z662593), to maximise temperature-cycling performance. Each reaction was set up as listed in Table 2-3 and cycled using the parameters outlined in Table 2-4.

QuickChange® Reaction	Volume (µl)
Reaction Buffer (10×)	5 µl
dsDNA Template	1 µl (10 ng)
Primer #1	1 µl (125 ng)
Primer #2	1 µl (125 ng)
dNTP Mix	1 µl
QuikSolution	3 µl
ddH_2O	To 50 µl final volume
PfuTurbo DNA Polymerase	1 µl (2.5 units)

Table 2-3. *Protocol for the QuickChange® XL site-directed mutagenesis kit (Stratagene, UK).*

This protocol was used to introduce the required mutations to pcDNA3.1-ABCB4wt vector. Reaction buffer (1×): 200 mM Tris-HCl (pH 8.8), 20 mM $MgSO_4$, 100 mM KCl, 100 mM $(NH_4)2SO_4$, 1% Triton® X-100, 1 mg/ml nuclease-free bovine serum albumin (BSA); dNTP mix and QuikSolution composition: *proprietary* (Agilent Technologies, UK).

Time (sec)	Temperature (°C)	No. Of Cycles	
60	95	1	Denaturation
50	95 (denaturation)	18	Cycling (Amplification)
50	60 (annealing)		
540	68 (extension)		
420	68	1	Extension

Table 2-4. *PCR programme used to mutagenise the pcDNA3.1-ABCB4wt vector.*

The sequence of the entire mutant cDNA was confirmed as described in Section 2.17.2.

2.16 Plasmid Constructions

2.16.1 pGEM3®-3Zf(-):PKCα

The PKCα cDNA from the EGFP-PKCα vector (50 ng) was amplified in a mutagenic PCR set-up as per Table 2-5 (RoboCycler Gradient 40, Agilent Technologies, UK). The mutagenic primers *Pci*I-F:PKCα and an *Age*I-R:PKCα were used at a temperature gradient (48°C – 62°C), in the thermal cycling summarised in Table 2-6. Through this, a *Pci*I and an *Age*I restriction site were introduced at the 5'- and 3'-ends, respectively, of the amplified product generating PKCα(*Age*I/*Pci*I).

Vent PCR Reaction	Volume (µl)	Final Concentration
ThermoPol Reaction Buffer (10×)	2.5 µl	1×
dNTP mix (2 mM)	2.5 µl	200 µM
*Pci*I-F PKCα (10 µ M)	1.5 µl	0.15 µM
*Age*I-R PKCα (10 µ M)	1.5 µl	0.15 µM
DNA template	50 ng	
$Vent_R$® DNA Polymerase	1.0 µl	2 units
ddH_2O	To 25 µl final volume	

Table 2-5. ***Protocol for Vent PCR Reaction used to amplify the PKCα cDNA from the pEGFP-PKCα.***

This protocol was used to introduce the *Pci*I and *Age*I restriction sites at 5'- and 3'- ends , respectively, of the PKCα cDNA. ThermoPol Reaction Buffer (1×): 20 mM Tris-HCl, 10 mM $(NH_4)_2SO_4$, 10 mM KCl, 2 mM $MgSO_4$, 0.1 % Triton X-100 pH 8.8 @ 25°C. dNTP mix: dATP, dCTP, dGTP and dTTP, each at 2 mM.

Time (min)	Temperature (°C)	No. Of Cycles	
2	95	1	Denaturation
1	95	30	Cycling (Amplification)
1	48-62		
1	72		
5	72	1	Extension

Table 2-6. ***Programme used in mutagenic PCR to amplify PKCα and define the optimal annealing temperature for the reaction.***

The blunt-ended, PCR product [PKCα(*Age*I/*Pci*I)] was cloned into the polylinker *Sma*I site of the pGEM3®-3Zf(-) vector (Promega, UK; P2261) to generate pGEM3®-3Zf(-):PKCα. Prior to the ligation, the digested vector and PCR product were run on a 1% (w/v) agarose gel (see Section 2.12) and purified by gel extraction using the PureLink™ Quick Gel

Extraction Kit (see Section 2.13). The ligation was carried out using Quick T4 DNA Ligase (NEB, UK; M2200L) for 10 min at 25°C. Vector and insert fragments were used at an approximate 1:1 molar ratio. The ligation product was transformed into XL10-Gold® Ultracompetent cells (as described in Section 2.9) for "blue/white" screening. White colonies, i.e. carrying the pGEM3®-3Zf(-) vector with the PKCα(*Age*I/*Pci*I) insert, were picked and incubated overnight in 5 ml LB-amp liquid medium at 37°C with shaking (250 rpm). Plasmid DNA was isolated from the overnight cultures as described in Section 2.11.2.1.

The presence of the PKCα cDNA (*Age*I/*Pci*I) was verified by restriction digest analysis using the enzymes *Hind*III and *Xmn*I (NEB, UK). DNA (400 ng) was digested from each individual clone. The digested products were resolved on 1% agarose gel (see Section 2.12).

The integrity of the construct was verified by DNA sequencing using the pUC/M13 forward and reverse primers as well as several other primers covering the whole length of the PKCα cDNA, namely, PKCaR1, PKCaF1, PKCaF2, PKCaF3, PKCaF4 and pEGFP-C1F1.

2.16.2 pPR3-STE:PKCα

pPR3-STE(*Age*I/*Nco*I) and PKCα(*Age*I/*Pci*I) were generated by digestion of the pPR3-STE:Caveolin (Wharton J., personal communication) and the pGEM3®-3Zf(-):PKCα(*Age*I/*Pci*I) (see above 2.16.1) with the appropriate enzymes (NEB, UK). The digested products were run on a 1% agarose gel (see Section 2.12) and the fragments corresponding to the expected size of the DNA fragment of interest were purified by gel extraction (see Section 2.13). Ligation of pPR3-STE(*Age*I/*Nco*I) and PKCα(*Age*I/*Pci*I) was carried out using Quick T4 DNA Ligase (NEB, UK; M2200L) for 10 min at 25°C. As a

control for the self-ligation of the vector, an additional ligation reaction was carried out using vector only DNA. The products of the ligation reactions were transformed into XL10-Gold® Ultracompetent as described in Section 2.9. Bacterial colonies, transformed with the pPR3-STE:PKCα ligation product, were picked and incubated overnight in 5 ml LB-amp liquid medium at 37°C with shaking (250 rpm). Plasmid DNA was isolated from the overnight cultures as described in Section 2.11.2.1.

The presence of the PKCα insert was verified by digesting the purified plasmid with *Dra*III (NEB, UK). A large-scale preparation of the pPR3-STE:PKCα construct was carried out as described in Section 2.11.2.2.

2.16.3 pcDNA3.1-ABCB4 WT and Mutant plasmids

pcDNA3.1-ABCB4wt plasmid encoding human ABCB4 as well as the inactive ABCB4_E558Q (c.1672G>C) derivative (replacing a conserved glutamate in the Walker B motif with a glutamine to prevent ATP hydrolysis) were kindly provided by Dr Marta Rodriguez-Romero and have been described elsewhere (Groen et al., 2011). ABCB4_A546D (c.1637C>A) and ABCB4_S320F (c.959C>T) were derived by site-directed mutagenesis from pcDNA3.1-ABCB4wt. They were provided by Dr Marta Rodriguez-Romero (personal communication) and confirmed by DNA sequencing (see Section 2.17.2).

2.16.3.1 Site-directed Mutagenesis

All other ABCB4 mutants were derived from pcDNA3.1-ABCB4wt using the QuickChange® XL site-directed mutagenesis kit (see Section 2.15) The primers used to derive each mutant were the following: ABCB4_G535D (c.1604G>A), ABCB4_M301T (c.902T>C), ABCB4_E528D (c.1584G>C), ABCB4_L591Q (c.1772T>A), ABCB4_P1161S (c.3481C>T), ABCB4_R545C (c.1633C>T), ABCB4_A286V (c.857C>T)

and their reverse complements (Table 2-2). Colonies from the mutagenesis reaction were picked and incubated overnight in 5 ml LB-amp liquid medium at 37°C with shaking (250 rpm). Plasmid DNA was isolated from the overnight cultures as described in Section 2.11.2.1.

2.16.3.2 Restriction Digests

Putative mutants were screened based on their restriction digest profiles as predicted by *in silico* analysis of the mutated constructs. Specifically 1 μg of template from each candidate was digested for 1 h at the appropriate conditions according to the requirements of the restriction endonuclease as stated by the manufacturer (NEB, UK). ABCB4_G535D were digested with *BstX*I, ABCB4_M301T with *Nco*I, ABCB4_E528D with *BsmA*I, ABCB4_L591Q with *Acc*I, ABCB4_P1161S with *TthIII*I and ABCB4_R545C with both *Pml*I and *Nhe*I-HF. The digested products were run on a 1% agarose gel (see Section 2.12) and candidates for each mutation with the expected restriction digest profile were confirmed either by automated DNA sequencing (see Section 2.17.1; Source BioScience, UK) or in-house sequencing (see Section 2.17.2). The primers used were designed to cover the whole ABCB4 cDNA, namely, ABCB4_389F, ABCB4_918F, ABCB4_1440F, ABCB4_ 1983F, ABCB4_2473F, ABCB4_2981F, ABCB4_3393F, ABCB4_491R (Table 2-2).

2.16.4 ATP8B1 and CDC50 Plasmids

pCI-neo-ATP8B1 and pCI-neo-CDC50 plasmids encoding human ATP8B1 and CDC50A respectively were kindly provided by Dr Marta Rodriguez-Romero (Groen et al., 2011).

2.17 DNA Sequencing

2.17.1 Automated DNA sequencing

Automated DNA sequencing was out sourced and performed by either: 1. The MRC Clinical Sciences Centre Genomics Core Laboratory or 2. LifeSciences (Source BioScience, UK).

2.17.2 In-house sequencing

In-house sequencing was carried out using the BigDye® Terminator v3.1 Cycle Sequencing Kit (Invitrogen, UK).

2.17.2.1 Cycle sequencing on plasmid DNA

The BigDye Terminator v3.1 Cycle Sequencing Kit provides the required reagent components for the sequencing reaction in a pre-mixed format. These reagents are suitable for performing fluorescence-based cycle sequencing reactions on single-stranded or double-stranded DNA templates and on PCR fragments.

Each reaction mixture was prepared as shown below in Table 2-7.

Reagent	Volume (µl)
Oligonucleotide (3.2 pmol/µl)	1.0 µl
BigDye® Terminator Buffer (5×)	2.0 µl
DNA template	1.0 µg
Ready Reaction Premix	0.5 µl
ddH_2O	To 10 µl final volume

Table 2-7. *Reaction mixture preparation for DNA sequencing.*
BigDye® Terminator Buffer and Ready Reaction Premix composition: *proprietary* (Invitrogen, UK)

Cycle sequencing was performed in the Touchgene Gradient Thermal Cycler (Techne LTD, UK) using the protocol summarised in Table 2-8.

Time (sec)	Temperature (°C)	No. Of Cycles
60	96	1
10	96	25
5	50	
240	60	
∞	10	∞

Table 2-8. ***Termocycling for plasmid DNA sequencing.***

2.17.2.2 Ethanol/EDTA precipitation of DNA

To ensure optimum results, unincorporated dye terminators (which can obscure data) should be completely removed prior to electrophoresis. In order to minimise unincorporated dyes the ethanol/EDTA (ethylenediaminetetraacetic acid) purification method was used.

Initially, the tubes containing the amplified products (in 10 μl volumes) were spun briefly before adding 2.5 μl of 125 mM EDTA (25 mM final; Sigma-Aldrich, UK) to each sample followed by 30 μl of 100% ethanol (Sigma-Aldrich, UK). The tubes were sealed, mixed by inverting 4 times, incubated at RT for 15 min and spun for 20 min at 17000 g at 4°C in a fixed-rotor centrifuge (Heraeus Fresco 17; ThermoFisher Scientific, Waltham, MA). Following centrifugation, the supernatant was discarded and 30 μl of 70% ethanol were added to each sample. The tubes were then spun for 10 min at 17000 g at 4°C and the supernatant was discarded. Finally, the samples were allowed to air-dry for 30 min in the dark, resuspended in 10 μl Hi-Di™ Formamide (Applied Biosystems, UK) and loaded onto a MicroAmp® Optical 96-Well Reaction Plate (Invitrogen, UK).

2.17.2.3 Sample electrophoresis

Prior to electrophoresis, the 96-well reaction plate was sealed and the samples were heated for 5 min at 96°C on a hot block (DRI Block® DB1.M; Techne LTD, UK) to denature the DNA and cooled down rapidly for 1 min on ice.

Automated sample electrophoresis and sequencing analysis were performed using the instrument protocol "sequencing_600bp_POP7" and analysis protocol "3130 POP7_BDTU3-KB_DENOVO_V.5.2" on ABI Prism® 3130*xl* Genetic Analyser (Applied Biosystems, UK).

2.17.2.4 Sequencing data analysis

Analysis of the electropherograms was performed using the Sequence Scanner V1.0 (Applied Biosystems, UK).

2.18 Isolation of whole-cell protein content

2.18.1 Yeast whole-cell extracts

SD medium (10 ml) was inoculated with several colonies of NMY51 transformed with the appropriate vector(s) (see Section 2.8.1) and incubated overnight at 30°C with shaking at 200 rpm to an OD_{546} of 0.6-1. The cells (~2.4×10^7 – 4.0×10^7) were harvested by centrifugation at 700 g for 5 min. The pellet was then washed once in 1 mM EDTA in water and the cells were lysed in 200 µl 2.0 M NaOH for 10 min on ice. The samples were precipitated using TCA (trichloroacetic acid) as described in Section 2.19 and stored at -80°C.

2.18.2 HEK293T whole-cell extracts

Total-cell extracts from mammalian cells for immunoblot analysis (see Section 2.21) were prepared 48 h post transfection (see Section 2.10.1). Prior to lysis, cells were washed three times in ice-cold phosphate-buffered saline (PBS, Sigma-Aldrich, UK) and lysed on the cell culture dish in 300 µl lysis buffer [1% sodium dodecyl sulfate in PBS supplemented with 150 mM NaCl, 10 mM HEPES, 25 U/µl Benzonase® Endonuclease (Merck Millipore, Darmstadt, DE), Protease Inhibitor Coctail (Roche, UK) and 1.0 mM PMSF

(phenylmethylsulfonyl fluoride) in ethanol]. The endonuclease was allowed to act for 15 min at RT before the samples were collected in 1.5 ml eppendorf test tubes (Eppendorf, UK) and centrifuged at 17,000 g for 15 min at 4°C to remove any insoluble material. The supernatant was collected in fresh tubes and stored at -80°C.

2.19 TCA (trichloroacetic acid) precipitation of protein extracts

Cell lysates were concentrated using trichloroacetic acid (TCA) precipitation. Sodium deoxycholate (0.1 volumes of a 0.15% solution) was added to the protein sample and incubated at room temperature for 5 minutes. Following this, 0.1 volumes of 72% trichloroacetic acid was added, the sample was mixed and incubated for a 10 minutes at RT. The protein was recovered by centrifugation at 20,000 g for 8 min. After the supernatant was carefully removed and discarded, the pellet was resuspended in 50 µl resuspension buffer (4% SDS, 0.2 M Tris pH 7.4, 0.15 M NaOH). Samples were stored at -80°C.

2.20 Protein quantitation

Protein concentration of whole-cell extracts was determined using the Bio-Rad *DC* Protein Assay (Bio-Rad, UK; 500-0116). The assay is based on the Lowry method (Lowry et al., 1951) and was carried out following the manufacturer's instructions. The reactions were set up in duplicates on 96-well microplates (ThermoFisher Scientific, Waltham, MA). A range of BSA concentrations (0, 0.25, 0.5, 1.0, 2.0, 4, 6, 8 and 10 mg ml^{-1}) was used to produce a standard curve.

2.21 Analysis of protein expression

2.21.1 General reagents and buffers

SDS gel-loading buffer (5×): 0.31 M Tris-HCl (pH 6.8), 0.25 M DTT (dithiothreitol), 0.1% (v/v) bromophenol blue, 50% (v/v) glycerol, 10% (w/v) SDS. **Running buffer (10×):** 0.25 M Tris, 2.5 M glycine (pH 8.3), 1.0% (v/v) SDS. **Transfer Buffer (5×):** 0.195 M glycine, 0.24 M Tris base, 0.185% (w/w) SDS. All reagents were supplied by Sigma-Aldrich, UK. The Running buffer was diluted to 1× with deionised water and used up to three times before discarding. The Transfer buffer was diluted to 1× with deionised water supplemented with 20% (v/v) methanol and used once.

2.21.2 Antibodies

Anti-ABCB1/B4: C219 (mouse monoclonal; SIG-38710-1000) was obtained from Cambridge Bioscience. **Anti-Caveolin:** pY14 (mouse monoclonal; 611338) was obtained from BD Biosciences. **Anti-LexA:** Lex (2-12) (mouse monoclonal; sc-7544) was obtained from Santa Cruz. **Anti-tubulin:** anti-β-tubulin (mouse monoclonal; E1C601) was obtained from EnoGene Biotech. **Secondary Anti-Mouse:** HRP-conjugated (goat anti-mouse polyclonal; P0447) was obtained from Dako.

2.21.3 SDS-PAGE (sodium dodecyl sulfate polyacrylamide gel electrophoresis)

Gels were prepared using the discontinuous buffer system devised by Davis (1964), Ornstein (1964), and Laemmli (1970) in which the buffer in the sample and the stacking gel contain Tris-Cl (pH 6.8) and the resolving gel contains Tris-Cl (pH 8.8). Such buffer system has the ability to concentrate the complexes in the samples into a very small volume and therefore increase the resolution of the gel.

All SDS-PAGE was performed using the Mini-PROTEAN® electrophoresis system from Bio-Rad and tris-glycine running buffer (see Section 2.21.1). Proteins were diluted in 5× SDS sample buffer (see Section 2.21.1) and denatured briefly (5 min at 70°C) prior to loading on a freshly-made 7.5% SDS-polyacrylamide resolving gel (with 5% stacking gel). For each sample, 2 μg of total protein extract (protein quantitation was determined as described in Section 2.20) was loaded per lane. For yeast whole cell extracts (Section 2.18.1) the whole volume (50 μl) of the TCA-precipitated samples (Section 2.19) was loaded per lane. A lane containing 10 μl of standard molecular weight marker (Precision Plus Protein All Blue Standards; Bio-Rad, UK) was loaded onto each gel to enable the subsequent determination of protein molecular weights. Proteins were initially separated using a constant voltage (90 V) until the molecular weight marker separation was evident. The voltage was then increased to 120 V, and the separation was continued until the dye-front had reached the base of the gel.

2.21.4 Immunoblot analysis

Western blotting was originally devised by Towbin (1979) and Burnette (1981) and involves the transfer of electrophoretically separated proteins from an SDS gel to a solid support (polyvinylidene fluoride (PVDF) membrane) and probed with antibodies specific for particular amino acid sequences. The bound (primary) antibody is detected by a secondary (horseradish peroxidase (HRP)-conjugated) antibody via chemiluminescence.

Following their separation by SDS-PAGE, proteins were transferred onto a PVDF membrane (Immobilon-P; Millipore, Billerica, MA), activated with 100% methanol (1 min) and washed in deionised water (1 min), for western blotting analysis. The transfer was carried out overnight at 20 mV using the Mini-PROTEAN® transfer system and accompanying ice-pack from Bio-Rad with constant stirring. After electroblotting, the

PVDF membrane was washed in PBS-T [PBS + 0.1% (v/v) Tween-20 (Sigma-Aldrich, UK)] and blocked in 5% (w/v) milk (Marvel, UK) in PBS-T for 1 h at RT on a rocking platform. Subsequently, the membrane was probed overnight with the appropriate primary antibody at 1:1000 dilution in 5% (w/v) milk in PBS-T inside a heat-sealed bag at 4°C with gentle agitation. For β-tubulin, the primary antibody was used at 1:100,000 dilution. The membrane was then given three 10 min washes with PBS-T before incubation (1 h at RT with gentle agitation in a heat-sealed bag) with secondary HRP-conjugated goat-anti mouse antibody (Dako, UK) at 1:1000 dilution in PBS-T. Following three 10 min washes in PBS-T, bound antibodies were visualized by chemiluminescence (ECL Plus™, Amersham, Piscataway, NJ) and exposed to Hyperfilm ECL (GE Healthcare, Piscataway, NJ).

2.22 Cellular efflux of ^{3}H-PC

HEK293T cells were subcultured and transfected as described in Section 2.10.2. One hour post-transfection, the cells were fed 2 μCi [*methyl*-^{3}H]choline (PerkinElmer, Waltham, MA) and cultured for 48 h. Subsequently, the "feeding" medium was removed and cells were washed 3× in 1 ml fresh "feeding" medium pre-warmed to 37°C followed by a 24 h incubation in 2 ml "feeding" medium supplemented with 2 mM sodium taurocholate hydrate (TC) (Sigma-Aldrich, UK; 86339) in DPBS. After the 24 h incubation, 50 μl of culture media from each well were analysed for radioactivity content in a Beckman LS 6000SC scintillation counter (Beckman Coulter, UK). The cells attached to the dish were washed 3× in 1 ml DPBS and lysed in 2 ml 0.5% (v/v) Triton-X 100. An aliquot (50 μl) from each lysate was analysed for radioactivity to determine the cellular content. The level of [*methyl*-^{3}H]PC efflux for each ABCB4 variant was calculated as a percentage of the total [*methyl*-^{3}H]PC using the following equation:

$$\%\ PC\ efflux = \frac{\text{PC recovered in the culture medium}}{\text{Total PC (PC in culture medium + Cellular PC)}} \times 100$$

Each set of transfections was repeated six independent times.Statistical analysis was performed by one-way ANOVA (analysis of variance) using the GraphPad PRISM® V5.0 software.

2.23 Immunocytochemistry

HEK293T cells were cultured and transfected 24 h post-seeding (see Section 2.10.3). Forty eight hours post-transfection, all the medium was aspirated from the wells, the cells were washed 3× in 1 ml PBS and then fixed with ice-cold 10% (v/v) acetone in ethanol, for 20 min at RT. Following 3 washes in PBS, the cells were blocked for 1 h at RT in 1 ml of 5% (w/v) BSA (bovine serum albumin; Sigma-Aldrich, UK) in PBS. Subsequently, the cells were washed 3× in 1 ml PBS before incubating the coverslips with 100 µl of the anti-ABCB4 antibody, P_3II-26 [50 µg ml^{-1} (Sigma-Aldrich, UK) in 1% (w/v) BSA in PBS] for 1 h at RT. Following 3 washes in 1 ml PBS, the coverslips were incubated with 100 µl of Alexa Fluor® 488 Dye-conjugated goat anti-mouse IgG [2 µg ml^{-1} (Invitrogen, UK; A10680) in 1% (w/v) BSA in PBS] for 1 h at RT; at the same time, nuclei were stained with 1.5 ng μl^{-1} DAPI (4',6-diamidino-2-phenylindole; Invitrogen, UK). Subsequently, the coverslips were washed 3× in 1 ml PBS and mounted onto microscope slides using FluorSave™ Reagent (Merck Millipore, Darmstadt, DE; 345789). Cells were viewed using a Zeiss LSM710 confocal laser scanning microscope based on an Axiovert inverted microscope (Carl Zeiss, DE) with a 63× oil immersion objective with a numerical aperture of 1.4. Laser lines 488 nm and 405 nm were used to excite Alexa Fluor® 488 and DAPI,

respectively. The pinhole was set to 1 airy unit at 2.0% laser power for all experiments. Images were acquired with sequential scanning to allow cross-talk free Alexa Fluor® 488 and DAPI images to be collected.

2.24 Flow cytometric analysis

All flow cytometry was performed using a BD FACSAria II flow cytometer (BD Biosciences). Polypropylene FACS tubes (5 ml) were purchased from BD Biosciences.

HEK293T cells were triple-transfected as described in Section 2.10.1 replacing pcDNA3.1-ABCB4wt, pCI-neo-ATP8B1 and pCI-neo-CDC50A with the pECFP-C1, pEGFP-C1 and pEYFP-C1 vectors and harvested 48 h post transfection, by brief incubation with TrypLE-Express (500 µl). TrypLE-Express was neutralised by the addition of 5 ml "feeding" medium (Section 2.7.2) prior to collecting the cell suspension. Cells were pelleted for 10 min at 200 g at 4 °C. The resulting cell pellets were resuspended in 5 ml PBS and subjected to flow cytometry. Efficiency of transfection with all three vectors was assessed by enhanced cyan fluorescent protein (ECFP), enhanced green fluorescent protein (EGFP) and enhanced yellow fluorescent protein (EYFP) fluorescence. The ECFP fluorophore was excited at 450 nm, the EGFP fluorophore was excited at 525 nm and the EYFP fluorophore was excited at 582 nm. The emission spectra were measured using the FL-1 channel. The level of expression of each fluorophore was measured in 10,000 cells of normal size and granularity. The ECFP/EGFP/EYFP population was compared to untransfected cells. Flow cytometry data were analysed using the FlowJo software package (Tree Star, Ashland, OR, USA).

2.25 FK506 assay

Single colonies of NMY51 yeast previously transformed with the ABCB1:Cub- or the CD36:Cub (control)-expressing vectors (as described in 2.8.1) were incubated overnight in 10 ml SD-*Leu* at 30°C with shaking to an OD_{600} of 1.0. Serial dilutions were prepared by diluting the cultures to an OD_{600} of 0.2 and further down to an OD_{600} of 0.02 and 0.002 in sterile water. The cell suspension (5 μl) from each dilution was spotted onto the appropriate 90 mm Petri YPAD agar plates and growth was monitored after incubation of the plates for 2 days at 30°C in the dark. The experiment was repeated at 0, 20, 30, 40 and 50 μg ml^{-1} FK506.

2.26 The NubI/NubG test (control assay)

Exponentially growing cells at an OD_{546} of 0.6-0.8 were transformed with 1.5 μg of the appropriate prey and bait vectors (see Table 2-9) as described in Section 2.8.1.

Amount of Vector each (μg)	Plasmid (Bait)	Plasmid (Prey)
1.5	pBT3-N:ABCB1	pAI-Alg5 (NubI)
1.5	pBT3-N:ABCB1	pDL2-Alg5 (NubG)

Table 2-9. ***List of vectors used in the NubI/NubG test.***

Each transformed yeast sample was resuspended in 150 μl 0.9% NaCl. Aliquots (50 μl) from each sample were spread on 90 mm SD-*Trp-Leu* (to select for plasmid maintenance) and SD-*Trp-Leu-His*, SD-*Trp-Leu-His-Ade* (to select for bait and prey interaction) agar plates. The plates were sealed with Parafilm "M" and the percentage of growth under selection was assessed after a 4 day incubation at 30°C and calculated using the following formula:

$$\%\ growth\ under\ selection = \frac{\#\ of\ colonies\ on\ selective\ plate}{\#\ of\ colonies\ on\ non\ selective\ plate} \times 100$$

If the bait is properly expressed and functional in the control assay, then the percentage of growth under selection for the pBT3-N:ABCB1/NubI co-expressing cells should be between 20% and 100% depending of the expression level of the bait. On the other hand, no significant growth should be observed under selection for the pBT3-N:ABCB1/NubG co-expressing cells.

2.27 The human adult liver cDNA library screens

2.27.1 Library complexity assay

For the NubG-X library this was done using an oligo dT sequence which anneals to polyA$^+$ mRNA. As the cDNA synthesis can terminate in any of the three different frames, only one-third of the cDNAs will be fused in frame (N-terminally) with the NubG. For the X-NubG library the use of the oligo dT primers for first-strand synthesis is not possible as this would produce cDNAs containing the stop codon of the gene and the 3'-untranslated region and. To circumvent this problem, random primers were used by the company (Dualsystems Biotech, Zurich, CH) to reverse-transcribe the mRNA and also add a leader sequence to the 5'-end to ensure efficient translation of the fusion product. Using this approach, two fusion points need to be in-frame with the cDNA clone, and only one-ninth of the cDNA clones will carry both the leader sequence (5') and the NubG sequence (3') in-frame with the cloned cDNA. First-strand synthesis was performed using M-MLV (Moloney Murine Leukemia Virus) reverse transcriptase. The first-strand cDNA was then purified and amplified by PCR to add an adapter to the 5'- and 3'-end of the cDNA to introduce asymmetric *Sfi*I restriction sites allowing for directional cloning into the appropriate library vector.

To confirm the quality of the cDNA libraries employed; a qualitative test was performed on isolated plasmid DNA from randomly selected clones. Plasmid DNA (400 ng) from the NubG-X and X-NubG was transformed into XL10-Gold® Ultracompetent cells as described in Section 2.9 and transformants were selected by resistance to ampicillin. DNA (1 μg) isolated from *E. coli* (see Section 2.11.2.1) was digested with *Sfi*I (NEB, UK) and run on 1% agarose gel at 120 mV until the desired resolution was obtained (see Section 2.12). The average insert size was expected to be between 1.2 and 1.3 kb for both libraries (as stated by the manufacturer; Dualsystems Biotech, Zurich, CH).

2.27.2 Optimisation of screening stringency

The level of the ABCB1:Cub self-activation was tested by assaying the level of growth of yeast cells co-transformed with the ABCB1:Cub-expressing vector and the pPR3-N empty vector on selective plates. A large-scale transformation was performed as described in Section 2.8.2. The concentration of 3-AT (2.5 mM) at which no growth was observed was chosen for the library screen.

2.27.3 The library screens

The NubG-X (pPR3-N) and X-NubG (pDL2xN-SUC/pDL2xN-STE) adult liver cDNA libraries were transformed into exponentially growing NMY51 cells bearing the ABCB1:Cub-expressing vector as described in Section 2.8.2 with slight modifications highlighted below [***note:*** the quantities described are for *one* library]. The amount of culture required to return 30 OD units was calculated (as instructed by the manufacturer; Dualsystems Biotech, Zurich, CH), spun down and re-suspended in 200 ml 2×YPAD. The transformation mixtures were prepared as follows: LiAc/TE mastermix (704 μl LiAc 1.0 M, 704 μl 10×TE pH 7.5, 5 ml sterile water); PEG/LiAc mastermix (1.0 ml LiAc 1.0 M, 1.0 ml 10×TE pH 7.5, 8 ml 50% w/v PEG), per 200 ml cell culture. A total of 28 μg of library plasmid mix was transformed in each culture. Cells were re-suspended in 4.8 ml of

0.9% (w/v) NaCl and spread on a total of 16 SD-*Trp-Leu-His-Ade* plates supplemented with 2.5 mM 3-AT (see Section 2.5.2). The plates were sealed with Parafilm "M" and incubated at 30°C for 5 days. Following the appearance of colonies, the plates were stored at 4°C for a further 4 days and monitored for the development red colouration (accumulation of a shunt intermediate product in the *ADE2* biosynthetic pathway indicative of a false-positive colony). The total number of transformants should be greater than 2×10^6 per transformation reaction (i.e. 4.8 ml of re-suspended culture) on the SD-*Trp-Leu* plates (as stated by the manufacturer; Dualsystems Biotech, Zurich, CH). The transformation efficiency was calculated using the formula listed in Section 2.8.2.

2.27.4 Recovery of plasmid DNA from yeast for transformation into bacteria

The library vector encoding a putative ABCB1-interactor was isolated by mechanical disruption of the yeast cells, expressing interacting proteins, using glass beads (see Section 2.11.1) and then retransformed into *E. coli* to obtain large amounts of plasmid DNA (see Sections 2.9 and 2.11.2.1).

2.27.5 Sequencing and Analysis of Recovered Plasmid DNA

Isolated plasmid DNA from *E. coli* (see Section 2.27.4) was sequenced using the forward primer pNubGx for the NubG-X library clones and the reverse primer pDSL-Nx for the X-NubG library clones. The retrieved sequence data was analysed using Vector NTI Advance™ software V11.0 (Invitrogen, UK) and the encoded genes were identified using the BLAST algorithm.

2.27.6 Confirmation of positive interaction and determination of its specificity for ABCB1

2.27.6.1 Confirmation of positive ABCB1-interactors

Prey plasmid DNA isolated from yeast from the initial screen, was transformed into *E. coli* (Section 2.9), recovered from *E. coli* (Section 2.11.2.1) and re-transformed into the

ABCB1:Cub-bearing yeast strain as described in Section 2.8.1. Each transformation (100 µl) was then plated on 90 mm SD-*Trp-Leu* agar plates, sealed with Parafilm "M" and incubated at 30°C until colonies had appeared (3 – 4 days). Single colonies were then picked and grown O/N into 5 ml of SD-*Trp-Leu* medium in individual, CultiFlask® 50 disposable bioreactor (Sartorius, UK; DF-050MB-SSH) to an OD_{546} of 1.0. Exponentially growing cell cultures were then diluted to an OD_{546} of 0.1 in SD-*Trp-Leu* medium and 10 µl of each was spotted SD-*Trp-Leu* plates and on SD-*Trp-Leu-His-Ade* plates supplemented with 0, 1, 2, 3, or 4 mM 3-AT. Cells carrying the control prey plasmids pAI-Alg5 (NubI) and pDL2-Alg5 (NubG) were also employed as positive and negative controls, respectively. Growth at 30°C was monitored after 3 – 4 days by means of colony-colour (white, pink or red depending on the strength of interaction) and colony growth (by eye).

2.27.6.2 Determination of the specificity of interaction with ABCB1:Cub

ABCB1:Cub, FATP4:Cub (Wharton J., personal communication) and Alg5p:Cub (Dualsystems Biotech, Zurich, CH) vectors were transformed into exponentially growing NMY51 yeast cells as described in Section 2.8.1 and grown on SD-*Leu* plates for 3 – 4 days at 30°C. Individual colonies were then used to inoculate the appropriate volume of SD-*Leu* medium (2 ml of yeast culture per bait/prey pair to be assayed) and grown overnight at 30°C with shaking at 200 rpm to an OD_{546} of 0.6-0.8. Exponentially growing cells were transformed with individual prey plasmids (isolated from the library screen) and 10 µl of each was spotted onto SD-*Trp-Leu* and SD-*Trp-Leu-His-Ade* plates supplemented with 3.0 mM 3-AT. Colour development was monitored at 30°C after 2 days on SD-*Trp-Leu* agar plates, and after 3 – 4 days on SD-*Trp-Leu-His-Ade* agar plates in the presence of 3-AT.

2.28 Testing the interaction of ABCB1 with Caveolin-1 and PKCα

The interaction of ABCB1 with Caveolin-1 and PKCα was tested using the transformation protocol outlined in Section 2.8.1. The pPR3-STE:Caveolin and pPR3-STE:PKCα prey vectors were transformed into the ABCB1:Cub(bait)-bearing yeast strain. The transformants were spread on SD-*Trp-Leu-His-Ade* plates, sealed with Parafilm "M" and assessed for growth density and colour development (where growth was evident) after 4 days at 30°C.

Chapter Three

3 Use of the split-ubiquitin yeast system to identify the “interactome” of the multidrug resistance P-glycoprotein (ABCB1)

3.1 Introduction

ABCB1 is a plasma membrane glycoprotein involved in many aspects of the normal human physiology. It functions primarily as an efflux pump in the variety of tissues that it is expressed (the BBB, liver, testes, heart, kidneys, intestines and stem-like progenitor cells) providing a protective role against xenobiotics (Chaudhary and Roninson, 1991, Cordon-Cardo et al., 1990, Cordon-Cardo et al., 1989, Fojo et al., 1987, Sharom, 2011, Thiebaut et al., 1987, Thiebaut et al., 1989). It may also be involved in intercellular signalling (Raggers et al., 2001).

Despite its protective role, overexpression of ABCB1 in tumour tissues is one of the major impediments to chemotherapeutic treatments for cancer patients (Gottesman et al., 2002). This phenomenon is known as multidrug resistance (MDR) and describes the state whereby tumours become spontaneously resistant to a variety of therapeutic agents that are structurally and/or functionally unrelated, including agents that the cells have not been previously exposed to. While direct inhibition of ABCB1 could improve the outcome of chemotherapeutic treatment in cancer patients, it imposes a risk for neurological toxicity and myelosuppression (Fisher et al., 1996). A plethora of pharmacological agents have been developed, and new drugs are constantly being designed that aim to circumvent drug resistance, yet pharmacokinetic interactions as well as dose-dependent toxicity in the patient present a recurring challenge that needs to be overcome (Gottesman et al., 2002).

Identification of ABCB1-interacting partners that influence trafficking and/or function could provide alternative targets for therapy. Although a number of proteins have been shown to interact with ABCB1 (Section 1.11), to date there has been no systematic approach to identify the ABCB1 interactome to better understand its mechanistic

functions, and physiological role(s) and regulation. Consequently, the primary aim of this part of the project was to use the SU-YTH system to identify proteins that interact with ABCB1.

3.1.1 Conventional techniques to study protein:protein interaction

3.1.1.1 Co-immunoprecipitation

Co-immunoprecipitation (co-IP) is one of the most valuable biochemical techniques used routinely in the lab for the identification of protein:protein interactions (Phizicky and Fields, 1995). It can either be employed to confirm an interaction between two known proteins or to identify unknown partners of a protein of interest. The basic principle involves the precipitation of a polypeptide from a whole-cell lysate using a specific antibody (Ab), washing away any non-specifically bound proteins while retaining those that bind directly to the protein of interest, elution of the precipitated complex and separation on a SDS-PAGE gel. The components of the complex can then be identified using mass spectrometry. The Ab used to precipitate the protein of interest (antigen) can either be a monoclonal Ab raised against a specific epitope or a preadsorbed polyclonal Ab. If an antigen is expressed heterologously in a cell system, the encoding vector can be designed to express the protein with a carboxy- or amino-terminal fusion to an epitope tag (such as c-Myc or FLAG-tag) or to protein tag (such as glutathione-S-transferase (GST) (Vikis and Guan, 2004) providing more options when choosing a precipitating Ab. Weak or transient interactions are difficult to detect with co-IP although sometimes this can be overcome by covalent cross-linking of the proteins prior to immunoprecipitation. Although co-IP is an invaluable approach, it is technically difficult when used for membrane proteins because it requires the use of detergents to solubilise the proteins from the lipid membrane. The detergent used must be strong enough to solubilise the membrane protein but it should also allow the maintenance of its quaternary structure (le Maire et al., 2000). An array of

non-ionic or zwitterionic detergents can be used at a range of different temperatures and incubation times in order to optimise the conditions required for the isolation of the complex of interest. However, these methods require extensive optimisation for each complex and are therefore not suited for use in large-scale screens for the simultaneous identification of several uncharacterised protein:protein interactions.

3.1.1.2 The yeast two-hybrid system

The yeast *Saccharomyces cerevisiae* has proven to be an important tool for the identification of protein:protein complexes (Forsburg, 2001, Kumar and Snyder, 2001) due to the ease of handling yeast in the laboratory and the development of several reporter strains. Genetic methods involving the yeast two-hybrid (YTH) system (Fields and Song, 1989) were developed to detect interactions between insoluble proteins in the yeast cytosol and to verify interaction networks, but these require the translocation of the interacting complexes to the nucleus (Ito et al., 2001, Uetz et al., 2000).

The classical YTH system is based on the reconstitution of an active transcription factor from the interaction of test proteins that are fused to the separated DNA-binding domain (BD) and transcription activation domain (AD) of a transcription factor such as GAL4 (Fields and Song, 1989). The interaction of the test proteins reunites the BD with the AD and is detected via the expression of reporter genes such as *lacZ* (β-galactosidase) which contain an upstream activation sequence to which the BD binds (Fields and Song, 1989).

The YTH system has been used successfully to detect interactions between particular membrane proteins (Bourette et al., 1997, Hellyer et al., 1998); however, in genome-wide YTH screens, the coverage of membrane proteins was shown to be poor (Ito et al., 2001, Uetz et al., 2000). Transmembrane proteins contain many strongly hydrophobic domains

and are therefore insoluble and tend to aggregate when in the cytosol. Furthermore, post-translational modifications (such as glycosylation) hinder nuclear localisation even further. The potency of the original YTH system is therefore limited in the identification of integral membrane protein interactors, however modified YTH systems have been developed to address these problems (Stagljar and Fields, 2002).

3.1.1.3 The "split-ubiquitin" yeast two-hybrid system

Several yeast-based systems have been developed to allow for the detection of interaction between integral membrane proteins. These include the reverse Ras recruitment system (Broder et al., 1998, Hubsman et al., 2001), the G-protein-based YTH system (Ehrhard et al., 2000), the rUra3-based YTH system (Wittke et al., 1999) and the "split-ubiquitin" yeast two-hybrid (SU-YTH) system (Stagljar et al., 1998).

In this chapter, the use of the commercially available SU-YTH system (Dualsystems Biotech, Zurich, CH) (Stagljar et al., 1998) to identify regulators of ABCB1 is described. The SU-YTH system has been used successfully to study ER (Scheper et al., 2003), vacuolar (Paumi et al., 2007) and plasma membrane proteins (Gisler et al., 2008, Stagljar et al., 1998, Thaminy et al., 2003).

The system is based on the observation that ubiquitin (Ub), a protein which when used to modify a target protein can designate the target protein for proteasomal degradation by the 26S proteasome (Hershko and Ciechanover, 1992), can be split into two parts; the N-terminal (Nub) and the C-terminal (Cub) (Johnsson and Varshavsky, 1994). In the SU-YTH system, the Cub moiety is linked to an artificial transcription factor (TF) fused to a transactivator protein. The two halves (Cub and Nub) can be autonomously expressed in the same cell, and retain their natural affinity for each other to re-assemble the "split-

ubiquitin". The reformed "split-ubiquitin" complex is recognised by ubiquitin-specific proteases (UBPs) which are recruited to cleave the Cub-linked TF which can translocate to the nucleus and activate expression of reporter genes. Thus, unlike the conventional YTH, the entire protein:protein interaction complex does not need to translocate to the nucleus to effect transcription of reporter genes.

The innate attraction of Nub and Cub can be abolished by a point mutation in the wild-type Nub (designated NubI) replacing an isoleucine at position 3 for a glycine (designated NubG) (Johnsson and Varshavsky, 1994). When co-expressed in the same cell, Cub and NubG do not innately re-assemble. If, however, a protein of interest X is fused to Cub and another protein of interest Y is fused to NubG, and X and Y interact, Cub and NubG are brought in close proximity to each other and reassemble the "split-ubiquitin" which can now be recognised by UBPs.

Stagljar *et al.* (1998) and Thaminy *et al.* (2003) modified this system for the *in vivo* screening of membrane protein interactions. In this method, one integral membrane protein (the "bait") is fused (N- or C-terminally) to Cub which is in turn fused to an artificial TF comprising the *E. coli* DNA-binding protein LexA and the activation domain of the *Herpes simplex* virus VP16. "Prey" are fused (N- or C-terminally) to NubG. If the "bait" and "prey" interact, "split-ubiquitin" is reconstituted, UBPs cleave the C-terminus of the Cub, the TF is released and this translocates to the nucleus to drive expression of the reporter genes independently of the membrane protein complex (Figure 3-1). A fundamental prerequisite for the detection of an interacting protein pair in the SU-YTH system is that the Cub-LexA-VP16 module fused to the N- or C-terminus of the bait and the NubG fused to the N- or C-terminus of the prey protein are both located on the cytosolic side of the membrane. The topology of ABCB1, based on primary sequence analysis, topological

analysis and the structures of homologues, shows that both the C- and the N-termini are cytoplasmic (Chen et al., 1986, Gerlach et al., 1986a, Gros et al., 1986b). Tagging ABCB1 on either end should therefore make the Cub-LexA-VP16 module available for interaction with NubG.

The interacting protein may be cytoplasmic or an integral membrane protein. Type I integral membrane proteins typically have a cytoplasmic C-terminus and a luminal N-terminus whereas for type II integral membrane proteins the converse is true (Singer et al., 1987) and for multiple transmembrane proteins, either, both or neither termini may be cytoplasmic. Two different cDNA libraries were therefore tested for candidates interacting with ABCB1. In a NubG-prey cDNA library (NubG-X), NubG is fused to the N-terminus

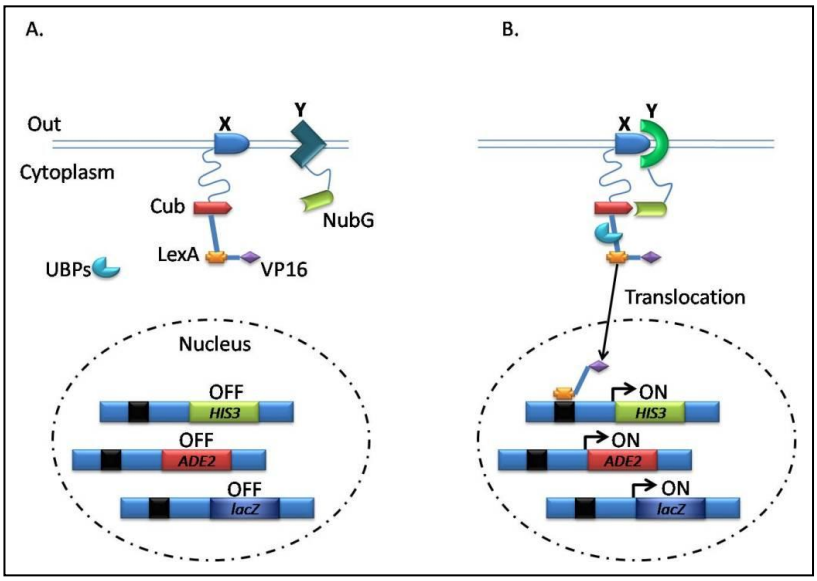

Figure 3-1. ***The split-ubiquitin system for the detection of mbrane-protein interactions.***

(A). The integral membrane protein of interest X is fused to the Cub which is in turn fused to the artificial transcription factor LexA and the transactivation domain VP16. Another protein of interest is fused to the NubG. If X and Y do not interact, Cub and NubG will not re-constitute the "split-ubiquitin". (B). If X and Y interact, Cub and NubG are brought into close proximity to each other which enables them to interact and re-assemble the "split-ubiquitin". This is recognised in-turn by Ubiquitin-specific proteases which cleave off the transcription factor. Consequently, the transcription factor translocates to the nucleus where it drives expression of reporter genes allowing the yeast expressing the interacting protein pair to survive on defined selective media by complementation of auxotrophic markers [modified from (Stagljar and Fields, 2002)].

of the prey protein making it suitable for the screening of membrane proteins with an amino-terminal cytoplasmic domain. On the other hand, a prey-NubG (X-NubG) cDNA library can be used for the screening of membrane proteins with a carboxy-terminal cytoplasmic domain. The topology of the candidates is an unknown factor. Furthermore, it is not possible to predict if a candidate will tolerate amino- or carboxy-terminal modifications or whether the quaternary interaction will survive either of these. For these reasons, it was deemed suitable to screen both libraries to ensure optimal recovery of putative interactors.

3.1.2 Aim

The overall aim of the project was to employ the SU-YTH system to identify proteins that interact with ABCB1.

3.2 Results

3.2.1 Expression of the ABCB1:bait construct in the reporter strain NMY51

3.2.1.1 Efficient transformation of yeast cells and expression of bait protein

Before the use of the SU-YTH system to identify putative ABCB1-interacting partners, it was important to verify the expression of the ABCB1:Cub fusion protein. The cDNA of human ABCB1 was cloned in-frame to the Cub in the pBT3-N (Dualsystems Biotech, Zurich, CH) bait vector (hereafter the ABCB1:Cub vector) and the correct sequence confirmed by DNA sequencing (Linton K. J., personal communication).

The bait vector carries the *LEU2* gene which will complement *LEU2*-deficient NMY51, allowing the cells bearing the bait vector to survive on defined selective media lacking leucine. Yeast cells are most competent when the culture used for the transformation is at an early log phase. In addition, use of freshly prepared transformation reagents (i.e., 50%

(w/v) PEG; poly[ethylene glycol]) as well as single-stranded carrier DNA increase the transformation efficiency by several-fold (Kawai et al., 2010). As shown in Figure 3-2, when NMY51 yeast cells were transformed with the ABCB1:Cub vector following the protocol described by Gietz and Schiestl (Gietz and Schiestl, 2007a), colonies appeared after three days of incubation at 30°C confirming that the yeast cells can be efficiently transformed: (125 colonies × 10,000 [dilution factor])/1.5 μg DNA = 8.0×10^5 cells μg^{-1} "bait" DNA and should express the ABCB1:Cub fusion protein (Figure 3-2). This high transformation efficiency will also be sufficient to express a representative cDNA library.

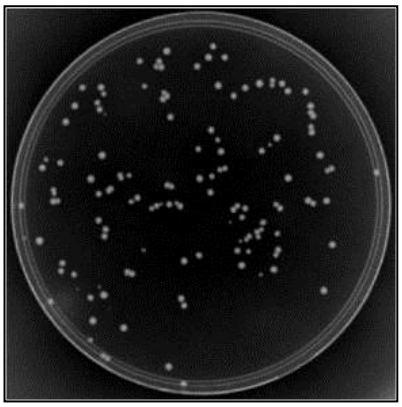

Figure 3-2. ***Representative growth on SD-Leu medium of NMY51 reporter strain transformed with 1.5 μg pBT3-N (ABCB1) bait vector.***

Transformation was carried out using the LiAc/SS carrier DNA/PEG method. Dilution shown 1:10,000 (100 μl plated, 125 colonies recovered).

3.2.1.2 Confirmation of bait protein expression using the "NubI/NubG" test

Following successful transformation of NMY51 cells with the ABCB1:Cub vector, the expression of the bait fusion protein was assayed. The yeast strain expressing the bait protein was co-transformed with the control prey plasmids pAI-Alg5 (NubI) and pDL2-Alg5 (NubG) (Dualsystems Biotech, Zurich, CH). Co-expression of ABCB1:Cub with the wild-type NubI that retains affinity for the Cub resulted in reconstitution of the split-ubiquitin and the activation of reporter genes allowing growth on selective medium by

complementation of auxotrophic markers *HIS3* and *ADE2* (Figure 3-3, panels B-C). Co-expression of the bait together with NubG which has little or no affinity for the Cub did not activate either reporter gene (Figure 3-3, panels E-F). It should be noted that growth on SD-*Trp-Leu* plates is expected for both transformations confirming that both the bait and the prey vectors were taken up by the yeast cells (Figure 3-3, panels A and D). Growth on the selective media strongly suggests that the ABCB1:Cub protein is made by the cells and is able to interact with NubI. However, with this test it can only be assumed that the fusion protein folds correctly and inserts properly in the membrane.

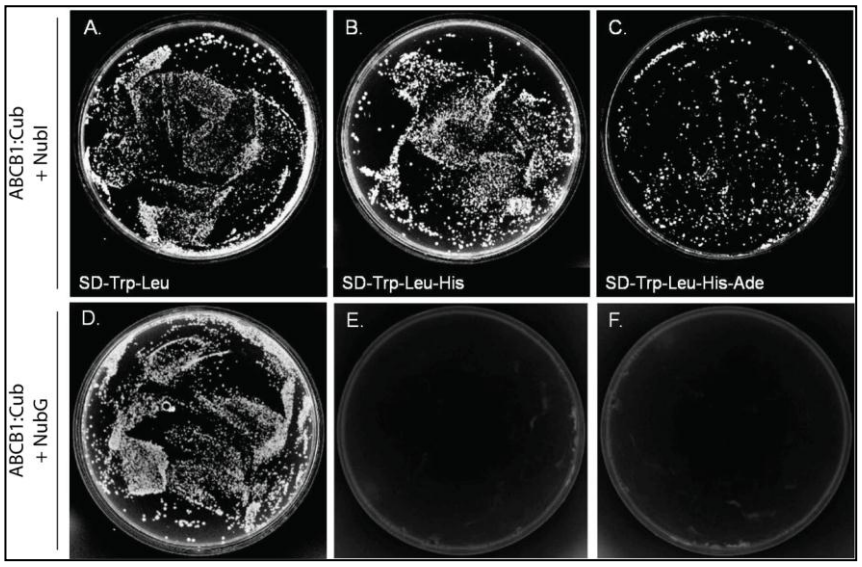

Figure 3-3. ***The "NubI/NubG" test.***

Panels A-C show growth of the yeast cells co-transformed with ABCB1:Cub and NubI on media of increasing stringency. Panels D-F show growth of yeast cells co-transformed with ABCB1:Cub and NubG on media of increasing stringency. The appearance of colonies on SD-*Trp-Leu* plates shows that the yeast were successfully transformed with both "bait" and "prey" vectors. Survival on SD-*Trp-Leu-His* (panel B) and on SD-*Trp-Leu-His-Ade* (panel C) plates confirms that ABCB1:Cub and NubI interact allowing complementation of the auxotrophic markers. When yeast were co-transformed with ABCB1:Cub and NubG, growth was only evident on SD-*Trp-Leu* plates. No survival was observed on the SD-*Trp-Leu-His* or on SD-*Trp-Leu-His-Ade* verifying the lack of interaction between ABCB1:Cub and NubG.

3.2.1.3 Western blotting analysis of bait protein expression

The expression of the ABCB1:Cub bait protein was also tested by western blot of total cell extracts, probed with antibodies specific for ABCB1 or LexA. The bait vector is

maintained at a very low copy number (1-2 copies/cell) and the expression of the fusion protein is under the control of a weak promoter (*CYC1*) in order to minimise the recovery of false positives during a library screen. The prey vector on the other hand, is maintained at a much higher copy number (20-50 copies/cell) and is under the control of a strong promoter (*ADH1*). To assay the differences in expression levels between the bait and prey vectors two additional control vectors (one bait and one prey) were employed that express . different membrane proteins unrelated to the ABC transporter family: (a) the multi-ligand, scavenger receptor CD36 (Greenwalt et al., 1992) which has been implicated in the

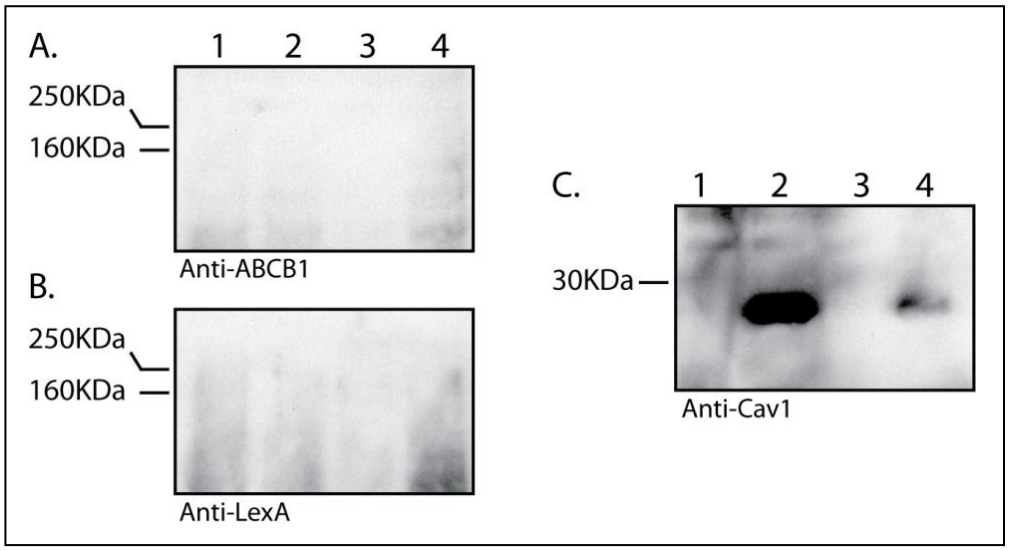

Figure 3-4. ***Western blot on NMY51 total-cell extracts.***

Trichloroacetic acid (TCA)-precipitated whole-cell protein extracts from ~2.4×10^7 – 4.0×10^7 yeast cells were loaded in each well and subjected to western analysis. [Lane 1] ABCB1:Cub + pAI-Alg5 (control vector); [Lane 2] ABCB1:Cub + pPR3-STE:Caveolin (prey vector); [Lane 3] empty; [Lane 4] CD36:Cub + pPR3-STE:Caveolin (prey vector). (A). Mouse ABCB1-specific antibody (C219). (B). Mouse LexA-directed antibody. (C). Rabbit caveolin-1 specific antibody. Apparent molecular masses are indicated in kDa. In lanes 1 and 2 (panels A and B), a protein of approximately 208 kDa (ABCB1:Cub-LexA-VP16 fusion) was expected. No protein was detected using either of the two antibodies. In lane 4 (panel B), a protein of size between 120-130 kDa was expected (CD36:Cub-LexA-VP16 fusion). In lanes 2 and 4 (panel C) a protein of approximately 22 kDa (Caveolin-1:NubG) was detected.

development of atherosclerosis (Febbraio et al., 2000) and insulin resistance (Aitman et al., 1999) and (b) caveolin-1, a structural component of lipid rafts (Galbiati et al., 2001, Simons and Ikonen, 1997) shown to act as a negative regulator of ABCB1 (Barakat et al., 2007,

Jodoin et al., 2003). The cDNA for CD36 was cloned into the pBT3-N bait vector (Linton K. J., and Wharton J., personal communication) and the cDNA for caveolin-1 was cloned into the pPR3-STE prey vector (Wharton J., personal communication).No ABCB1-fusion proteins were detected in the lanes where total cell extracts from the transformed yeast cells were loaded and probed with the mouse ABCB1-specific antibody (Figure 3-4; lanes 1 and 2 on panels A and B). This contrasts with the result of the NubI/NubG test whereby expression of ABCB1:Cub was confirmed by auxotrophic complementation.

The reason for this discrepancy may lie in the design features of the pBT3-N bait vector outlined earlier. As the bait vector is maintained at a very low copy number and the expression of the fusion protein is under the control of the *CYC1* promoter, it is likely that ABCB1:Cub is expressed at levels below the detection threshold of the western. This is also likely to be true for the CD36:Cub fusion on the anti-LexA blot for which no signal was detected at the appropriate molecular weight (Figure 3-4; panel B, lane 4). Although CD36:Cub fusion protein was not detected on the western blot, the library screen with CD36 as bait (Snippe M., personal communication) provides evidence that the CD36:Cub is expressed as CD36:Nub interactors were recovered including CD36 itself (CD36 is known to dimerise; (Daviet et al., 1997, Thorne et al., 1997). The prey vector on the other hand, is maintained at high copy number and is under the control of the *ADH1* promoter. As shown in Figure 3-4 (panel C, lanes 2 and 4) caveolin-1 was detectable as it is expressed at a higher level from the pPR3-STE vector.

3.2.1.4 Analysis of ABCB1 functionality using the anti-fungal reagent FK506

In the absence of detectable ABCB1:Cub by western analysis, the functional activity of the drug pump in yeast cells was tested to assess ABCB1:Cub expression. This assay was based on work carried out previously which showed that ABCB1 can be expressed and is

functional in yeast by measuring the resistance of ABCB1-expressing cells to the anti-fungal drug FK506 (Raymond et al., 1994, Saeki et al., 1993). No difference was observed between the survival rates of ABCB1:Cub-expressing yeast cells and the control cells expressing CD36:Cub at concentrations of FK506 between 10-100 μg ml^{-1} (see methods for details, data not shown). This observation could again be attributed to the low level of expression of the ABCB1:Cub fusion protein from the bait plasmid.

3.2.2 Testing the interaction of ABCB1 with its putative interactors Caveolin-1 and PKCα

ABCB1 has already been suggested to interact with caveolin-1 (Barakat et al., 2007, Jodoin et al., 2003) and to be a substrate of PKCα (Fine et al., 1988, Germann et al., 1996, Goodfellow et al., 1996). To further confirm these interactions and to test the capacity of the SU-YTH system to be used with ABCB1, caveolin:Nub and PKCα:Nub fusion constructs were generated.

3.2.2.1 Investigating the interaction of ABCB1 with Caveolin-1

When the Cav:NubG was co-expressed with ABCB1:Cub no colonies were observed on SD-*Trp-Leu-His*/SD-*Trp-Leu-His-Ade* selective plates (data not shown), although growth was observed on the SD-*Trp-Leu* medium indicating uptake of both plasmids into the yeast. This lack of growth in the absence of histidine and adenine suggests that ABCB1 and caveolin do not interact in the yeast-based system at least under the screening conditions used. The possibility that the interaction is affected by the C-terminal fusion of the Cub on ABCB1 is unlikely as the proposed caveolin-binding motif (FTMFRYAGW) is located on the cytosolic N-terminus of ABCB1 (Demeule et al., 2000, Jodoin et al., 2003). The reason(s) for the lack of interaction in the yeast are presently unknown but perhaps is due to the carboxy-terminal modification of caveolin with NubG which may prevent interaction with ABCB1.

3.2.2.2 Investigating the interaction of ABCB1 with PKCα

In order to test the interaction of ABCB1 with PKCα *in vivo*, the cDNA for PKCα first had to be fused to the cDNA for NubG in the pPR3-STE prey vector (Figure 3-5).

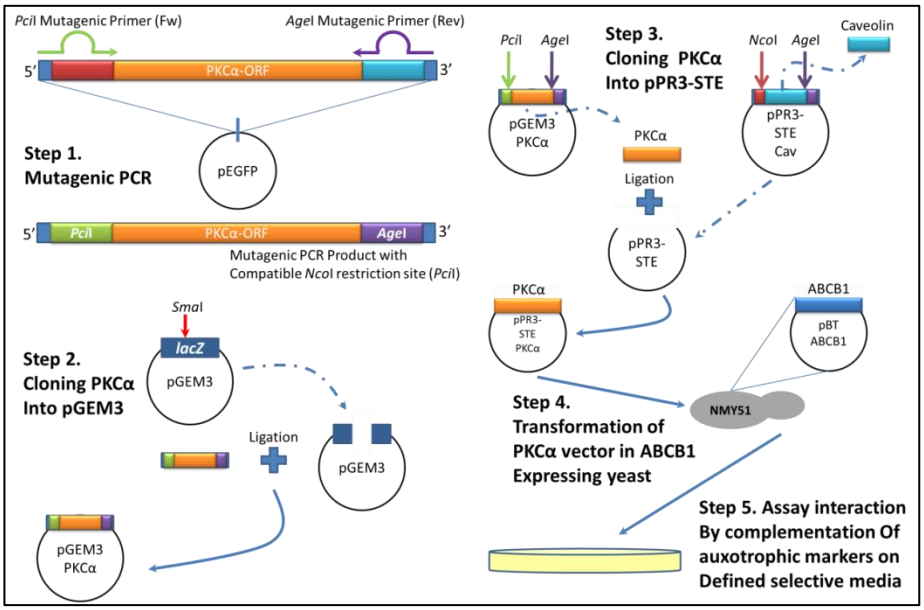

Figure 3-5. ***Summary of the strategy followed to clone the PKCα cDNA into the pPR3-STE yeast expression vector.***

Initially the PKCα-ORF was amplified by mutagenic PCR introducing a 5'-*PciI* and a 3'-*AgeI* restriction site (Step 1). Next, the blunt-ended PCR product was introduced into the *SmaI* restriction site of the pGEM3 vector (Step 2). The ligated products were then transformed into bacteria and recombinants were selected in a blue/white screen. The sequence-verified pGEM3:PKCα vector was then digested with *AgeI*/*PciI* restriction enzymes to excise the PKCα sequence. At the same time, the pPR3-STE:Cav vector was digested with *AgeI*/*NcoI* to excise the caveolin sequence. PKCα and pPR3-STE were purified from an agarose gel, ligated (Step 3) and transformed into bacteria. The pPR3-STE:PKCα vector was confirmed by restriction digest with *Dra*III and transformed into the ABCB1:Cub-expressing NMY51 yeast strain (Step 4). Colony-formation on defined selective media by complementation of auxotrophic markers aimed to test the interaction between ABCB1 and PKCα (Step 5).

The caveolin cDNA was cloned between the *Nco*I and *Age*I restriction sites introduced into the modified pPR3-STE vector (Linton K. J., and Wharton J., personal communication) to generate an in-frame fusion with NubG. *In silico* analysis of PKCα sequence identified an *Nco*I restriction site within its cDNA, however, *Pci*I generates compatible cohesive ends suitable for cloning into an *Nco*I site. Mutagenic primers were therefore designed to amplify the PKCα-cDNA from a GFP-PKCα vector (obtained from A. Sardini) and simultaneously

introduce a *Pci*I site at the 5'-end and an *Age*I site at the 3'-end of the PCR product (Figure 3-5; Step 1).

Following successful amplification of the sequence of interest (Figure 3-6A), the blunt-ends of the PCR product were ligated to the pGEM3®-3Zf(-) vector cut with *Sma*I (Figure 3-5; Step 2), transformed into *E. coli* and plated onto LB (Lysogeny broth) agar plates supplemented with ampicillin (the selectable marker on the plasmid), IPTG (Isopropyl 1-thio-β-D galactopyranoside) and X-gal (5-bromo-4-chloro-3-indolyl-beta-D-galactopyranoside). The pGEM3®-3Zf(-) vector was chosen because it can offer α-complementation when transformed into an appropriate bacterial host strain (e.g. XL10-Gold® Ultracompetent cells) allowing blue/white screening for recombinants. When *lacZ* expression is induced by IPTG in the presence of the chromogenic substrate X-gal, colonies containing plasmids with inserts will be white, while colonies containing plasmids without inserts will be blue. After a 24 h incubation at 37°C, several white colonies (i.e. likely to carry the PKCα insert within the *lacZ* coding sequence) were selected. The plasmid DNA was recovered and digested with *Hind*III (Figure 3-6B; top panel) and *Xmn*I (Figure 3-6B; bottom panel) to identify recombinant plasmids carrying the PKCα cDNA.

The restriction profiles indicated that "Clone#46" carried the PKCα cDNA (Figure 3-6B). The integrity of the insert was verified by DNA sequencing. "Clone#46" was then digested with *Pci*I/*Age*I to excise the PKCα-ORF, and the pPR3-STE:Cav with *Nco*I/*Age*I to excise the caveolin-cDNA (Figure 3-5; Step 3 and Figure 3-6C).

The pPR3-STE(*Nco*I/*Age*I) vector and the PKCα-cDNA(*Pci*I/*Age*I) were purified and ligated (Figure 3-5; Step 3). The ligation product was transformed into XL10-Gold® ultracompetent cells and several colonies were selected for DNA extraction/purification.

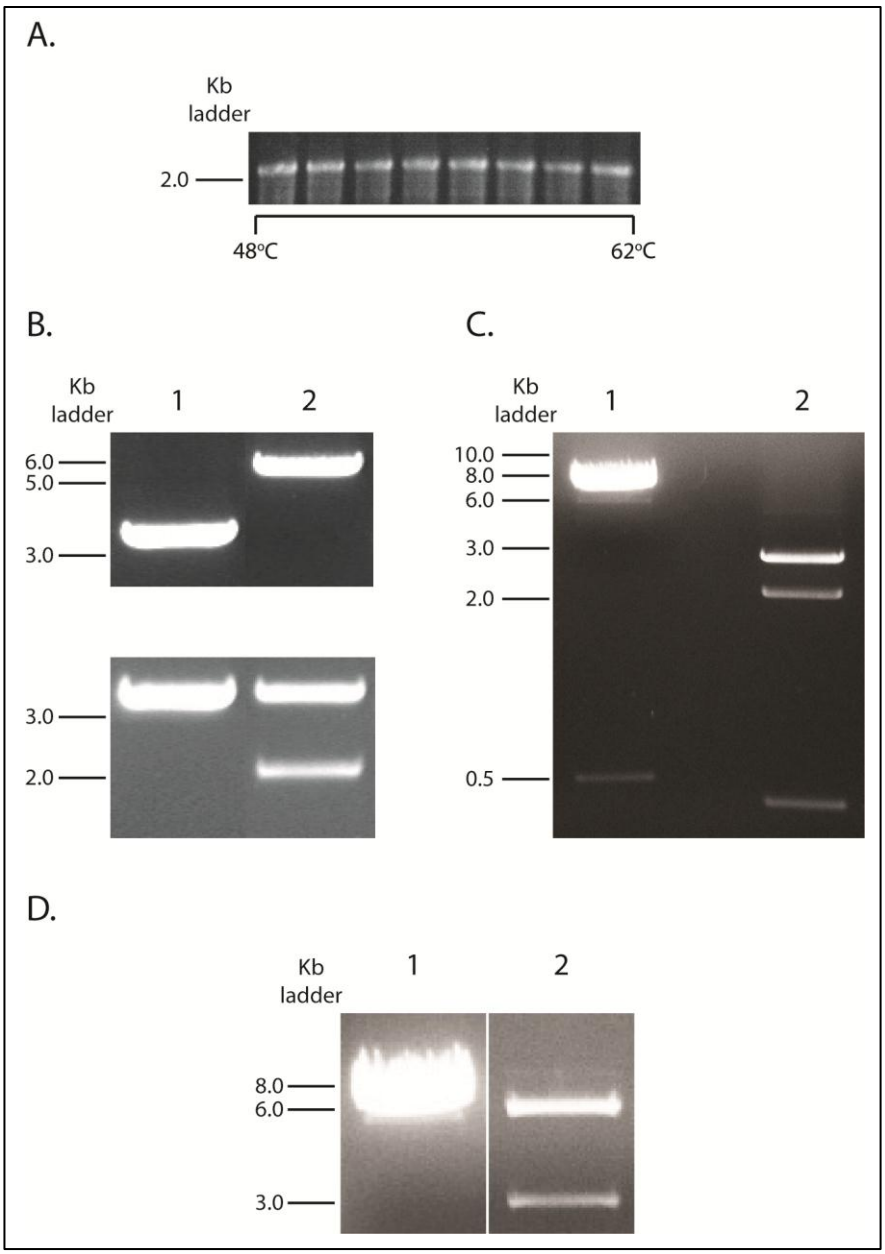

Figure 3-6. ***Cloning the the PKCα cDNA into the pPR3-STE expression vector.***

(A). Mutagenic PCR to amplify the PKCα-cDNA from the GFP-PKCα vector and introduce a *Pci*I (5'-end) and an *Age*I (3'-end) restriction site. The reaction was carried out at a temperature gradient (48^{o}C – 62^{o}C) to identify the best annealing temperature for the primers. (B). Restriction digest profile of "clone#46" using *Hind*III (top panel) and *Xmn*I (bottom panel). Sample DNA (400 ng) was digested and run on 1.0% (w/v) agarose gel. *Hind*III digest: for the pGEM3®-3Zf(-) empty vector only one fragment was expected of 3197 bp (top panel, lane 1) and for the pGEM3®-3Zf(-):PKCα a fragment at 5242 bp was expected (top panel, lane 2). *Xmn*I digest: for the empty vector, a single fragment of size 3157 bp was expected (bottom panel, lane 1) and for the pGEM3®-3Zf(-):PKCα construct two fragments of size 3185 bp and 2057 bp were expected (bottom panel, lane 2). (C). Restriction digest profile of pPR3-STE:Cav (lane 1) and pGEM3:PKCα (lane 2) using the restriction enzymes *Nco*I/*Age*I and *Pci*I/*Age*I respectively. The digested products (750 ng for pPR3-STE:Cav; 1 µg pGEM3:PKCα) were run on 1.0% (w/v) agarose gel. *Nco*I/*Age*I digest (lane 1): Two fragments of size 6591 bp (pPR3-STE [*Age*I/*Nco*I]) and 533 bp (caveolin [*Age*I/*Nco*I]) were expected. *Pci*I/*Age*I digest (lane 2): Three fragments of size 2788 bp (pGEM3 [*Pci*I/*Pci*I]), 2012 bp (PKCα [*Pci*I/*Age*I]) and 442 bp (pGEM3 [*Pci*I/*Age*I]) were expected. (D). Restriction profiles of pPR3-STE:Cav (lane 1) and pPR3-STE:PKCα (lane 2). The constructs were digested with *Dra*III. As *Dra*III only cuts once within the vector sequence, only one fragment at 7124 bp was expected (lane 1). For the pPR3-STE:PKCα digest, two fragments of size 5817 bp and 2786 bp were expected (right lane).

The extracted DNA was digested with *Dra*III to verify the cloning of PKCα into the pPR3-STE vector (Figure 3-6D).

Finally, the NMY51 reporter strain was co-transformed with the ABCB1:Cub bait and the PKCα:NubG prey vectors and tested for an interaction by complementation of auxotrophic markers. Growth was detected on the SD-*Trp-Leu* plates (i.e. yeast cells had taken up both bait and prey vectors; data not shown), however, no colonies were visible on the SD-*Trp-Leu-His-Ade* plates indicating a lack of interaction between ABCB1:Cub and PKCα:NubG (data not shown).

The lack of a good positive control for the library screen (i.e. no complementation of the auxotrophic markers on co-expressing ABCB1:Cub with either PKCα:Nub or Cav:Nub) was a concern, and indicated the SU-YTH system will not identify every protein interacting with ABCB1. However, there could be a perfectly reasonable explanation. For example, fusion of Nub to the C-terminus of PKCα or caveolin-1 could sterically hinder interaction with ABCB1, or perhaps PKCα requires stimulation to engage ABCB1. Nevertheless, the prior description of functional ABCB1 expression in yeast (Goodfellow et al., 1996, Raymond et al., 1994), and the behaviour of the ABCB1:Cub with the NubI positive control, suggested that a library screen was likely to be productive.

3.2.3 Evaluation of the level of self-activation and determination of the optimal conditions for the library screen

For a library screen the optimal screening conditions have to be determined. This was achieved by co-transformation of NMY51 with ABCB1:Cub and the pPR3-N NubG-X empty library vector. No interaction is expected between the ABCB1:Cub and NubG proteins therefore any colonies arising on plates of selective medium (SD-*Trp-Leu-His*/SD-*Trp-Leu-His-Ade*) are non-specific background. To ensure that as few as possible false

positives arise on the selection plates, the medium was supplemented with 1-10 mM of 3-AT, a competitive inhibitor of the *HIS3* gene product that increases the stringency of selection. At a 3-AT concentration of 2.5 mM on SD-*Trp-Leu-His-Ade* plates all growth of yeast containing the ABCB1:Cub and the NubG vectors was inhibited. Transformation efficiency was also measured in this experiment; i.e., the number of colonies appearing on the SD-*Trp-Leu* plates. The total number of transformants on SD-*Trp-Leu* was 1.9×10^6 clones per μg DNA (or a total of 4×10^7 colonies); a transformation efficiency almost 20× greater than recommended by the manufacturer (Dualsystems Biotech, Zurich, CH) for introducing the cDNA library.

3.2.4 Library transformation and selection of interactors

ABCB1 is highly expressed on the canalicular membrane of the hepatocyte (Thiebaut et al., 1987). The ABCB1:Cub bait was therefore screened against two human adult liver libraries, NubG-X and X-NubG (Dualsystems Biotech, Zurich, CH). In NubG-X libraries the NubG is fused to the N-terminus of the prey. Any protein whose N-terminus is located in the cytoplasm and which tolerates an N-terminal fusion, will be available to interact with the Cub on the carboxy terminus of ABCB1:Cub. The X-NubG libray was also screened, in which NubG is fused to the C-terminus of the prey suitable for use with proteins when their C-terminus is cytoplasmic.

3.2.4.1 Library characterisation

The cDNA libraries from Dualsystems Biotech were derived from cells of an adult human liver. The company literature reports that the cDNAs were digested with *Sfi*I, size-fractionated and purified before cloning into the NubG-X or the X-NubG library vectors, as appropriate.

The NubG-X cDNA library should have a complexity of 1.5×10^6 independent clones ranging in size from 0.5 – 2.5 Kb (average size 1.3 Kb; see below) and the X-NubG library should have a complexity of 1.3×10^6 independent clones ranging in size from 0.3 – 4 Kb (average size 1.2 Kb) as stated by the supplier (Dualsystems Biotech, Zurich, CH). To achieve a reasonable likelihood of sampling each clone in the library a minimum of 1.3×10^7 clones in the library screen was desirable (i.e., 10× the number of clone equivalents).

To confirm the quality of the cDNA libraries employed; a qualitative test was performed on isolated plasmid DNA from randomly selected clones. As mentioned earlier the average insert size cloned between the *Sfi*I sites of the library vectors should be between 1.2 and 1.3 Kb (minimum 0.3 Kb and maximum 4.0 Kb). Consequently, digesting the vectors with *Sfi*I should release an insert within this range. As shown in Figure 3-7, cDNA inserts covering a range of sizes were released from the NubG-X or the X-NubG vectors confirming the manufacturer's description. On average, from ten clones from each library, the mean insert size was 1.3 Kb for both the NubG-X and the X-NubG. The insert sizes vary from 0.5 Kb to 3.0 Kb but most are within the range of 1.0 to 1.5 Kb (Figure 3-7).

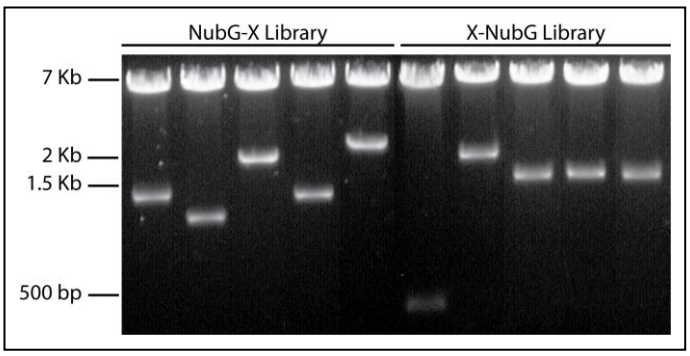

Figure 3-7. ***SfiI digestion of plasmid DNA from the NubG-X and the X-Nub-G libraries.***

Plasmid DNA (1 µg) was digested with *Sfi*I and run on 1.0% (w/v) agarose gel. An array of insert sizes ranging from 0.3 – 4.0 Kb was expected. Average insert size from a total of 10 samples for each library: 1.3 Kb. Size of empty library vectors: 6.3 and 6.6 Kb for the NubG-X and X-NubG library vectors, respectively.

3.2.4.2 Library screen

Using 28 μg of prey DNA and obtaining a transformation efficiency of ~9.7×10^5 and ~8.2×10^5 clones per μg DNA (as detected by growth on SD-*Trp-Leu* plates) for the NubG-X and the X-NubG libraries, respectively, a total of 18 clone equivalents were screened for each library. Since a cDNA library represents the expression pattern in the hepatocyte, highly expressed genes will be over-represented. Furthermore, since the digested cDNA fragments were separated according to size, genes smaller than the minimum insert size would be not represented in the library. For larger genes it is hoped that domains that fold independently will be represented.

Interacting bait and prey are recognised by growth of their yeast host on the SD-*Trp-Leu-His-Ade* plates supplemented with 2.5mM 3-AT, and also by colonies that are faint-pink to white in colour (see below for a more detailed account on the basis of the coloured shunt intermediate accumulation). Upon completion of the NubG-X and the X-NubG library screen, a total of 130 and 12 colonies were isolated from each library, respectively. Each colony should express a putative interacting protein pair.

3.2.4.2.1 Clone identification

To reveal the identity of each putative ABCB1 interactor, the library plasmid was isolated from the yeast colonies, transformed into *E. coli*, isolated from the bacterial colonies and sent for sequencing analysis. The bait and prey vectors are bifunctional and can therefore be maintained in both yeast and *E. coli*. Prey plasmids carry the β-lactamase gene so bacteria that have been transformed successfully can be propagated on LB agar plates supplemented with ampicillin. Bait plasmids encode only the kanamycin selectable marker, therefore only *E. coli* which have taken up the library plasmid grow in the presence of ampicillin.

From the 130 putative interactors isolated from the NubG-X library screen, fifteen (~12%) could not be transformed and amplified in *E. coli* and may well encode a product deleterious to the bacteria.

Isolation of the plasmids which gave rise to bacterial colonies, sequencing and *in silico* analysis using the BLAST algorithm allowed for further sorting of the candidates. During transformation, yeast can take up more than one plasmid and it is possible that the recovered plasmid is not the one that is able to rescue growth on the selective yeast-medium. Accordingly, twelve (~9%) appeared to be empty vectors i.e. not carrying a cDNA insert based on sequence analysis and five (~4%) of the isolated clones did not form colonies in the clone-confirmation assay (Section 3.2.4.2.2). Four (~3%) encoded ubiquitin which has been reported to be isolated occasionally from NubG-X libry screens (Iyer et al., 2005).

Twenty (~15%) encoded proteins which, based on what is known for ABCB1 function and localisation, were not likely to interact. These included peroxisomal proteins such as enoyl CoA hydratase 1 (ECH1) which is involved in the β-oxidation of fatty acids (Hiltunen et al., 2003, Reddy and Mannaerts, 1994) as well as the mitochondrial malate dehydrogenase 2 (MDH2) involved in the citric acid cycle (Musrati et al., 1998).

A total of seventy four (~57%) encoded a potentially interesting candidate. Many clones were isolated more than once. Alignment of the sequence of the isolated clones originating from the same gene revealed that not all inserts were equal in length but all aligned to the 3'-end of the respective gene's coding sequence, as expected based on the strategy used to create the library (Dualsystems Biotech, Zurich, CH). For example, cDNA from the gene

STAT6 (signal transducer and activator of transcription 6) was the most prevalent in the screen (isolated 17 times; Table 3-1, column 1). All 17 clones aligned to the 3'-end of the *STAT6* coding sequence but most of them had a different length of coding sequence meaning that they are likely the product of different cloning events rather than the result of the plasmid being amplified through a selective advantage in *E. coli*. In addition, some of the clones, such as those encoding for VKOR (vitamin K oxido-reductase), an enzyme involved in the recycling of oxidised vitamin K (Zimmermann and Matschiner, 1974, Li et al., 2004, Rost et al., 2004), carried the whole coding sequence of the gene.

Sequence analysis of the twelve candidates isolated from the X-NubG screen revealed that they all encoded for the amino terminus of ubiquitin cloned from the liver library and were therefore considered false positives. Isolation of ubiquitin as an interacting partner is perhaps not surprising as ABCB1 is regulated via a ubiquitination-dependent pathway (Zhang et al., 2004).

3.2.4.2.2 Clone retransformation and confirmation of interaction with ABCB1

To confirm the findings of the NubG-X screen, isolated prey plasmids were re-transformed into the ABCB1:Cub-bearing yeast strain. This was done in order to identify more false positives. As mentioned earlier, it is possible that during library transformation, the yeast cells take up more than one prey vector or the yeast may have survived due to an endogenous genetic change.

Individual clones of retransformed NMY51 were grown on plates lacking tryptophan and leucine (SD-*Trp-Leu*), selecting only for the maintenance of the two plasmids. The clones were then spotted on SD-*Trp-Leu-His-Ade* plates supplemented with a range of 0-4 mM of 3-AT. The clones were also spotted on SD-*Trp-Leu* plates at the same time for comparison

of colony growth. The control prey plasmids pAI-Alg5 (NubI) and pDL2-Alg5 (NubG; a control vector that codes for Cub fused to the endoplasmic reticulum transmembrane protein Alg5p) supplied by the manufacturer (Dualsystems Biotech, Zurich, CH), were also employed as positive and negative controls, respectively.

Figure 3-8 is a representative example of the result obtained after 3-4 days of growth at 30°C. All prey vectors were successfully transformed into the yeast complementing the auxotrophic markers on the SD-*Trp-Leu* plates (*LEU2* for "bait", *TRP1* for "prey"; Figure 3-8A). The lack of growth on the SD-*Trp-Leu-His-Ade* media for some of the transformants carrying both vectors (Figure 3-8B shows growth on SD-*Trp-Leu-His-Ade* plates plus 3 mM 3-AT but is comparable to plates with 2 mM and 4 mM 3-AT), indicates that some clones do not encode an ABCB1-interacting partner. For example clone 4i when co-expressed with ABCB1:Cub supports yeast growth on the SD-*Trp-Leu-His-Ade* plate suggesting that 4i is a true ABCB1 interactor. In contrast, when clone 25i was co-expressed with ABCB1:Cub, although the yeast cells were able to grow on SD-*Trp-Leu* plate (i.e., had taken up both bait and prey vectors) no growth was observed on the SD-*Trp-Leu-His-Ade* plate. Using this approach, 5 candidates (~4%) were discarded.

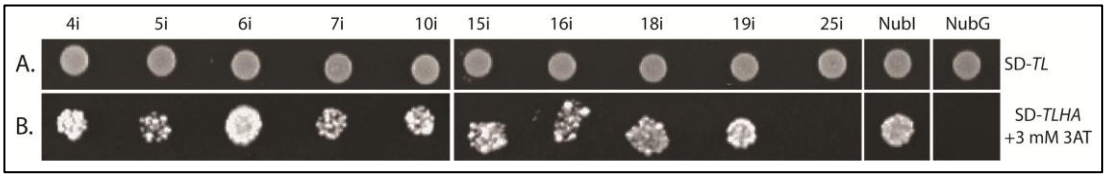

Figure 3-8. ***Reconfirmation of the interaction between ABCB1 and candidate partner proteins in yeast.***

(A). Yeast growth on SD-*Trp-Leu* media. Growth on this plate denotes that both bait (ABCB1:Cub) and prey vectors were taken up by the yeast cells during the transformation. (B). Replicate SD-*Trp-Leu-His-Ade* plate supplemented with 3 mM of 3-AT, an inhibitor of the *HIS3* gene product. Growth on this plate indicates that the proteins encoded by bait and prey vectors interact and drive expression of the reporter genes (*His* and *Ade*). Clone numbers are indicated in the top row. NubI, positive control; NubG, negative control.

Following the elimination of all false positives 29 unique putative intetacting partners were recovered (Table 3-1; final 3 columns).

Sequence ID (BLAST) and Clone ID	Clones	Colour			Growth on SD-TLHA + 3mM 3AT		
		ABCB1:Cub	FATP4:Cub	Alg5p:Cub	ABCB1:Cub	FATP4:Cub	Alg5p:Cub
STAT6 Clone(s): 23i, 37i, 39i, 41i, 48i, 52i, 62i, 65i, 69i, 83i, 88i, 89i, 105i, 110i, 121i, 122i, 130i	17				++	+++	+++
EBP Clone(s): 27i, 29i, 34i, 40i, 42i, 49i, 58i, 81i, 91i, 97i, 104i, 106i, 116i, 119i	14				+++	+++	+++
IFITM3 Clone(s): 10i, 24i, 46i, 54i, 71i, 75i, 77i, 82i, 85i, 102i	10				Ø	++	+++
SERP1/RAMP4 Clone(s): 18i, 20i, 22i, 38i, 64i, 78i, 80i, 101i, 112i, 126i	10				++	++	+++
VKORC1 Clone(s): 4i, 14i, 53i, 92i, 114i	5				+++	+++	+++
TMBIM4 Clone(s): 43i, 59i, 61i	3				++	++	+++
ARL6IP5 Clonse(s): 57i, 74i	2				+	++	++
ASGR2 Clones(s): 44i, 111i	2				+	+++	+++
CYB5A Clone(s): 55i, 107i	2				Ø	+++	+++
PLP2 Clone(s): 63i, 66i	2				Ø	Ø	+++
VAPB Clone(s): 11i, 72i	2				++	+++	+++
acylCoA Dehydrogenase Clone(s): 7i	1				++	+++	+++
ATP6V0B Clone(s): 45i	1				Ø	Ø	+++

Table 3-1. ***Phenotype of the 29 candidates isolated from the NubG-X library screen.***

The numbers highlighted in blue, indicate the putative interactors that were compared for specificity and strength of interaction with ABCB1:Cub in comparison with the FATP4:Cub and the Alg5p:Cub controls. In cases where a candidate was isolated more than once, one was selected and used in the experiment. "+" indicates the degree of yeast cell growth on the selective plates (SD-*Trp-Leu* or SD-*Trp-Leu-His-Ade*) in the following order: +++ > ++ > + > Ø. Shaded boxes indicate the colour of the yeast colonies on SD-*Trp-Leu* plates: white= a strong interaction between the proteins encoded by the co-transformed "bait" and "prey" vectors, pink= intermediate interaction and red= lack of interaction. All the co-transformed cells gave rise to colonies on SD-*Trp-Leu* selective plates indicating that they had taken up both "bait" and "prey" vectors. *STAT6*, signal transducer and activator of transcription 6; *IFITM3*, interferon induced transmembrane protein 3; *SERP1*, stress-associated endoplasmic reticulum protein 1; *VKORC1*, vitamin K epoxide reductase complex (subunit 1); *TMBIM4*, transmembrane BAX inhibitor motif containing 4; *ARL6IP5*, ADP-ribosylation-like factor interacting protein 5; *ASGR2*, asialoglycoprotein receptor 2 (transcript variant 1); *CYB5A*, cytochrome b5 type A; *PLP2*, proteolipid protein 2; *VAPB*, vesicle-associated membrane protein-associated protein B; *ATP6V0B*, ATPase H^+ transporting lysosomal 21kDa V0 subunit b.

Sequence ID (BLAST) and Clone ID	Clones	Colour			Growth on SD-TLHA + 3mM 3AT		
		ABCB1:Cub	FATP4:Cub	Alg5p:Cub	ABCB1:Cub	FATP4:Cub	Alg5p:Cub
CD63 Clone(s): 128i	1				++	+++	+++
CD81 Clone(s): 96i	1				++	+++	+++
CRP Clone(s): 108i	1				Ø	Ø	Ø
Ergic32 Clone(s): 16i	1				+++	+++	+++
Ferritin Light Polypeptide Clone(s): 13i	1				Ø	Ø	Ø
FXYD5 Clone(s): 100i	1				++	+++	+++
HDAC6 Clone(s): 73i	1				+++	+++	+++
LASS2 Clone(s): 99i	1				+++	+++	+++
MDH2 Clone(s): 51i	1				Ø	Ø	Ø
SERPINA1 Clone(s): 125i	1				Ø	Ø	+++
SOX4 Clone(s): 113i	1				Ø	+++	+++
SSR3 Clone(s): 32i	1				+++	+++	+++
TM9SF4 Clone(s): 56i	1				Ø	+++	+++
TMEM85 Clone(s): 21i	1				+	+	+++
TNFSF13B Clone(s): 90i	1				++	+++	+++
YIF1A Clone(s): 33i	1				Ø	++	+++
UB Clone(s): 6i, 36i, 70i, 76i	4				+++	+++	+++

Table 3-1. (continued) Phenotype of the 29 candidates isolated from the NubG-X library screen. ; *CRP*, C-reactive protein; *Ergic32*, ER-Golgi intermediate compartment protein 32; FXDY5, FXYD domain-containing ion transport regulator 5; *HDAC6*, histone de-acetylase 6; *LASS2*, ceramide synthase 2.*MDH2*, malate dehydrogenase 2*; SERPINA1*, serpin peptidase inhibitor member 1; *SOX4*, sex-determining region box 4; *SSR3*, signal sequence receptor gamma; *TM9SF4*, transmembrane 9 superfamily protein member 4; *TMEM85*, transmembrane protein 85; *TNFSF13B*, tumour necrosis factor superfamily member 13; *YIF1A*, Yip1 interacting factor homolog A; UB, ubiquitin.

3.2.5 Determination of the specificity of interaction between ABCB1:Cub and its interactors

The cDNA of the mouse long-chain fatty acid transporter FATP4 (Doege and Stahl, 2006, Hirsch et al., 1998, Gimeno et al., 2003) had been cloned into the pBT3-N bait vector

(Linton K. J., and Wharton J., personal communication). This construct has been used to screen a mouse heart expression library recovering prey proteins implicated in fat metabolism. Interaction has also been confirmed by co-IP, thus it is clear that FATP4:Cub expresses appropriately in yeast.

In order to assess the specificity of interaction between the proteins identified from the library screen and ABCB1:Cub, each of the confirmed candidates was co-expressed in the NMY51 strain with (a) ABCB1:Cub, (b) FATP4:Cub and (c) pCCW-Alg5p:Cub. The rationale behind this experiment was that the FATP4:Cub and the Alg5p:Cub would act as more stringent negative controls as neither FATP4 nor Alg5p are related to ABCB1 but both proteins, linked to Cub, should be present in the membrane. No growth or dramatically reduced growth was therefore expected for cells co-expressing any of the candidates that specifically interact with ABCB1 and the two negative controls when plated on SD-*Trp-Leu-His-Ade* selective plates.

For this experiment, colony colour was also monitored as this is related to the strength of bait and prey interaction. The NMY51 yeast strain carries a mutation in the *ADE2* gene which codes for a key enzyme in the adenine biosynthetic pathway. This enzyme, phosphoribosylaminoimidazole carboxylase (or AIR carboxylase), catalyses the conversion of 5'-phosphoribosyl-5-aminoimidazole (AIR) to 5'-phosphoribosyl-4-carboxy-5-aminoimidazole (CAIR). In the presence of low concentrations of adenine, AIR accumulates in the yeast cells and is oxidised into a red shunt intermediate (Roman, 1956, Dorfman, 1969, Gedvilaite and Sasnauskas, 1994, Stotz et al., 1993). Supplementation of high concentrations of adenine negatively inhibits the adenine biosynthetic pathway and the NMY51 strain fails to accumulate the red shunt product. This observation can be exploited to provide a measure of the strength of the interaction between the library

protein and ABCB1 on the SD-*Trp-Leu* medium containing low concentrations of adenine sufficient to allow growth, but insufficient to fully inhibit the adenine biosynthetic pathway. White colonies would result from the presence of an interacting pair inducing *ADE2* gene expression via the released LexA-VP16 transcription factor. On the other hand, red colonies would be expected for cells co-transformed with FATP4:Cub or Alg5p:Cub and any of the putative interactors on the SD-*Trp-Leu* plates as the lack of interaction (for candidates that interact specifically with ABCB1) would be unable to drive expression of AIR carboxylase. AIR would therefore accumulate and be converted into the red shunt product.

Figure 3-9 shows a representative result of such an experiment. The first observation is that all transformation experiments were carried out successfully as indicated by the visible growth of colonies on the SD-*Trp-Leu* plates (Figure 3-9, panels A and C) i.e. both "bait" and "prey" vectors were taken up by the yeast. The Alg5p:NubI and Alg5p:NubG transformants (respective positive and negative controls from Dualsystems Biotech) returned the expected result. Specifically, good growth was observed in the presence of Alg5p:NubI irrespective of the bait (Figure 3-9; column 8 on panel B and column 6 on panel D), and no growth, or markedly reduced growth, was observed in the presence of Alg5p:NubG on SD-*Trp-Leu-His-Ade* medium (Figure 3-9; column 9 on panel B and column 7 on panel D).

The ideal ABCB1 interactor would be able to rescue growth on SD-*Trp-Leu-His-Ade* plates only when co-expressed with ABCB1:Cub and not with FATP4:Cub or Alg5p:Cub. Supplementing the plates with the 3-AT inhibitor should inhibit any non-specific growth. Surprisingly, at 3mM 3-AT growth is inhibited for some cells transformed ABCB1:Cub and some of the putative interactors whereas in the cells transformed with the equivalent

interactor and FATP4:Cub or Alg5p:Cub growth is less affected (for example see Figure 3-9; clone 44i on panel B and clone 63i on panel D). This observation did not change at different concentrations of 3-AT (data not shown). Such clones were therefore considered not to interact specifically with ABCB1 and were discarded.

If colony growth on the SD-*Trp-Leu-His-Ade* plates was not a good discriminating phenotype, then the colony colour on SD-*Trp-Leu* was used to gauge the specificity and strength of interaction. The colonies in the top row on panels A and C, where ABCB1 was co-expressed with its putative interactors or the positive control Alg5p:NubI, were expected to be white or faint pink, while colonies in which any of the candidate preys were co-expressed with either FATP4:Cub (second row on Figure 3-9 panels A and C) or Alg5p:Cub (third row on Figure 3-9 panels A and C) were expected to be red because of the accumulation of the coloured, adenine shunt intermediate. A similar result is anticipated when any of the three baits (ABCB1:Cub, FATP4:Cub, Alg5p:Cub) is co-expressed with the negative control Alg5p:NubG (Figure 3-9; column 9 on panel A and column 7 on panel C; the variability in the colour phenotype is evident here with ABCB1 and Alg5p colonies turning red and the FATP4 remaining a paler colour, so results should be interpreted with care). In Figure 3-9A and C, the colonies transformed with ABCB1:Cub and any of its putative interactors were red or faint pink in colour (for example see Figure 3-9; clones 29i and 44i on panel A and clones 33i and 63i on panel C). Pale colouration may be indicative of a strong interaction but in the cases where this was observed it also occurred in the colonies transformed with the candidate interactor and either of the two negative control baits (for example see Figure 3-9; clone 4i on panel A and clone 33i on panel C). The results of this experiment for all 29 putative interacting proteins are summarised in the "colour" section of Table 3-1.

This experiment was designed to discriminate between specific ABCB1-interacting partners and candidates that would interact with any bait (i.e. "sticky" proteins or proteins generally involved in membrane protein translation, translocation and trafficking).

A list of the "sticky" proteins that tend to come up in screens using the SU-YTH system is available online (http://www.dualsystems.com/support/highly-connected-interactors-in-the-dualmembrane-system.html) but none of those isolated from the NubG-X screen presented here appears on this list. One could argue that the isolated interactors are involved in a translation, folding or trafficking pathway common to all the baits. Although

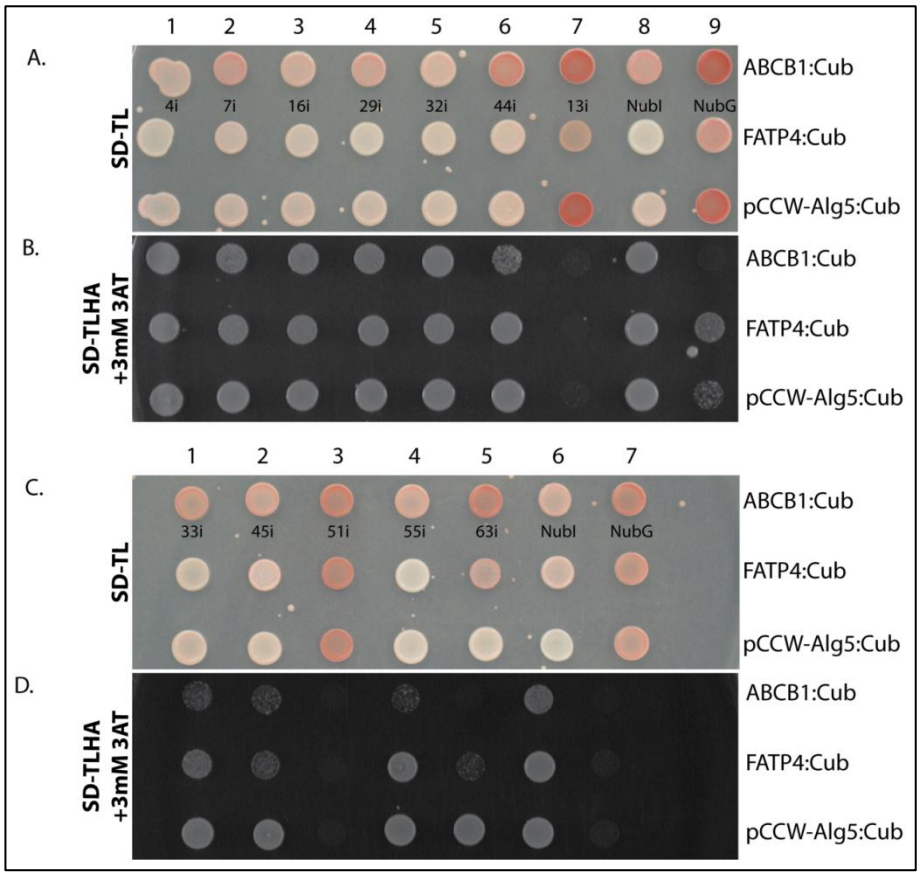

Figure 3-9. ***Assessment of the specificity and strength of interaction between ABCB1:Cub bait and the putative interacting candidates ("preys").***

Yeast cells were co-transformed with "preys" and either the original ABCB1:Cub bait or one of the negative control vectors FATP4:Cub and Alg5p:Cub. Growth was evaluated on SD-*Trp-Leu-His-Ade* plates supplemented with 3mM 3-AT. Accumulation of coloured shunt intermediate was examined on SD-*Trp-Leu* plates. NubI: positive control (Alg5p:NubI), NubG: negative control (Alg5p:NubG) as described in the text.

this is unlikely to be true of all candidates, VAPB (vesicle-associated, membrane protein-associated protein B), SERP1/RAMP4 (stress-associated endoplasmic reticulum protein 1/ribosome-associated membrane protein 4) and Ergic32 (endoplasmic reticulum-Golgi intermediate compartment protein 32) were among the putative interactors isolated and are all involved in the general folding and trafficking of proteins (Breuza et al., 2004, Hori et al., 2006, Lev et al., 2008, Nishimura et al., 1999, Yamaguchi et al., 1999a). Other "false positives" may include factors that drive the direct activation of genes in the nucleus. One such candidate could be STAT6 (signal transducer and activator of transcription 6) which was isolated several times from the NubG-X library screen. It is a member of a family of transcription factors that reside in the cytoplasm and accumulate in the nucleus upon activation/phosphorylation by tyrosine kinases in response to extracellular signals (Bromberg and Darnell, 2000, Levy and Darnell, 2002). STAT6 may therefore, directly or indirectly, influence transcription of the reporter genes independently of the bait protein. Even if this is not the case, STAT6 appears significantly less potent in the presence of ABCB1, where colonies are red on SD-*Trp-Leu* media, than with FATP4 or Alg5p which are much paler, indicating a distinct lack of specificity for ABCB1.

The yeast system employed in this project proved to be unfruitful for identifying specific interaction partners for ABCB1 as all candidates have been ruled out as false positives or non-specific. However, it has been demonstrated that it can be used to screen for regulators of FATP4 and CD36 (Wharton J., and Linton K. J., unpublished data). In Figure 3-10, an example of the system's capacity to discriminate between a "true" and a "false" FATP4 putative interacting partner is shown.

The yeast are red when co-expressing the LPL:NubG (lipoprotein lipase) "prey" and each of the three "bait" vectors (FATP4:Cub used as the bait for the library screen, CD36:Cub

used as a bait for the CD36 library screen (Snippe M., personal communication) and ABCB1:Cub used as a bait for the ABCB1 library screen described in this report) on the SD-*Trp-Leu* plates indicating that there is little or no interaction between LPL and each "prey" (Figure 3-10A). This is consistent with the lack of growth on the SD-*Trp-Leu-His-Ade* medium. However, when cells co-express YIP1B:NubG (Yip1 interacting factor homolog B) "prey" and the "bait" vectors a different result was obtained. A white colony is apparent when FATP4:Cub and YIP1B:NubG vectors are co-expressed whereas a red

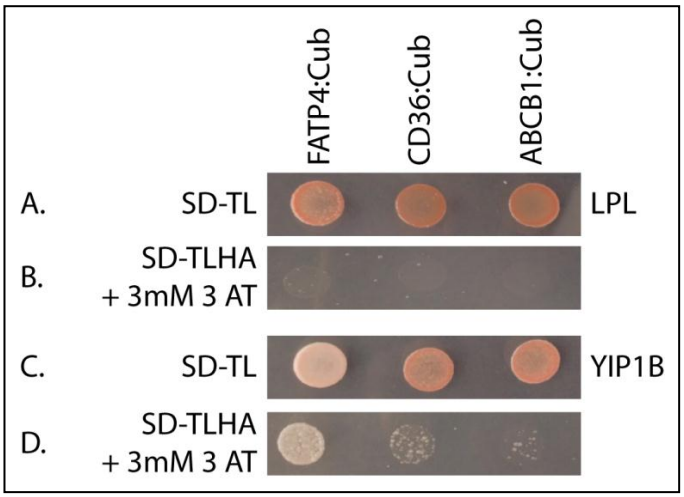

Figure 3-10. ***Specificity and strength of interaction between FATP4:Cub bait and two of the putatively interacting candidates ("preys").***

Yeast cells were co-transformed with "preys" (LPL:NubG or YIP1B:NubG) and either the original FATP4:Cub bait or the negative controls CD36:Cub and ABCB1:Cub. Growth was evaluated on SD-*Trp-Leu-His-Ade* plates supplemented with 3mM 3-AT. Accumulation of coloured shunt intermediate was examined on SD-*Trp-Leu* plates. *LPL*: lipoprotein lipase, *YIP1B*: Yip1 interacting factor homolog B.

colony is observed with the YIP1B:NubG prey and the CD36:Cub or the ABCB1:Cub baits (Figure 3-10C) signifying a strong and specific interaction between FATP4 and YIP1B and a lack of interaction between YIP1B and either CD36 or ABCB1. Further confirmation is provided when the co-transformed cells were grown on SD-*Trp-Leu-His-Ade* medium. Very good growth is achieved for the cells co-transformed with FATP4:Cub and YIP1B:NubG vectors but poor growth was observed for cells co-transformed with the

YIP1B:NubG vector and either of the CD36:Cub or ABCB1:Cub vectors (Figure 3-10D). It was later shown that YIP1B could be co-immunoprecipitated from mammalian cells with FATP4 (Wharton J., and Linton K. J., personal communication).

3.3 Discussion

ABCB1, a multispecific efflux transporter, has a role in normal physiology to protect the body against the harmful effects of xenotoxins. Overexpression of this well-studied member of the ABC superfamily can confer MDR in cancer patients (Gottesman et al., 2002, Higgins, 2007). The aim of this aspect of my project was to utilise the SU-YTH system to identify novel regulators of the MDR ABCB1 with a view to studying their effects on ABCB1 trafficking and function. Unfortunately, the candidates isolated from two adult mouse cDNA library screens proved not to interact with ABCB1 in a specific manner.

Before screening for putative interacting partners it was considered important to demonstrate expression of the "bait" protein. The ABCB1:Cub fusion protein could not be detected by western blotting (Figure 3-4) or by function (i.e., resistance to the antifungal FK506; Section 3.2.1.4) but was shown to be expressed by the "NubI/NubG" test (Figure 3-3). A plausible explanation for this ambiguity may lie in two of the main design features of the bait vector. First, the vector is a centromeric plasmid that carries an ARS (autonomously replicating sequence) origin of replication and one CEN (centromeric locus) thus it is maintained at a maximum of two copies per cell. Second, *CYC1* is a weak promoter which only allows for low levels of bait protein expression (Iyer et al., 2005). It has been demonstrated previously that overexpression of the bait protein can result in unstable and mislocalised fusion protein, and also to activation of the reporter genes in the

absence of an interacting prey (Miller et al., 2005). These two characteristics are therefore crucial to minimise the number of false-positives due to self-activation of the bait. Furthermore, ABCB1 has been expressed successfully in yeast by other groups and shown to function as a drug efflux pump, however in these prior experiments the ABCB1 protein was overexpressed (Goodfellow et al., 1996, Raymond et al., 1994, Saeki et al., 1993),

There is evidence, both direct and indirect, that ABCB1 interacts with several different proteins (Elliott et al., 2005, Goodfellow et al., 1996, Jodoin et al., 2003, Ortiz et al., 2004, Sardini et al., 1994, Valverde et al., 1992). In an attempt to demonstrate the interaction of ABCB1 with caveolin-1 and validate the SU-YTH system, the ABCB1:Cub bait vector was co-expressed with the Cav:NubG prey vector in the NMY51 yeast strain. Unfortunately no interaction was detected. Caveolin-1 has been shown to function when fused, either N- or C-terminally, to GFP (Razani et al., 1999, Volonte et al., 1999) and to be able to interact with the Orf3a viral protein in the Y2H system (Padhan et al., 2007). The consensus N-terminal caveolin-1-binding motif Φ*XXXX*Φ*XX*Φ (where Φ = F, Y or W and *X* = any amino acid) has been proposed to be between amino acid residues 36 and 44 in ABCB1 (36-**F**TMFR**Y**AG**W**-44) indicating that an interaction between caveolin-1 and ABCB1 likely occurs at the cytosolic N-terminus of ABCB1 (Demeule et al., 2000). Experiments performed in Cos-7 cells demonstrated that mutations in that domain do not affect the expression levels of ABCB1 but reduced its interaction with caveolin-1 by up to 48% as shown by co-immunoprecipitation assays (Jodoin et al., 2003). The Cav:Nub fusion protein was detected in the yeast by western analysis but whether or not the fusion protein is able to form functional caveolin in the yeast plasma membrane is not known. The available evidence suggests that it should have been possible to detect an interaction between ABCB1:Cub and Cav:Nub in the SU-YTH system, however, none was detected and it is difficult to reach a definitive conclusion from negative data.

ABCB1 has been shown to interact directly with PKCα (Goodfellow et al., 1996). In an effort to demonstrate this interaction, the PKCα cDNA was C-terminally fused to NubG. Fusion of large coding sequences to either end of PKCα has not proven to affect its normal folding and function (Ng et al., 1999, Prevostel et al., 2000) therefore the fusion of NubG to its carboxy-terminus was not expected to affect its behaviour. Similar to the caveolin-1 co-expression experiment, an interaction between PKCα and ABCB1 could not be demonstrated in the SU-YTH system. However, the interaction between ABCB1 and PKCα might be dependent on the activation of the latter, for example by phorbol ester (Castagna et al., 1982). Heterologous expression of functional mammalian PKC isoforms has been demonstrated in yeast in the presence of cell-membrane permeable activators such as phorbol esters (Parissenti and Riedel, 2003). The presence of such activators on the selective plates might have enabled the detection of an interaction between ABCB1 and PKCα but this was not tested.

ABCB1 is highly expressed in the canalicular membrane of the hepatocyte (Thiebaut et al., 1987). Screening of two liver cDNA expression libraries, NubG-X and X-NubG, identified a total 130 and 12 colonies, respectively, likely to express an interacting protein pair. The library plasmids encoding the putative interactors were isolated, sequenced and retransformed back into yeast cells already carrying the ABCB1:Cub vector in an attempt to replicate the findings (Figure 3-8). The sequence data from the candidates isolated from the X-NubG screen revealed that only ubiquitin was cloned from the expression library. Recurrent isolation of the N-terminal fragments of wild-type ubiquitin has been reported to be a common problem when using X-NubG libraries and is a much less frequent problem when using NubG-X libraries but the reason behind this is unknown (Iyer et al., 2005). It is not clear why no plausible candidates were picked out in the X-NubG screen but similar

screens with an X-NubG heart library have also provided few candidates for interaction with CD36 or FATP4 (Snippe M.; Wharton J., and Linton K. J.; personal communication).

Sequence data of the putative interactors from the NubG-X libary screen, *in silico* analysis and retransformation into ABCB1:Cub-bearing cells (Figure 3-8) identified 29 possible ABCB1-interacting proteins. These proteins are listed in Table 3-1. One would have expected to detect PKCα, caveolin-1 or HAX-1 based on the evidence of a physical association between ABCB1 and PKCα (Goodfellow et al., 1996), caveolin-1 (Jodoin et al., 2003) and HAX-1 (Ortiz et al., 2004). As discussed earlier, the association between ABCB1 and PKCα may depend on activation of the latter. The library screen was not performed in the presence of a phorbol ester which may provide for a plausible explanation as to why PKCα was not detected. The downregulation of ABCB1 function by caveolin-1 was detected at the blood-brain barrier (Jodoin et al., 2003) whereas, here, an adult human liver cDNA library was used for the screen. Although caveolin-1 has been shown to be expressed in membrane microdomains (caveolae) at the canalicular membrane of rat hepatocytes (Ismair et al., 2009), it is possible that ABCB1 and caveolin-1 do not interact in hepatic cells. Interaction of HAX-1 and ABCB1 has been shown in rat liver cells by co-immunoprecipitation (Ortiz et al., 2004). It is possible that this is species-specific and does not occur in human hepatocytes. It is also possible that other co-factors may be required for the correct trafficking of HAX-1 to the membrane which may not be present in the yeast or that the interaction may be indirect through a larger multiprotein complex. Furthermore, because of the way the cDNA libraries are constructed (Section 3.2.4.1), it is possible that only a part of HAX-1 was represented which may not be adequate for the interaction with ABCB1.

The strength and specificity of the interaction between ABCB1 and the 29 isolated candidates was assessed in comparison with two different control vectors (Figure 3-9 and Table 3-1). One encoding an unrelated FATP4:Cub fusion protein (Wharton J., personal communication) and the other a non-interacting Alg5p:Cub fusion protein (Dualsystems Biotech, Zurich, CH). The purpose of the controls was to ensure that the isolated prey proteins interact with the bait protein because of their specificity for ABCB1 and not simply due to their close proximity to any "bait" on the plasma membrane or in the ER/Golgi during folding and trafficking. The prey proteins did not discriminate between any of the bait controls and are therefore likely to be a mixture of proteins with a general role in protein folding and trafficking, such as VAPB, Ergic32 and SERP1/RAMP4, factors controlling gene transcription, such as STAT6, and proteins that based on our knowledge did not qualify as physiologically relevant regulators of ABCB1, for example the ferritin light polypeptide involved in the control of iron uptake/export in different tissues, or the Yip1 interacting factor (YIF1A) involved in the maintenance of the Golgi structure (Figure 3-9 and Table 3-1).

A modified version of the SU-YTH system (iMYTH; integrated split-ubiquitin membrane yeast two hybrid) has been used successfully to screen for potential regulators of a member of the yeast ABCC subfamily (Ycf1p) in yeast (Paumi et al., 2007). In humans, the ABCC subfamily comprises 13 members, 9 of which (ABCC1-6 and ABCC10-12) are multidrug-resistance associated proteins (MRPs) and are involved primarily in the export of anionic conjugates from cells (Borst et al., 1999, Kruh and Belinsky, 2003). The sulphonylurea receptors ABCC8 and ABCC9 (SUR1 and SUR2 respectively) act as ion channel regulators and control the gating of the K^+ channel Kir6.2 (Nichols, 2006). ABCC7 (most widely known as CFTR) is expressed at the apical border of epithelial cells of exocrine glands where it functions as a chloride channel (Gadsby et al., 2006, Vankeerberghen et al., 2002).

Ycf1p is a vacuolar glutathione *S*-conjugate pump involved in the detoxification pathway in yeast cells (Li et al., 1996) which displays a 63% sequence similarity (at the amino acid level) to ABCC1 (Szczypka et al., 1994). Furthermore, it has been demonstrated that Ycf1p mutants can be complemented by heterologous expression of mammalian ABCC1 in yeast (Tommasini et al., 1996). In the approach undertaken by Paumi *et al.* (2007), Tus1p, an exchange factor for the small GTPase Rho1p involved in actin cytoskeleton remodelling during bud growth in yeast (Schmelzle et al., 2002), was isolated as a potential Ycf1p regulator. The authors were also able to show that the effect of Tus1p on Ycf1p was specifically through Rho1p demonstrating the modulation of an ABC transporter by a cytosolic factor. Nevertheless, their modified iMYTH approach involved a native yeast protein and the bait was integrated into the yeast genome ensuring an endogenous level of expression to maintain the correct stoichiometry of protein complexes and avoid inappropriate interactions.

The use of other proteins (FATP4 and CD36) to discriminate between specific and non-specific interactors of ABCB1 (and preys that autoactivate) was useful in this study, providing a rapid approach to corroborate (or dismiss) interactions with ABCB1. Following a negative outcome, the decision was taken to discontinue this line of study as the likelihood of identifying a specific factor for ABCB1 maturation or regulation was remote.

Chapter Four

4 Expression of ABCB4 wild-type and non-synonymous genetic variants in HEK293T cells

4.1 Introduction

Progressive familial intrahepatic cholestasis (PFIC) refers to a group of autosomal recessive liver disorders of childhood presenting with intrahepatic cholestasis within the first year of life which can lead to severe growth retardation and ultimately to death from liver failure. Progression to liver failure may occur within the first decades of life and in its most severe form, orthotopic liver transplantation represents the only treatment for patients (Davit-Spraul et al., 2009).

PFIC can be subdivided in three types which differ in their clinical presentation, liver histology and biochemical features (i.e. bile composition, serum gamma-glutamyltransferase activity and level of cholesterol in the serum) (Davit-Spraul et al., 2009, Jacquemin, 1999, Morotti et al., 2011). PFIC type 1 (or FIC1 deficiency) is due to mutations in *ATP8B1* (*FIC1*), PFIC type 2 (or ABCB11 deficiency) is due to mutations in *ABCB11* (*BSEP*) and PFIC type 3 (or ABCB4 deficiency) is due to mutations in *ABCB4* (or *MDR3*) (for a more detailed account on the identification of the three genes and their link to cholestatic liver disease see Chapter 1; Section 1.13.5.3).

As described in Chapter 1 (Section 1.13.5.3.2), ABCB4 is a phosphatidylcholine (PC) translocase which functions at the canalicular membrane of the hepatocyte (Smith et al., 1998, van Helvoort et al., 1996). Lipid secreted from the liver into the bile duct protects the liver from the detergent action of bile (Donovan et al., 1991). Consequently, mutations in *ABCB4* are associated with a spectrum of liver diseases, ranging from the benign and episodic to the malign and fatal. In the rare and fatal condition, PFIC type 3 (PFIC3), the link between mutation and disease is clear, but in the majority of liver diseases the underlying causes are complex and include diet, physiological conditions such are

pregnancy or therapeutic drug use, as well as genetics (Oude Elferink and Groen, 2002, Oude Elferink and Paulusma, 2007, van Mil et al., 2005). In these cases, which include intrahepatic cholestasis of pregnancy (ICP or obstetric cholestasis), drug-induced cholestasis (DIC), low phospholipid-associated cholelithiasis (LPAC, a form of cholesterol gallstone disease), primary sclerosing cholangitis (PSC) and primary biliary cirrhosis (PBC), association with particular mutations in *ABCB4* is implicated by human genetic studies and animal models, but critical evidence at the functional and mechanistic level of protein expression and floppase activity is lacking.

Some insights into the functional consequences of *ABCB4* mutation have been obtained by our group (Dixon et al., 2000) and more recently by the group of Michele Maurice in Paris (Delaunay et al., 2009) by mimicking clinically-relevant mutations in ABCB1 (the closest relative of ABCB4) and measuring the effect of the mutation on drug efflux by ABCB1. Although this approach can provide useful information on the possible effects of the mutations on ABCB4, it is limited and only relevant if the particular amino acid is conserved between the two proteins and performs the same function. Amino acid changes which influence PC binding or flopping, or responses to hormones of pregnancy, contraceptives or drugs are therefore ruled out.

Critical evidence at the functional and mechanistic level of ABCB4 protein expression and floppase activity is lacking. This is because ABCB4 expression *in vitro* can be deleterious to recipient cells. This problem has been resolved recently, allowing for the transient expression of ABCB4 in naïve HEK293T cells. This is essential to analyse the phenotype of the large number of missense SNPs and has been achieved by co-expressing ABCB4 with the ATP8B1/CDC50A flippase complex, which flips a different lipid, phosphatidylserine (PS), in the opposite direction to PC (Groen et al., 2011) [Chapter1;

Section 1.13.6.]. Co-expression of the ATP8B1/CDC50A PS flippase appears to stabilise the plasma membrane of the recipient cells *in vitro* (as it does the canalicular membrane *in vivo*), and allows expression and function of ABCB4 to be measured. I have exploited this method to analyse expression (by western blot), trafficking to the plasma membrane (by confocal microscopy) and lipid flopping activity (by bile salt-dependent extraction of radiolabelled PC into the culture medium) of 9 variant ABCB4 with missense SNPs that are implicated in the aetiology of liver disease (Table 4-1).

a.a. Change	Domain	Relevant patient genotype where known	Disease Class	Reference
A286V	ICL2	S320F [on 2nd allele]	PFIC3	(Degiorgio et al., 2007)
M301T	MSH5	HET	LPAC	(Rosmorduc et al., 2003)
S320F	MSH5	A286V [on 2nd allele]	PFIC3	(Degiorgio et al., 2007)
		Y279X [on 2nd allele]	PFIC3	(Degiorgio et al., 2007)
		A953D [on 2nd allele] + V444A [on ABCB11] (HET)	LPAC to PFIC3	(Poupon et al., 2010)
		HOM	LPAC	(Rosmorduc et al., 2001)
		HOM	LPAC	(Rosmorduc et al., 2003)
		HOM	ICP	(Pauli-Magnus et al., 2004b)
		HET + V444A [on ABCB11] + -1G>T [on *FXR*] (HET)	ICP	(Zimmer et al., 2009)
		HOM + V444A [on ABCB11]	ICP	(Keitel et al., 2006)
		HET	ICP	(Bacq et al., 2009)
E528D	NBD1	HET	LPAC	(Rosmorduc et al., 2003)
		HET	LPAC	(Nakken et al., 2009)
		HET	ICP	(Floreani et al., 2008)
G535D	NBD1	HET	LPAC (juvenile) to ICP (2× pregnancy) to BC (at 47 years)	(Lucena et al., 2003)
R545C	NBD1	Unknown	PSC	(Pauli-Magnus et al., 2004a)
A546D	NBD1	HET	ICP	(Dixon et al., 2000)
L591Q	NBD1	HOM	LPAC	(Rosmorduc et al., 2003)
P1161S	NBD2	HOM	LPAC	(Rosmorduc et al., 2001)
		HET	LPAC	(Rosmorduc et al., 2003)

Table 4-1. ***Summary of the 9 ABCB4 missense mutants analysed in this investigation.***

Where appropriate, additional mutations identified within the same patient(s) either on the other *ABCB4* allele or on *ABCB11*, are indicated. a.a., amino acid; ICL, intracellular loop; MSH, membrane spanning helix; NBD, nucleotide-binding domain; PFIC, progressive familial intrahepatic cholestasis; LPAC, low phospholipid-associated cholelithiasis; ICP, intrahepatic cholestasis of pregnancy; BC, biliary cirrhosis; PSC, primary sclerosing cholangitis; HOM, homozygous; HET, heterozygous; c.HET, compound heterozygote; n/a, not available; FXR, farnesoid X receptor.

These nine variants were chosen because they cover a wide range of liver disease phenotypes that have been linked to mutations in the *ABCB4* gene. The S320F (c.959C>T)

variant has been implicated in three different disease phenotype; PFIC3 (Degiorgio et al., 2007), LPAC (Rosmorduc et al., 2003, Rosmorduc et al., 2001) and ICP (Bacq et al., 2009, Keitel et al., 2006, Pauli-Magnus et al., 2004b). The E528D (c.1584G>C) variant has also been linked to more than one disease phenotypes; LPAC (Nakken et al., 2009, Rosmorduc et al., 2003) and ICP (Floreani et al., 2008). The A286V (c.857C>T) variant was identified in a PFIC3 patient as a compound heterozygous alteration with S320F (Degiorgio et al., 2007). The M301T (c.902T>C), L591Q (c.1772T>A) and P1161S (c.3481C>T) variants have all been implicated in LPAC (Rosmorduc et al., 2003, Rosmorduc et al., 2001). The A546D (c.1637C>A) variant has been identified in an ICP patient (Dixon et al., 2000). The G535D (1605G>A) is unique in that it was found in a female patient presenting with juvenile cholelithiasis who then developed ICP during both of her pregnancies followed by biliary cirrhosis in adulthood (Lucena et al., 2003). Finally, the R545C (c.1633C>T) variant was identified as PSC-specific (Pauli-Magnus et al., 2004a).

4.2 Results

In this chapter the heterologous expression system for the transient expression of WT ABCB4 in HEK293T cells is described and optimised. In addition, the generation of the 9 *ABCB4* variants (summarised in Table 4-1), using site-directed mutagenesis, is outlined. Finally, the study of the expression level of the different variants in the HEK293T cell system is presented.

4.2.1 Expression of wild-type ABCB4 in HEK293T cells

Before attempting to characterise a number of ABCB4 variants in the heterologous expression system, it was important to demonstrate the expression of wild-type (WT) ABCB4 in HEK293T cells in the presence and in the absence of the ATP8B1/CDC50A PS flippase, recapitulating the results of a previous report to serve as a baseline for the

effect of the SNPs (Groen et al., 2011). Success of the experiment is dependent on triple transfection of the recipient cells with high efficiency because each of the components is encoded on a separate plasmid. Cell density at the time of transfection can influence the transfection efficiency (i.e., the uptake of the PEI (polyethylenimine)-DNA complexes into the cells) and the expression levels of the genes of interest; therefore the optimal confluency at the time of transfection was investigated.

4.2.1.1 Co-transfection of cells with *ABCB4* and the *ATP8B1/CDC50A* PS flippase improves ABCB4 expression

Initially, it was essential to confirm that the presence of the ATP8B1/CDC50A PS flippase improves the expression level of *ABCB4* in HEK293T cells as previously reported (Groen et al., 2011).

To this end, HEK293T cells were seeded on 6-well plates and transfected with the pcDNA3.1-ABCB4wt (coding for WT ABCB4) or pcDNA3.1-ABCB4_E558Q (coding for a Walker B motif mutant of ABCB4 that is likely to be deficient in ATP hydrolysis) mammalian expression vectors. Transfections were set up either in the presence (triple transfection) or in the absence (single transfection) of the pCI-neo-ATP8B1 (coding for ATP8B1) and pCI-neo-CDC50 (coding for CDC50A) mammalian expression vectors. In the case where cells were transfected with the *ABCB4*-expressing vector in the absence of the *ATP8B1*- and *CDC50A*-expressing vectors, the PEI:DNA ratio was kept constant by co-transfecting with the parental, empty form of the pcDNA3.1 vector. All vectors were kindly provided by Dr Marta Rodriguez-Romero (Groen et al., 2011).

Both the pcDNA3.1 (Invitrogen) and the pCI-neo (Promega) vectors permit efficient and high-level expression of recombinant proteins in mammalian cells under the control of the human cytomegalovirus (CMV) immediate-early enhancer/promoter (Schmidt et al., 1990).

In addition, both vectors also contain the SV40 enhancer and early promoter region. The SV40 early promoter contains the SV40 origin of replication which induces transient, episomal replication of the vectors in cells constitutively expressing the SV40 large T antigen, e.g. HEK293T cells (Gluzman, 1981).

The expression level of ABCB4 (WT or WB mutant) in the presence or in the absence of the ATP8B1/CDC50A PS flippase was assayed by western blotting using the monoclonal antibody C219 which recognises ABCB4 (Georges et al., 1990). C219 recognizes an internal, highly conserved amino acid sequence (VQEALD and VQAALD) found in ABCB4 (and ABCB1 and ABCB11). To allow comparison of the ABCB4 data, β-tubulin was employed as a loading control for the experiment. In the case where uneven loading is revealed (i.e., variations in the intensity of the signal detected for β-tubulin in the different samples), the level of ABCB4 detected was normalised against the level of β-tubulin. To achieve this, densitometry analysis was performed using the ImageJ image analysis software (http://rsb.info.nih.gov/ij/index.html). Initially, an arbitrary value for the level of intensity (i.e., density) of the bands was obtained by measurement of the number of pixels on a digital image of the loading control (β-tubulin) and ABCB4 blots (Figure 4-1; panel A). Next, the relative intensities of each of the loading control bands were calculated against a reference band. In this case the most intense band, based on its density, was selected as a standard and given the arbitrary value of 1. Finally, the density value of each of the ABCB4 bands was multiplied by the relative value of the corresponding loading control to reflect the true band intensity which would have been detected for ABCB4 following equal loading of total protein. In doing so, a direct comparison between different samples was achieved.

No ABCB4 could be detected in the untransfected (UT) sample, indicating that HEK293T cells do not express endogenous ABCB4 (Figure 4-1; panel A, lane 5). WT ABCB4 was expressed 1.4-fold higher in the triple transfection as compared to the single (Figure 4-1; panel A, compare lane 1 with lane 2) when normalised against the loading control (Figure 4-1; panel B). In contrast, the inactive WB mutant expressed 2.0× higher than WT *ABCB4* in the single transfection (Figure 4-1; panel A, lane 3) when normalised against the loading control (Figure 4-1; panel B). These data are in general agreement with previous results (Groen et al., 2011). Co-expression of *ABCB4* with *ATP8B1/CDC50A* in HEK293T cells therefore increases the expression level of ABCB4, whereas it has little effect on the inactive WB mutant (Figure 4-1; panel A, lanes 3 and 4, and panel B).

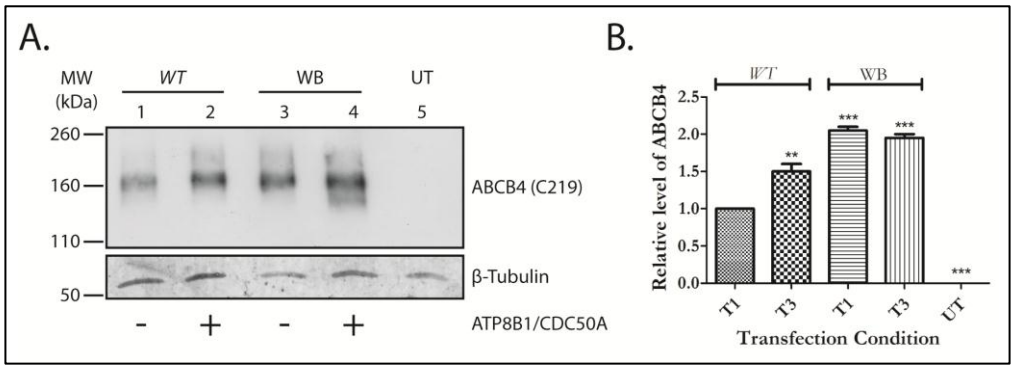

Figure 4-1. ***Expression of WT and mutant (WB, E558Q) ABCB4 in the absence or in the presence of the ATP8B1/CDC50A PS flippase.***

(A) HEK293T cells (3.0×10^5) were seeded on 6-well plates and transfected 24 h post-seeding. The vectors encoding either WT or mutant/inactive (WB) ABCB4 were co-transfected with the vectors coding for ATP8B1 and CDC50A where indicated. Samples were harvested 48 h post-transfection and the level of ABCB4 was determined by western blotting using the anti-ABCB4 monoclonal antibody C219 (upper panel). No ABCB4 could be detected in the untransfected (UT) sample. β-tubulin was used as a loading control (lower panel). Co-expression of *ABCB4* and *ATP8B1/CDC50A* improves the level of ABCB4 in the samples (compare lanes 1 and 2). The presence of ATP8B1/CDC50A has little effect on the level of the WB mutant detected in the samples (compare lanes 3 and 4). The WB mutant expresses at a higher level than WT *ABCB4* in the single transfection samples (compare lanes 1 and 3). Apparent molecular masses are indicated in kDa. (B) Densitometry analysis of ABCB4 in the samples shown in panel A. The relative density of ABCB4 in each sample was corrected against the β-tubulin loading control and plotted using the WT ABCB4 single-transfected cell population as a reference. T1, single strasfection; T3, triple transfection. Densitometry was performed in ImageJ (http://rsb.info.nih.gov/ij/index.html) and plotted using GraphPad Prism 5.01. The experiment was performed three times (*n* = 3) for statistical analysis by one-way ANOVA (analysis of variance) in the GraphPad PRISM® V5.0 software. ***P*<0.01, ****P*<0.005 (with respect to wild-type single transfection); error bars, standard error of the mean.

Together, these data confirm that the presence of WT ABCB4 is deleterious to HEK293T cells suggesting a negative selective pressure against ABCB4 function. In the presence of the ATP8B1/CDC50A PS flippase, the deleterious effect of ABCB4 function is alleviated allowing higher levels of ABCB4 in the cells (see also Section 1.13.6). The inactive form of ABCB4 (the WB mutant), is detected in the single- and triple-transfected cell population approximately 1.4-fold higher than WT ABCB4 achieved in the triple transfection. As the WB mutant is thought to be catalytically inactive, it is expected to have limited influence on the lipid composition of the plasma membrane. Consequently, in HEK293T cells the expression of this mutant is tolerated more than the expression of the WT protein even in the presence of ATP8B1 and CDC50A (Figure 4-1; panel B).

4.2.1.2 Optimisation of HEK293T seeding density for efficient expression of ABCB4

In the experiments described above, the expression of ABCB4 (WT or WB mutant) was tested in the absence or in the presence of the ATP8B1/CDC50 PS flippase which had been shown previously to increase the level of ABCB4 in HEK293T cells and improve plasma membrane localisation (Groen et al., 2011). Although the expression of WT ABCB4 was improved with concomitant expression of ATP8B1/CDC50A, it did not appear to be as high as reported by Groen *et al.* This could be due to inefficient transfection. Cell density at the time of transfection can have an important influence on the transfection efficiency. The expression of WT and WB ABCB4 in HEK293T cells was therefore tested at different cell densities.

HEK293T cells were seeded on 6-well plates at 1.5, 3.0 or 6.0×10^5 cells per well, 24 h prior to transfection. The expression level of ABCB4 (WT or WB mutant) was assayed by western blotting using β-tubulin as a loading control (Figure 4-2; panel A). The results of this analysis were plotted as the relative level of ABCB4 in each well using the level of

ABCB4 in the aliquot collected from the wells seeded with 1.5×10^5 cells as a reference (Figure 4-2; panel B). The analysis was achieved by means the densitometry method described in Section 4.2.1.1.

As shown in Figure 4-2, the highest level for WT ABCB4 expression, when normalised against the β-tubulin loading control, was obtained at a seeding density of 3.0×10^5 cells per well (Figure 4-2; panel B), suggesting that wells can be over- and under-seeded. The optimal seeding density for transfection and efficient expression of ABCB4 variants in all future experiments was thus selected as 3.0×10^5 cells per well. As shown later, optimisation of the seeding density resulted in a high transfection efficiency of HEK293T cells (Figure 4-3) and increased the ratio between the WT ABCB4 detected in the triple transfection over the single transfection (Figure 4-5).

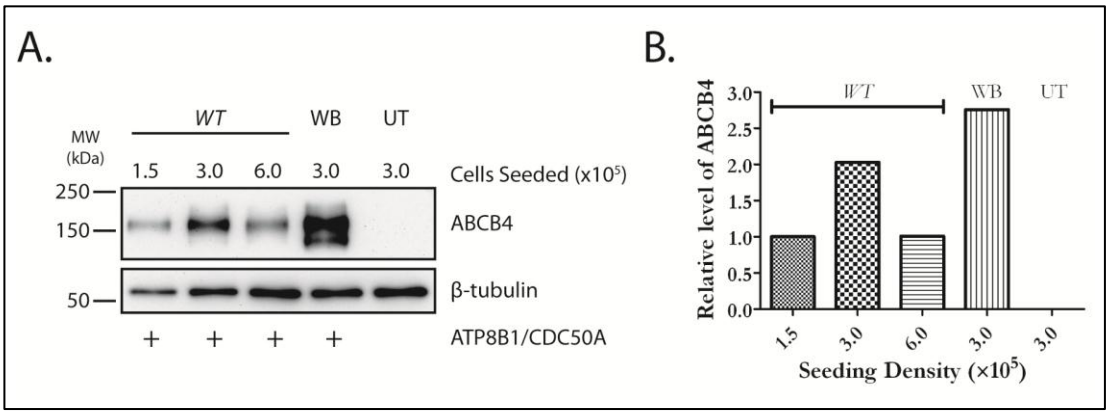

Figure 4-2. ***Optimisation of seeding density for efficient transfection of HEK293T cells.***

(A) HEK293T cells, 1.5×10^5, 3.0×10^5 or 6.0×10^5, were seeded on 6-well plates and transfected 24 h post-seeding. The vectors encoding either WT or mutant/inactive (WB) ABCB4 were co-transfected with the vectors coding for ATP8B1 and CDC50A. Samples were harvested 48 h post-transfection and the level of ABCB4 was determined by western blotting using the anti-ABCB4 monoclonal antibody C219 (upper panel). No ABCB4 could be detected in the untransfected (UT) sample. β-tubulin was used as a loading control (lower panel). The mature, fully glycosylated form of ABCB4 migrates at 170 kDa. The second, lower molecular weight band (~140 kDa) detected in the WB sample corresponds to the immature, unglycosylated form of ABCB4 (see Section 4.2.4). Highest level of ABCB4 was detected in the samples collected from the wells seeded with 3.0×10^5 cells. Apparent molecular masses are indicated in kDa. (B) Densitometry analysis of ABCB4 in the samples shown in panel A. The relative density of ABCB4 in each sample was corrected against the β-tubulin loading control and plotted using the sample collected from the wells seeded with 1.5×10^5 cells as a reference. Densitometry was performed in ImageJ (http://rsb.info.nih.gov/ij/index.html) and plotted using GraphPad Prism 5.01.

A high level of protein was also detected in the samples for the WB mutant (1.36× that of WT) when transfected at the same cell density (Figure 4-2). In the WB sample, two forms of the protein were evident which differed in their glycosylation status (Figure 4-2; panel A). The top, high molecular weight band, corresponds to the mature, fully glycosylated form of the protein, whereas the bottom, lower molecular mass band represents the unglycosylated form of the protein (see Section 4.2.4).

4.2.1.3 The HEK293T cells are efficiently transfected at optimal seeding density

Having determined the seeding density for optimal expression of the constructs, it was important to assay the transfection efficiency under the experimental conditions used for the triple transfection. This was performed using flow cytometric analysis.

4.2.1.3.1 Flow cytometric analysis

In a flow cytometer a cell suspension is taken up into the sample stream of the flow cytometer under negative pressure. This sample stream is then mixed with the sheath stream and injected into the flow manifold. Within the flow manifold, the cells are subjected to a laser beam which excites any fluorophores associated with the cell. Light emitted by the fluorophores passes through a series of filters onto photomultipliers, enabling the measurement of emissions at specific wavelengths. In addition, the forward- and sideways-scattering of the excitation light can be used to measure the size, granularity, and morphology of each cell that passes through the manifold. All these individual measurements are recorded by the data processing unit, and multiple scattering or fluorescence signals can be used to divide, or 'gate', the cells into subpopulations for further analysis, or to examine cellular physiology.

4.2.1.3.2 Measurement of HEK293T transfection efficiency

Flow cytometry can be used to assess cell-surface expression of membrane glycoproteins. Lack of an antibody that specifically recognises an extracellular epitope of ABCB4 means that a direct measurement of the level of plasma membrane localisation of the protein would be difficult. A different experiment was therefore employed as a means of assaying the transfection efficiency of HEK293T cells.

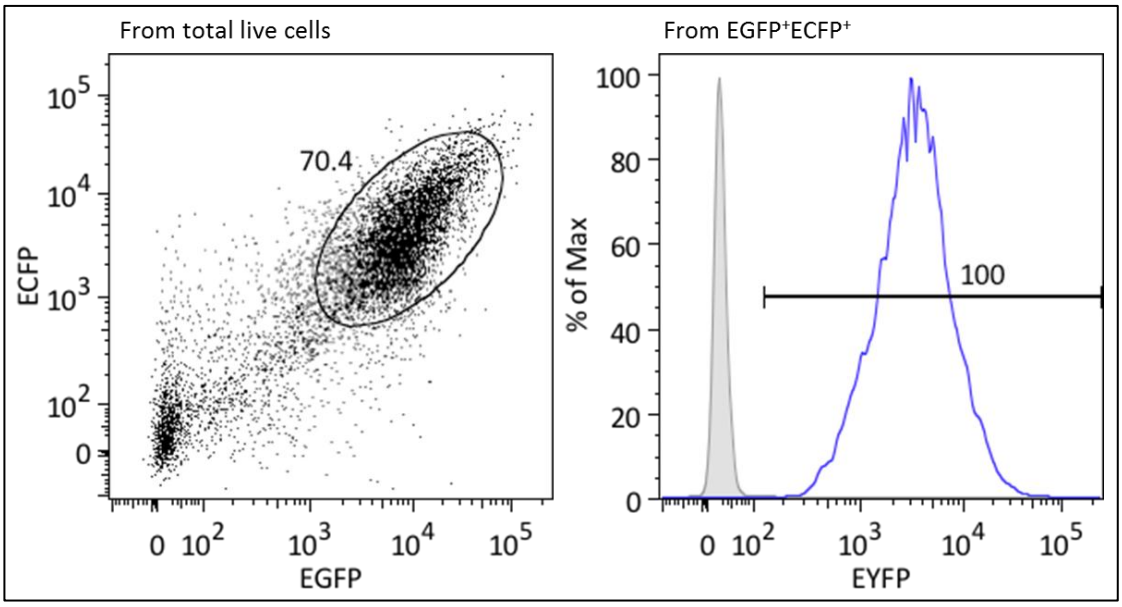

Figure 4-3. ***Transfection efficiency of HEK293T cells.***

HEK293T cells were transfected with a total 7.5 µg of plasmid DNA at a 1:1:1 ratio of pEGFP-C1:pECFP-C1:pEYFP-C1. The cells were harvested 48 h post-transfection. Fluorescence data was acquired on a BD FACSAria II flow cytometer (Becton Dickinson). Cells (10,000) were gated for normal size and granularity. The EGFP fluorophore was excited at 525 nm, the ECFP fluorophore was excited at 582 nm and the EYFP fluorophore was excited at 450 nm. Emission spectra were measured using the FL-1 channel. Cells from the ECFP/EGFPexpressing population (left panel) were also gated for EYFP expression (blue trace; right panel) and compared to untransfected cells (grey trace; right panel). Flow cytometry data were analysed using the FlowJo software package (Tree Star, Ashland, OR, USA). Under these conditions, 70% of the cells were successfully transfected of which 100% were positive for all three fluorescent markers.

HEK293T cells (3×10^5) were transiently transfected with 2.5 µg each of plasmids that express, respectvely, an enhanced green fluorescent protein (EGFP), an enhanced yellow fluorescent protein (EYFP), and an enhanced cyan fluorescent protein (ECFP) under the conditions used for the ABCB4/ATP8B1/CDC50A triple transfection. Forty eight hours

post-transfection, the cells were analysed by flow cytometry. The level of expression of each fluorophore was measured in 10,000 cells of normal size and granularity. Seventy percent (70%) of the analysed cell population was positive for ECFP and EGFP (Figure 4-3; left panel). The ECFP/EGFP-positive ($ECFP^+/EGFP^+$) population was then gated for EYFP expression and compared to the untransfected population. One hundred percent (100%) of the $ECFP^+/EGFP^+$ population was also positive for EYFP (Figure 4-3; right panel). In this experiment, the conditions for efficient triple transfection of HEK293T cells have been demonstrated which should be sufficient to allow measurement of ABCB4 function.

These data, together with the expression difference of WT ABCB4 in the single and triple transfected cells suggests that a cell-based system for the transient expression of ABCB4 is achievable in the presence of the ATP8B1/CDC50A PS flippase. The difference in *ABCB4* expression in the single, compared to the triple transfection could also provide tentative insights into the functionality of the ABCB4 variants. Thus, variants that express equally well in single and triple transfections are likely to be relatively inactive for flopping PC. This system was therefore applied to the characterisation of ABCB4 variants involved in the development of cholestatic liver disease.

4.2.2 Generation of ABCB4 mutants implicated in cholestatic liver disease

The 9 ABCB4 variants selected for characterisation (Table 4-1) using the HEK293T heterologous expression system harbour missense mutations identified in patients suffering from one or more of the several forms of cholestatic liver. None of the mutations is located in TMD2. There is one mutation in NBD2 (P1161S) and five in NBD1 (E528D, G535D, R545C, A546D and L591Q). The rest of the mutations are centred on MSH5 (M301T, S320F) and its preceding ICL (A286V).

The mutations were introduced into pcDNA3.1-ABCB4wt by site-directed mutagenesis. However, because the mutagenesis protocol is not 100% efficient, not all plasmid molecules in the reaction will be modified therefore generating both mutant and non-mutant progenies. As a result, it is helpful to be able to quickly and conveniently identify the mutated plasmid DNA isolated from the bacterial colonies.

Mutagenic oligonucleotides are often designed to introduce, along with the desired non-synonymous mutation, a synonymous change in the same vicinity of the coding region. Although it does not change the encoded amino acid, the secondary change is designed to remove or introduce a restriction site. This alters the restriction digest profile of the mutant plasmid DNA. This type of manipulation allows for the rapid screening of putative mutant plasmids (isolated from transformed *E. coli*), using specific restriction endonucleases. *In silico* analysis of the expected DNA sequence of all mutants generated for the purpose of this study revealed that the non-synonymous mutation introduced to the WT *ABCB4* coding sequence, serendipitously resulted in a change of the restriction digest profile of each mutant, except for ABCB4_A286V (c.857C>T). Consequently, no further changes were introduced to the design of these mutagenic oligonucleotides to allow for rapid screening of putative mutants. In the case of ABCB4_A286V, no restriction analysis was performed and mutants were identified by DNA sequencing. Following the identification of plasmid DNA likely to harbour the desired mutation by restriction analysis (or sequencing over the mutation site), the integrity of the entire cDNA in the construct was validated by DNA sequencing to ensure no additional mutations were introduced during the mutagenesis or replication process in *E. coli*.

Figure 4-4 depicts an example of the screening process. Within the pcDNA3.1-ABCB4wt plasmid, there are four *Bst*XI restriction sites (CCANNNNN▼NTGG; where N = A or C or G or T). When digested with the *Bst*XI restriction endonuclease (NEB, UK) and the

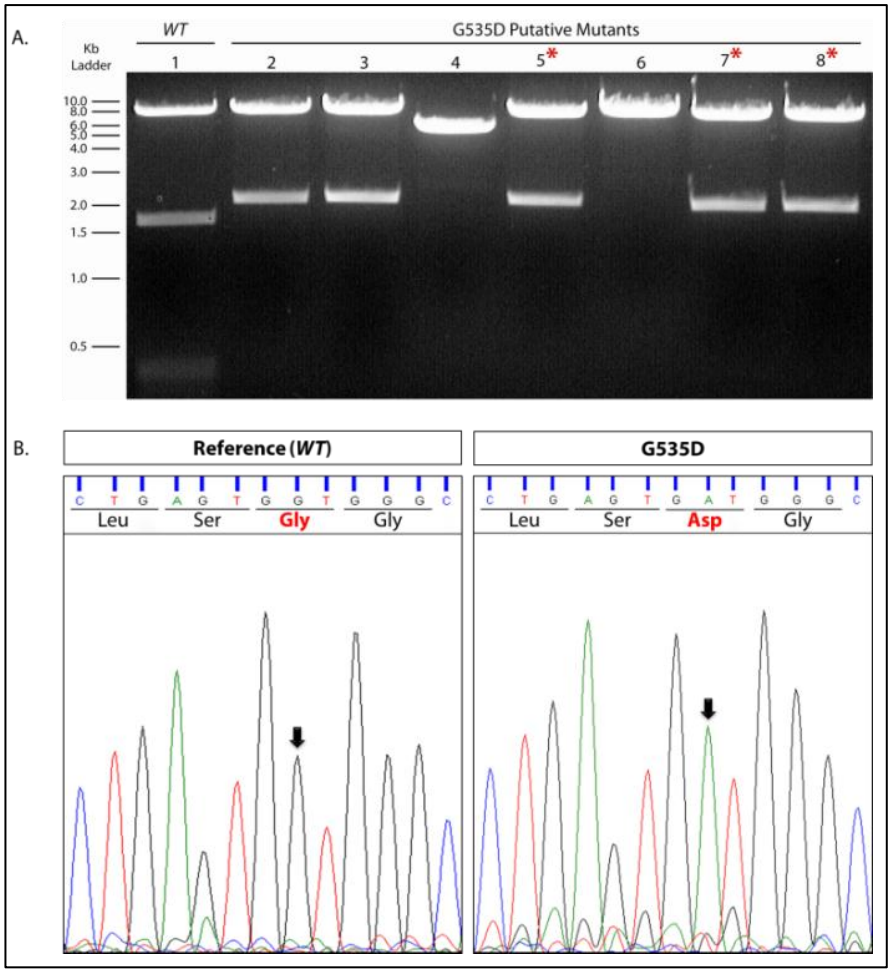

Figure 4-4. ***Screening for putative ABCB4 mutant plasmids.***

(A). Restriction digest profile of plasmid DNA of WT ABCB4 (lane 1) and G535D (lanes 2-8) putative mutants. Each sample (1 µg) was digested with *Bst*XI restriction endonuclease for 90 min at 37°C and run on 0.75% (w/v) agarose gel. For WT ABCB4, four fragments were expected: 7269, 1642, 356 and 14 nucleotide bases in length. For the G535D mutants, three fragments were expected: 7269, 1998 and 14 nucleotide bases in length. The candidates in lanes 2, 3, 5, 7 and 8 reveal the restriction digest profile expected for plasmid DNA carrying the desired mutation (c.1605G>A). The putative mutants in lanes 5, 7 and 8, highlighted by a red asterisk, were subjected to DNA sequencing. (B). Electropherogram of DNA sequencing of wild-type *ABCB4* and the putative mutant in lane 8. A guanine (G) at position 1605 of the *ABCB4* coding region (left panel) is replaced with an adenine (A) (right panel) following successful mutagenesis. The integrity of the whole ABCB4 G535D coding region was verified by careful inspection of the electropherograms.

sample subjected to agarose gel electrophoresis, four fragments of different sizes are therefore expected: 7269, 1642, 356 and 14 nucleotide bases in length (Figure 4-4A; lane 1)

[*note:* the smallest band (14 base pairs) is too small to detect]. The ABCB4_G535D codon change removes one *Bst*XI restriction site from the ABCB4 coding region. Consequently, only three fragments are expected: 7269, 1998, 14. Out of the seven individual plasmid samples digested, five had the anticipated profiles (Figure 4-4A; lanes 2, 3, 5, 7 and 8) of which three (Figure 4-4A; lanes 5, 7 and 8) were sequenced to confirm the presence of the desired mutation. The amino acid change at position 535 of the ABCB4 polypeptide is a result of a point mutation whereby a guanine (G) at position 1605 of the *ABCB4* coding region is replaced with an adenine (A). This results in the replacement of the wild-type glycine (Gly, G) residue with an aspartic acid (Asp, D) residue. DNA sequencing of the putative mutant depicted in lane 8 of Figure 4-4A confirmed that the c.1605G>A modification was present (Figure 4-4B; right panel). Following careful inspection of the whole *ABCB4* coding region no further changes were detected, therefore this plasmid was selected for downstream applications.

Mutant	Change Introduced	Screen with	# of Restriction Sites		Fragments	
			WT	Putative Mutant	WT	Putative Mutant
G535D	*Bst*XI (-)	*Bst*XI	4	3	7269, 1642, 356, 14	7269, 1998, 14
M301T	*Nco*I (-)	*Nco*I	5	4	3342, 3331, 1279, 735, 594	3342, 3331, 1873, 735
E528D	*Bsm*AI (+)	*Bsm*AI	9	10	3136, 2460, 1503, 776, 770, 328, 192, 74, 42	2460, 1776, 1503, 1360, 776, 770, 328, 192, 74, 42
L591Q	*Acc*I (-)	*Acc*I	5	4	4324, 2185, 1420, 1345, 7	5669, 2185, 1420, 7
P1161S	*Tth*IIII (+)	*Tth*IIII	1	2	9281	7513, 1768
R545C	*Pml*I (-)	*Pml*I & *Nhe*I-HF	1 (*each*)	1 (*Nhe*I)	7553, 1728	9281
S320F	*Bam*HI (-)	*Bam*HI	2	1	8265, 1016	9281
A546D	*Sex*AI (+)	*Sex*AI	2	3	7085, 2196	6234, 2196, 851
A286V	None	n/a	n/a	n/a	n/a	n/a

Table 4-2. ***Restriction digest profiles of WT and mutant vector (pcDNA3.1) DNA carrying the ABCB4 coding region.***

DNA base changes introduced a restriction site change in all but one of the non-synonymous mutants. This change was used to screen for putative mutants during the mutagenesis experiments. Addition or removal of a restriction site is indicated with a (+) or a (-) sign, respectively, next to the change introduced. The expected fragments in the WT and putative mutants are also outlined. In the A286V variant, no alteration in the restriction profile was introduced by the mutation and putative mutants were confirmed by DNA sequencing of the ABCB4 coding region. WT, wild type; n/a, not applicable.

The same process was exploited to obtain all nine of the desired ABCB4 non-synonymous genetic variants. As stated earlier, eight of the mutations introduced to the *ABCB4* coding region resulted in a change of the restriction profile. Specifically, the ABCB4_M301T (c.902T>C) codon change removes one of the five *Nco*I sites; the ABCB4_E528D (c.1584G>C) codon change inserts one *Bsm*AI site resulting in a total of nine *Bsm*AI restriction sites; the ABCB4_L591Q (c.1772T>A) codon change removes one of the five *Acc*I sites; the ABCB4_P1161S (c.3481C>T) codon change inserts one *Tth*IIII resulting in a total of two *Tth*IIII restriction sites; and the ABCB4_R545C (c.1633C>T) codon change removes the unique *Pml*I site (Table 4-2). The ABCB4_A546D (c.1637C>A) and ABCB4_S320F (c.959C>T) were provided by Dr Marta Rodriguez-Romero (personal communication) and reconfirmed by DNA sequencing.

4.2.3 Expression of ABCB4 mutants in HEK293T cells

To investigate the role of ABCB4 in the development of cholestatic liver disease I have introduced a series of mutations into the transporter, that are found in the human population and linked to various liver conditions (Table 4-1). The 9 non-synonymous ABCB4 variants gave a range of different mutant phenotypes which could be divided into 3 categories: 1. WT-like (active or unaffected) mutants, 2. WB-like (non-active/stable) and 3. non-active/unstable mutants (Figure 4-5).

4.2.3.1 WT-like (active or unaffected) mutants

Mutants which display a similar expression profile to WT ABCB4 are designated here as WT-like and represent one third (3/9) of the total number of mutants studied [Figure 4-5; panel B (E528D and L591Q) and panel C (P1161S)]. E528D, P1161S and L591Q mutants are detected at a very low level when expressed in HEK293T cells in the absence of ATP8B1/CDC50A, but when these mutants are co-expressed with *ATP8B1/CDC50A*, the level of expression is dramatically improved (Figure 4-5F). These data, mimicking the

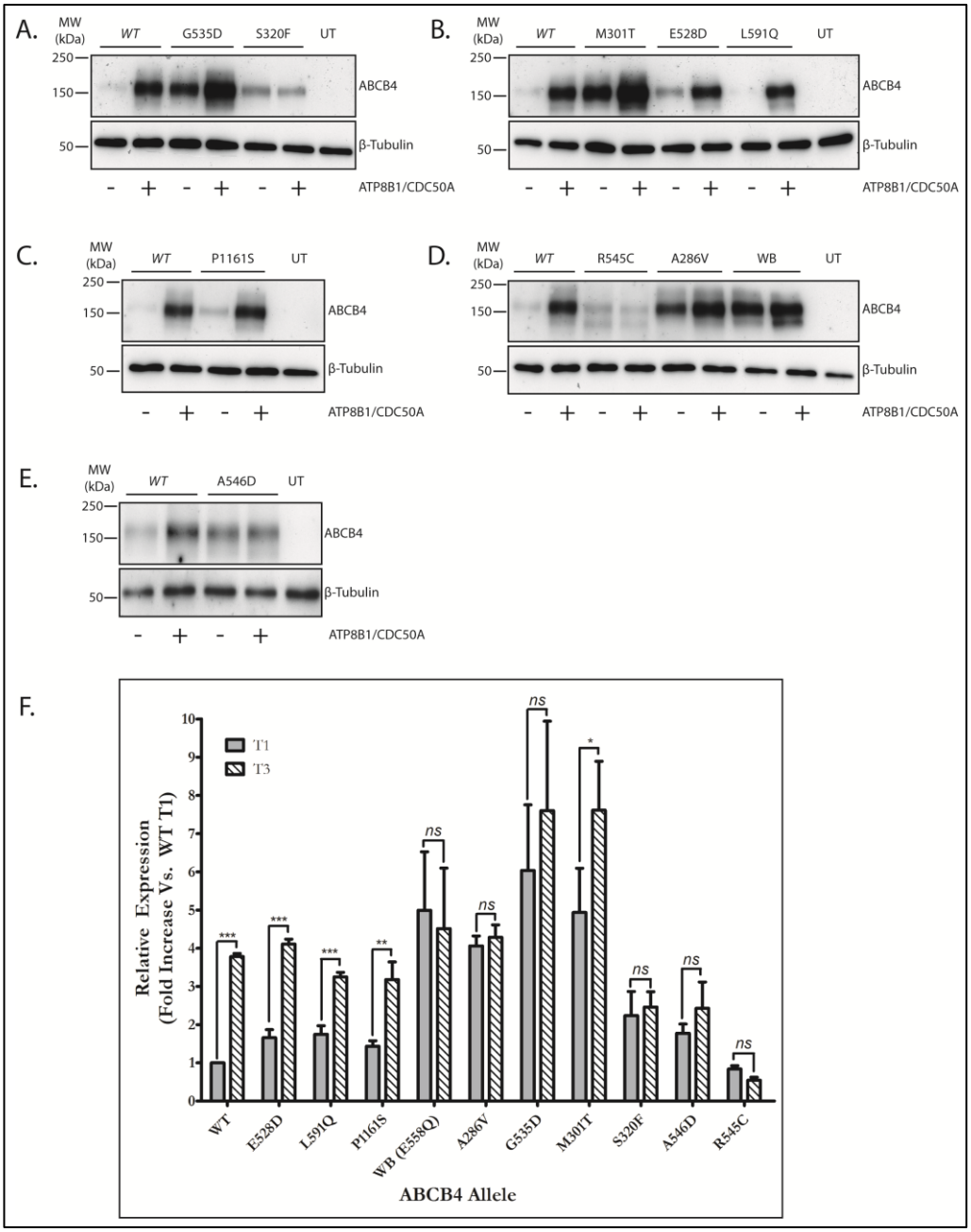

Figure 4-5. ***Expression of ABCB4 mutants in HEK293T cells.***

HEK293T cells were transiently transfected with WT or mutant *ABCB4*-expressing vector in the presence (+) and in the absence (-) of the ATP8B1/CDC50A PS flippase. Samples were harvested 48 h post-transfection and whole-cell lysate (2 µg of total protein) from each sample was subjected to western analysis. The level of ABCB4 was determined using anti-ABCB4 monoclonal antibody C219. β-tubulin was used to ensure equal loading for all samples. A representative blot for each set of mutants is shown in panels A-E. No ABCB4 could be detected in the untransfected samples. *WT*, wild type; UT, untransfected; WB, walker B (E558Q) mutant. Apparent molecular masses are indicated in kDa. Densitometry analysis of ABCB4 expression in the samples shown in panels A-E is presented in panel F. The relative density of ABCB4 in each sample was corrected against the β-tubulin loading control and plotted using the WT ABCB4 single-transfected cell population as a reference. T1, single strasfection; T3, triple transfection. Densitometry was performed in ImageJ (http://rsb.info.nih.gov/ij/index.html). The experiment was performed three independent times (*n* = 3) for statistical analysis in the GraphPad PRISM® V5.0 software. **P*<0.05, ***P*<0.01, ****P*<0.005 (with respect to the single transfection); *ns*, not significant; error bars, standard error of the mean.

phenotype of WT ABCB4 shown as a control on each panel, suggests that the mutants are deleterious to the cells. These mutants are therefore expected to localise to the plasma membrane and flop PC similar to WT ABCB4 (see Chapter 5).

4.2.3.2 WB-like (non-active/stable) mutants

Mutants which display a similar expression profile to the E558Q (WB) mutant (Figure 4-5; panel D) are designated here as WB-like and also represent one third (3/9) of the total number of mutants studied [Figure 4-5; panel A (G535D), panel B (M301T) and panel D (A286V)]. All three mutants behave in a manner more comparable to the WB mutant than WT. Specifically, these are detected at a high level in the absence of ATP8B1/CDC50A. However, expression of each of the 3 mutants is improved by co-expression with *ATP8B1/CDC50A* suggesting that each may retain some PC floppase activity, but this is likely to be less than the WT activity (Figure 4-5F). In this type of analysis it is difficult to distinguish between non-functional mutants (i.e., those that reach the plasma membrane but are unable to flop PC) and trafficking mutants (i.e., those that fold inefficiently and therefore do not progress through the trafficking pathway although it is possible that these mutants may migrate faster through SDS-PAGE due to the presence of core rather than mature glycosylation). Both phenotypes likely result in protein that has limited influence on the lipid asymmetry, and hence the integrity, of the plasma membrane and therefore their expression is tolerated by HEK293T cells in the absence of the ATP8B1/CDC50A PS flippase. These two possible sub-phenotypes are addressed further in Chapter 5.

4.2.3.3 Non-active/unstable mutants

The remaining three mutants (S320F, A546D and R545C), are detected at a similar level both in the presence and in the absence of ATP8B1/CDC50A [Figure 4-5; panel A (S320F), panel D (R545C) and panel E (A546D)]. Notably none of the mutants reaches the level of expression of the WT ABCB4 achieved in the presence of ATP8B1/CDC50A

(although A546D consistently achieves about 70% of WT as indicated by densitometry analysis); but each is present at a higher level than WT ABCB4 in the absence of ATP8B1/CDC50A. These mutations *may* cause a folding defect which makes the protein unstable resulting in an increased rate of degradation. These proteins are also likely to have reduced activity hence expression is not improved in the presence of ATP8B1/CDC50A. Some insight into the effect of these mutations may be offered by studying the subcellular localisation of the recombinant protein by confocal microscopy, and measurement of its lipid flopping activity (by bile salt-dependent extraction of radiolabelled PC into the culture medium). The results of these studies are reported in Chapter 5.

Of note, two forms of the R545C protein are evident which differ in electrophoretic mobility [Figure 4-5; panel D (R545C)]. This variation is likely due to a difference in the glycosylation status of the two protein species and this is tested and described below (see Section 4.2.4).

4.2.4 Transient expression of ABCB4 R545C results in two protein forms which differ in their glycosylation status

Western analysis of the expression levels of several ABCB4 variants following transient expression in HEK293T cells revealed that some mutants express as two forms with different apparent molecular weights [Figure 4-5; panel D (R545C, A286V and WB); panel B (L591Q)]. The peptide *N*-Glycosidase F (PNGase F; NEB, UK) cleaves mature and immature *N*-linked glycans present on a polypeptide and was used to test whether the two forms of ABCB4 detected differed in their glycosylation status. In the untreated WT ABCB4 samples, the mature, 170-kDa is the main form present (Figure 4-6; lanes 1 and 3) although some immature 140-kDa form is detected when ABCB4 is overexpressed in the presence of ATP8B1/CDC50A (Figure 4-6; lane 3, black arrowhead). Enzymatic deglycosylation of the WT ABCB4 samples shows that the larger, 170-kDa band is

sensitive to the treatment (Figure 4-6; compare the untreated samples in lanes 1 and 3 with the treated samples in lanes 2 and 4). In the R545C samples, the higher molecular weight species is the mature form of the protein which migrates with the same mobility as the mature WT protein and which is sensitive to deglycosylation with PNGase F. The deglycosylated R545C migrates with the same mobility as the deglycosylated WT protein (Figure 4-6; compare lane 2 with lane 6 and lane 4 with lane 8). The lower molecular weight proteins present in the untreated R545C samples in the absence and in the presence of ATP8B1/CDC50A likely represent the nascent immature protein (Figure 4-6; lanes 5 and 7). In addition, a small fraction of the deglycosylated R545C protein appears to migrate faster than the predominant 140-kDa deglycosylated form the PNGase F-treated samples and likely represents a degradation product of the mature protein (Figure 4-6; lanes 6 and 8, red arrowheads). This fraction is possibly present in the treated WT ABCB4 sample but is masked by the high signal detected from the deglycosylated protein (Figure 4-6; lanes 2 and 4).

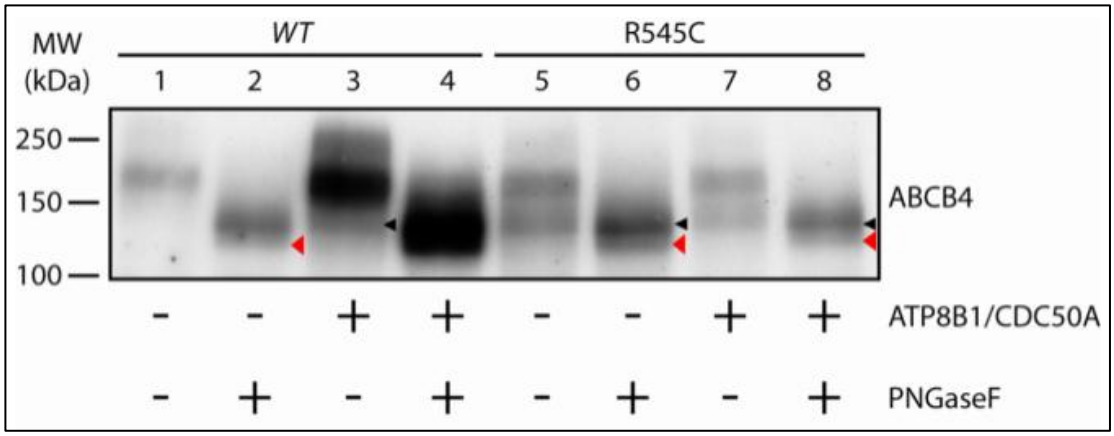

Figure 4-6. ***Two forms of ABCB4 are expressed in HEK293T cells which differ in their glycosylation status.***

Aliquots (20 µg total protein) were subjected to PNGase F (lanes 2, 4, 6 and 8) digestion or left untreated (lanes 1, 3, 5 and 7), and processed for electrophoresis and immunoblotting using a monoclonal anti-ABCB4 antibody C219. Lanes 1-4: wild type ABCB4. Lanes 5-8: ABCB4_R545C mutant. Black arrowhead, nascent immature protein. Red arrowhead, degradation product of the mature ABCB4 protein. Apparent molecular masses are indicated in kDa.

4.3 Discussion

ABCB4 is a PC floppase most abundantly expressed at the canalicular membrane of the hepatocyte (Smith et al., 1998, van Helvoort et al., 1996). Variations in the *ABCB4* coding region cause PFIC3, a rare autosomal recessive disease characterised by the early onset of cholestasis that ultimately leads to liver failure at a young age (Jacquemin et al., 2001). There is now evidence that in addition to PFIC3, mutations in *ABCB4* are involved in ICP, LPAC, DIC and PSC (Dixon et al., 2000, Jacquemin et al., 1999, Jacquemin et al., 2001, Lang et al., 2007, Lucena et al., 2003, Pauli-Magnus et al., 2004a, Pauli-Magnus et al., 2004b, Rosmorduc et al., 2003, Rosmorduc et al., 2001, Poupon et al., 2010). Patients with these less severe conditions are generally heterozygous, in contrast to PFIC3 patients who are generally homozygous or compound heterozygous at the locus (Pauli-Magnus et al., 2005). Although the genetic evidence describes a causative link between *ABCB4* mutations and the disease phenotype, it is often not definitive for the complex conditions and the affect of these mutations on ABCB4 expression, membrane localisation and its PC-flopping activity remains untested.

The generation and expression in HEK293T cells of non-synonymous ABCB4 variants in the presence and in the absence of a PS flippase (ATP8B1/CDC50A) is reported. The mechanism notwithstanding, ATP8B1/CDC50A has a profound effect on the ability of the cells to tolerate ABCB4 function (Groen et al., 2011). Consequently, this heterologous triple expression system was used to analyse the *ABCB4* mutations that have been linked to cholestatic liver disease by genetic studies.

Nine non-synonymous ABCB4 variants were selected for testing. These have been associated with a range of phenotypes in cholestatic patients (Tables 4-1 and 4-3). The

mutations were introduced into the coding region of WT ABCB4 by site-directed mutagenesis and confirmed by DNA sequencing (Section 4.2.2). HEK293T cells were then transiently-transfected with mutant *ABCB4*-expressing vectors in the presence and in the absence of the ATP8B1/CDC50 PS flippase. Importantly, for each experiment, the WT ABCB4 and catalytically inactive Walker B mutant (E558Q) were included as controls. The level of expression of each mutant was then determined by western analysis of whole-cell extracts (Section 4.2.3). A range of different mutant phenotypes was observed (Figure 4-5) which could be divided broadly into 3 categories (Table 4-3).

Allele	Mutated domain	Patient phenotype	Expression level		Implied impact on ABCB4
			ABCB4 only	ABCB4 ATP8B1 CDC50A	
WT	n/a	n/a	+	++++	n/a
WB (E558Q)	NBD1	n/a	++++	++++	Inactive
E528D	NBD1	ICP, LPAC	++	++++	Apparently unaffected
L591Q	NBD1	LPAC	+	++++	
P1161S	NBD2	LPAC	+	++++	
A286V	ICL2	PFIC3	++++	++++	Loss of deleterious PC-flopping activity
M301T	MSH5	LPAC	++++	+++++	
G535D	NBD1	LPAC to ICP to BC	++++	+++++	
S320F	MSH5	PFIC3, ICP, LPAC	+++	+++	Loss of activity and stability
R545C	NBD1	PSC	++	++	
A546D	NBD1	ICP	+++	+++	

Table 4-3. ***Summary of the expression of WT and mutant ABCB4 in HEK293T cells.***

The expression of ABCB4 non-synonymous genetic variants was analysed following transient expression of ABCB4 in the presence and in the absence of ATP8B1/CDC50A in HEK293T cells. The level of expression is summarised here as: +++++ > ++++ > +++ > ++ > +. ABCB4 expression was detected in all samples tested but revealed different phenotypes which can be divided in three broad categories (far right column). ICL, intracellular loop; MSH, membrane-spanning helix; NBD, nucleotide-binding domain; n/a, not applicable; ICP, intrahepatic cholestasis of pregnancy; LPAC, low phospholipid-associated cholelithiasis; PFIC3, progressive familial intrahepatic cholestasis Type 3; BC, biliary cirrhosis; PSC, primary sclerosing cholangitis.

One third of the mutants displayed an expression profile comparable to that of WT ABCB4; i.e. the level of ABCB4 detected was dramatically increased in the presence of ATP8B1/CDC50A (Figure 4-5F; E528D, L591Q and P1161S). These apparently unaffected variants have been associated mainly with LPAC (Floreani et al., 2008, Nakken et al., 2009, Rosmorduc et al., 2003, Rosmorduc et al., 2001) although the E528D mutation

has also been identified in an ICP patient (Floreani et al., 2008). LPAC is a multifactorial syndrome characterised by low phospholipid content in the bile and symptomatic and recurring cholestasis in young adults with an apparent prevalence in the female population (Rosmorduc and Poupon, 2007). Since all three variants display an expression profile analogous to that of the WT protein, it is unlikely that the disease phenotypes are a result of a defect in the PC-efflux activity of ABCB4 under normal conditions. However, it is plausible that the mutations predispose to the condition which only manifests under the influence of environmental and dietary factors. In the ICP patient carrying the E528D variant Floreani *et al.* only sequenced exons 14-16 of the *ABCB4* gene, and additional mutations might have been missed (Floreani et al., 2008). Alternatively, since ICP is likely to be modulated by pregnancy hormones and their metabolites (Arrese and Reyes, 2006, Lammert et al., 2000), it is possible that E528D confers a genetic susceptibility to the disease which manifests during the third trimester of pregnancy when hormone levels are high.

The second group of mutants revealed an expression profile similar to that of the WB (E558Q) mutant (an inactive derivative of ABCB4 carrying a point mutation in the Walker B motif likely rendering it unable to hydrolyse ATP) (Figure 4-5; panel D). These ABCB4 mutants could be detected in the presence and in the absence of ATP8B1/CDC50A at comparable levels that were also similar to the level of WT ABCB4 when co-expressed with ATP8B1/CDC50A (Figure 4-5; G535D, M301T, A286V). However, these mutant phenotypes are not identical to one another. Both M301T and G535D reproducibly express at a significantly higher level in the triple transfection experiment suggesting that they retain a small level of PC-efflux activity that is deleterious in the absence of ATP8B1/CDC50A (a more modest increase in expression is observed with A286V). The low impact of these mutants on HEK293T cells in the absence of ATP8B1/CDC50A

compared to the effect of WT ABCB4 suggests a threshold effect under which low levels of PC-flopping activity are tolerated. These three ABCB4 variants (A286V, M301T and G535D) have been implicated in a variety of cholestatic phenotypes ranging from the most severe PFIC3 (A286V) to the milder LPAC (M301T) and to what appears to be a clinical continuum of diseases progressing from a mild (LPAC) to a progressive (biliary cirrhosis) phenotype (G535D) in a single patient. The western analysis suggests that these variants have lost their deleterious PC-flopping activity. Since they express at a level either comparable (A286V) or slightly elevated (M301T and G535D) compared to the WT protein in the triple transfection, and in the absence of core glycosylated fraction or degradation products, it is likely that they can adopt a normal conformation and traffic to the plasma membrane and that the mutation impacts their ability to flop PC. The M301T and G535D variants have been identified in the heterozygous state (Lucena et al., 2003, Rosmorduc et al., 2003). The expression of the normal allele in each patient probably compensates for the presumably reduced activity of the two variants resulting in the development of relatively mild phenotypes. The development of ICP and the slow, gradual progress to biliary cirrhosis (BC) in the patient expressing the G535D ABCB4 variant (Lucena et al., 2003) possibly reflects the complex, heterogeneous and multifactorial nature of ABCB4-related disease. Degiorgio *et al.* identified the c.857C>T (A286V) mutation in a PFIC3 patient as compound heterozygote with the recurrent c.959C>T (S320F) mutation on the *ABCB4* locus (Degiorgio et al., 2007). The combination of a presumed loss-of-PC-flopping activity variant (A286V) with another variant (S320F) which appears to lack PC-flopping activity as well as stability (possibly due to a folding defect), would most likely result in a severe reduction in PC-efflux, failure of bile flow and progressive liver disease.

The final group of mutants displayed a unique expression pattern in that they do not resemble the profile observed for either WT ABCB4 or the WB mutant. The presence of

ATP8B1/CDC50A had little effect on their expression level. Although none of the mutants could be detected at a level approaching that of the WT expressed in the presence of the PS flippase (Figure 4-5S320F, A286V and A546D); all three are detectable at a higher level than WT ABCB4 in the absence of the PS flippase. The phenotype of these mutants suggests that they lack activity because they express at a higher level than WT ABCB4 in the absence of the PS flippase, and because they are unable to achieve the level of expression of the WB mutant, they may also fail to fold properly or may lack stability. The mutation c.959C>T (S320F) has been associated with a range of disparate phenotypes (PFIC3, LPAC and ICP) and identified in the homozygous, heterozygous as well as in the compound heterozygous states (Bacq et al., 2009, Degiorgio et al., 2007, Keitel et al., 2006, Pauli-Magnus et al., 2004b, Poupon et al., 2010, Rosmorduc et al., 2003, Rosmorduc et al., 2001). Dixon *et al.* identified the A546D variant in an ICP patient heterozygous for this locus (Dixon et al., 2000). Finally, the R545C variant was only detected in a population with PSC although no correlation could be established between *ABCB4* (or *ABCB11*) mutations and the development of PSC or PBC in this prior study (Pauli-Magnus et al., 2004a).

In the earlier studies the level of expression of the S320F variant appeared to be low in western analysis, but immunostaining on liver sections identified the protein at the canalicular membrane suggesting that the variant can traffic to the plasma membrane and probably retains a level of PC-efflux activity (Keitel et al., 2006, Poupon et al., 2010). Several different cholestatic disease phenotypes have been associated with the S320F variant. These can probably be explained by the differences in zygosity in the patients (Degiorgio et al., 2007, Poupon et al., 2010) or the presence of additional mutations in other gene loci implicated in liver disease such as *ABCB11* or the farnesoid X receptor (FXR) (Keitel et al., 2006, Poupon et al., 2010, Zimmer et al., 2009). The influence of endogenous (i.e., pregnancy hormones) or exogenous factors (i.e., environment and/or

diet), or a combination of the two, concomitantly with the S320F mutation may also play a role in the development of the disease phenotype (Bacq et al., 2009, Pauli-Magnus et al., 2004b, Rosmorduc et al., 2003, Rosmorduc et al., 2001).

Dixon *et al.* identified the A546D variant in an ICP patient (Dixon et al., 2000). When the equivalent residue (A544) was mutated in ABCB1, the closest homologue of ABCB4, it caused a trafficking defect in ABCB1 depleting the protein from the plasma membrane. However, the fraction that reached the plasma membrane could efflux drugs suggesting that this variant of ABCB1 was functional (Dixon et al., 2000). The results reported by Dixon *et al.* are in agreement with the reduced stability observed here (Table 4-3). In the triple transfection, the level of expression of the A546D variant is lower than that of WT ABCB4 suggesting that the mutation causes a folding defect which leads to the degradation of the A546D protein by the ERAD (ER-associated degradation) pathway (Meusser et al., 2005, Vembar and Brodsky, 2008). Nevertheless, it is possible that a proportion of the expressed protein can reach the plasma membrane and efflux PC when stimulated by a bile salt. Likewise, the R545C variant could harbour a similar defect. Despite the lack of genetic association between *ABCB4* mutations and the development of PSC and PBC (based on haplotype structure and variant segregation), the c.1633C>T (R545C) mutation was found to be PSC-specific (Pauli-Magnus et al., 2004a). It is possible therefore, that his non-synonymous change has a functional impact on ABCB4 and is involved in the pathogenesis of PSC.

In general, PFIC3 results from the most severe mutations to ABCB4, i.e. of nonsense or frame-shift mutations in the *ABCB4* gene locus which result in truncation of the open reading frame (Chen et al., 2001, de Vree et al., 1998, Jacquemin et al., 2001, Pauli-Magnus et al., 2004b). mRNAs with a premature termination codon are recognised by the

nonsense-mediated mRNA decay (NMD) surveillance system and targeted for degradation (Chang et al., 2007). Consequently, ABCB4 canalicular staining was absent from liver biopsies of PFIC3 patients carrying nonsense or frame-shift mutations (de Vree et al., 1998, Jacquemin et al., 2001). In contrast, missense mutations cause a range of phenotypes with the type and severity of cholestatic disease usually dependent on the zygosity of the patient (Pauli-Magnus et al., 2005). As summarised in Table 4-3, some of the variants characterised in this report associate with a single disease phenotype (L591Q, P1161S, A286V, M301T, R545C and A546D) whereas others have been linked to more than one (E528D and S320F). Furthermore, one mutant (G535D) has been associated with a range of liver disease phenotypes within a single patient suggesting that *ABCB4* mutations can result in a clinical continuum of diseases progressing from a mild to a severe phenotype.

A more detailed biochemical and molecular analysis of mutant ABCB4 protein is required to further characterise the contribution of ABCB4 in the development of cholestatic liver disease. In the following chapter, the localisation of each mutant in HEK293T cells is studied by confocal microscopy providing insight into the trafficking of mutant ABCB4 species to the plasma membrane, and the ability of mutant ABCB4 to efflux PC in a bile salt-dependent manner is measured in order to clarify the link between mutant protein phenotype and patient presentation.

Chapter Five

5 Localisation and phospholipid efflux activity of ABCB4 variants in HEK293T cells

5.1 Introduction

In the previous chapter the generation and expression of *ABCB4* non-synonymous missense mutants was described. HEK293T cells were transfected with the pcDNA3.1-ABCB4wt or pcDNA3.1-ABCB4_X vectors, where X is any of the 9 ABCB4 variants summarised in Table 4-1, either in the presence (triple transfection) or in the absence (single transfection) of the pCI-neo-ATP8B1 and pCI-neo-CDC50A vectors. The level of expression of each mutant was then determined by western analysis of whole-cell extracts and compared with the phenotype of the WT and non-functional Walker B mutant (E558Q). This revealed a range of different mutant phenotypes (Figure 4-5) which could be divided broadly into 3 categories (Table 4-3). Although tentative conclusions could be drawn concerning the effect of the particular mutation on the folding, trafficking and even the function of the protein based on the western analysis, further biochemical evaluation was required.

To this end, confocal laser scanning microscopy (CLSM) was employed to study the trafficking of mutant ABCB4 to the plasma membrane (Section 5.2.1) and the ^{3}H-PC efflux assay (see below) was used to determine the level of PC-flopping activity retained in each variant (Section 5.2.2). Because all variants were shown by western analysis to be expressed following triple transfection (Figure 4-5), and because the co-expression of the PC-floppase alongside the PS-flippase is more physiologically relevant, both the CLSM analysis and the [*methyl*-^{3}H]-PC efflux assay were performed in HEK293T cells co-transfected with the ATP8B1/CDC50A constructs. The basis of the [*methyl*-^{3}H]-PC efflux assay is described in the following section.

5.1.1 Phosphatidylcholine biosynthesis

The major structural lipids in eukaryotic membranes are the *glycerophospholipids* (phosphatidylcholine, PC; phosphatidylethanolamine, PE; phosphatidylserine, PS; phosphatidylinositol, PI; and phosphatidic acid, PA) and the *sphingolipids* (shingomyelin, SM and glycosphingolipids; GS). Within the lipid bilayer of the plasma membrane of eukaryotic cells, there is an asymmetric distribution of lipids with PS and PE predominantly facing the cytosolic side and PC and SM almost exclusively on the outer leaflet (Devaux and Morris, 2004, van Meer et al., 2008).

PC is the principal component of eukaryotic cellular membranes (>50% of the total phospholipid content) and in mammalian cells it is synthesised *de novo* via two different pathways residing in the ER: (i) the PEMT (phosphatidylethanolamine *N*-methyltransferase) pathway (Vance et al., 2008); and, (ii) the CDP (cytidine diphosphate)-choline (or Kennedy) pathway (Kennedy and Weiss, 1956). Although the PEMT pathway only accounts for a small fraction of PC synthesis in most tissues, in the liver it is responsible for ~30% of the total PC synthesis (Kent, 1995). In this pathway, PC is formed by a series of sequential methylations of PE by PEMT (Sundler and Akesson, 1975). In contrast, in the CDP-choline biosynthetic pathway (which occurs in all nucleated cells) PC formation requires the sequential conversion of dietary choline to phosphocholine, CDP-choline and finally PC (Kennedy and Weiss, 1956). The rate-limiting step in this series of reactions requires CTP (cytidine triphosphate) to provide energy for the cytidylyltransferase-catalysed conversion of phosphocholine to CDP-choline which is in turn converted to PC by choline phosphotransferase (Kent, 1995, Vance et al., 2008).

5.1.1.1 The ^{3}H-PC efflux assay

A number of mutations have been reported, following genetic studies in cholestatic patients, which implicate ABCB4 in the manifestation of the disease. To establish cause and effect definitively would require an assay whereby the activity of ABCB4 could be demonstrated (and quantified) in an *in vitro* system to permit the characterisation of ABCB4 variants with non-synonymous changes. Such an assay has been developed recently in our lab (Groen et al., 2011), in which HEK293T cells that have been co-transfected with vectors expressing WT *ABCB4* and *ATP8B1* and *CDC50A*, are fed [*methyl*-^{3}H]choline (a radioactive labelled PC precursor for the Kennedy pathway). The cells are allowed to incorporate [*methyl*-^{3}H]choline PC resulting in the generation of radiolabelled PC species. Forty-eight hours post-transfection, the cells are washed extensively and incubated with culture medium containing taurocholate (TC; 2 mM) to extract labelled PC flopped by ABCB4 to the outer leaflet of the plasma membrane of HEK293T cells. After 24 h incubation, the culture media is recovered and the radioactivity content is quantified. In addition, the cells attached to the culture dish are lysed and the radioactivity associated with the cellular fraction is also measured. The amount of labelled PC effluxed by ABCB4 (i.e., the radioactivity present in the recovered culture medium) is calculated as a percentage of the total radioactivity present in the dish (i.e., the radioactivity in the culture medium plus the radioactivity retained by the cells). Quantification of the fraction of labelled PC effluxed to the culture medium mimics the situation at the canalicular membrane and provides a powerful tool to characterise ABCB4 variants. The results of this investigation are reported in Section 5.2.2.

5.2 Results

5.2.1 Localisation of ABCB4 variants in HEK293T cells

Most proteins adopt a particular three dimensional conformation to function. Failure to do so often has detrimental effects on the protein and misfolded membrane proteins are normally degraded by the ERAD (ER-associated degradation) pathway (Meusser et al., 2005, Vembar and Brodsky, 2008). In fact, many inherited diseases such as cystic fibrosis (CF) are due to defective protein folding (Welch, 2004) caused by mutations that prevent the protein (ABCC7/CFTR in the case of CF) from adopting its native fold resulting in its retention in the ER and subsequent degradation. For example, the ΔF508 mutation in ABCC7 which is present in approximately 70% of patients with cystic fibrosis results in the loss of a phenylalanine residue at amino acid position 508 (Riordan et al., 1989, Kerem et al., 1989). Consequently, the protein is retained in the ER and rapidly degraded preventing it from reaching the plasma membrane (Cheng et al., 1990). Mutations in the *ABCB4* coding region could have similar effects on protein processing which would prevent its correct trafficking to the plasma membrane.

To examine the cellular localisation of ABCB4, HEK293T cells were transiently-transfected with plasmid DNA encoding WT ABCB4 or a non-synonymous missense variant in the presence of the ATP8B1/CDC50A PS flippase and studied by CLSM. Cells were seeded onto glass coverslips at a low density in order to observe some cells in isolation by microscopy. A transfection efficiency of 40 – 60% was therefore generally achieved. Immunofluorescence was studied 48 hours post-transfection after detecting ABCB4 using the monoclonal antibody P_3II-26. The epitope of the P_3II-26 antibody is located in NBD1 of human ABCB4 between the amino acid residues 629 and 692 and so all the variant ABCB4 proteins generated for this study should be detectable (Scheffer et

al., 2000). In the untransfected cells, no ABCB4 was present (Figure 5-1A); the low level of green fluorescent signal detected arises from endogenous fluorophores which emit light when excited at 499 nm, and is known as autofluorescence. In contrast, in the cell populations transiently-transfected with the ABCB4-expressing vector, a strong fluorescent signal could be detected in a number of the recipient cells (Figure 5-1B-L) demonstrating expression of ABCB4 in the presence of ATP8B1/CDC50A and that the protein can be detected by the P_3II-26 primary antibody on fixed cell preparations.

In the majority of cells transfected with plasmid DNA encoding WT or WB (E558Q) mutant ABCB4, the protein appears to be almost exclusively at the periphery of the cell consistent with plasma membrane localisation (Figure 5-1B and C). This observation is in agreement with previous results (Groen et al., 2011). The subcellular localisation of variant ABCB4 reveals two distinct phenotypes. For the majority of mutants (7/9) a fluorescent staining pattern analogous to that of WT and WB ABCB4 is detected which is consistent with plasma membrane localisation of the protein (Figure 5-1D-J). In contrast, in cells transiently expressing either the R545C or the A546D ABCB4 variants, a punctate intracellular signal is evident (Figure 5-1K-L). This is suggestive of a trafficking defect in these two mutants which causes the intracellular retention of a large fraction of the transporter protein. The precise intracellular localisation of variant ABCB4 was not determined but, colocalisation with an organelle-specific antibody such as calnexin and protein disulphide isomerase (ER) or Golgi matrix protein (Golgi), would likely identify the subcellular compartment of the protein.

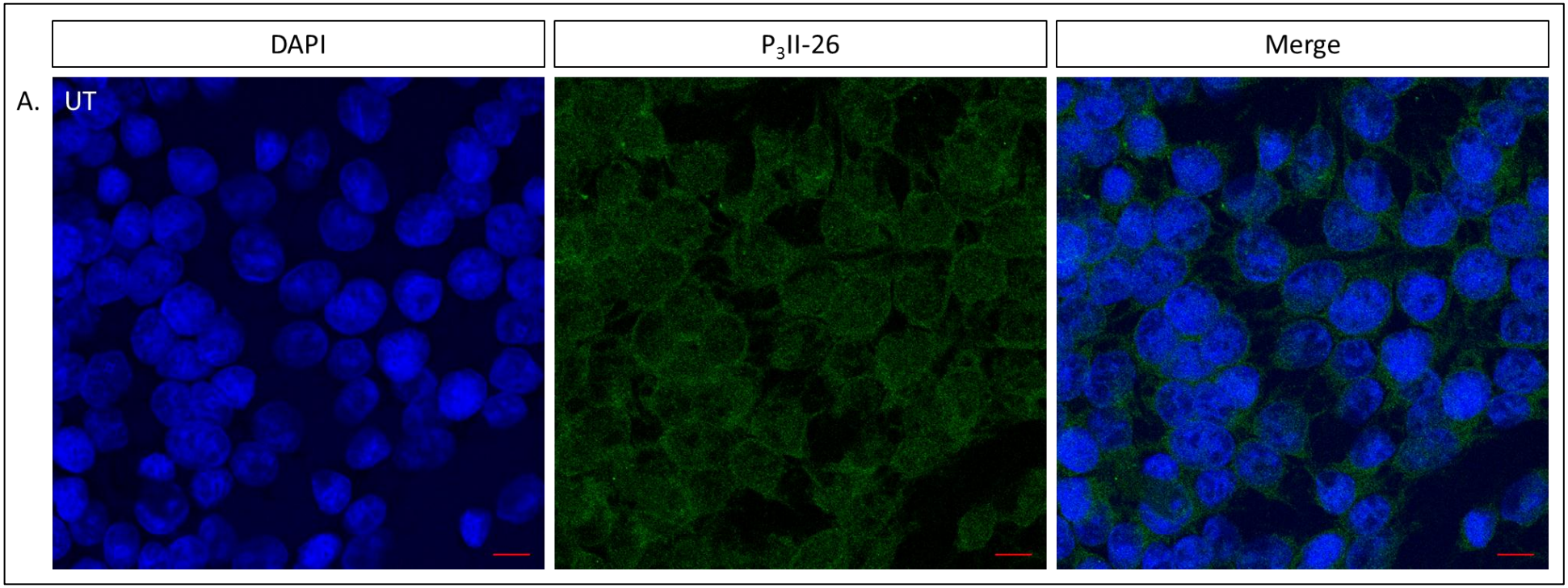

Figure 5-1. ***Expression of ABCB4 WT and missense variants in HEK293T cells in the presence of the ATP8B1/CDC50A PS flippase.***

HEK293T cells transiently expressing WT or missense variant ABCB4 and ATP8B1/CDC50A, were fixed with 10% (v/v) acetone in ethanol. ABCB4 was detected by immunofluorescence using the P_3II-26 monoclonal antibody and Alexa Fluor® 488 Dye-conjugated goat anti-mouse IgG. Nuclei were stained with DAPI (4',6-diamidino-2-phenylindole). Untransfected cells were used as a negative control to account for background fluorescence. WT ABCB4 and the WB (E558Q) mutant were employed as positive controls to confirm that P_3II-26 is specific to ABCB4. Scale bars, 10 µm. Images representative of the whole population are shown in each case.

(A). Untransfected (UT) HEK293T cells. A low level green fluorescent signal (autofluorescence) is detected in all cells.

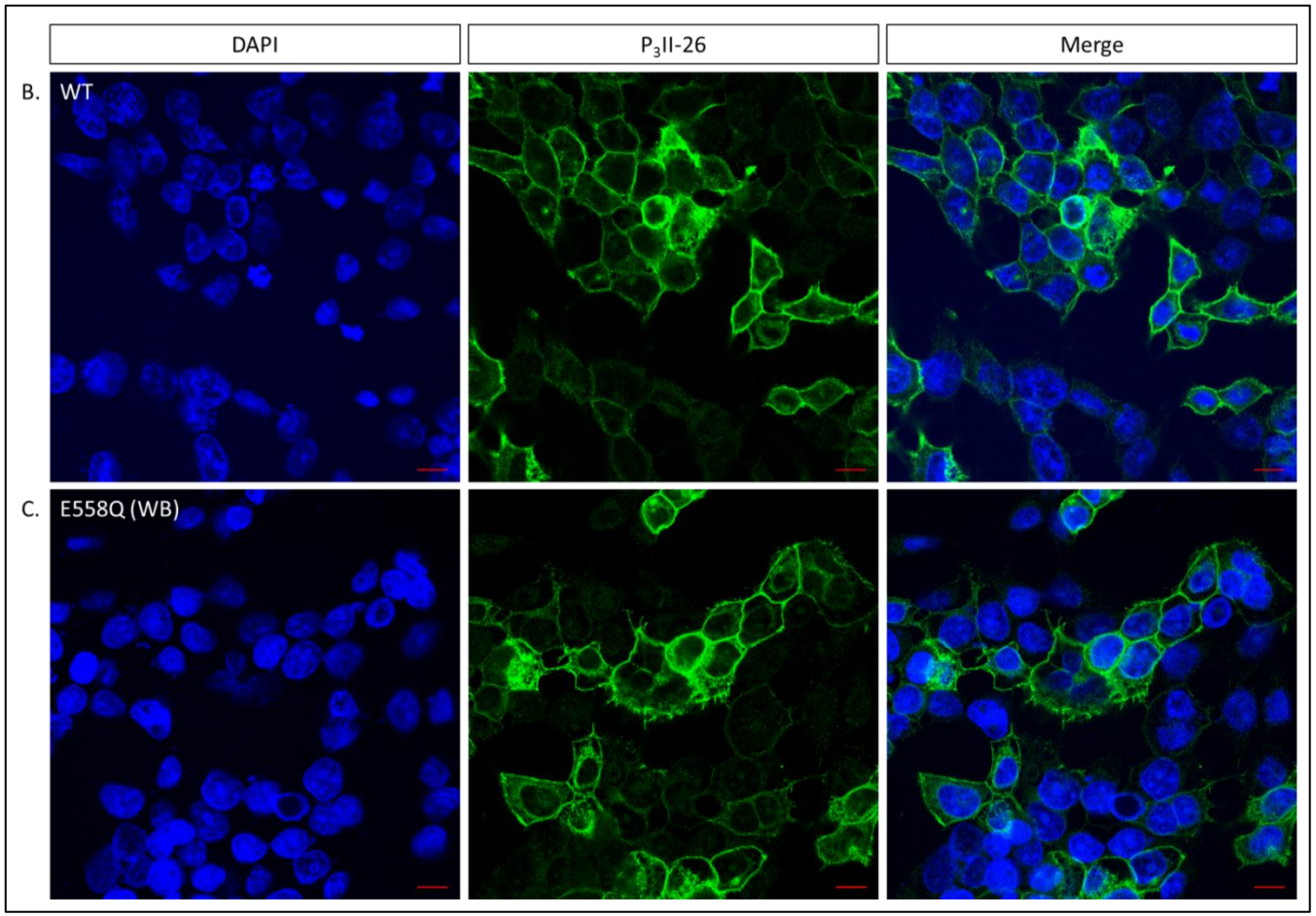

Figure 5-1. ***(continued) Expression of ABCB4 WT and missense variants in HEK293T cells in the presence of the ATP8B1/CDC50A PS flippase.***

HEK293T cells transiently expressing (B) WT and (C) WB mutant (E558Q) ABCB4 in the presence of ATP8B1/CDC50A. The green signal (ABCB4) is consistent with plasma membrane localisation of the protein.

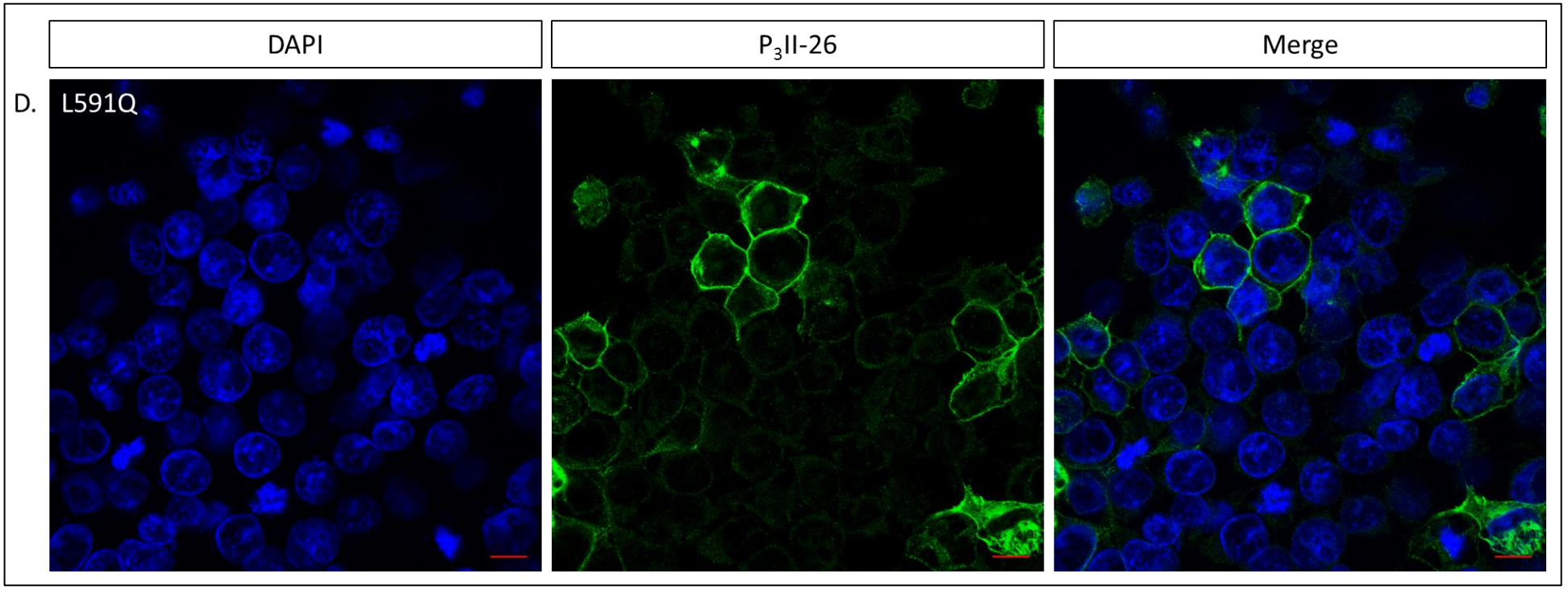

Figure 5-1. ***(continued) Expression of ABCB4 WT and missense variants in HEK293T cells in the presence of the ATP8B1/CDC50A PS flippase.***

(D). HEK293T cells transiently expressing the L591Q non-synonymous ABCB4 variant in the presence of ATP8B1/CDC50A. The green signal (ABCB4) is consistent with plasma membrane localisation of the protein.

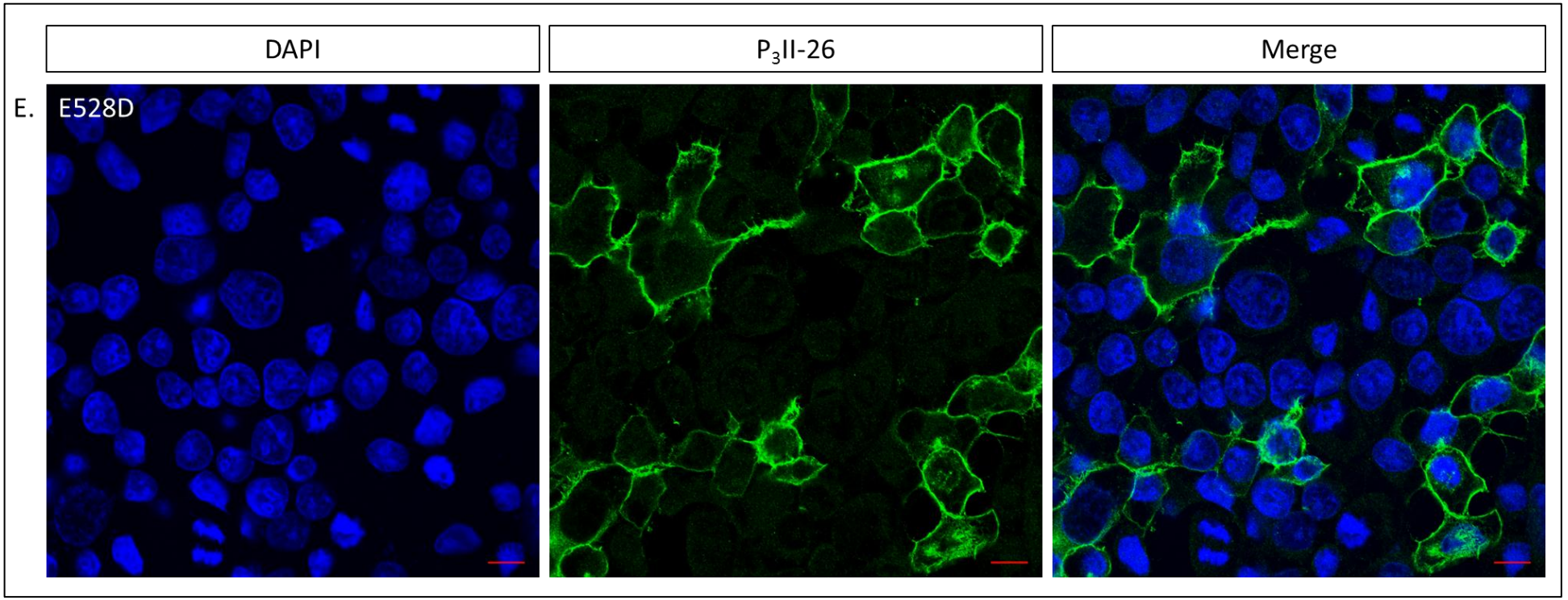

Figure 5-1. ***(continued) Expression of ABCB4 WT and missense variants in HEK293T cells in the presence of the ATP8B1/CDC50A PS flippase.***

(E). HEK293T cells transiently expressing the E528D non-synonymous ABCB4 variant in the presence of ATP8B1/CDC50A. The green signal (ABCB4) is consistent with plasma membrane localisation of the protein.

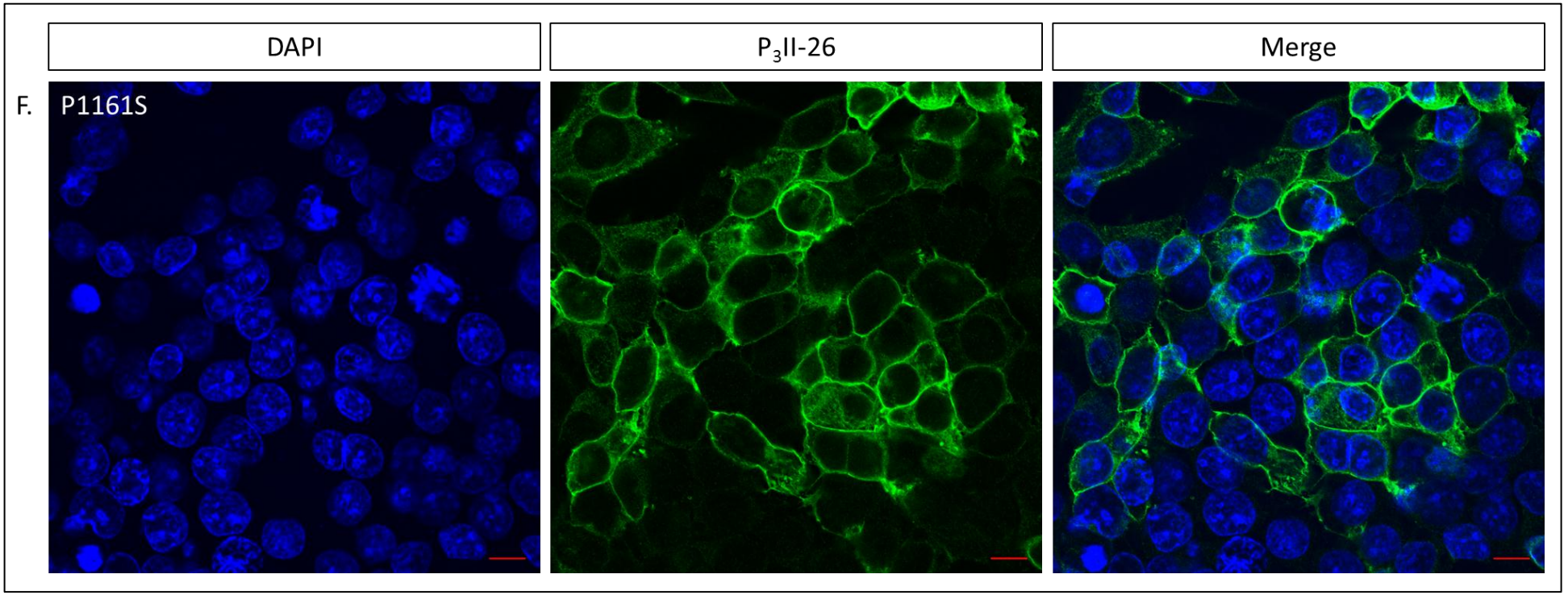

Figure 5-1. ***(continued) Expression of ABCB4 WT and missense variants in HEK293T cells in the presence of the ATP8B1/CDC50A PS flippase.***

(F). HEK293T cells transiently expressing the P1161S non-synonymous ABCB4 variant in the presence of ATP8B1/CDC50A. The green signal (ABCB4) is consistent with plasma membrane localisation of the protein.

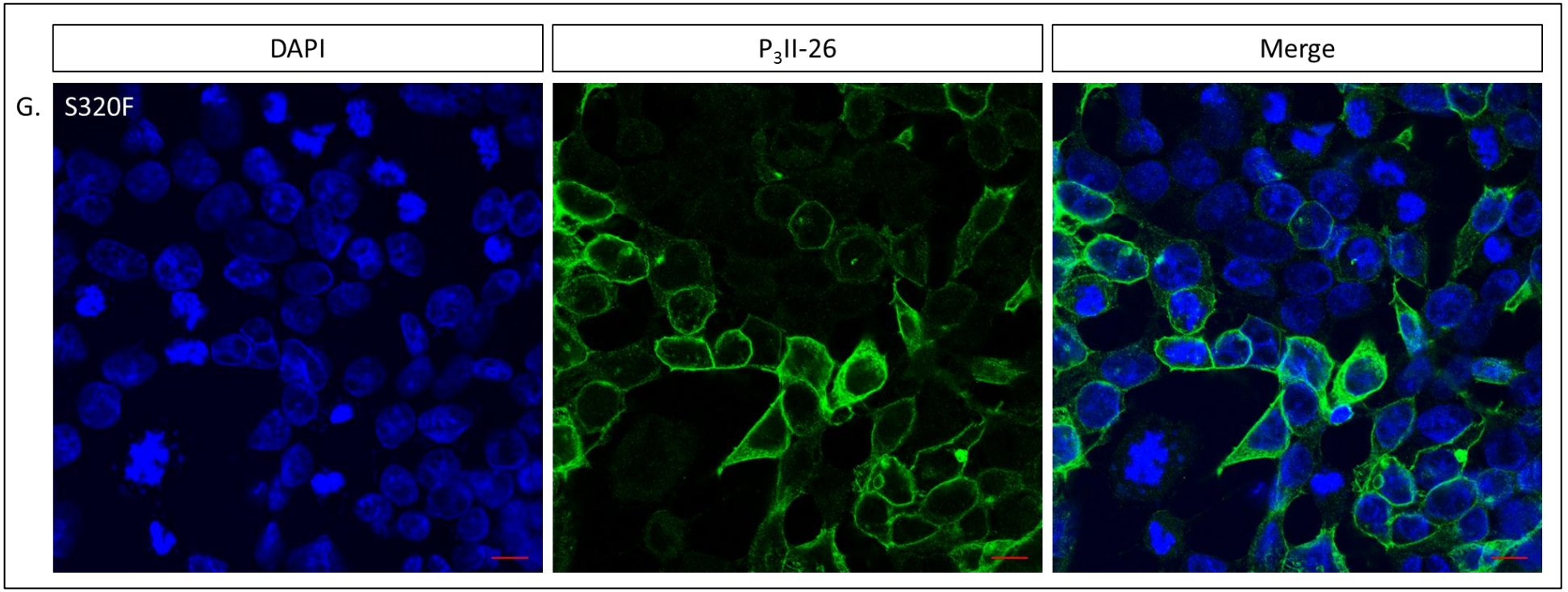

Figure 5-1. ***(continued) Expression of ABCB4 WT and missense variants in HEK293T cells in the presence of the ATP8B1/CDC50A PS flippase.***

(G). HEK293T cells transiently expressing the S320F non-synonymous ABCB4 variant in the presence of ATP8B1/CDC50A. The green signal (ABCB4) is consistent with plasma membrane localisation of the protein.

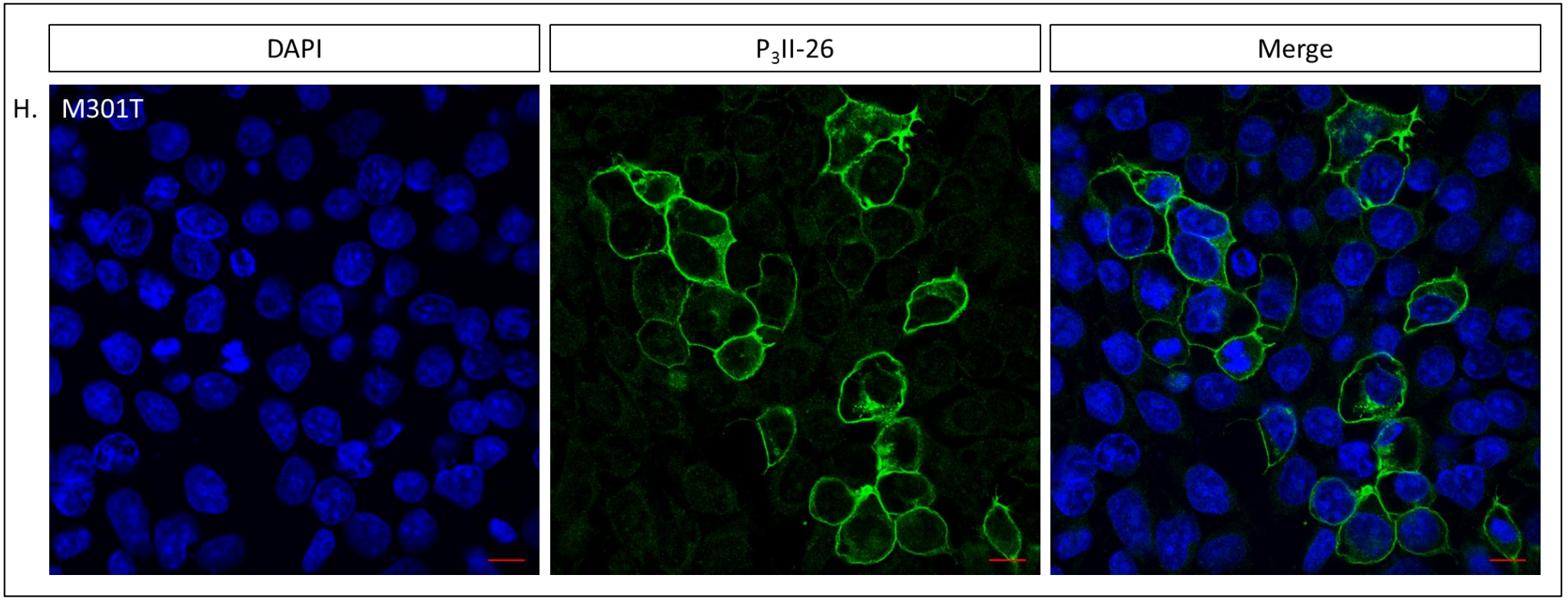

Figure 5-1. ***(continued) Expression of ABCB4 WT and missense variants in HEK293T cells in the presence of the ATP8B1/CDC50A PS flippase.***

(H). HEK293T cells transiently expressing the M301T non-synonymous ABCB4 variant in the presence of ATP8B1/CDC50A. The green signal (ABCB4) is consistent with plasma membrane localisation of the protein.

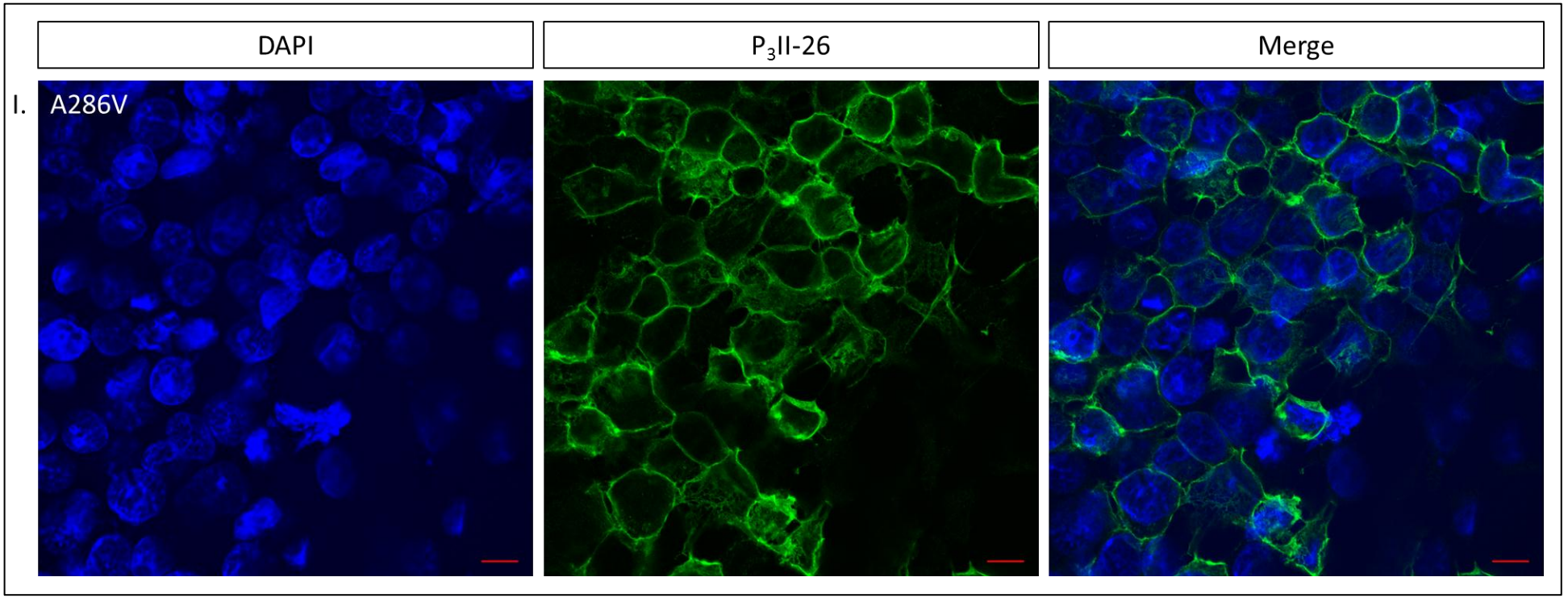

Figure 5-1. ***(continued) Expression of ABCB4 WT and missense variants in HEK293T cells in the presence of the ATP8B1/CDC50A PS flippase.***

(I). HEK293T cells transiently expressing the A286V non-synonymous ABCB4 variant in the presence of ATP8B1/CDC50A. The green signal (ABCB4) is consistent with plasma membrane localisation of the protein.

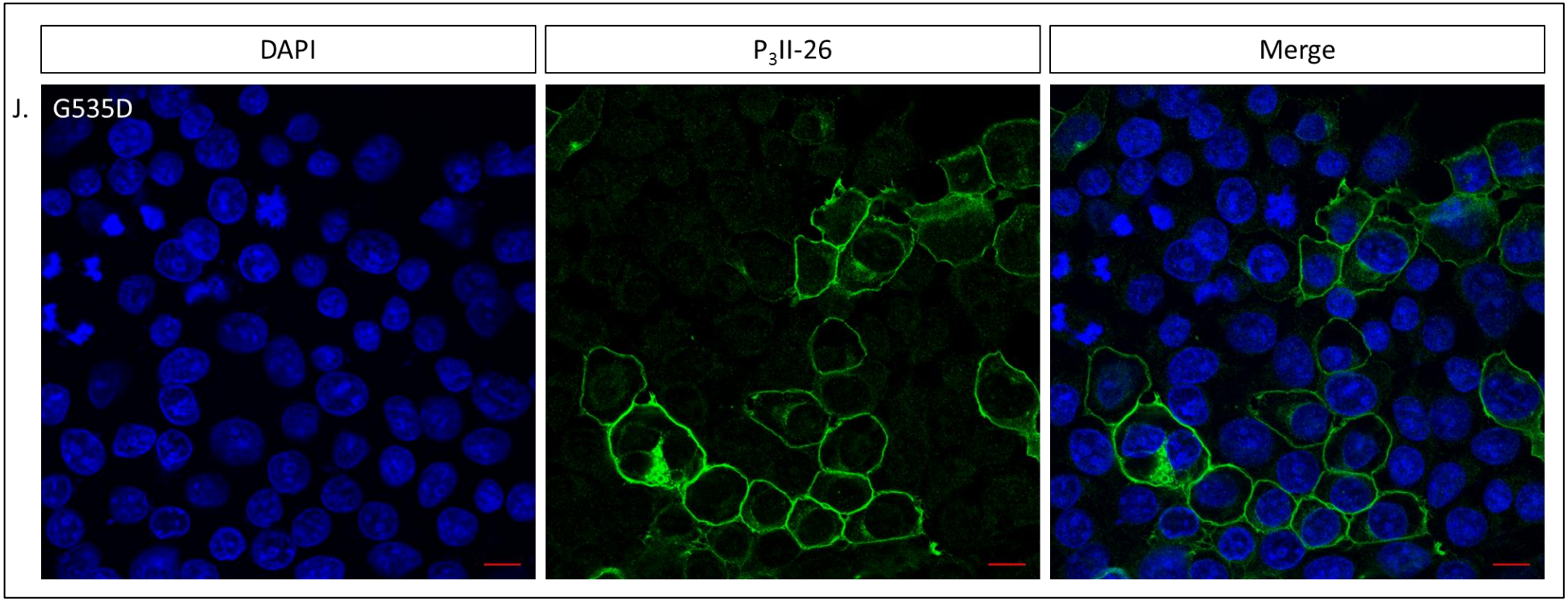

Figure 5-1. ***(continued) Expression of ABCB4 WT and missense variants in HEK293T cells in the presence of the ATP8B1/CDC50A PS flippase.***

(J). HEK293T cells transiently expressing the G535D non-synonymous ABCB4 variant in the presence of ATP8B1/CDC50A. The green signal (ABCB4) is consistent with plasma membrane localisation of the protein.

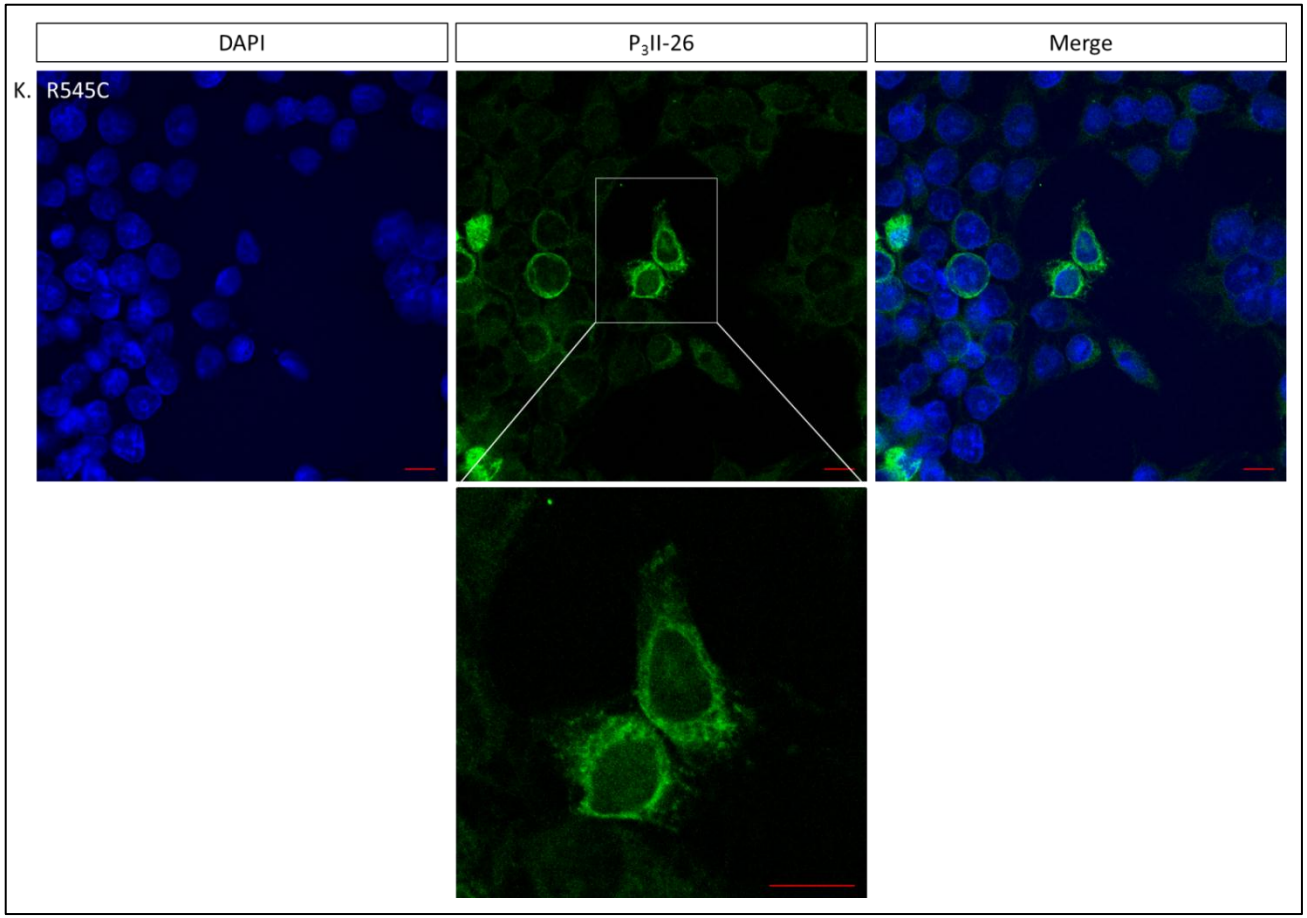

Figure 5-1. ***(continued) Expression of ABCB4 WT and missense variants in HEK293T cells in the presence of the ATP8B1/CDC50A PS flippase.***

(K). HEK293T cells transiently expressing the R545C non-synonymous ABCB4 variant in the presence of ATP8B1/CDC50A. The green signal (ABCB4) is consistent with cytosolic localisation of the protein suggesting a trafficking defect for this mutant. Lower panel; scale bar, 10 µm.

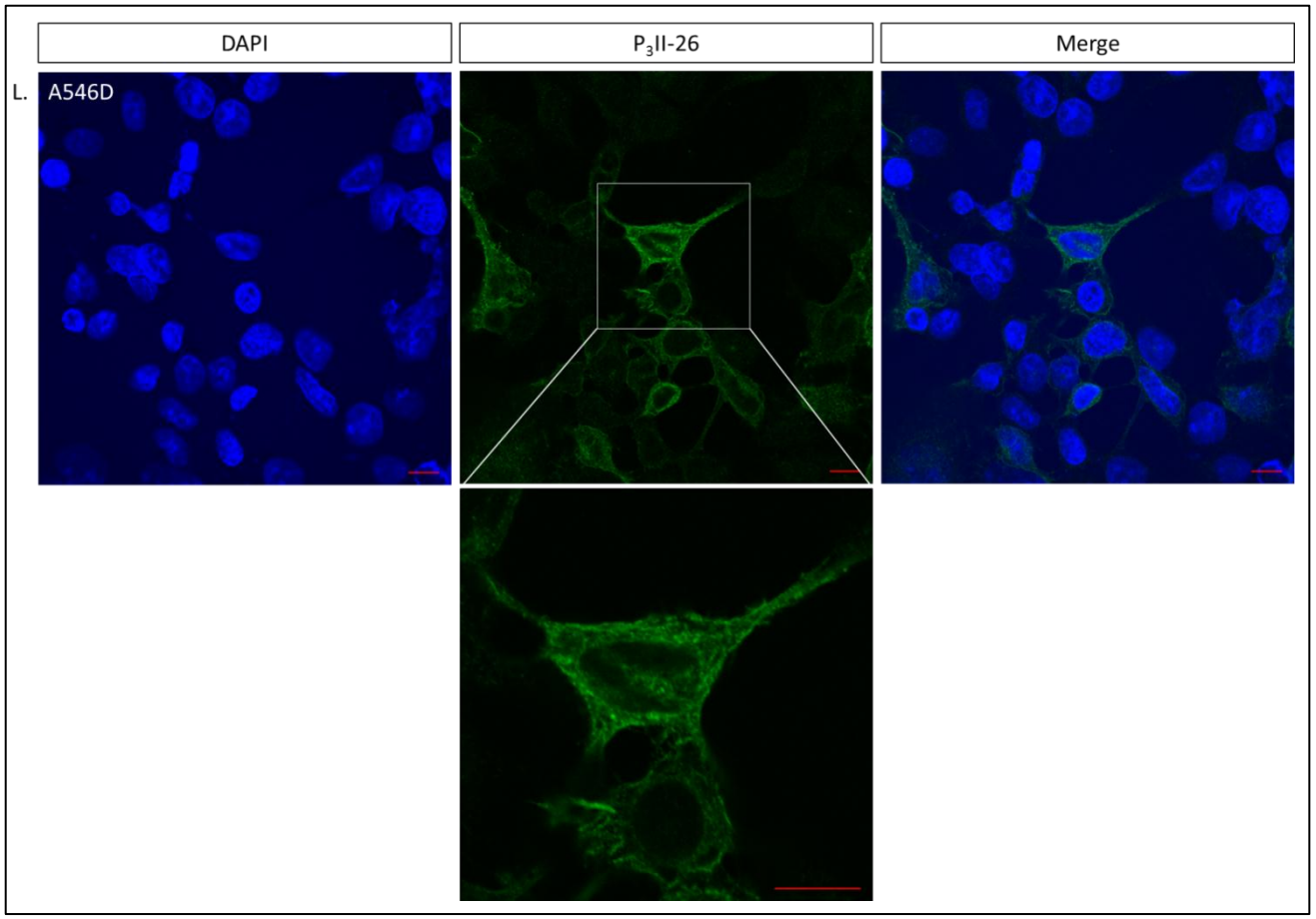

Figure 5-1. ***(continued) Expression of ABCB4 WT and missense variants in HEK293T cells in the presence of the ATP8B1/CDC50A PS flippase.***

(L). HEK293T cells transiently expressing the A546D non-synonymous ABCB4 variant in the presence of ATP8B1/CDC50A. The green signal (ABCB4) is consistent with cytosolic localisation of the protein suggesting a trafficking defect for this mutant. Lower panel; scale bar, 10 µm.

5.2.2 PC-efflux activity of ABCB4 variants in HEK293T cells

The co-expression of WT *ABCB4* with *ATP8B1* and *CDC50A* allows HEK293T cells to tolerate the function of ABCB4 enabling the measurement of the efflux of PC in a bile salt-dependent manner (Groen et al., 2011). As shown by pulse-chase experiments performed in rat hepatocytes, after a 30 min incubation with [*methyl*-^{3}H]choline, more than 90% of the radioactivity was present as phosphocholine. Following a chase with unlabelled choline, the radiolabelled phosphocholine was converted to PC as determined by thin-layer chromatography of the various choline metabolites (Pelech et al., 1983). It should therefore be possible to measure the level of PC floppase activity of ABCB4, by "feeding" cells [*methyl*-^{3}H]choline and analysing the amount of radiolabelled PC effluxed into the culture medium. To mimic the situation at the canalicular membrane (because there is no lipid flow unless there is there is bile salt flow) sodium taurocholate (TC) was added to the medium, to accept the PC flopped by ABCB4. The efficiency of [*methyl*-^{3}H]choline uptake by the cells can vary within an experiment probably due to a combination of micropipetting errors and the efflux of PC by active ABCB4 within the first two days. To account for differences in [*methyl*-^{3}H]choline incorporation between wells, the radioactivity effluxed to the medium in the presence of 2 mM TC was calculated as the percentage of the total radioactivity in each well; i.e. amount of radioactivity in the medium following the addition of TC divided by the sum of the radioactivity in the medium plus the radioactivity retained intracellularly.

It is particularly important to have a healthy monolayer of cells because all cells contain PC in their outer leaflet and dying cells are relatively easily solubilised by a natural detergent like TC. It was crucial therefore to include in each experiment a positive control (WT ABCB4 co-expressed with ATP8B1/CDC50A) and a negative control (the non-functional WB mutant co-expressed with ATP8B1/CDC50A). The level of TC-dependent PC efflux

should be significantly different in these two conditions, as shown in Figure 5-2, signifying the health of the cells. Mock-transfected cells (parental, empty form of the pcDNA3.1 vector co-expressed with ATP8B1/CDC50A) display a low level of TC-dependent PC extraction but it is significantly lower than the level observed when the WB mutant is expressed (Figure 5-2).

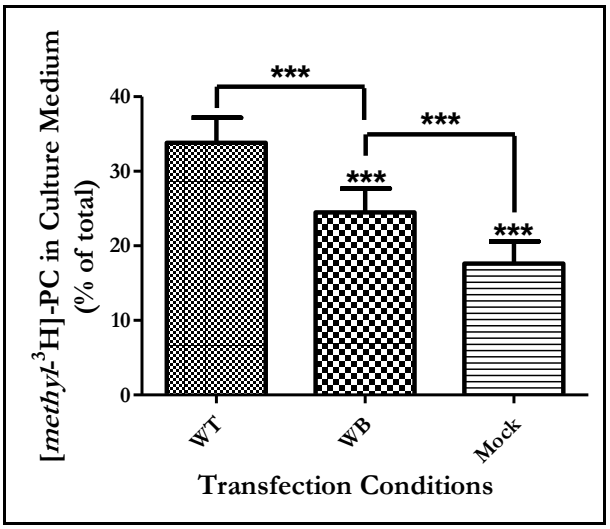

Figure 5-2. ***TC-dependent PC efflux in triple transfected HEK293T cells.***

HEK293T cells were triple transfected with plasmid DNA encoding for WT or WB (E558Q) ABCB4 or the parental empty vector pcDNA3.1 (mock) and the ATP8B1 and CDC50A-expressing vectors, and fed [*methyl*-^{3}H]choline for 48 h. The radioactivity effluxed to the medium in the presence of 2 mM sodium taurocholate hydrate (TC) was calculated as the percentage of the total radioactivity in each well. Cells expressing WT ABCB4 efflux significantly more PC than cells expressing the WB mutant. Mock-transfected cells consistently display a low level of TC-dependent PC extraction which is significantly lower than the level observed in the WB-transfected cells. Statistical analysis by one-way ANOVA (analysis of variance) was performed in the GraphPad PRISM® V5.0 software. *n* = 6; ****P*<0.005; error bars, standard error of the mean.

The effect of the E558Q mutation has not been characterised in ABCB4. However, it has been shown that when the equivalent glutamate residue (E556) in ABCB1 (the closest homologue of ABCB4) was mutated to a glutamine (Q), the catalytic activity of ABCB1 was abolished (Sauna et al., 2002, Zolnerciks et al., 2007). This suggests that the presence of ABCB4 protein in the plasma membrane may cause some destabilisation of the membrane leading to extraction (rather than flopping) of radiolabelled PC. The E558Q

WB mutant was therefore used as a negative control to account for background radioactivity present in the culture medium.

To measure the PC-efflux activity of variant ABCB4, HEK293T cells were transiently co-transfected with plasmid DNA expressing variant ABCB4, and ATP8B1 and CDC50A. Cells were then fed [*methyl*-^{3}H]choline for 48 h. The cell medium was subsequently replaced with fresh medium containing TC (2 mM) to drive the efflux of [*methyl*-^{3}H]-PC from the triple-transfected cells. The background level of radioactivity (i.e., percentage of [*methyl*-^{3}H]-PC effluxed by the WB mutant in each experiment) was then subtracted from each sample and the corrected levels of radiolabelled TC-dependent PC efflux by the variant ABCB4 were plotted and compared to the level of activity of WT ABCB4 (Figure 5-3).

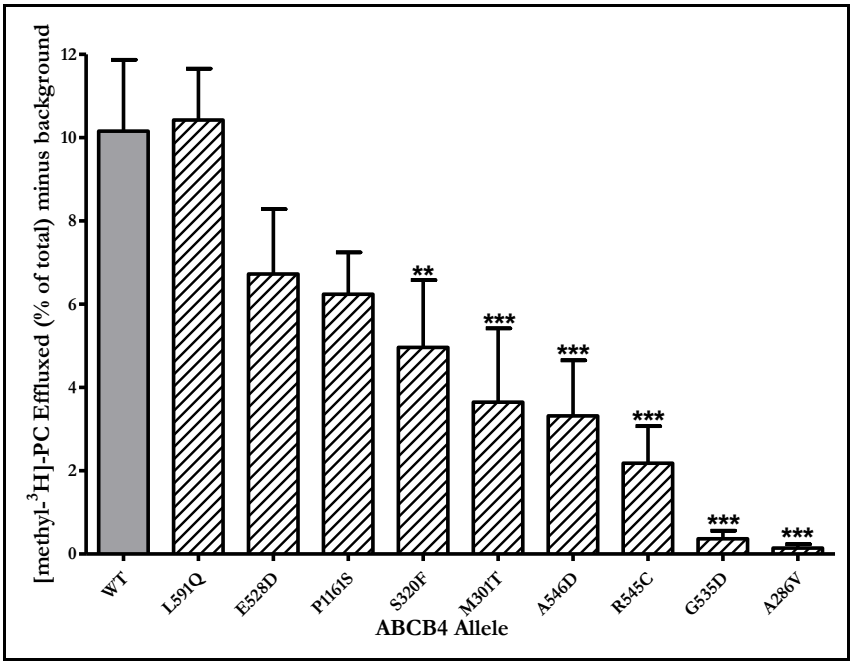

Figure 5-3. ***TC-stimulated PC efflux by ABCB4 in the presence of the ATP8B1/CDC50A PS flippase.***

HEK293T cells transiently co-expressing WT ABCB4 and ATP8B1 and CDC50A were fed [*methyl*-^{3}H]choline for 48 h. The radioactivity effluxed to the medium in the presence of 2 mM sodium taurocholate hydrate (TC) was calculated as the percentage of the total radioactivity in each well after subtraction of the background level from similarly treated cells transfected with the Walker B (E558Q) mutant. The experiment was performed six independent times (*n* = 6) for statistical analysis by one-way ANOVA (analysis of variance) using the GraphPad PRISM® V5.0 software. *****P*<0.01, ******P*<0.005 (with respect to wild-type); error bars, standard error of the mean.

The level of [*methyl*-^{3}H]-PC effluxed by each variant in the presence of TC was then used to calculate the relative activity of each mutant protein when normalised to the 100% level of TC-dependent [*methyl*-^{3}H]-PC efflux by WT ABCB4.

The data show that the different mutations affect the ability of ABCB4 to efflux radiolabelled PC to varying degrees. Specifically, cells expressing the L591Q variant retain a very high level of PC-floppase activity comparable to cells expressing the WT protein. Although the E528D and P1161S variants appear, consistently, to have a lower activity than WT, these are not statistically different from that of the WT protein. The activity of cells expressing the S320F variant is reduced by 50% compared to WT ABCB4 ($P<0.01$). Both the M301T and A546D variants efflux PC at about one third of the level of activity of the WT protein ($P<0.005$) whereas the R545C variant has only 20% of the PC-efflux activity compared to cells expressing WT ABCB4 ($P<0.005$). Finally, the G535D and A286V variants confer little or no PC-efflux activity to the host cells.

Cells expressing different variants of ABCB4 can therefore have distinct phenotypes. The phenotypes range from full (L591Q) or close to full (E528D and P1161S) activity, to no activity (G535D and A286V) to efflux PC. Some variants that confer an intermediate level of PC-floppase activity (S320F, M301T, A546D and R545C) that is significantly different compared to the efflux activity of WT ABCB4 in HEK293T cells are arguably the most interesting as these offer the best possibility for clinical intervention.

5.3 Discussion

In Chapter 4 it was demonstrated that a non-synonymous change in the *ABCB4* coding region can affect the expression level of ABCB4 in HEK293T cells (Figure 4-1). This may

be due to the mutation preventing the protein folding efficiently and trafficking to the plasma membrane or in single-transfected cells it may be due to impairment of ABCB4 function abrogating a deleterious effect on the host cell membrane, or a combination of both.

To further characterise the molecular pathogenesis of ABCB4 missense mutations, the nine variant forms of the protein (Table 4-1) were transiently co-expressed in HEK293T cells with the ATP8B1/CDC50A PS flippase. Their subcellular localisation (Section 5.2.1) and their ability to efflux radiolabelled PC in a bile salt-dependent manner were studied (Section 5.2.2).

Allele	Mutated domain	Patient phenotype	Predominant localisation (PM/IC)	Efflux Activity (% of WT)
WT	n/a	n/a	PM	100
WB (E558Q)	NBD1	n/a	PM	n/a
L591Q	NBD1	LPAC	PM	102
E528D	NBD1	ICP, LPAC	PM	66
P1161S	NBD2	LPAC	PM	61
S320F	MSH5	PFIC3, ICP, LPAC	PM	49
M301T	MSH5	LPAC	PM	36
A546D	NBD1	ICP	IC	33
R545C	NBD1	PSC	IC	21
G535D	NBD1	LPAC to ICP to BC	PM	4
A286V	ICL2	PFIC3	PM	1

Table 5-1. ***Summary of the subcellular localisation and relative bile salt-dependent PC-efflux activity of WT and mutant ABCB4 in HEK293T cells.***

The subcellular localisation and ability to efflux [*methyl*-^{3}H]-PC in a TC-dependent manner of WT and mutant ABCB4 was studied following transient expression in HEK293T cells in the presence of the ATP8B1/CDC50A PS-flippase. n/a, not applicable; NBD, nucleotide-binding domain; MSH, membrane-spanning helix; ICL, intracellular loop; LPAC, low phospholipid-associated cholelithiasis; ICP, intrahepatic cholestasis of pregnancy; PFIC3, progressive familial intrahepatic cholestasis Type 3; PSC, primary sclerosing cholangitis; BC, biliary cirrhosis; PM, plasma membrane; IC, intracellular compartment.

So far in the analysis none of the data has been corrected for expression level. The level of expression of the L591Q, E528D and P1161S variants was very low in the single transfection and dramatically improved in the triple transfection similar to levels

comparable to WT ABCB4 (Figure 4-5). This western blot data suggested that these mutants are able to traffic to the plasma membrane where they are likely to flop PC with high efficiency. When expressed in HEK293T cells and examined by CLSM, all three variants revealed a staining pattern consistent with efficient plasma membrane localisation of the protein (Table 5-1). Furthermore, in the [*methyl*-^{3}H]-PC efflux assay all three variants maintained a high level of TC-dependent PC-flopping activity comparable to WT ABCB4 (Table 5-1). Taken together, these data suggest that the mutations do not appear to affect protein expression, plasma membrane localisation or the lipid-translocase activity of ABCB4 *per se* under the test conditions.

The expression of the M301T, A286V and G535D variants when analysed by western blot was high in the single transfection and slightly improved in the triple transfection (Figure 4-5). From the localisation studies presented in this chapter, it is evident that these mutants traffic to the plasma membrane (Table 5-1). Their high level of expression in the single transfection, in combination with their apparent plasma membrane localisation, suggests that these variants have reduced lipid-flopping activity. In fact, the G535D and A286V missense alterations appear to have a dramatic influence on the level of TC-dependent PC-efflux activity (i.e., 4% and 1% of WT ABCB4 activity, respectively, $P<0.005$) whereas M301T is only able to efflux PC at 36% of WT ABCB4 ($P<0.005$) (Table 5-1). In each of these three cases the non-synonymous mutation most likely affects the molecular mechanism of PC-flopping activity of ABCB4, but to different degrees. This is also reflected in the patient phenotypes with which the variants are associated. For example, it is not surprising, given the lack of activity of A286V ABCB4, that it is associated with PFIC3. The relationship between genotype and phenotype is discussed further in the general discussion (Chapter 6).

The remaining three mutants (S320F, A546D and R545C), were detected by western blot at a similar level in the presence and in the absence of ATP8B1/CDC50A (Figure 4-5). However, none of the mutants reached the level of expression of the WT ABCB4 achieved in the presence of ATP8B1/CDC50A, but each was present at a higher level than WT ABCB4 in the absence of the PS-flippase (Figure 4-5). The subcellular localisation of the S320F variant is consistent with efficient trafficking to the plasma membrane and when subjected to the [*methyl*-^{3}H]-PC efflux assay, S320F was shown to efflux radiolabelled PC with half the efficiency of WT ABCB4 (Table 5-1). In contrast, the A546D and R545C variants accumulated in an intracellular compartment which indicates a trafficking defect most likely caused by inefficient folding of the polypeptide during the maturation steps in the ER and Golgi (Table 5-1). Nevertheless, it is likely that some A546D and R545C ABCB4 protein can reach the plasma membrane because cells harbouring these two mutants can efflux PC in a bile salt-dependent manner to 33% and 21% (P<0.005), respectively, of the WT activity (Table 5-1).

Collectively, the data presented in Chapters 4 and 5 describe a novel approach undertaken to characterise a group of ABCB4 non-synonymous variants linked to cholestatic liver disease. Biochemical characterisation of the variant proteins has provided insights into the effect of each mutation on ABCB4 expression, localisation and PC-floppase function. Correlations between genotype and patient phenotype and future prospects for genetic screening and clinical intervention are discussed in the following chapter.

Chapter Six

6 General Discussion

This thesis encompasses the work undertaken to characterise two related members of the ATP-binding cassette superfamily of proteins, ABCB1 and ABCB4. In Chapter 3, the use of the "split-ubiquitin" yeast two-hybrid system to screen for regulators of ABCB1 is described. This approach proved to be unfruitful as all the candidates isolated have been ruled out as false positives or non-specific. The underlying reasons for this unsuccessful attempt were discussed in Chapter 3 and are therefore not considered further here. In Chapters 4 and 5, the effect of ABCB4 missense mutations linked to abnormal bile flow is investigated. It was demonstrated that cells expressing different variants of ABCB4 can have distinct phenotypes. The effect of the missense mutations on ABCB4 and possible genotype-phenotype correlations are discussed below. Future perspectives for clinical intervention are also considered.

6.1 ABCB4 and cholestatic liver disease

Impairment of bile flow into the small intestine is known as cholestasis and can cause a wide range of hepatic disease from the benign and episodic to the malign and fatal. The most severe phenotype, PFIC, is characterised by progressive cholestatic liver disease which eventually leads to liver failure and can only be treated by liver transplantation (Davit-Spraul et al., 2009). There are three types of PFIC (1-3), each caused by mutations in the genes encoding hepatic transporters involved in bile formation. The genes mutated in PFIC1, 2 and 3 are ATP8B1, ABCB11 and ABCB4 respectively (reviewed in van Mil et al., 2005).

Sequence analysis in PFIC3 patients has resulted in the cataloguing of approximately 40 different mutations in patients with high level of serum γ-GT, a normal level of serum cholesterol and moderately raised concentrations of serum primary bile acids (Chen et al.,

2001, de Vree et al., 1998, Degiorgio et al., 2007, Jacquemin et al., 2001). The patient is usually homozygous for the mutation or compound heterozygous. Typically the mutation is a nonsense alteration that could encode only for a truncated protein, in line with the absence of ABCB4 staining in liver biopsies from PFIC3 patients (Jacquemin et al., 2001). The near absence of *ABCB4* mRNA in northern blot analysis on liver samples from several patients indicates that the truncations result in instability of ABCB4 mRNA which is then degraded (de Vree et al., 1998, Deleuze et al., 1996) although this could be secondary to the progressive liver disease. In these cases the link between patient genotype and disease phenotype is clear. The lack of ABCB4 protein causes the accumulation of toxic bile acids in bile which is not neutralised by phospholipids, eventually leading to damage to the bile canaliculi and biliary epithelium (Jacquemin et al., 2001).

It is becoming increasingly apparent that missense mutations in *ABCB4* are also associated with PFIC3, ICP, DIC, LPAC, PBC and PSC and in these cases the link between the genetic alteration and disease outcome is less clear. Whether the patient phenotype is due to an affect on protein expression, or on the ability of the protein to reach the plasma membrane or efflux phospholipids, is addressed in this study. A total of nine *ABCB4* missense variants implicated in cholestatic liver disease were generated and their expression, trafficking to the plasma membrane and ability to efflux PC in a bile salt-dependent manner was investigated using a heterologous expression system (Table 6-1).

6.2 The expression system

In a recent study, our group reported that *ABCB4* expression was very poor in HEK293T cells and that this was due to cytotoxicity of ABCB4 function. In contrast, an inactive mutant form of the protein expressed very well in the cells and trafficked to the plasma

a.a. Change	Base Change	Domain	Relevant patient genotype where known	Disease Class	Reference	Expression Level		Predominant Localisation (PM/IC)	Efflux Activity (% of WT)
						ABCB4 Only	ABCB4 ATP8B1/CDC50A		
WT	n/a	n/a	n/a	n/a	n/a	+	++++	PM	100
E558Q	1672G>C	NBD1	n/a	n/a	(Groen et al., 2011)	++++	++++	PM	n/a
L591Q	1772T>A	NBD1	HOM	LPAC	(Rosmorduc et al., 2003)	+	++++	PM	102
E528D	1584G>C	NBD1	HET	LPAC	(Rosmorduc et al., 2003)	++	++++	PM	66
			HET	LPAC	(Nakken et al., 2009)				
			HET	ICP	(Floreani et al., 2008)				
P1161S	3481C>T	NBD2	HOM	LPAC	(Rosmorduc et al., 2001)	+	++++	PM	61
			HET	LPAC	(Rosmorduc et al., 2003)				
S320F	959C>T	MSH5	A286V [on 2nd allele]	PFIC3	(Degiorgio et al., 2007)	+++	+++	PM	49
			Y279X [on 2nd allele]	PFIC3	(Degiorgio et al., 2007)				
			A953D [on 2nd allele] + V444A [on *ABCB11*] (HET)	LPAC to PFIC3	(Poupon et al., 2010)				
			HOM	LPAC	(Rosmorduc et al., 2001)				
			HOM	LPAC	(Rosmorduc et al., 2003)				
			HOM	ICP	(Pauli-Magnus et al., 2004b)				
			HET + V444A [on *ABCB11*] + -1G>T [on *FXR*] (HET)	ICP	(Zimmer et al., 2009)				
			HOM + V444A [on *ABCB11*]	ICP	(Keitel et al., 2006)				
			HET	ICP	(Bacq et al., 2009)				
M301T	902T>C	MSH5	HET	LPAC	(Rosmorduc et al., 2003)	++++	+++++	PM	36
A546D	1637C>A	NBD1	HET	ICP	(Dixon et al., 2000)	+++	+++	IC	33
R545C	1633C>T	NBD1	Unknown	PSC	(Pauli-Magnus et al., 2004a)	++	++	IC	21
G535D	1605G>A	NBD1	HET	LPAC (juvenile) to ICP (2× pregnancy) to BC (at 47 years)	(Lucena et al., 2003)	++++	+++++	PM	4
A286V	857C>T	ICL2	S320F [on 2nd allele]	PFIC3	(Degiorgio et al., 2007)	++++	++++	PM	1

Table 6-1. ***ABCB4 non-synonymous mutations analysed in this study.***

The zygosity of index patients is indicated as: homozygous (HOM), heterozygous (HET) or compound heterozygous (c.HET). The data obtained from the experiments described here are outlined in the last four columns. The level of expression of WT and variant ABCB4 as obtained by western analysis is summarised as: +++++ > ++++ > +++ > ++ > +. The subcellular localisation and ability to efflux PC in a taurocholate-dependent manner of WT and variant ABCB4 are also indicated. ICL, intracellular loop; MSH, membrane-spanning helix; NBD, nucleotide-binding domain; n/a, not applicable; ICP, intrahepatic cholestasis of pregnancy; LPAC, low phospholipid-associated cholelithiasis; PFIC3, progressive familial intrahepatic cholestasis Type 3; BC, biliary cirrhosis; PSC, primary sclerosing cholangitis; PM, plasma membrane; IC, intracellular compartment.

membrane. The cytotoxicity of ABCB4 was reduced to a background level upon co-expression of the ATP8B1/CDC50A complex. This led to a dramatic increase in the level of ABCB4 and permitted the localisation of the protein to the plasma membrane. Furthermore, ABCB4 was able to flop PC in a bile salt-dependent manner (Groen et al., 2011). Most importantly, these observations were confirmed in an *in vivo* mouse model whereby the canalicular membrane of mice deficient in both *Atp8b1* and *Abcb4* expression was more resistant to bile salt-mediated damage than the membrane of mice deficient on only Atp8b1 or Abcb4 (Groen et al., 2011). These observations are the basis for the heterologous expression system employed here for the characterisation of nine ABCB4 variants that had been linked to cholestatic liver disease by genetic studies.

ABCB4 has been expressed successfully in polarised cells [human hepatocellular carcinoma (HepG2) and Madin-Darby canine kidney (MDCK) II cells (Delaunay et al., 2009), pig kidney epithelial cells (LLC-PK1) (van Helvoort et al., 1996), and HEK293 (Morita et al., 2007)] and shown to translocate PC across the plasma membrane in apparent contradiction of the results reported by Groen *et al*. However, although HepG2 cells express *ATP8B1* endogenously (Martinez-Fernandez et al., 2009), the level of endogenous ATP8B1 expression was not investigated in any of the other cell lines where ABCB4 function has been investigated. In addition, in these earlier and contemporaneous studies, ABCB4 expression and function were studied in stably-transfected cells (rather than by transient transfection employed in the present study). This may have led to the selection of cells expressing low levels of WT ABCB4 or mutated ABCB4, due to negative selective pressure against ABCB4 function. It is also possible that compensatory secondary changes, for example upregulation of a PS-flippase, ensued allowing for the deleterious effect of the PC-floppase to be tolerated.

HEK293T cells do not express ABCB4 endogenously (Figure 4-1) making them an ideal expression system to study the transporter. They are also highly transfectable and recombinant ATP8B1 and CDC50A can be expressed without deleterious effect on the cells (Groen et al., 2011). WT ABCB4 expression is significantly and consistently improved in the triple transfected cells (Figure 4-2) suggesting that endogenous ATP8B1 expression in HEK293T cells is limited.

6.3 Variant protein phenotype

The three lines of *in vitro* evidence, expression, localisation and function, described in this report are used to characterise variant protein phenotype. These are summarised here and related to the published patient phenotypes and genotypes.

6.3.1 S320F and A286V ABCB4

S320F and A286V have been linked to the most severe ABCB4-related liver disease, PFIC3 (Degiorgio et al., 2007). S320F ABCB4 was identified in two patients, in one case as a compound heterozygote with the missense mutation A286V in the second allele and in the second case as a compound heterozygote with the nonsense mutation Y279X. Poupon *et al.* also reported the S320F variant in two siblings as a compound heterozygous alteration with A593D (c.2858C>A) (Poupon et al., 2010), a mutation previously linked to PFIC3 in the homozygous state (Keitel et al., 2005). In these two patients, a heterozygous alteration (V444A; c.1331T>C) affecting *ABCB11* was also detected which is reported to predispose to cholestatic disorders (Lang et al., 2007, Meier et al., 2006, Meier et al., 2008, Pauli-Magnus et al., 2004b). Both subjects were diagnosed with LPAC in their early twenties which progressed to PFIC3 several years later necessitating liver transplantation (Poupon et al., 2010).

According to the western analysis performed in this study (Table 4-3), the high level of expression of A286V in the single-transfected cells suggests that the protein has lost its deleterious PC-flopping activity. The improved expression of S320F compared to WT in the single-transfected cells, and its low level of expression in the triple-transfected cells suggested this variant to have lost activity as well as stability, possibly due to a folding defect. However, by CLSM, it was evident that both mutants are able to traffic to the plasma membrane (Table 6-1). In keeping, immunostaining on liver sections from two PFIC3 patients harbouring both the S320F and the A593D variants revealed normal canalicular membrane localisation of mutant ABCB4 (Poupon et al., 2010). However, the TC-dependent PC-efflux activity of the S320F variant was reduced to half the level of the WT protein whereas, the A286V was inactive (Table 6-1). Taken together, these data provide an explanation for the PFIC3 phenotype observed in compound heterozygous patients (Degiorgio et al., 2007, Poupon et al., 2010). The reduced expression of the S320F variant results in a 50% reduction in PC-efflux that when combined with the inactivity of the A286V or Y279X variants in the same patient, likely results in a severe reduction in PC efflux. The low lipid content of the bile would make the relatively high bile salt concentration toxic and this would plausibly lead to chronic and progressive liver disease eventually leading to liver failure, characteristic of PFIC3 (Davit-Spraul et al., 2009). The late onset of PFIC3 in these two patients is most likely due to the PC-efflux activity of the small amount of S320F variant present in the canalicular membrane. Given this interpretation it is most likely that the uncharacterised A593D variant in the patient identified by Poupon *et al.*, will be unable to efflux PC.

The S320F variant has also been reported in ICP (Bacq et al., 2009, Keitel et al., 2006, Pauli-Magnus et al., 2004b) and LPAC patients (Rosmorduc et al., 2003, Rosmorduc et al., 2001). LPAC is characterised by low phospholipid content in the bile and symptomatic and

recurring cholestasis in young adults with an apparent prevalence in the female population (Rosmorduc and Poupon, 2007). The LPAC patients were all homozygous for S320F indicating that the affect of the S320F mutation on ABCB4 function is not so severe as to result in PFIC3. Indeed, a 50% TC-dependent PC-efflux compared to cells expressing the WT protein suggests that this residual PC-flopping activity permits adequate efflux of PC to partially alleviate the detergent effect of bile salts in the biliary tract preventing progressive deterioration of the biliary epithelium.

ICP presents in the third trimester of pregnancy with maternal pruritus and abnormal liver function (Reyes and Simon, 1993). Mutations in the coding regions of *ABCB4* and *ABCB11* confer genetic susceptibility to the development of the disease (Geenes and Williamson, 2009). Although the genetic predisposition plays an important role in the occurrence of ICP, the expression of the disease is also likely to be modulated by pregnancy hormones such as progesterone and oestrogens as well as by environmental factors (Arrese and Reyes, 2006, Lammert et al., 2000). In ICP patients, the S320F variant has been identified both in the homozygous state (Keitel et al., 2006, Pauli-Magnus et al., 2004b) and heterozygous with the WT allele (Bacq et al., 2009). In one ICP patient homozygous for the S320F mutation, ABCB4 localisation at the canalicular membrane did not seem to be affected as shown by immunostaining of ABCB4 in liver sections (Keitel et al., 2006). This is in agreement with the observations presented here following CLSM analysis of the variant *in vitro*, but the immunostaining data are unlikely to be sufficiently sensitive to demonstrate quantitative differences in the level of the transporter at the cell membrane. It is likely, therefore, that the elevated levels of pregnancy hormones or their metabolites during the third trimester negatively modulate S320F ABCB4 function or, transiently, further reduce the level of the transporter in the canalicular membrane allowing the condition to manifest.

6.3.2 M301T, P1161S, L591Q and E528D ABCB4

The genetic contribution in the development of gallstones is still under investigation but *ABCB4* gene defects are thought to impose a high risk factor in acquiring the LPAC syndrome. The ABCB4 variants M301T, P1161S, L591Q and E528D have all been identified in patients with LPAC (Nakken et al., 2009, Rosmorduc et al., 2003, Rosmorduc et al., 2001).

The M301T variant was described as a heterozygous alteration (Rosmorduc et al., 2003). Based on the western analysis performed here, M301T is amongst the mutants that appear to have lost their deleterious PC-flopping activity (Table 4-3). CLSM analysis revealed a staining pattern consistent with plasma membrane localisation (Table 6-1) but, the TC-dependent PC-efflux activity of M301T was only 36% of the level of WT ABCB4 (Table 6-1). The expression of this variant along with the WT protein in the heterozygous patient, probably means that there is a significant amount of PC effluxed into the bile resulting in slow disease progression and the appearance of symptoms only later in life [mean age at presentation 38.1 years; (Rosmorduc et al., 2003)]. Environmental and/or dietary factors, are likely to play a role leading to the formation of bile with decreased PC content and increased lithogenicity, injury of the biliary membrane and eventually the development LPAC in patients with accompanying increased γ-glytamiltransferase (γ-GT) activity in the serum (Rosmorduc and Poupon, 2007).

Western analysis of the L591Q, E528D and P1161S variants suggested a WT phenotype (Table 4-3) and CLSM analysis suggests normal plasma membrane localisation (Table 6-1). Moreover, all three variants maintain a high level of TC-dependent PC-efflux activity (Table 6-1). Although the E528D and P1161S variants consistently present with lower PC-

efflux activity than the WT activity (means of 66 and 61%, respectively), they are not statistically different (Figure 5-2).

Environment and/or dietary factors therefore, likely play an important role in the development of LPAC in patients with the P1161S, L591Q and E528D mutations. Of note, the E528D variant has also been linked to ICP in a study where only exons 14-16 of the *ABCB4* gene locus was sequenced from each patient (Floreani et al., 2008). As discussed earlier, it is possible that the elevated hormonal levels during the third trimester of pregnancy lead to the development of ICP in this patient (Jacquemin et al., 1999) or that additional mutations were present on any of the exons which were not sequenced by Floreani *et al.*

Another possibility is that these represent normal variants in the population and the LPAC has a different aetiology in these patients. It is also possible that additional mutations were present in other gene loci involved in bile synthesis and flow, such as *ABCB11* or *FXR*, which were not identified in the analyses performed by Rosmorduc *et al.* and Nakken *et al.* but have been described in other patients with cholestatic syndromes (Keitel et al., 2006, Poupon et al., 2010, Zimmer et al., 2009).

It is also becoming increasingly apparent that mutations which disrupt the splicing machinery can have a causative role in a number of human diseases (Wang and Cooper, 2007). Byrne *et al.* recently reported the impact of 62 missense mutations and 21 SNPs in *ABCB11* on pre-messenger RNA (pre-mRNA)-splicing that have been linked to cholestatic liver disease (Byrne et al., 2009). Mutant sequences were cloned into a minigene vector and differentially-spliced products were amplified and quantified by real-time polymerase chain reaction (RT-PCR). Using this technique, Byrne *et al.* demonstrated that a number of

mutations caused exon skipping and therefore decreased the amount of normally spliced product generated by the minigene construct (Byrne et al., 2009). Of note was the effect on pre-mRNA splicing of c.1445A>G (p.D482G), which results in a mRNA that introduces 14 novel amino acids and a premature stop codon to the polypeptide (Byrne et al., 2009).

In vitro studies on the subcellular localisation and bile salt-efflux function of the same D482G mutant expressed from a cDNA have reported inconsistent results and this could be attributable to differences in the assay systems used by each group or inter-species differences between the rat, mouse and human protein (Hayashi et al., 2005, Kagawa et al., 2008, Plass et al., 2004, Wang et al., 2002). Expression of the human D482G ABCB11 in MDCK II cells revealed that the protein was mostly present in the immature unglycosylated form which accumulated intracellularly, however, the mutant protein displayed normal bile-salt transport function in isolated inside-out membrane vesicles from HEK293 cells (Hayashi et al., 2005).

The altered pre-mRNA splicing identified by Byrne *et al.* offers a plausible explanation for the linkage of D482G in PFIC2 patients. If altered pre-mRNA splicing of the D482G mutant allele is the predominant allele in PFIC2 patients, very little, if any, D482G ABCB11 will be present at the bile canaliculi. This would be consistent with immunostaining patterns in the liver of PFIC2 patients with the D482G mutation where ABCB11 is severely reduced or completely undetectable (Strautnieks et al., 2008). It remains possible therefore that the ABCB4 variants, L591Q, P1161S and E528D, are indeed mutations that lead to altered pre-mRNA splicing which affects the abundance of full-length ABCB4 in these patients.

6.3.3 G535D ABCB4

The G535D variant was identified in a patient with a heterozygous genotype and a complex phenotype (Lucena et al., 2003). The patient developed LPAC during adolescence which was followed by ICP in two pregnancies and finally biliary cirrhosis (BC) at the age of 47 (Lucena et al., 2003). Immunostaining of liver sections from the patient revealed reduced staining for ABCB4 at the canalicular membrane compared to sections from a control liver (Lucena et al., 2003). Lucena *et al.* postulated that the affect of G535D on ABCB4 is relatively mild resulting in a slow progression of liver disease. From my data, recorded *in vitro*, the level of G535D ABCB4 at the plasma membrane of HEK293T cells was high in the single-transfected cells and higher still in the triple-transfected cells. CLSM analysis showed that this variant can traffic to the plasma membrane (Table 6-1). However, TC-dependent PC-efflux showed that the G535D ABCB4 variant retains only 4% of the PC-flopping activity of the WT protein (Table 6-1). Since the patient was heterozygous at the *ABCB4* locus suggests that expression of the normal allele partially compensates for the reduced activity of the G535D variant. This would allow for the slow formation of cholesterol gallstones as a result of the high lithogenicity of the low PC-content bile. During pregnancy, negative modulation of ABCB4 by sex hormones would likely contribute to the development of ICP (Jacquemin et al., 1999) and the progressive damage caused by the built-up of cholesterol and the toxic effect of bile may eventually have led to BC in this patient.

6.3.4 A546D and R545C ABCB4

Another ABCB4 variant which has been implicated in ICP is A546D which was identified in a patient heterozygous for this locus (Dixon et al., 2000). The mutation was reproduced in ABCB1, the closest homologue of ABCB4, and shown to cause a trafficking defect because the protein failed to traffic efficiently to the plasma membrane. However, the

fraction that reached the plasma membrane was functional and could efflux drugs, the normal allocrites for ABCB1 (Dixon et al., 2000). The data presented here (Table 4-3) are in agreement with these earlier observations. The fact that the level of expression of the A546D variant does not achieve the level of expression of the WT protein in the triple transfection suggests difficulty with folding or trafficking; a folding defect would likely result in degradation of the A546D protein by the ERAD (ER-associated degradation) pathway (Meusser et al., 2005, Vembar and Brodsky, 2008). Indeed, when the subcellular localisation of A546D ABCB4 protein was analysed by CLSM, the majority of protein appeared to accumulate in an intracellular compartment which is consistent with the reduced TC-dependent PC-efflux activity (33% of the WT protein) observed for cells expressing this variant (Table 6-1).

In a study by Pauli-Magnus et al., the role of *ABCB4* and *ABCB11* genetic variations in the pathogenesis of PBC and PSC was investigated (Pauli-Magnus et al., 2004a). Although the authors could not conclude definitely that *ABCB4* (and *ABCB11*) genes co-segregate with the development of PSC or PBC in patients, the R545C variant was found to be specific to the PSC population (Pauli-Magnus et al., 2004a). Western analysis shows that the expression of R545C ABCB4 is greatly reduced and not influenced by the co-expression of ATP8B1 and CDC50A. The subcellular localisation of the R545C ABCB4 protein closely resembles the pattern observed for the A546D variant; i.e., intracellular accumulation, in line with the reduced TC-dependent PC-efflux activity (21% of WT ABCB4) (Table 6-1).

6.4 Modelling of the ABCB4 mutations on the structural data for Abcb1a and Sav1866

A crystal structure of ABCB4 is currently unavailable. However, the crystal structures of related ABC transporters, drug-efflux pumps from mouse (Abcb1a) and bacteria (Sav1866) have been resolved, albeit at a medium resolution (Aller et al., 2009, Dawson and Locher, 2006). Alignment of the primary sequence of ABCB4 with Abcb1a and Sav1866 in ClustalW (Appendix I) allowed specific ABCB4 amino acid residues to be mapped on the structural models to gain insight into how specific mutations affect the PC-floppase. ABCB4 was found to be 73% identical, 83% similar to Abcb1a, and 27% identical, 44% similar to Sav1866 (aligned to the amino-terminal half of ABCB4).

The A546D, R545C, S320F, M301T G535D and A286V ABCB4 mutants, all displayed reduced cellular TC-dependent PC-efflux activity compared to the WT protein (Table 6-1). S320F, A545D and A546D appear to affect the protein primarily at the level of folding and/or trafficking, while M301T G535D and A286V appear to affect the PC-transport activity.

The mutated amino acid residues in ABCB4 and their equivalent residues in Abcb1a and Sav1866 following sequence alignment are shown in Table 6-2. Some ABCB4 residues are perfectly conserved in all three transporters (e.g. G535 and R545), some are only conserved between the more closely related ABCB4 and Abcb1a ($ABCB4^{A286}$, $ABCB4^{M301}$ and $ABCB4^{A546}$), whereas $ABCB4^{S320}$ is represented by a semi-conservative change in Abcb1a (threonine) and in Sav1866 by another amino acid with a relatively small side-chain but no hydroxyl group (alanine).

Amino Acid Residue		
ABCB4	**Abcb1a**	**Sav1866**
A286V	A280	F233
M301T	M295	F248
S320F	T314	A267
G535D	G529	G480
R545C	R539	R490
A546D	A540	I491

Table 6-2. ***ABCB4 mutant amino acid residues and their equivalents in murine Abcb1a and bacterial Sav1866.***

6.4.1 ABCB4^{A546}

In Figure 6-1, a cartoon model of Abcb1a is presented in a colour-coded format: TMD1, yellow; NBD1, grey; TMD2, purple; NBD2, green. The ABCB4^{A546} equivalent is shown in Abcb1a (Abcb1a^{A540}) as red spheres on NBD1 (Figure 6-1A) and as elemental spheres in close up in Figure 6-1B and C. The structural fold of NBD1 is given in Figure 6-1B and the comprising alpha (α) helices and beta (β) sheets are numbered in ascending order from the amino terminus of the domain. The order is as follows: β1-β2-β3-α1-β4-α2-β5-α3-α4-α5-α6-α7-β6-α8-β7-α9-β8-β9-α10-α11. Abcb1a^{A540} is located in α7, the final α-helix of the α-helical subdomain (Figure 1-3). All of the amino acid residues within 5Å of Abcb1a^{A540} are shown in stick format and include several in the adjacent β-strand, β5. In the Abcb1a model A540 is only involved in intra-helical hydrogen bonds that would be no different if replaced by an aspartic acid, so long as α7 adopts the same secondary structure. However, alanine has a volume of 88.6Å^3 whereas the volume of aspartic acid is 111.1Å^3 (http://www.fli-leibniz.de/IMAGE_AA.html). Replacing an alanine (Ala; A) with the larger and negatively charged aspartate (Asp; D) is therefore likely to sterically and electrostatically hinder the approximation of α7 and β5 of NBD1 preventing the domain from folding efficiently resulting in its intracellular retention and increased likelihood of degradation in the proteasome.

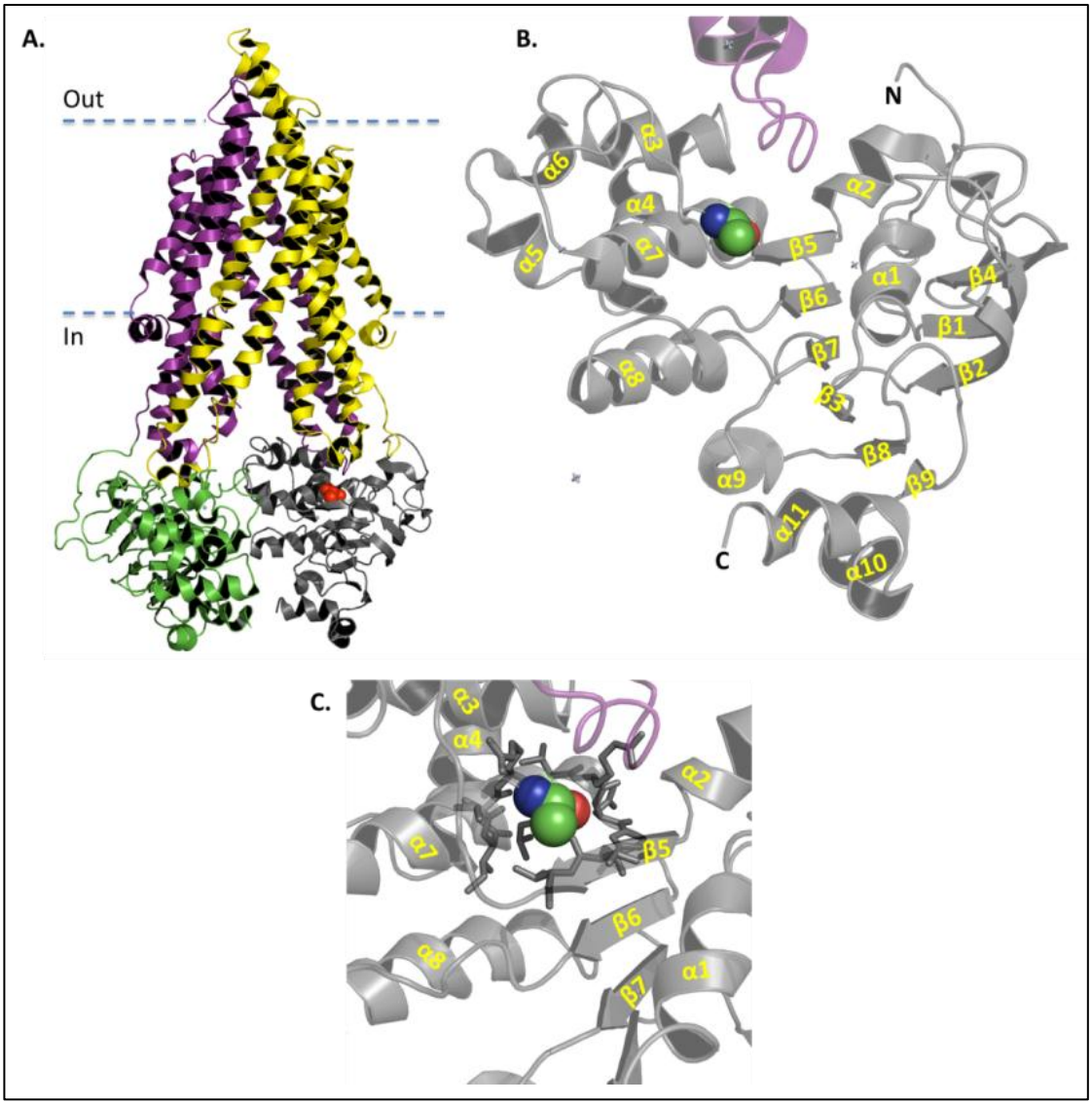

Figure 6-1. ***Mapping the ABCB4^{A546} residue on Abcb1a (Abcb1a^{A540}).***

(A). Cartoon model of Abcb1a (PDB: 3G5U). NBD1 is coloured grey and NBD2 is coloured green. TMD1 is coloured yellow and TMD2 is coloured purple. The horizontal dashed lines represent the approximate positioning of the lipid bilayer. Abcb1a^{A540} is represented by red spheres. (B). Secondary structure of NBD1. The α-helices and β-sheets of the NBD1 fold are numbered in ascending order from the amino-terminal of the domain as follows: β1-β2-β3-α1-β4-α2-β5-α3-α4-α5-α6-α7-β6-α8-β7-α9-β8-β9-α10-α11. (C). Abcb1a^{A540} is shown in coloured elemental spheres (C, green; N, blue; O, red) in alpha (α)-helix 7. Amino acid residues within 5Å of Abcb1a^{A540} are shown in stick format.

6.4.2 ABCB4^{R545}

Abcb1a^{R539} (ABCB4^{R545}) is adjacent to Abcb1a^{A540} on α7 (Figure 6-2A). In Figure 6-2B, Abcb1a^{R539} is illustrated in stick format on α7 and coloured elementally. In this close up view the side chain of Abcb1a^{R539} can be seen to hydrogen bond (orange dashes) to the

carbonyl group of the peptide backbone of Abcb1a^{V474} in the loop region between β5 and α3 which includes the Q-loop (Hopfner et al., 2000).

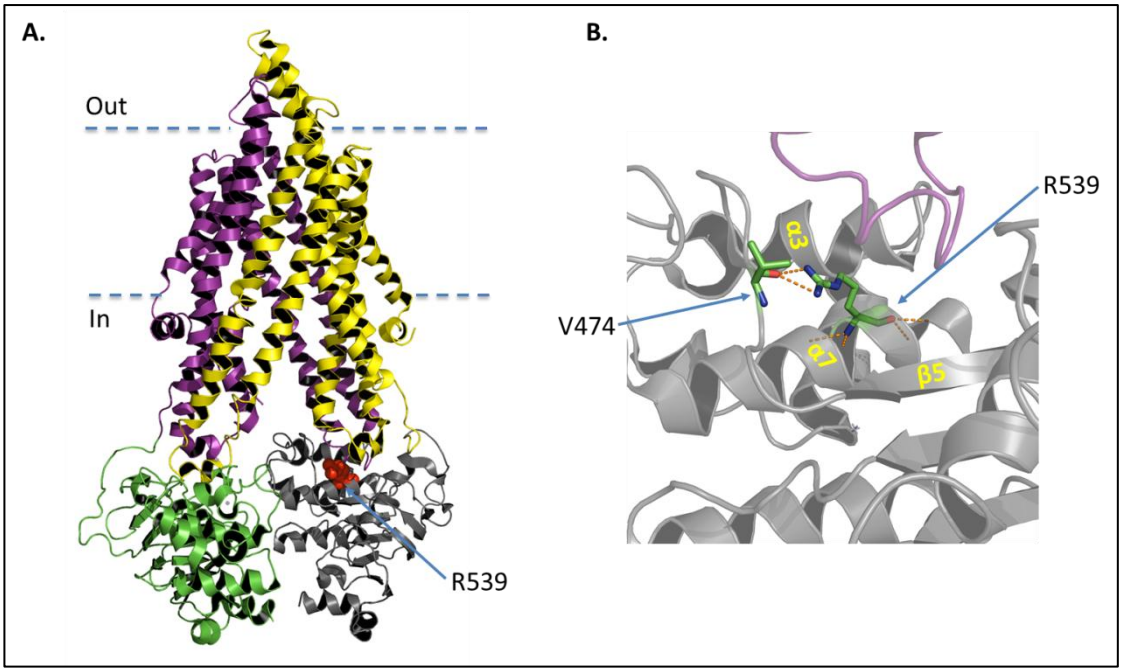

Figure 6-2. ***Mapping the ABCB4^{R545} residue on Abcb1a (Abcb1a^{R539}).***

(A). Cartoon model of Abcb1a (PDB: 3G5U). NBD1 is coloured grey and NBD2 is coloured green. TMD1 is coloured yellow and TMD2 is coloured purple. The horizontal dashed lines represent the approximate positioning of the lipid bilayer. Abcb1a^{R539} is represented by red spheres. (B). Abcb1a^{R539} and Abcb1a^{V474} illustrated in stick format on α7 and the loop region between β5 and α3, respectively, and coloured elementally (C, green; N, blue; O, red). Abcb1a^{R539} hydrogen bonds (orange dashes) to the carbonyl group of the peptide backbone of Abcb1a^{V474}. Alpha (α)-helices and beta (β)-sheets are numbered as per Figure 6-1B.

The Q-loop contains a highly conserved glutamine (Q) residue in an eight-residue loop which links the "core" subdomain with the α-helical subdomain of the NBD (Figure 1-3). It has been proposed that conformational changes in the Q-loop during the catalytic cycle transmit information between the NBDs and the TMDs (Dalmas et al., 2005, Jones and George, 2002). The hydrogen bond between Abcb1a^{R539} and Abcb1a^{V474} likely stabilizes the tertiary structure of this region. When ABCB4^{R545} is replaced by a cysteine (ABCB4^{R545C}) the absence of this hydrogen bond could make folding, and therefore stability and trafficking of ABCB4-R545C difficult.

6.4.3 ABCB4^{S320}

Abcb1a^{T314} (ABCB4^{S320}) is shown as red spheres in the extracellular loop at the end of MSH5 (Figure 6-3A).

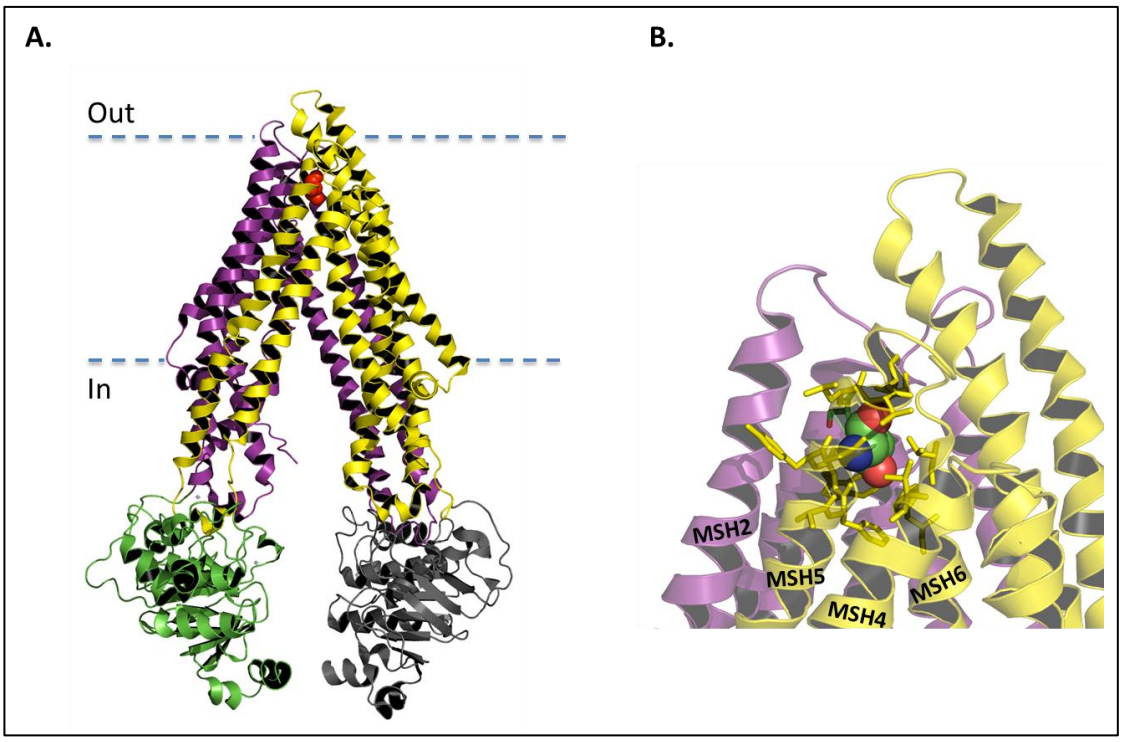

Figure 6-3. ***Mapping the ABCB4^{S320} residue on Abcb1a (Abcb1a^{T314}).***

(A). Cartoon model of Abcb1a (PDB: 3G5U). NBD1 is coloured grey and NBD2 is coloured green. TMD1 is coloured yellow and TMD2 is coloured purple. The horizontal dashed lines represent the approximate positioning of the lipid bilayer. Abcb1a^{T314} is represented by red spheres. (B). Close up view of the Abcb1a extracellular loops. Abcb1a^{T314} is shown as spheres coloured elementally (C, green; N, blue; O, red). All residues within 5Å of Abcb1a^{T314} are shown in stick format.

Abcb1a^{T314} is the first of a threonine (T)-serine (S) dipeptide in Abcb1a, i.e. Abcb1a$^{T314\text{-}S315}$. This dipeptide is reversed in ABCB4 as ABCB4$^{S320\text{-}T321}$ perhaps suggesting that the side chain hydroxyls of these two residues form important inter-helical hydrogen bonds. In the model of Abcb1a, while Abcb1a^{S315} is close enough for its side-chain to form a hydrogen bond with Abcb1a^{N747} (asparagine) in MSH2, Abcb1a^{T314} appears to form only intra-helical hydrogen bonds. While side-chain interactions of Abcb1a^{T314} in other conformations of the transport cycle cannot be ruled out, it is possible to speculate that in the 'inwardly open

conformation' shown for Abcb1a, replacing Abcb1a^{T314} with a bulkier phenylalanine (F) would hinder the formation of the tight extracellular turn of MSH5 into MSH6 and may sterically hinder the close packing of MSH4 (all residues within 5Å of Abcb1a^{T314} are shown in stick format in Figure 6-3B).

6.4.4 ABCB4^{G535}

Abcb1a^{G529} (ABCB4^{G535}) is shown as red spheres in NBD1 of Abcb1a (Figure 6-4A; grey). This amino acid residue is part of the ABC signature motif. The ABC signature (LSGGQ) which is also known as the C-motif is unique to the ABC superfamily (Hyde et al., 1990). In a full ABC transporter, the NBDs align in a "head-to-tail" arrangement such that the Walker A motif of one NBD is in close association with the ABC signature motif of the apposing NBD allowing two ATP molecules to be trapped at the interface (Jones et al., 2009, Rees et al., 2009, Zolnerciks et al., 2011).

The importance of this residue is best illustrated in Sav1866 (color-coded elemental spheres of Sav1866^{G480} in grey NBD) which was crystallized in closed conformation with 2×ADP at the interface (Dawson and Locher, 2007) imaged from above (Figure 6-4B; top panel), and in the α-helical subdomain of the isolated Sav1866 NBD with ADP and with the rest of the ABC signature motif in stick format (L^{478}S^{479}G^{480}G^{481}Q^{482}; Figure 6-4B; bottom panel). The two glycine (G) residues in the ABC signature motif are essential to form the tight α-helical turn leading in to α7. Replacing one of these glycine residues with a larger, negatively-charged aspartate as in the ABCB4-G535D mutant would likely alter the conformation of the ABC signature motif which is necessary for interaction with the juxtaposed ATP. With a misfolded ABC-signature motif the G535D mutant would likely

be unable to bind ATP in this pocket and would therefore be unlikely to function as a transporter.

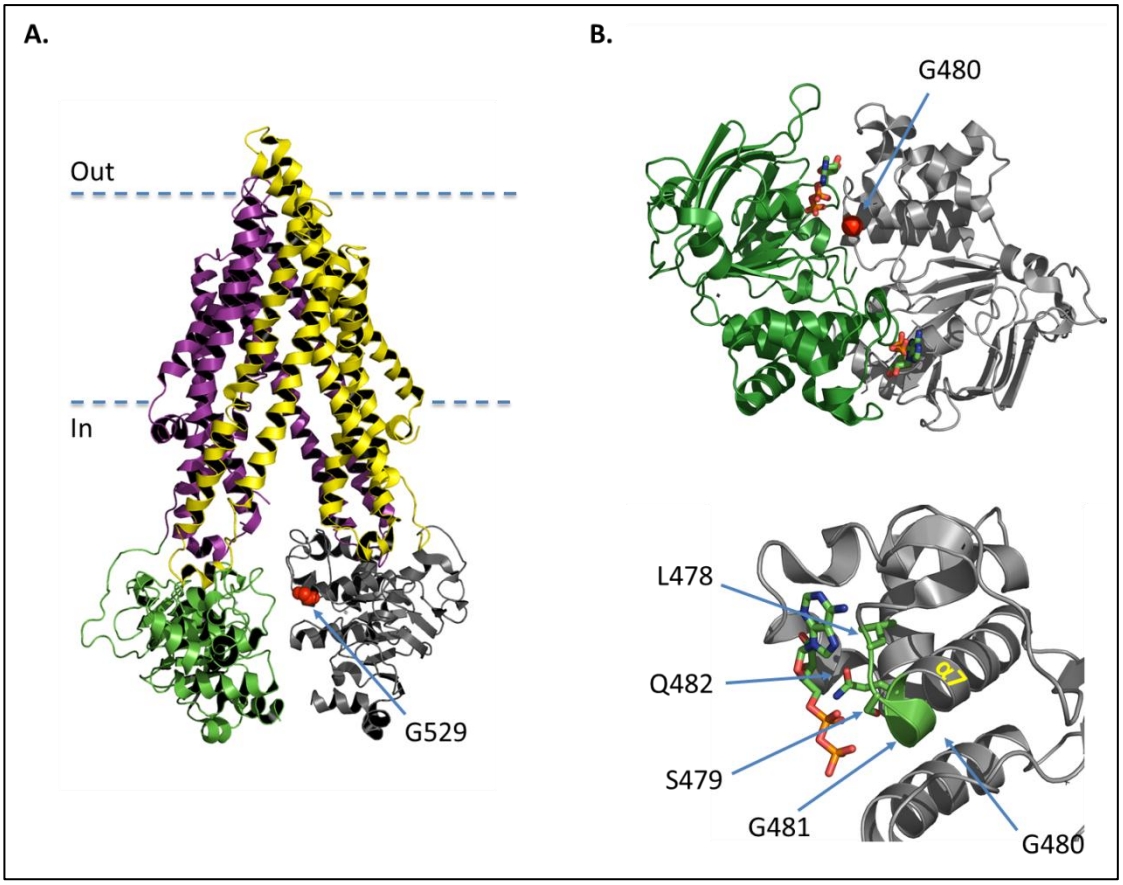

Figure 6-4. ***Mapping the ABCB4^{G535} residue on Abcb1a (Abcb1a^{G529}).***

(A). Cartoon model of Abcb1a (PDB: 3G5U). NBD1 is coloured grey and NBD2 is coloured green. TMD1 is coloured yellow and TMD2 is coloured purple. The horizontal dashed lines represent the approximate positioning of the lipid bilayer. Abcb1a^{G529} is represented by red spheres. (B). Secondary structure of the NBD-NBD dimer in Sav1866 with 2×ADP trapped at the interface (PDB: 2ONJ) (Dawson and Locher, 2007) imaged from above (top panel), and as an isolated NBD with ADP and with the ABC signature motif in stick format (bottom panel) coloured elementally (C, green; N, blue; O, red). The two glycine (Gly; G) residues (G529 and G530) in the ABC signature motif are essential to form the tight alpha helical turn leading in to α7. Alpha (α)-helices and beta (β)-sheets are numbered as per Figure 6-1B.

6.4.5 ABCB4^{A286} and ABCB4^{M301}

Abcb1a^{A280} and Abcb1a^{M295}, the equivalents of ABCB4^{A286} and ABCB4^{M301} respectively, are indicated as red spheres on MSH5 of TMD1 in Figure 6-5A. Neither residue is involved in inter-helical interactions; Abcb1a^{M295} is expected to be exposed to the lipid bilayer if the

Abcb1a conformation is correctly interpreted and Abcb1a^{A280} would be at the intracellular face of the membrane.

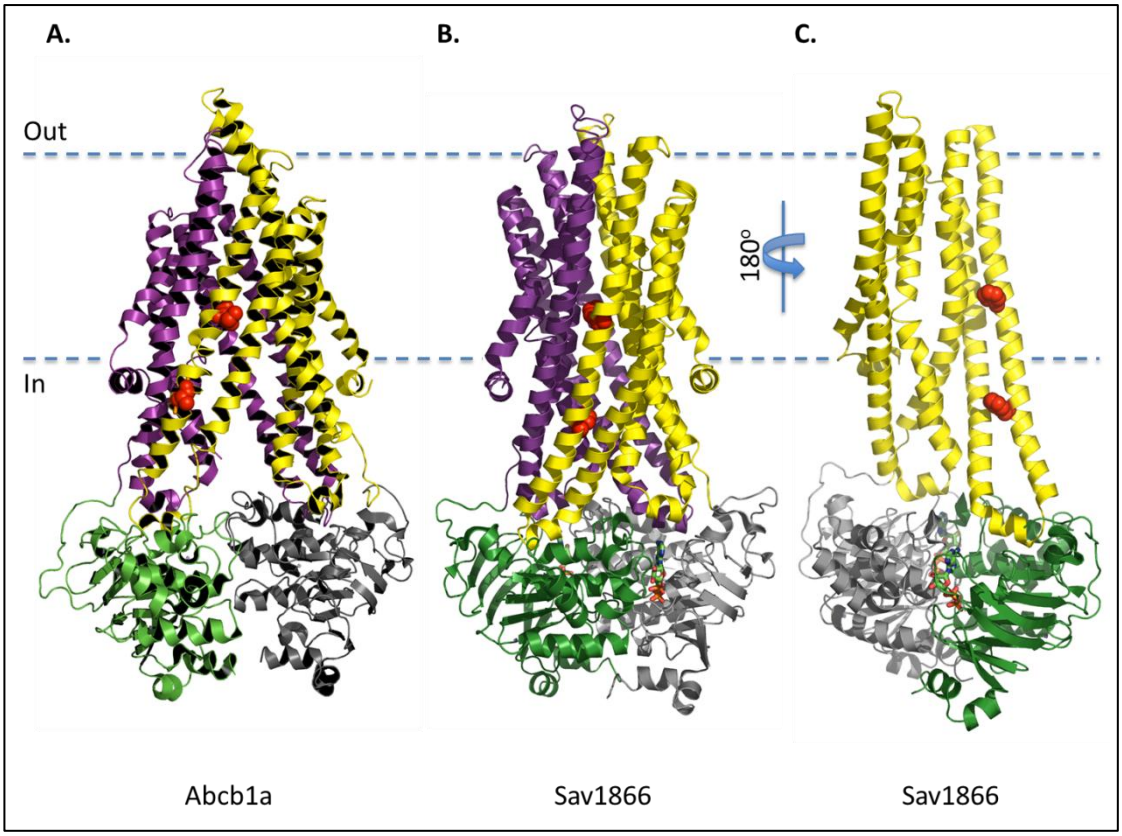

Figure 6-5. ***Mapping the ABCB4^{A286} and ABCB4^{M301} residues on Abcb1a (Abcb1a^{A280}/Abcb1a^{M295}) and Sav1866 (Sav1866^{F233}/Sav1866^{F248}).***

(A). Cartoon model of Abcb1a (PDB: 3G5U). NBD1 is coloured grey and NBD2 is coloured green. TMD1 is coloured yellow and TMD2 is coloured purple. The horizontal dashed lines represent the approximate positioning of the lipid bilayer. Abcb1a^{M280} and Abcb1a^{M295} are represented by red spheres. Both residues are exposed on the outside of MSH5. (B). Cartoon model of Sav1866 (PDB: 2ONJ) with similar colour coding as in A. Sav1866^{F233} and Sav1866^{F248} on MSH5 are orientated to face the internal cavity. (C). As in (B) but with TMD2 removed for clarity and the structure rotated 180^{o} clockwise through the central Y axis to show the side chains of the two phenylalanines pointing towards the centre of the protein.

When modelled on the Sav1866 structure the equivalents of ABCB4 A286 and M301 (Sav1866^{F233} and Sav1866^{F248}, respectively) are positioned such that their side chains point towards the central cavity of bacterial drug efflux pump (Figure 6-5B and C). Replacing an alanine (neutral, non-polar side chain) with a valine (neutral, non-polar side chain), or a methionine (neutral, non-polar side chain) with a threonine (neutral, polar side chain)

introduces a subtle change in the polypeptide that appears unlikely to affect the secondary structure of ABCB4. It is not clear why these mutations (ABCB4-A286V and ABCB4-M301T) have an impact on function but both are in the same MSH which may change conformation during the transport cycle and so it is possible that they are involved directly in the binding of PC.

6.5 Future Work

6.5.1 The ICP-associated ABCB4 variants. Are they influenced by hormones?

ICP usually develops during the third trimester of pregnancy and is characterised by raised serum bile acids and γ-GT as well as severe pruritus. The condition persists until delivery after which the symptoms usually resolve within 48 hours (Geenes and Williamson, 2009). In addition to the genetic susceptibility conferred by mutations in the *ABCB4*, *ABCB11* and *ATP8B1* gene loci (Dixon and Williamson, 2008), hormonal factors and environmental cues are thought to contribute to the pathogenesis of the disease (Geenes and Williamson, 2009).

Seasonal variation, dietary regime, geographical location as well as ethnicity, all appear to have an influence on the development of ICP (Pusl and Beuers, 2007). The fact that ICP is more common in twin pregnancies (Gonzalez et al., 1989), develops during the third trimester when oestrogen levels are at their maximum and resolves soon after delivery when pregnancy-related hormone levels return to their normal (Reyes and Simon, 1993), suggests that reproductive hormones play a role in the pathogenesis.

Studies performed using estrogen (estradiol-17β-glucuronide; $E_2$17βG) and sulphated progesterone (5α-pregan-3α-ol-20-one; PM4-S and 5α-pregan-3β-ol-20-one; PM5-S)

metabolites have provided evidence that they can trans-inhibit ABCB11 and reduce bile flow (Stieger et al., 2000, Vallejo et al., 2006). In isolated vesicles from the canalicular plasma membrane of rat liver (cLPM), $E_2$17βG exhibited dose-dependent inhibition of TC transport into inside out cLPM vesicles but not in Abcb11-expressing vesicles from Sf9 insect cells. However, co-expression of Abcc2 and Abcb11 in Sf9 cells restored the $E_2$17βG dose-dependent inhibition of TC transport prompting the authors to conclude that $E_2$17βG can only inhibit Abcb11 function, and thereby induce cholestasis, after it is excreted into the bile canaliculus by Abcc2 (Stieger et al., 2000).

In experiments performed in isolated perfused rat liver, it was demonstrated that PM4-S could negatively modulate bile salt efflux (Vallejo et al., 2006). Vallejo *et al.* then used *Xenupus laevis* oocytes as an experimental model to investigate whether the reduction in bile salt efflux was due to an inhibition of Abcb11 function. Rat Abcb11 was expressed in *X. laevis* oocytes and the effect of PM4 and PM5 and their sulphated derivatives (PM4-S and PM5-S, respectively) as well as $E_2$17βG, on Abcb11-mediated efflux, was measured from bile salt loaded oocytes (Vallejo et al., 2006). It was shown that PM4 and PM5 had no effect on Abcb11-mediated efflux whereas PM4-S, PM5-S and $E_2$17βG had a significant negative effect (Vallejo et al., 2006).

It is plausible therefore, that $E_2$17βG and/or progesterone metabolites induce a similar effect on ABCB4 function and increased effect on E528D, S320F, A546D and G535D. This is now testable for the ICP-related ABCB4 variants using the TC-dependent PC efflux assay described in this thesis. This may help to clarify the role of reproductive hormones in the aetiology of ICP.

6.5.2 The S320F, R545C and A456D ABCB4 mutants; candidates for therapeutic intervention?

It seems likely that the apparently low level of activity of the S320F, R545C and A546D ABCB4 mutants is, at least in part, due to a folding defect which results in depletion of the protein from the membrane. The PC-efflux activity of cells expressing these three mutants [49% (P<0.01) for S320F; 33% (P<0.005) for A546D; and 21% (P<0.005) for R545C; compared to WT ABCB4] suggests that the fraction of the protein that is able to fold properly and reach the plasma membrane is able to efflux PC efficiently.

For other proteins it has been demonstrated *in vitro* that some mutants can be fully functional provided they can escape the quality control machinery. This has been achieved by growth at reduced temperature or in the presence of pharmacological agents (Delaunay et al., 2009, Denning et al., 1992, Gautherot et al., 2012, Hayashi and Sugiyama, 2007, Plass et al., 2004, Wang et al., 2006). Pharmacological agents have also been used successfully in the clinic to improve disease outcome. In ABCC7 the ΔF508 mutation is a deletion of a phenylalanine at position 508 and it is the most common mutation amongst CF patients (Cutting et al., 1990). The mutation causes retention of the ABCC7 ΔF508 species in the ER and its subsequent degradation by the proteasome (Cheng et al., 1990). However, if it can escape degradation it can fold and traffic to the plasma membrane where it retains its chloride channel function (Li et al., 1993). Sodium 4-phenylbutyrate (4-PBA) is a clinically-approved pharmacological chaperone that has been used successfully in patients homozygous for the ΔF508 mutation and shown to induce ABCC7 function in the nasal epithelia (Rubenstein et al., 1997). 4-PBA has also been used successfully in a patient with PFIC2 (with a homozygous *ABCB11* mutation) and shown to improve liver function and reduce clinical cholestasis (Gonzales et al., 2012).

At present, there is limited evidence on the effect of pharmacological chaperones on ABCB4 mutants. ABCB4 I541F has been reported in a homozygous patient with PFIC3 (Jacquemin et al., 2001) and shown to cause a folding defect that prevents the correct localisation of the protein at the canalicular membrane of hepatic HepG2 cells (Delaunay et al., 2009). The use of cyclosporin A (CsA) [better known as an immunosuppressant and a substrate and competitive inhibitor of ABCB1 (Tamai and Safa, 1990)], improved plasma membrane localisation of ABCB4 I541F *in vitro* (Gautherot et al., 2012). Although Gautherot *et al.* were not able to verify whether the rescued protein was functional at the cell surface, they postulate that because the equivalent I541F mutation in ABCB1 allowed the drug-efflux pump to localise to the plasma membrane and efflux calcein-AM from MDCK cells in the presence of low concentrations of CsA, the ABCB4 I541F variant is likely to be functional as well (Gautherot et al., 2012).

The discovery and development of pharmacological agents that enhance the transport activity or the plasma membrane localisation of mutant ABCB4 associated with cholestatic liver disease poses a major challenge. Although the functional rescue of disease-related mutations by a pharmacological chaperone has been well documented for other membrane proteins (Morello et al., 2000, Ulloa-Aguirre et al., 2004, Bernier et al., 2004), until now only one such agent (CsA) has been tested on ABCB4 I541F (Gautherot et al., 2012). The systematic screening of ABCB4 mutants to determine which are likely to be amenable to chemical intervention would be a good place to start.

The S320F, R545C and A546D ABCB4 mutants are characterised by reduced expression but all retain TC-dependent PC-efflux activity. It is likely that each causes a folding defect which results in reduced abundance of the transporter in the membrane. Restoration of the expression level therefore represents a route to therapeutic intervention in patients carrying

these mutations. The use of pharmacological or chemical chaperones such as glycerol, thapsigargin, 4-PBA or CsA, which have been used and shown to improve plasma membrane localisation of other membrane proteins (Delisle et al., 2003, Egan et al., 2002, Hayashi and Sugiyama, 2007, Rubenstein et al., 1997, Sobolewski et al., 2008, Tveten et al., 2007), would be good candidates to demonstrate the efficacy of this approach *in vitro* before seeking small molecules suitable for use in the clinic.

6.6 Concluding remarks

The link between genotype and clinical phenotype is not straightforward as some mutations that are apparently innocuous (following *in silico* analysis of amino acid changes) can have a dramatic impact on the protein and result in the development of disease (Thorisson et al., 2009). In order to appreciate the contribution of ABCB4 in the development of cholestatic liver disease, a detailed biochemical and molecular characterisation of mutant ABCB4 proteins associated with disease phenotypes is required.

As part of the work described in this thesis, the affects of nine ABCB4 variants on protein expression, subcellular localisation and phospholipid efflux activity were studied revealing a variety of phenotypes *in vitro*. Deciphering the molecular pathogenesis of cholestatic disease can establish the foundations for the development of new pharmacological treatments.

The prospect of discovering and designing small-molecule chemical agents that can target specific mutations in cholestatic patients is an exciting one. Mutants which retain PC-flopping activity but are limited by folding or stability to a low level of abundance at the plasma membrane (e.g. S320F, R545C and A546D) would be particularly suited to intervention. In the work presented here I have identified three ABCB4 mutants that fall

into this category; S320F, R545C and A546D. These mutants are implicated in all of the liver diseases linked to ABCB4 including the most debilitating PFIC3. They also represent one third of the variants tested and so there are likely to be more among the 1334 SNPs reported in the literature and on databases (http://www.ncbi.nlm.nih.gov/snp). Screens to identify *modulators* of these and similar mutants would be the natural extension to this work and should be possible using the *in vitro* expression system described herein.

Bibliography

ADACHI, Y., KOBAYASHI, H., KURUMI, Y., SHOUJI, M., KITANO, M. & YAMAMOTO, T. 1991. ATP-dependent taurocholate transport by rat liver canalicular membrane vesicles. *Hepatology,* 14**,** 655-9.

ADAMS, D. H. & EKSTEEN, B. 2006. Aberrant homing of mucosal T cells and extra-intestinal manifestations of inflammatory bowel disease. *Nat Rev Immunol,* 6**,** 244-51.

AGELLON, L. B. & TORCHIA, E. C. 2000. Intracellular transport of bile acids. *Biochim Biophys Acta,* 1486**,** 198-209.

AHMAD, S. & GLAZER, R. I. 1993. Expression of the antisense cDNA for protein kinase C alpha attenuates resistance in doxorubicin-resistant MCF-7 breast carcinoma cells. *Mol Pharmacol,* 43**,** 858-62.

AHMAD, S., SAFA, A. R. & GLAZER, R. I. 1994. Modulation of P-glycoprotein by protein kinase C alpha in a baculovirus expression system. *Biochemistry,* 33**,** 10313-8.

AITMAN, T. J., GLAZIER, A. M., WALLACE, C. A., COOPER, L. D., NORSWORTHY, P. J., WAHID, F. N., AL-MAJALI, K. M., TREMBLING, P. M., MANN, C. J., SHOULDERS, C. C., GRAF, D., ST LEZIN, E., KURTZ, T. W., KREN, V., PRAVENEC, M., IBRAHIMI, A., ABUMRAD, N. A., STANTON, L. W. & SCOTT, J. 1999. Identification of Cd36 (Fat) as an insulin-resistance gene causing defective fatty acid and glucose metabolism in hypertensive rats. *Nat Genet,* 21**,** 76-83.

ALLER, S. G., YU, J., WARD, A., WENG, Y., CHITTABOINA, S., ZHUO, R., HARRELL, P. M., TRINH, Y. T., ZHANG, Q., URBATSCH, I. L. & CHANG, G. 2009. Structure of P-glycoprotein reveals a molecular basis for poly-specific drug binding. *Science,* 323**,** 1718-22.

ALLIKMETS, R., GERRARD, B., HUTCHINSON, A. & DEAN, M. 1996. Characterization of the human ABC superfamily: isolation and mapping of 21 new genes using the expressed sequence tags database. *Hum Mol Genet,* 5**,** 1649-55.

ALREFAI, W. A. & GILL, R. K. 2007. Bile acid transporters: structure, function, regulation and pathophysiological implications. *Pharm Res,* 24**,** 1803-23.

AMBUDKAR, S. V. 1995. Purification and reconstitution of functional human P-glycoprotein. *J Bioenerg Biomembr,* 27**,** 23-9.

AMBUDKAR, S. V., LELONG, I. H., ZHANG, J., CARDARELLI, C. O., GOTTESMAN, M. M. & PASTAN, I. 1992. Partial purification and reconstitution of the human multidrug-resistance pump: characterization of the drug-stimulatable ATP hydrolysis. *Proc Natl Acad Sci U S A,* 89**,** 8472-6.

ANANTHANARAYANAN, M., BALASUBRAMANIAN, N., MAKISHIMA, M., MANGELSDORF, D. J. & SUCHY, F. J. 2001. Human bile salt export pump promoter is transactivated by the farnesoid X receptor/bile acid receptor. *J Biol Chem,* 276**,** 28857-65.

ANDERSON, B. O., BENSARD, D. D. & HARKEN, A. H. 1991. The role of platelet activating factor and its antagonists in shock, sepsis and multiple organ failure. *Surg Gynecol Obstet,* 172**,** 415-24.

ANDO, T., KUSUHARA, H., MERINO, G., ALVAREZ, A. I., SCHINKEL, A. H. & SUGIYAMA, Y. 2007. Involvement of breast cancer resistance protein (ABCG2) in the biliary excretion mechanism of fluoroquinolones. *Drug Metab Dispos,* 35**,** 1873-9.

ARIAS, I. M., BOYER, J. L., FAUSTO, N., JAKOBY, W. B., SCHACHTER, D. & SHAFRITZ, D. A. 1994. *The Liver: biology and pathobiology*, Raven Press Ltd.

ARRESE, M. & REYES, H. 2006. Intrahepatic cholestasis of pregnancy: a past and present riddle. *Ann Hepatol,* 5**,** 202-5.

ASPINALL, R. J. & TAYLOR-ROBINSON, S. D. 2002. *Mosby's Color Atlas and Text of Gastroenterology and Liver Disease*, Mosby.

AUERBACH, M. & LIEDTKE, C. M. 2007. Role of the scaffold protein RACK1 in apical expression of CFTR. *Am J Physiol Cell Physiol,* 293**,** C294-304.

BACQ, Y., GENDROT, C., PERROTIN, F., LEFROU, L., CHRETIEN, S., VIE-BURET, V., BRECHOT, M. C. & ANDRES, C. R. 2009. ABCB4 gene mutations and single-nucleotide

polymorphisms in women with intrahepatic cholestasis of pregnancy. *J Med Genet,* 46**,** 711-5.

BARAKAT, S., DEMEULE, M., PILORGET, A., REGINA, A., GINGRAS, D., BAGGETTO, L. G. & BELIVEAU, R. 2007. Modulation of p-glycoprotein function by caveolin-1 phosphorylation. *J Neurochem,* 101**,** 1-8.

BATES, S. E., LEE, J. S., DICKSTEIN, B., SPOLYAR, M. & FOJO, A. T. 1993. Differential modulation of P-glycoprotein transport by protein kinase inhibition. *Biochemistry,* 32**,** 9156-64.

BEAULIEU, E., DEMEULE, M., GHITESCU, L. & BELIVEAU, R. 1997. P-glycoprotein is strongly expressed in the luminal membranes of the endothelium of blood vessels in the brain. *Biochem J,* 326 (Pt 2)**,** 539-44.

BELANGER, M. M., ROUSSEL, E. & COUET, J. 2003. Up-regulation of caveolin expression by cytotoxic agents in drug-sensitive cancer cells. *Anticancer Drugs,* 14**,** 281-7.

BENDAYAN, R., RONALDSON, P. T., GINGRAS, D. & BENDAYAN, M. 2006. In situ localization of P-glycoprotein (ABCB1) in human and rat brain. *J Histochem Cytochem,* 54**,** 1159-67.

BERGE, K. E., TIAN, H., GRAF, G. A., YU, L., GRISHIN, N. V., SCHULTZ, J., KWITEROVICH, P., SHAN, B., BARNES, R. & HOBBS, H. H. 2000. Accumulation of dietary cholesterol in sitosterolemia caused by mutations in adjacent ABC transporters. *Science,* 290**,** 1771-5.

BERNIER, V., LAGACE, M., BICHET, D. G. & BOUVIER, M. 2004. Pharmacological chaperones: potential treatment for conformational diseases. *Trends Endocrinol Metab,* 15**,** 222-8.

BLOBE, G. C., SACHS, C. W., KHAN, W. A., FABBRO, D., STABEL, S., WETSEL, W. C., OBEID, L. M., FINE, R. L. & HANNUN, Y. A. 1993. Selective regulation of expression of protein kinase C (PKC) isoenzymes in multidrug-resistant MCF-7 cells. Functional significance of enhanced expression of PKC alpha. *J Biol Chem,* 268**,** 658-64.

BORST, P. & ELFERINK, R. O. 2002. Mammalian ABC transporters in health and disease. *Annu Rev Biochem,* 71**,** 537-92.

BORST, P., EVERS, R., KOOL, M. & WIJNHOLDS, J. 1999. The multidrug resistance protein family. *Biochim Biophys Acta,* 1461**,** 347-57.

BOSCH, I., DUNUSSI-JOANNOPOULOS, K., WU, R. L., FURLONG, S. T. & CROOP, J. 1997. Phosphatidylcholine and phosphatidylethanolamine behave as substrates of the human MDR1 P-glycoprotein. *Biochemistry,* 36**,** 5685-94.

BOURETTE, R. P., MYLES, G. M., CHOI, J. L. & ROHRSCHNEIDER, L. R. 1997. Sequential activation of phoshatidylinositol 3-kinase and phospholipase C-gamma2 by the M-CSF receptor is necessary for differentiation signaling. *EMBO J,* 16**,** 5880-93.

BOUSSIF, O., LEZOUALC'H, F., ZANTA, M. A., MERGNY, M. D., SCHERMAN, D., DEMENEIX, B. & BEHR, J. P. 1995. A versatile vector for gene and oligonucleotide transfer into cells in culture and in vivo: polyethylenimine. *Proc Natl Acad Sci U S A,* 92**,** 7297-301.

BOYER, J. L., NG, O. C., ANANTHANARAYANAN, M., HOFMANN, A. F., SCHTEINGART, C. D., HAGENBUCH, B., STIEGER, B. & MEIER, P. J. 1994. Expression and characterization of a functional rat liver Na+ bile acid cotransport system in COS-7 cells. *Am J Physiol,* 266**,** G382-7.

BREUZA, L., HALBEISEN, R., JENO, P., OTTE, S., BARLOWE, C., HONG, W. & HAURI, H. P. 2004. Proteomics of endoplasmic reticulum-Golgi intermediate compartment (ERGIC) membranes from brefeldin A-treated HepG2 cells identifies ERGIC-32, a new cycling protein that interacts with human Erv46. *J Biol Chem,* 279**,** 47242-53.

BRODER, Y. C., KATZ, S. & ARONHEIM, A. 1998. The ras recruitment system, a novel approach to the study of protein-protein interactions. *Curr Biol,* 8**,** 1121-4.

BROMBERG, J. & DARNELL, J. E., JR. 2000. The role of STATs in transcriptional control and their impact on cellular function. *Oncogene,* 19**,** 2468-73.

BROWN, D. A. & LONDON, E. 1998. Functions of lipid rafts in biological membranes. *Annu Rev Cell Dev Biol,* 14**,** 111-36.

BULL, L. N., VAN EIJK, M. J., PAWLIKOWSKA, L., DEYOUNG, J. A., JUIJN, J. A., LIAO, M., KLOMP, L. W., LOMRI, N., BERGER, R., SCHARSCHMIDT, B. F., KNISELY, A. S., HOUWEN, R. H. & FREIMER, N. B. 1998. A gene encoding a P-type ATPase mutated in two forms of hereditary cholestasis. *Nat Genet,* 18**,** 219-24.

BURNETTE, W. N. 1981. "Western blotting": electrophoretic transfer of proteins from sodium dodecyl sulfate--polyacrylamide gels to unmodified nitrocellulose and radiographic detection with antibody and radioiodinated protein A. *Anal Biochem,* 112**,** 195-203.

BUSCHMAN, E., ARCECI, R. J., CROOP, J. M., CHE, M., ARIAS, I. M., HOUSMAN, D. E. & GROS, P. 1992. mdr2 encodes P-glycoprotein expressed in the bile canalicular membrane as determined by isoform-specific antibodies. *J Biol Chem,* 267**,** 18093-9.

BYRNE, J. A., STRAUTNIEKS, S. S., IHRKE, G., PAGANI, F., KNISELY, A. S., LINTON, K. J., MIELI-VERGANI, G. & THOMPSON, R. J. 2009. Missense mutations and single nucleotide polymorphisms in ABCB11 impair bile salt export pump processing and function or disrupt pre-messenger RNA splicing. *Hepatology,* 49**,** 553-67.

BYRNE, J. A., STRAUTNIEKS, S. S., MIELI-VERGANI, G., HIGGINS, C. F., LINTON, K. J. & THOMPSON, R. J. 2002. The human bile salt export pump: characterization of substrate specificity and identification of inhibitors. *Gastroenterology,* 123**,** 1649-58.

CAMERON, P. L., RUFFIN, J. W., BOLLAG, R., RASMUSSEN, H. & CAMERON, R. S. 1997. Identification of caveolin and caveolin-related proteins in the brain. *J Neurosci,* 17**,** 9520-35.

CAMPBELL, I. 2006. Liver: metabolic functions. *Anaesthesia & Intensive Care Medicine,* 7**,** 51-54.

CASTAGNA, M., TAKAI, Y., KAIBUCHI, K., SANO, K., KIKKAWA, U. & NISHIZUKA, Y. 1982. Direct activation of calcium-activated, phospholipid-dependent protein kinase by tumor-promoting phorbol esters. *J Biol Chem,* 257**,** 7847-51.

CHAMBERS, T. C., MCAVOY, E. M., JACOBS, J. W. & EILON, G. 1990. Protein kinase C phosphorylates P-glycoprotein in multidrug resistant human KB carcinoma cells. *J Biol Chem,* 265**,** 7679-86.

CHAMBERS, T. C., POHL, J., GLASS, D. B. & KUO, J. F. 1994. Phosphorylation by protein kinase C and cyclic AMP-dependent protein kinase of synthetic peptides derived from the linker region of human P-glycoprotein. *Biochem J,* 299 (Pt 1)**,** 309-15.

CHAMBERS, T. C., POHL, J., RAYNOR, R. L. & KUO, J. F. 1993. Identification of specific sites in human P-glycoprotein phosphorylated by protein kinase C. *J Biol Chem,* 268**,** 4592-5.

CHAMBERS, T. C., ZHENG, B. & KUO, J. F. 1992. Regulation by phorbol ester and protein kinase C inhibitors, and by a protein phosphatase inhibitor (okadaic acid), of P-glycoprotein phosphorylation and relationship to drug accumulation in multidrug-resistant human KB cells. *Mol Pharmacol,* 41**,** 1008-15.

CHANG, Y. F., IMAM, J. S. & WILKINSON, M. F. 2007. The nonsense-mediated decay RNA surveillance pathway. *Annu Rev Biochem,* 76**,** 51-74.

CHAUDHARY, P. M. & RONINSON, I. B. 1991. Expression and activity of P-glycoprotein, a multidrug efflux pump, in human hematopoietic stem cells. *Cell,* 66**,** 85-94.

CHAWLA, A., SAEZ, E. & EVANS, R. M. 2000. "Don't know much bile-ology". *Cell,* 103**,** 1-4.

CHEN, C. J., CHIN, J. E., UEDA, K., CLARK, D. P., PASTAN, I., GOTTESMAN, M. M. & RONINSON, I. B. 1986. Internal duplication and homology with bacterial transport proteins in the mdr1 (P-glycoprotein) gene from multidrug-resistant human cells. *Cell,* 47**,** 381-9.

CHEN, H. L., CHANG, P. S., HSU, H. C., LEE, J. H., NI, Y. H., HSU, H. Y., JENG, Y. M. & CHANG, M. H. 2001. Progressive familial intrahepatic cholestasis with high gamma-glutamyltranspeptidase levels in Taiwanese infants: role of MDR3 gene defect? *Pediatr Res,* 50**,** 50-5.

CHEN, H. L., CHANG, P. S., HSU, H. C., NI, Y. H., HSU, H. Y., LEE, J. H., JENG, Y. M., SHAU, W. Y. & CHANG, M. H. 2002. FIC1 and BSEP defects in Taiwanese patients with chronic intrahepatic cholestasis with low gamma-glutamyltranspeptidase levels. *J Pediatr,* 140**,** 119-24.

CHEN, J., LU, G., LIN, J., DAVIDSON, A. L. & QUIOCHO, F. A. 2003. A tweezers-like motion of the ATP-binding cassette dimer in an ABC transport cycle. *Mol Cell,* 12**,** 651-61.

CHEN, K. G., SZAKACS, G., ANNEREAU, J. P., ROUZAUD, F., LIANG, X. J., VALENCIA, J. C., NAGINENI, C. N., HOOKS, J. J., HEARING, V. J. & GOTTESMAN, M. M. 2005. Principal expression of two mRNA isoforms (ABCB 5alpha and ABCB 5beta) of the ATP-binding cassette transporter gene ABCB 5 in melanoma cells and melanocytes. *Pigment Cell Res,* 18**,** 102-12.

CHENG, S. H., GREGORY, R. J., MARSHALL, J., PAUL, S., SOUZA, D. W., WHITE, G. A., O'RIORDAN, C. R. & SMITH, A. E. 1990. Defective intracellular transport and processing of CFTR is the molecular basis of most cystic fibrosis. *Cell,* 63**,** 827-34.

CHILDS, S., YEH, R. L., GEORGES, E. & LING, V. 1995. Identification of a sister gene to P-glycoprotein. *Cancer Res,* 55**,** 2029-34.

CLAYTON, R. J., IBER, F. L., RUEBNER, B. H. & MCKUSICK, V. A. 1969. Byler disease. Fatal familial intrahepatic cholestasis in an Amish kindred. *Am J Dis Child,* 117**,** 112-24.

COHEN, A. W., HNASKO, R., SCHUBERT, W. & LISANTI, M. P. 2004. Role of caveolae and caveolins in health and disease. *Physiol Rev,* 84**,** 1341-79.

COLE, S. P. 1990. Patterns of cross-resistance in a multidrug-resistant small-cell lung carcinoma cell line. *Cancer Chemother Pharmacol,* 26**,** 250-6.

COLE, S. P., BHARDWAJ, G., GERLACH, J. H., MACKIE, J. E., GRANT, C. E., ALMQUIST, K. C., STEWART, A. J., KURZ, E. U., DUNCAN, A. M. & DEELEY, R. G. 1992. Overexpression of a transporter gene in a multidrug-resistant human lung cancer cell line. *Science,* 258**,** 1650-4.

COPPOLA, C. P., GOSCHE, J. R., ARRESE, M., ANCOWITZ, B., MADSEN, J., VANDERHOOF, J. & SHNEIDER, B. L. 1998. Molecular analysis of the adaptive response of intestinal bile acid transport after ileal resection in the rat. *Gastroenterology,* 115**,** 1172-8.

CORDON-CARDO, C., O'BRIEN, J. P., BOCCIA, J., CASALS, D., BERTINO, J. R. & MELAMED, M. R. 1990. Expression of the multidrug resistance gene product (P-glycoprotein) in human normal and tumor tissues. *J Histochem Cytochem,* 38**,** 1277-87.

CORDON-CARDO, C., O'BRIEN, J. P., CASALS, D., RITTMAN-GRAUER, L., BIEDLER, J. L., MELAMED, M. R. & BERTINO, J. R. 1989. Multidrug-resistance gene (P-glycoprotein) is expressed by endothelial cells at blood-brain barrier sites. *Proc Natl Acad Sci U S A,* 86**,** 695-8.

CORNWELL, M. M., PASTAN, I. & GOTTESMAN, M. M. 1987a. Certain calcium channel blockers bind specifically to multidrug-resistant human KB carcinoma membrane vesicles and inhibit drug binding to P-glycoprotein. *J Biol Chem,* 262**,** 2166-70.

CORNWELL, M. M., SAFA, A. R., FELSTED, R. L., GOTTESMAN, M. M. & PASTAN, I. 1986. Membrane vesicles from multidrug-resistant human cancer cells contain a specific 150- to 170-kDa protein detected by photoaffinity labeling. *Proc Natl Acad Sci U S A,* 83**,** 3847-50.

CORNWELL, M. M., TSURUO, T., GOTTESMAN, M. M. & PASTAN, I. 1987b. ATP-binding properties of P glycoprotein from multidrug-resistant KB cells. *FASEB J,* 1**,** 51-4.

CUTTING, G. R., KASCH, L. M., ROSENSTEIN, B. J., ZIELENSKI, J., TSUI, L. C., ANTONARAKIS, S. E. & KAZAZIAN, H. H., JR. 1990. A cluster of cystic fibrosis mutations in the first nucleotide-binding fold of the cystic fibrosis conductance regulator protein. *Nature,* 346**,** 366-9.

DALMAS, O., ORELLE, C., FOUCHER, A. E., GEOURJON, C., CROUZY, S., DI PIETRO, A. & JAULT, J. M. 2005. The Q-loop disengages from the first intracellular loop during the catalytic cycle of the multidrug ABC transporter BmrA. *J Biol Chem,* 280**,** 36857-64.

DANO, K. 1973. Active outward transport of daunomycin in resistant Ehrlich ascites tumor cells. *Biochim Biophys Acta,* 323**,** 466-83.

DAVIET, L., MALVOISIN, E., WILD, T. F. & MCGREGOR, J. L. 1997. Thrombospondin induces dimerization of membrane-bound, but not soluble CD36. *Thromb Haemost,* 78**,** 897-901.

DAVIS, B. J. 1964. Disc Electrophoresis. Ii. Method and Application to Human Serum Proteins. *Ann N Y Acad Sci,* 121**,** 404-27.

DAVIT-SPRAUL, A., GONZALES, E., BAUSSAN, C. & JACQUEMIN, E. 2009. Progressive familial intrahepatic cholestasis. *Orphanet J Rare Dis,* 4**,** 1.

DAWSON, P. A., HUBBERT, M., HAYWOOD, J., CRADDOCK, A. L., ZERANGUE, N., CHRISTIAN, W. V. & BALLATORI, N. 2005. The heteromeric organic solute transporter alpha-beta, Ostalpha-Ostbeta, is an ileal basolateral bile acid transporter. *J Biol Chem,* 280**,** 6960-8.

DAWSON, P. A., LAN, T. & RAO, A. 2009. Bile acid transporters. *J Lipid Res,* 50**,** 2340-57.

DAWSON, R. J. & LOCHER, K. P. 2006. Structure of a bacterial multidrug ABC transporter. *Nature,* 443**,** 180-5.

DAWSON, R. J. & LOCHER, K. P. 2007. Structure of the multidrug ABC transporter Sav1866 from Staphylococcus aureus in complex with AMP-PNP. *FEBS Lett,* 581**,** 935-8.

DE PAGTER, A. G., VAN BERGE HENEGOUWEN, G. P., TEN BOKKEL HUININK, J. A. & BRANDT, K. H. 1976. Familial benign recurrent intrahepatic cholestasis. Interrelation with intrahepatic cholestasis of pregnancy and from oral contraceptives? *Gastroenterology,* 71**,** 202-7.

DE VREE, J. M., JACQUEMIN, E., STURM, E., CRESTEIL, D., BOSMA, P. J., ATEN, J., DELEUZE, J. F., DESROCHERS, M., BURDELSKI, M., BERNARD, O., OUDE ELFERINK, R. P. & HADCHOUEL, M. 1998. Mutations in the MDR3 gene cause progressive familial intrahepatic cholestasis. *Proc Natl Acad Sci U S A,* 95**,** 282-7.

DEAN, M., RZHETSKY, A. & ALLIKMETS, R. 2001. The human ATP-binding cassette (ABC) transporter superfamily. *Genome Res,* 11**,** 1156-66.

DEGIORGIO, D., COLOMBO, C., SEIA, M., PORCARO, L., COSTANTINO, L., ZAZZERON, L., BORDO, D. & COVIELLO, D. A. 2007. Molecular characterization and structural implications of 25 new ABCB4 mutations in progressive familial intrahepatic cholestasis type 3 (PFIC3). *Eur J Hum Genet,* 15**,** 1230-8.

DELAUNAY, J. L., DURAND-SCHNEIDER, A. M., DELAUTIER, D., RADA, A., GAUTHEROT, J., JACQUEMIN, E., AIT-SLIMANE, T. & MAURICE, M. 2009. A missense mutation in ABCB4 gene involved in progressive familial intrahepatic cholestasis type 3 leads to a folding defect that can be rescued by low temperature. *Hepatology,* 49**,** 1218-27.

DELEUZE, J. F., JACQUEMIN, E., DUBUISSON, C., CRESTEIL, D., DUMONT, M., ERLINGER, S., BERNARD, O. & HADCHOUEL, M. 1996. Defect of multidrug-resistance 3 gene expression in a subtype of progressive familial intrahepatic cholestasis. *Hepatology,* 23**,** 904-8.

DELISLE, B. P., ANDERSON, C. L., BALIJEPALLI, R. C., ANSON, B. D., KAMP, T. J. & JANUARY, C. T. 2003. Thapsigargin selectively rescues the trafficking defective LQT2 channels G601S and F805C. *J Biol Chem,* 278**,** 35749-54.

DEMEULE, M., JODOIN, J., GINGRAS, D. & BELIVEAU, R. 2000. P-glycoprotein is localized in caveolae in resistant cells and in brain capillaries. *FEBS Lett,* 466**,** 219-24.

DEMEULE, M., LABELLE, M., REGINA, A., BERTHELET, F. & BELIVEAU, R. 2001. Isolation of endothelial cells from brain, lung, and kidney: expression of the multidrug resistance P-glycoprotein isoforms. *Biochem Biophys Res Commun,* 281**,** 827-34.

DENNING, G. M., ANDERSON, M. P., AMARA, J. F., MARSHALL, J., SMITH, A. E. & WELSH, M. J. 1992. Processing of mutant cystic fibrosis transmembrane conductance regulator is temperature-sensitive. *Nature,* 358**,** 761-4.

DEVAUX, P. F. & MORRIS, R. 2004. Transmembrane asymmetry and lateral domains in biological membranes. *Traffic,* 5**,** 241-6.

DIETSCHY, J. M. 1966. Recent developments in solute and water transport across the gall bladder epithelium. *Gastroenterology,* 50**,** 692-707.

DIETZEN, D. J., HASTINGS, W. R. & LUBLIN, D. M. 1995. Caveolin is palmitoylated on multiple cysteine residues. Palmitoylation is not necessary for localization of caveolin to caveolae. *J Biol Chem,* 270**,** 6838-42.

DIXON, P. H., VAN MIL, S. W., CHAMBERS, J., STRAUTNIEKS, S., THOMPSON, R. J., LAMMERT, F., KUBITZ, R., KEITEL, V., GLANTZ, A., MATTSSON, L. A., MARSCHALL, H. U., MOLOKHIA, M., MOORE, G. E., LINTON, K. J. &

WILLIAMSON, C. 2009. Contribution of variant alleles of ABCB11 to susceptibility to intrahepatic cholestasis of pregnancy. *Gut,* 58**,** 537-44.

DIXON, P. H., WEERASEKERA, N., LINTON, K. J., DONALDSON, O., CHAMBERS, J., EGGINTON, E., WEAVER, J., NELSON-PIERCY, C., DE SWIET, M., WARNES, G., ELIAS, E., HIGGINS, C. F., JOHNSTON, D. G., MCCARTHY, M. I. & WILLIAMSON, C. 2000. Heterozygous MDR3 missense mutation associated with intrahepatic cholestasis of pregnancy: evidence for a defect in protein trafficking. *Hum Mol Genet,* 9**,** 1209-17.

DIXON, P. H. & WILLIAMSON, C. 2008. The molecular genetics of intrahepatic cholestasis of pregnancy. *Obstet Med,* 1**,** 65-71.

DOEGE, H. & STAHL, A. 2006. Protein-mediated fatty acid uptake: novel insights from in vivo models. *Physiology (Bethesda),* 21**,** 259-68.

DONOVAN, J. M., TIMOFEYEVA, N. & CAREY, M. C. 1991. Influence of total lipid concentration, bile salt:lecithin ratio, and cholesterol content on inter-mixed micellar/vesicular (non-lecithin-associated) bile salt concentrations in model bile. *J Lipid Res,* 32**,** 1501-12.

DORFMAN, B. Z. 1969. The isolation of adenylosuccinate synthetase mutants in yeast by selection for constitutive behavior in pigmented strains. *Genetics,* 61**,** 377-89.

DOYLE, L. A., YANG, W., ABRUZZO, L. V., KROGMANN, T., GAO, Y., RISHI, A. K. & ROSS, D. D. 1998. A multidrug resistance transporter from human MCF-7 breast cancer cells. *Proc Natl Acad Sci U S A,* 95**,** 15665-70.

DUPREE, P., PARTON, R. G., RAPOSO, G., KURZCHALIA, T. V. & SIMONS, K. 1993. Caveolae and sorting in the trans-Golgi network of epithelial cells. *EMBO J,* 12**,** 1597-605.

EASL 2009. EASL Clinical Practice Guidelines: management of cholestatic liver diseases. *J Hepatol,* 51**,** 237-67.

ECKFORD, P. D. & SHAROM, F. J. 2005. The reconstituted P-glycoprotein multidrug transporter is a flippase for glucosylceramide and other simple glycosphingolipids. *Biochem J,* 389**,** 517-26.

EGAN, M. E., GLOCKNER-PAGEL, J., AMBROSE, C., CAHILL, P. A., PAPPOE, L., BALAMUTH, N., CHO, E., CANNY, S., WAGNER, C. A., GEIBEL, J. & CAPLAN, M. J. 2002. Calcium-pump inhibitors induce functional surface expression of Delta F508-CFTR protein in cystic fibrosis epithelial cells. *Nat Med,* 8**,** 485-92.

EHRHARD, K. N., JACOBY, J. J., FU, X. Y., JAHN, R. & DOHLMAN, H. G. 2000. Use of G-protein fusions to monitor integral membrane protein-protein interactions in yeast. *Nat Biotechnol,* 18**,** 1075-9.

EHRHARDT, C., SCHMOLKE, M., MATZKE, A., KNOBLAUCH, A., WILL, C., WIXLER, V. & LUDWIG, S. 2006. Polyethylenimine, a cost-effective transfection reagent. *Signal Transduction,* 6**,** 179-184.

ELLIOTT, J. I., SURPRENANT, A., MARELLI-BERG, F. M., COOPER, J. C., CASSADY-CAIN, R. L., WOODING, C., LINTON, K., ALEXANDER, D. R. & HIGGINS, C. F. 2005. Membrane phosphatidylserine distribution as a non-apoptotic signalling mechanism in lymphocytes. *Nat Cell Biol,* 7**,** 808-16.

ELORANTA, M. L., HEISKANEN, J. T., HILTUNEN, M. J., MANNERMAA, A. J., PUNNONEN, K. R. & HEINONEN, S. T. 2002. Multidrug resistance 3 gene mutation 1712delT and estrogen receptor alpha gene polymorphisms in Finnish women with obstetric cholestasis. *Eur J Obstet Gynecol Reprod Biol,* 105**,** 132-5.

ESTELLER, A. 2008. Physiology of bile secretion. *World J Gastroenterol,* 14**,** 5641-9.

FEBBRAIO, M., PODREZ, E. A., SMITH, J. D., HAJJAR, D. P., HAZEN, S. L., HOFF, H. F., SHARMA, K. & SILVERSTEIN, R. L. 2000. Targeted disruption of the class B scavenger receptor CD36 protects against atherosclerotic lesion development in mice. *J Clin Invest,* 105**,** 1049-56.

FIELDS, S. & SONG, O. 1989. A novel genetic system to detect protein-protein interactions. *Nature,* 340**,** 245-6.

FINE, R. L., CHAMBERS, T. C. & SACHS, C. W. 1996. P-glycoprotein, multidrug resistance and protein kinase C. *Stem Cells,* 14**,** 47-55.

FINE, R. L., PATEL, J. & CHABNER, B. A. 1988. Phorbol esters induce multidrug resistance in human breast cancer cells. *Proc Natl Acad Sci U S A,* 85**,** 582-6.

FISHER, G. A., LUM, B. L., HAUSDORFF, J. & SIKIC, B. I. 1996. Pharmacological considerations in the modulation of multidrug resistance. *Eur J Cancer,* 32A**,** 1082-8.

FLOREANI, A., CARDERI, I., PATERNOSTER, D., SOARDO, G., AZZAROLI, F., ESPOSITO, W., MONTAGNANI, M., MARCHESONI, D., VARIOLA, A., ROSA RIZZOTTO, E., BRAGHIN, C. & MAZZELLA, G. 2008. Hepatobiliary phospholipid transporter ABCB4, MDR3 gene variants in a large cohort of Italian women with intrahepatic cholestasis of pregnancy. *Dig Liver Dis,* 40**,** 366-70.

FOJO, A. T., UEDA, K., SLAMON, D. J., POPLACK, D. G., GOTTESMAN, M. M. & PASTAN, I. 1987. Expression of a multidrug-resistance gene in human tumors and tissues. *Proc Natl Acad Sci U S A,* 84**,** 265-9.

FORSBURG, S. L. 2001. The art and design of genetic screens: yeast. *Nat Rev Genet,* 2**,** 659-68.

FRA, A. M., WILLIAMSON, E., SIMONS, K. & PARTON, R. G. 1994. Detergent-insoluble glycolipid microdomains in lymphocytes in the absence of caveolae. *J Biol Chem,* 269**,** 30745-8.

FRANK, N. Y., MARGARYAN, A., HUANG, Y., SCHATTON, T., WAAGA-GASSER, A. M., GASSER, M., SAYEGH, M. H., SADEE, W. & FRANK, M. H. 2005. ABCB5-mediated doxorubicin transport and chemoresistance in human malignant melanoma. *Cancer Res,* 65**,** 4320-33.

FU, D. & ROUFOGALIS, B. D. 2007. Actin disruption inhibits endosomal traffic of P-glycoprotein-EGFP and resistance to daunorubicin accumulation. *Am J Physiol Cell Physiol,* 292**,** C1543-52.

GADSBY, D. C., VERGANI, P. & CSANADY, L. 2006. The ABC protein turned chloride channel whose failure causes cystic fibrosis. *Nature,* 440**,** 477-83.

GALBIATI, F., RAZANI, B. & LISANTI, M. P. 2001. Emerging themes in lipid rafts and caveolae. *Cell,* 106**,** 403-11.

GAUTHEROT, J., DURAND-SCHNEIDER, A. M., DELAUTIER, D., DELAUNAY, J. L., RADA, A., GABILLET, J., HOUSSET, C., MAURICE, M. & AIT-SLIMANE, T. 2012. Effects of cellular, chemical, and pharmacological chaperones on the rescue of a trafficking-defective mutant of the ATP-binding cassette transporter proteins ABCB1/ABCB4. *J Biol Chem,* 287**,** 5070-8.

GEDVILAITE, A. & SASNAUSKAS, K. 1994. Control of the expression of the ADE2 gene of the yeast Saccharomyces cerevisiae. *Curr Genet,* 25**,** 475-9.

GEENES, V. & WILLIAMSON, C. 2009. Intrahepatic cholestasis of pregnancy. *World J Gastroenterol,* 15**,** 2049-66.

GENDROT, C., BACQ, Y., BRECHOT, M. C., LANSAC, J. & ANDRES, C. 2003. A second heterozygous MDR3 nonsense mutation associated with intrahepatic cholestasis of pregnancy. *J Med Genet,* 40**,** e32.

GEORGES, E., BRADLEY, G., GARIEPY, J. & LING, V. 1990. Detection of P-glycoprotein isoforms by gene-specific monoclonal antibodies. *Proc Natl Acad Sci U S A,* 87**,** 152-6.

GERLACH, J. H., ENDICOTT, J. A., JURANKA, P. F., HENDERSON, G., SARANGI, F., DEUCHARS, K. L. & LING, V. 1986a. Homology between P-glycoprotein and a bacterial haemolysin transport protein suggests a model for multidrug resistance. *Nature,* 324**,** 485-9.

GERLACH, J. H., KARTNER, N., BELL, D. R. & LING, V. 1986b. Multidrug resistance. *Cancer Surv,* 5**,** 25-46.

GERLOFF, T., STIEGER, B., HAGENBUCH, B., MADON, J., LANDMANN, L., ROTH, J., HOFMANN, A. F. & MEIER, P. J. 1998. The sister of P-glycoprotein represents the canalicular bile salt export pump of mammalian liver. *J Biol Chem,* 273**,** 10046-50.

GERMANN, U. A., CHAMBERS, T. C., AMBUDKAR, S. V., LICHT, T., CARDARELLI, C. O., PASTAN, I. & GOTTESMAN, M. M. 1996. Characterization of phosphorylation-defective mutants of human P-glycoprotein expressed in mammalian cells. *J Biol Chem,* 271**,** 1708-16.

GIETZ, R. D. & SCHIESTL, R. H. 2007a. High-efficiency yeast transformation using the LiAc/SS carrier DNA/PEG method. *Nat Protoc,* 2**,** 31-4.

GIETZ, R. D. & SCHIESTL, R. H. 2007b. Large-scale high-efficiency yeast transformation using the LiAc/SS carrier DNA/PEG method. *Nat Protoc,* 2**,** 38-41.

GIMENO, R. E., ORTEGON, A. M., PATEL, S., PUNREDDY, S., GE, P., SUN, Y., LODISH, H. F. & STAHL, A. 2003. Characterization of a heart-specific fatty acid transport protein. *J Biol Chem,* 278**,** 16039-44.

GISLER, S. M., KITTANAKOM, S., FUSTER, D., WONG, V., BERTIC, M., RADANOVIC, T., HALL, R. A., MURER, H., BIBER, J., MARKOVICH, D., MOE, O. W. & STAGLJAR, I. 2008. Monitoring protein-protein interactions between the mammalian integral membrane transporters and PDZ-interacting partners using a modified split-ubiquitin membrane yeast two-hybrid system. *Mol Cell Proteomics,* 7**,** 1362-77.

GLENNEY, J. R., JR. 1992. The sequence of human caveolin reveals identity with VIP21, a component of transport vesicles. *FEBS Lett,* 314**,** 45-8.

GLUZMAN, Y. 1981. SV40-transformed simian cells support the replication of early SV40 mutants. *Cell,* 23**,** 175-82.

GOLDBERG, A. L. 2003. Protein degradation and protection against misfolded or damaged proteins. *Nature,* 426**,** 895-9.

GONG, Y. Z., EVERETT, E. T., SCHWARTZ, D. A., NORRIS, J. S. & WILSON, F. A. 1994. Molecular cloning, tissue distribution, and expression of a 14-kDa bile acid-binding protein from rat ileal cytosol. *Proc Natl Acad Sci U S A,* 91**,** 4741-5.

GONZALES, E., GROSSE, B., CASSIO, D., DAVIT-SPRAUL, A., FABRE, M. & JACQUEMIN, E. 2012. Successful mutation-specific chaperone therapy with 4-phenylbutyrate in a child with progressive familial intrahepatic cholestasis type 2. *J Hepatol,* 57**,** 695-8.

GONZALEZ, M. C., REYES, H., ARRESE, M., FIGUEROA, D., LORCA, B., ANDRESEN, M., SEGOVIA, N., MOLINA, C. & ARCE, S. 1989. Intrahepatic cholestasis of pregnancy in twin pregnancies. *J Hepatol,* 9**,** 84-90.

GOODFELLOW, H. R., SARDINI, A., RUETZ, S., CALLAGHAN, R., GROS, P., MCNAUGHTON, P. A. & HIGGINS, C. F. 1996. Protein kinase C-mediated phosphorylation does not regulate drug transport by the human multidrug resistance P-glycoprotein. *J Biol Chem,* 271**,** 13668-74.

GOODWIN, B., JONES, S. A., PRICE, R. R., WATSON, M. A., MCKEE, D. D., MOORE, L. B., GALARDI, C., WILSON, J. G., LEWIS, M. C., ROTH, M. E., MALONEY, P. R., WILLSON, T. M. & KLIEWER, S. A. 2000. A regulatory cascade of the nuclear receptors FXR, SHP-1, and LRH-1 represses bile acid biosynthesis. *Mol Cell,* 6**,** 517-26.

GOTO, K., SUGIYAMA, K., SUGIURA, T., ANDO, T., MIZUTANI, F., TERABE, K., BAN, K. & TOGARI, H. 2003. Bile salt export pump gene mutations in two Japanese patients with progressive familial intrahepatic cholestasis. *J Pediatr Gastroenterol Nutr,* 36**,** 647-50.

GOTTESMAN, M. M., FOJO, T. & BATES, S. E. 2002. Multidrug resistance in cancer: role of ATP-dependent transporters. *Nat Rev Cancer,* 2**,** 48-58.

GRAHAM, F. L., SMILEY, J., RUSSELL, W. C. & NAIRN, R. 1977. Characteristics of a human cell line transformed by DNA from human adenovirus type 5. *J Gen Virol,* 36**,** 59-74.

GRAUMANN, P. L., LOSICK, R. & STRUNNIKOV, A. V. 1998. Subcellular localization of Bacillus subtilis SMC, a protein involved in chromosome condensation and segregation. *J Bacteriol,* 180**,** 5749-55.

GREENWALT, D. E., LIPSKY, R. H., OCKENHOUSE, C. F., IKEDA, H., TANDON, N. N. & JAMIESON, G. A. 1992. Membrane glycoprotein CD36: a review of its roles in adherence, signal transduction, and transfusion medicine. *Blood,* 80**,** 1105-15.

GRIBAR, J. J., RAMACHANDRA, M., HRYCYNA, C. A., DEY, S. & AMBUDKAR, S. V. 2000. Functional characterization of glycosylation-deficient human P-glycoprotein using a vaccinia virus expression system. *J Membr Biol,* 173**,** 203-14.

GROEN, A., ROMERO, M. R., KUNNE, C., HOOSDALLY, S. J., DIXON, P. H., WOODING, C., WILLIAMSON, C., SEPPEN, J., VAN DEN OEVER, K., MOK, K. S., PAULUSMA, C. C., LINTON, K. J. & OUDE ELFERINK, R. P. 2011. Complementary functions of the flippase ATP8B1 and the floppase ABCB4 in maintaining canalicular membrane integrity. *Gastroenterology,* 141**,** 1927-37 e1-4.

GROS, P., BEN NERIAH, Y. B., CROOP, J. M. & HOUSMAN, D. E. 1986a. Isolation and expression of a complementary DNA that confers multidrug resistance. *Nature,* 323**,** 728-31.

GROS, P., CROOP, J. & HOUSMAN, D. 1986b. Mammalian multidrug resistance gene: complete cDNA sequence indicates strong homology to bacterial transport proteins. *Cell,* 47**,** 371-80.

GROS, P. & SHUSTIK, C. 1991. Multidrug resistance: a novel class of membrane-associated transport proteins is identified. *Cancer Invest,* 9**,** 563-9.

GRUNICKE, H., HOFMANN, J., UTZ, I. & UBERALL, F. 1994. Role of protein kinases in antitumor drug resistance. *Ann Hematol,* 69 Suppl 1**,** S1-6.

HAGENBUCH, B. & DAWSON, P. 2004. The sodium bile salt cotransport family SLC10. *Pflugers Arch,* 447**,** 566-70.

HAGENBUCH, B. & MEIER, P. J. 1994. Molecular cloning, chromosomal localization, and functional characterization of a human liver Na+/bile acid cotransporter. *J Clin Invest,* 93**,** 1326-31.

HAGENBUCH, B. & MEIER, P. J. 1996. Sinusoidal (basolateral) bile salt uptake systems of hepatocytes. *Semin Liver Dis,* 16**,** 129-36.

HAGENBUCH, B. & MEIER, P. J. 2003. The superfamily of organic anion transporting polypeptides. *Biochim Biophys Acta,* 1609**,** 1-18.

HAGENBUCH, B. & MEIER, P. J. 2004. Organic anion transporting polypeptides of the OATP/ SLC21 family: phylogenetic classification as OATP/ SLCO superfamily, new nomenclature and molecular/functional properties. *Pflugers Arch,* 447**,** 653-65.

HAMADA, H., HAGIWARA, K., NAKAJIMA, T. & TSURUO, T. 1987. Phosphorylation of the Mr 170,000 to 180,000 glycoprotein specific to multidrug-resistant tumor cells: effects of verapamil, trifluoperazine, and phorbol esters. *Cancer Res,* 47**,** 2860-5.

HAMMERLE, S. P., ROTHEN-RUTISHAUSER, B., KRAMER, S. D., GUNTHERT, M. & WUNDERLI-ALLENSPACH, H. 2000. P-Glycoprotein in cell cultures: a combined approach to study expression, localisation, and functionality in the confocal microscope. *Eur J Pharm Sci,* 12**,** 69-77.

HARDY, S. P., GOODFELLOW, H. R., VALVERDE, M. A., GILL, D. R., SEPULVEDA, V. & HIGGINS, C. F. 1995. Protein kinase C-mediated phosphorylation of the human multidrug resistance P-glycoprotein regulates cell volume-activated chloride channels. *EMBO J,* 14**,** 68-75.

HATA, S., WANG, P., EFTYCHIOU, N., ANANTHANARAYANAN, M., BATTA, A., SALEN, G., PANG, K. S. & WOLKOFF, A. W. 2003. Substrate specificities of rat oatp1 and ntcp: implications for hepatic organic anion uptake. *Am J Physiol Gastrointest Liver Physiol,* 285**,** G829-39.

HAWKINS, B. T., SYKES, D. B. & MILLER, D. S. 2010. Rapid, reversible modulation of blood-brain barrier P-glycoprotein transport activity by vascular endothelial growth factor. *J Neurosci,* 30**,** 1417-25.

HAYASHI, H. & SUGIYAMA, Y. 2007. 4-phenylbutyrate enhances the cell surface expression and the transport capacity of wild-type and mutated bile salt export pumps. *Hepatology,* 45**,** 1506-16.

HAYASHI, H., TAKADA, T., SUZUKI, H., AKITA, H. & SUGIYAMA, Y. 2005. Two common PFIC2 mutations are associated with the impaired membrane trafficking of BSEP/ABCB11. *Hepatology,* 41**,** 916-24.

HELLYER, N. J., CHENG, K. & KOLAND, J. G. 1998. ErbB3 (HER3) interaction with the p85 regulatory subunit of phosphoinositide 3-kinase. *Biochem J,* 333 (Pt 3)**,** 757-63.

HERSHKO, A. & CIECHANOVER, A. 1992. The ubiquitin system for protein degradation. *Annu Rev Biochem,* 61**,** 761-807.

HIGGINS, C. F. 1992. ABC transporters: from microorganisms to man. *Annu Rev Cell Biol,* 8**,** 67-113.

HIGGINS, C. F. 2007. Multiple molecular mechanisms for multidrug resistance transporters. *Nature,* 446**,** 749-57.

HIGGINS, C. F., HILES, I. D., SALMOND, G. P., GILL, D. R., DOWNIE, J. A., EVANS, I. J., HOLLAND, I. B., GRAY, L., BUCKEL, S. D., BELL, A. W. & ET AL. 1986. A family of

related ATP-binding subunits coupled to many distinct biological processes in bacteria. *Nature,* 323**,** 448-50.

HIGH, S., LECOMTE, F. J., RUSSELL, S. J., ABELL, B. M. & OLIVER, J. D. 2000. Glycoprotein folding in the endoplasmic reticulum: a tale of three chaperones? *FEBS Lett,* 476**,** 38-41.

HILTUNEN, J. K., MURSULA, A. M., ROTTENSTEINER, H., WIERENGA, R. K., KASTANIOTIS, A. J. & GURVITZ, A. 2003. The biochemistry of peroxisomal beta-oxidation in the yeast Saccharomyces cerevisiae. *FEMS Microbiol Rev,* 27**,** 35-64.

HIRSCH, D., STAHL, A. & LODISH, H. F. 1998. A family of fatty acid transporters conserved from mycobacterium to man. *Proc Natl Acad Sci U S A,* 95**,** 8625-9.

HOFMANN, A. F. 2009. The enterohepatic circulation of bile acids in mammals: form and functions. *Front Biosci,* 14**,** 2584-98.

HOFMANN, A. F. & HAGEY, L. R. 2008. Bile acids: chemistry, pathochemistry, biology, pathobiology, and therapeutics. *Cell Mol Life Sci,* 65**,** 2461-83.

HOPFNER, K. P., KARCHER, A., SHIN, D. S., CRAIG, L., ARTHUR, L. M., CARNEY, J. P. & TAINER, J. A. 2000. Structural biology of Rad50 ATPase: ATP-driven conformational control in DNA double-strand break repair and the ABC-ATPase superfamily. *Cell,* 101**,** 789-800.

HORI, O., MIYAZAKI, M., TAMATANI, T., OZAWA, K., TAKANO, K., OKABE, M., IKAWA, M., HARTMANN, E., MAI, P., STERN, D. M., KITAO, Y. & OGAWA, S. 2006. Deletion of SERP1/RAMP4, a component of the endoplasmic reticulum (ER) translocation sites, leads to ER stress. *Mol Cell Biol,* 26**,** 4257-67.

HORIO, M., GOTTESMAN, M. M. & PASTAN, I. 1988. ATP-dependent transport of vinblastine in vesicles from human multidrug-resistant cells. *Proc Natl Acad Sci U S A,* 85**,** 3580-4.

HRYCYNA, C. A., AIRAN, L. E., GERMANN, U. A., AMBUDKAR, S. V., PASTAN, I. & GOTTESMAN, M. M. 1998. Structural flexibility of the linker region of human P-glycoprotein permits ATP hydrolysis and drug transport. *Biochemistry,* 37**,** 13660-73.

HUANG, L., ZHAO, A., LEW, J. L., ZHANG, T., HRYWNA, Y., THOMPSON, J. R., DE PEDRO, N., ROYO, I., BLEVINS, R. A., PELAEZ, F., WRIGHT, S. D. & CUI, J. 2003. Farnesoid X receptor activates transcription of the phospholipid pump MDR3. *J Biol Chem,* 278**,** 51085-90.

HUBSMAN, M., YUDKOVSKY, G. & ARONHEIM, A. 2001. A novel approach for the identification of protein-protein interaction with integral membrane proteins. *Nucleic Acids Res,* 29**,** E18.

HUG, H. & SARRE, T. F. 1993. Protein kinase C isoenzymes: divergence in signal transduction? *Biochem J,* 291 (Pt 2)**,** 329-43.

HYDE, S. C., EMSLEY, P., HARTSHORN, M. J., MIMMACK, M. M., GILEADI, U., PEARCE, S. R., GALLAGHER, M. P., GILL, D. R., HUBBARD, R. E. & HIGGINS, C. F. 1990. Structural model of ATP-binding proteins associated with cystic fibrosis, multidrug resistance and bacterial transport. *Nature,* 346**,** 362-5.

IDRISS, H., URQUIDI, V. & BASAVAPPA, S. 2000. Selective modulation of P-glycoprotein's ATPase and anion efflux regulation activities with PKC alpha and PKC epsilon in Sf9 cells. *Cancer Chemother Pharmacol,* 46**,** 287-92.

IKEBUCHI, Y., TAKADA, T., ITO, K., YOSHIKADO, T., ANZAI, N., KANAI, Y. & SUZUKI, H. 2009. Receptor for activated C-kinase 1 regulates the cellular localization and function of ABCB4. *Hepatol Res,* 39**,** 1091-107.

ISHIBASHI, H., NAKAMURA, M., KOMORI, A., MIGITA, K. & SHIMODA, S. 2009. Liver architecture, cell function, and disease. *Semin Immunopathol,* 31**,** 399-409.

ISMAIR, M. G., HAUSLER, S., STUERMER, C. A., GUYOT, C., MEIER, P. J., ROTH, J. & STIEGER, B. 2009. ABC-transporters are localized in caveolin-1-positive and reggie-1-negative and reggie-2-negative microdomains of the canalicular membrane in rat hepatocytes. *Hepatology,* 49**,** 1673-82.

ITO, T., CHIBA, T., OZAWA, R., YOSHIDA, M., HATTORI, M. & SAKAKI, Y. 2001. A comprehensive two-hybrid analysis to explore the yeast protein interactome. *Proc Natl Acad Sci U S A,* 98**,** 4569-74.

IYER, K., BURKLE, L., AUERBACH, D., THAMINY, S., DINKEL, M., ENGELS, K. & STAGLJAR, I. 2005. Utilizing the split-ubiquitin membrane yeast two-hybrid system to identify protein-protein interactions of integral membrane proteins. *Sci STKE,* 2005**,** pl3.

JACQUEMIN, E. 1999. Progressive familial intrahepatic cholestasis. *J Gastroenterol Hepatol,* 14**,** 594-9.

JACQUEMIN, E., CRESTEIL, D., MANOUVRIER, S., BOUTE, O. & HADCHOUEL, M. 1999. Heterozygous non-sense mutation of the MDR3 gene in familial intrahepatic cholestasis of pregnancy. *Lancet,* 353**,** 210-1.

JACQUEMIN, E., DE VREE, J. M., CRESTEIL, D., SOKAL, E. M., STURM, E., DUMONT, M., SCHEFFER, G. L., PAUL, M., BURDELSKI, M., BOSMA, P. J., BERNARD, O., HADCHOUEL, M. & ELFERINK, R. P. 2001. The wide spectrum of multidrug resistance 3 deficiency: from neonatal cholestasis to cirrhosis of adulthood. *Gastroenterology,* 120**,** 1448-58.

JANSEN, P. L., STRAUTNIEKS, S. S., JACQUEMIN, E., HADCHOUEL, M., SOKAL, E. M., HOOIVELD, G. J., KONING, J. H., DE JAGER-KRIKKEN, A., KUIPERS, F., STELLAARD, F., BIJLEVELD, C. M., GOUW, A., VAN GOOR, H., THOMPSON, R. J. & MULLER, M. 1999. Hepatocanalicular bile salt export pump deficiency in patients with progressive familial intrahepatic cholestasis. *Gastroenterology,* 117**,** 1370-9.

JODOIN, J., DEMEULE, M., FENART, L., CECCHELLI, R., FARMER, S., LINTON, K. J., HIGGINS, C. F. & BELIVEAU, R. 2003. P-glycoprotein in blood-brain barrier endothelial cells: interaction and oligomerization with caveolins. *J Neurochem,* 87**,** 1010-23.

JOHNSSON, N. & VARSHAVSKY, A. 1994. Split ubiquitin as a sensor of protein interactions in vivo. *Proc Natl Acad Sci U S A,* 91**,** 10340-4.

JONES, P. M. & GEORGE, A. M. 2002. Mechanism of ABC transporters: a molecular dynamics simulation of a well characterized nucleotide-binding subunit. *Proc Natl Acad Sci U S A,* 99**,** 12639-44.

JONES, P. M., O'MARA, M. L. & GEORGE, A. M. 2009. ABC transporters: a riddle wrapped in a mystery inside an enigma. *Trends Biochem Sci,* 34**,** 520-31.

JULIANO, R. L. & LING, V. 1976. A surface glycoprotein modulating drug permeability in Chinese hamster ovary cell mutants. *Biochim Biophys Acta,* 455**,** 152-62.

KAGAWA, T., WATANABE, N., MOCHIZUKI, K., NUMARI, A., IKENO, Y., ITOH, J., TANAKA, H., ARIAS, I. M. & MINE, T. 2008. Phenotypic differences in PFIC2 and BRIC2 correlate with protein stability of mutant Bsep and impaired taurocholate secretion in MDCK II cells. *Am J Physiol Gastrointest Liver Physiol,* 294**,** G58-67.

KAPLOWITZ, N. 1992. *Liver and biliary diseases*, Williams & Wilkins.

KARPOWICH, N., MARTSINKEVICH, O., MILLEN, L., YUAN, Y. R., DAI, P. L., MACVEY, K., THOMAS, P. J. & HUNT, J. F. 2001. Crystal structures of the MJ1267 ATP binding cassette reveal an induced-fit effect at the ATPase active site of an ABC transporter. *Structure,* 9**,** 571-86.

KARTNER, N., RIORDAN, J. R. & LING, V. 1983. Cell surface P-glycoprotein associated with multidrug resistance in mammalian cell lines. *Science,* 221**,** 1285-8.

KATZ, N. R. 1992. Metabolic heterogeneity of hepatocytes across the liver acinus. *J Nutr,* 122**,** 843-9.

KAWAI, S., HASHIMOTO, W. & MURATA, K. 2010. Transformation of Saccharomyces cerevisiae and other fungi: methods and possible underlying mechanism. *Bioeng Bugs,* 1**,** 395-403.

KEITEL, V., BURDELSKI, M., WARSKULAT, U., KUHLKAMP, T., KEPPLER, D., HAUSSINGER, D. & KUBITZ, R. 2005. Expression and localization of hepatobiliary transport proteins in progressive familial intrahepatic cholestasis. *Hepatology,* 41**,** 1160-72.

KEITEL, V., VOGT, C., HAUSSINGER, D. & KUBITZ, R. 2006. Combined mutations of canalicular transporter proteins cause severe intrahepatic cholestasis of pregnancy. *Gastroenterology,* 131**,** 624-9.

KENNEDY, E. P. & WEISS, S. B. 1956. The function of cytidine coenzymes in the biosynthesis of phospholipides. *J Biol Chem,* 222**,** 193-214.

KENT, C. 1995. Eukaryotic phospholipid biosynthesis. *Annu Rev Biochem,* 64**,** 315-43.

KEREM, B., ROMMENS, J. M., BUCHANAN, J. A., MARKIEWICZ, D., COX, T. K., CHAKRAVARTI, A., BUCHWALD, M. & TSUI, L. C. 1989. Identification of the cystic fibrosis gene: genetic analysis. *Science,* 245**,** 1073-80.

KERR, I. D. 2002. Structure and association of ATP-binding cassette transporter nucleotide-binding domains. *Biochim Biophys Acta,* 1561**,** 47-64.

KIPP, H. & ARIAS, I. M. 2000. Newly synthesized canalicular ABC transporters are directly targeted from the Golgi to the hepatocyte apical domain in rat liver. *J Biol Chem,* 275**,** 15917-25.

KLOMP, L. W., VARGAS, J. C., VAN MIL, S. W., PAWLIKOWSKA, L., STRAUTNIEKS, S. S., VAN EIJK, M. J., JUIJN, J. A., PABON-PENA, C., SMITH, L. B., DEYOUNG, J. A., BYRNE, J. A., GOMBERT, J., VAN DER BRUGGE, G., BERGER, R., JANKOWSKA, I., PAWLOWSKA, J., VILLA, E., KNISELY, A. S., THOMPSON, R. J., FREIMER, N. B., HOUWEN, R. H. & BULL, L. N. 2004. Characterization of mutations in ATP8B1 associated with hereditary cholestasis. *Hepatology,* 40**,** 27-38.

KNISELY, A. S. & GISSEN, P. 2010. Trafficking and transporter disorders in pediatric cholestasis. *Clin Liver Dis,* 14**,** 619-33.

KNISELY, A. S., STRAUTNIEKS, S. S., MEIER, Y., STIEGER, B., BYRNE, J. A., PORTMANN, B. C., BULL, L. N., PAWLIKOWSKA, L., BILEZIKCI, B., OZCAY, F., LASZLO, A., TISZLAVICZ, L., MOORE, L., RAFTOS, J., ARNELL, H., FISCHLER, B., NEMETH, A., PAPADOGIANNAKIS, N., CIELECKA-KUSZYK, J., JANKOWSKA, I., PAWLOWSKA, J., MELIN-ALDANA, H., EMERICK, K. M., WHITINGTON, P. F., MIELI-VERGANI, G. & THOMPSON, R. J. 2006. Hepatocellular carcinoma in ten children under five years of age with bile salt export pump deficiency. *Hepatology,* 44**,** 478-86.

KORNFELD, R. & KORNFELD, S. 1985. Assembly of asparagine-linked oligosaccharides. *Annu Rev Biochem,* 54**,** 631-64.

KOZAK, L., GOPAL, G., YOON, J. H., SAUNA, Z. E., AMBUDKAR, S. V., THAKURTA, A. G. & DHAR, R. 2002. Elf1p, a member of the ABC class of ATPases, functions as a mRNA export factor in Schizosacchromyces pombe. *J Biol Chem,* 277**,** 33580-9.

KRAMER, W., GIRBIG, F., GUTJAHR, U. & KOWALEWSKI, S. 1995. Radiation-inactivation analysis of the Na+/bile acid co-transport system from rabbit ileum. *Biochem J,* 306 (Pt 1)**,** 241-6.

KRAMER, W., STENGELIN, S., BARINGHAUS, K. H., ENHSEN, A., HEUER, H., BECKER, W., CORSIERO, D., GIRBIG, F., NOLL, R. & WEYLAND, C. 1999. Substrate specificity of the ileal and the hepatic Na(+)/bile acid cotransporters of the rabbit. I. Transport studies with membrane vesicles and cell lines expressing the cloned transporters. *J Lipid Res,* 40**,** 1604-17.

KRUH, G. D. & BELINSKY, M. G. 2003. The MRP family of drug efflux pumps. *Oncogene,* 22**,** 7537-52.

KULLAK-UBLICK, G. A., ISMAIR, M. G., STIEGER, B., LANDMANN, L., HUBER, R., PIZZAGALLI, F., FATTINGER, K., MEIER, P. J. & HAGENBUCH, B. 2001. Organic anion-transporting polypeptide B (OATP-B) and its functional comparison with three other OATPs of human liver. *Gastroenterology,* 120**,** 525-33.

KULLAK-UBLICK, G. A., STIEGER, B., HAGENBUCH, B. & MEIER, P. J. 2000. Hepatic transport of bile salts. *Semin Liver Dis,* 20**,** 273-92.

KULLAK-UBLICK, G. A., STIEGER, B. & MEIER, P. J. 2004. Enterohepatic bile salt transporters in normal physiology and liver disease. *Gastroenterology,* 126**,** 322-42.

KUMAR, A. & SNYDER, M. 2001. Emerging technologies in yeast genomics. *Nat Rev Genet,* 2**,** 302-12.

KURZCHALIA, T. V., DUPREE, P., PARTON, R. G., KELLNER, R., VIRTA, H., LEHNERT, M. & SIMONS, K. 1992. VIP21, a 21-kD membrane protein is an integral component of trans-Golgi-network-derived transport vesicles. *J Cell Biol,* 118**,** 1003-14.

LAEMMLI, U. K. 1970. Cleavage of structural proteins during the assembly of the head of bacteriophage T4. *Nature,* 227**,** 680-5.

LAM, C. W., CHEUNG, K. M., TSUI, M. S., YAN, M. S., LEE, C. Y. & TONG, S. F. 2006. A patient with novel ABCB11 gene mutations with phenotypic transition between BRIC2 and PFIC2. *J Hepatol,* 44**,** 240-2.

LAM, P., WANG, R. & LING, V. 2005. Bile acid transport in sister of P-glycoprotein (ABCB11) knockout mice. *Biochemistry,* 44**,** 12598-605.

LAMMERT, F., MARSCHALL, H. U., GLANTZ, A. & MATERN, S. 2000. Intrahepatic cholestasis of pregnancy: molecular pathogenesis, diagnosis and management. *J Hepatol,* 33**,** 1012-21.

LANG, C., MEIER, Y., STIEGER, B., BEUERS, U., LANG, T., KERB, R., KULLAK-UBLICK, G. A., MEIER, P. J. & PAULI-MAGNUS, C. 2007. Mutations and polymorphisms in the bile salt export pump and the multidrug resistance protein 3 associated with drug-induced liver injury. *Pharmacogenet Genomics,* 17**,** 47-60.

LANG, T., HABERL, M., JUNG, D., DRESCHER, A., SCHLAGENHAUFER, R., KEIL, A., MORNHINWEG, E., STIEGER, B., KULLAK-UBLICK, G. A. & KERB, R. 2006. Genetic variability, haplotype structures, and ethnic diversity of hepatic transporters MDR3 (ABCB4) and bile salt export pump (ABCB11). *Drug Metab Dispos,* 34**,** 1582-99.

LANKAT-BUTTGEREIT, B. & TAMPE, R. 2002. The transporter associated with antigen processing: function and implications in human diseases. *Physiol Rev,* 82**,** 187-204.

LAVIE, Y., FIUCCI, G. & LISCOVITCH, M. 1998. Up-regulation of caveolae and caveolar constituents in multidrug-resistant cancer cells. *J Biol Chem,* 273**,** 32380-3.

LE MAIRE, M., CHAMPEIL, P. & MOLLER, J. V. 2000. Interaction of membrane proteins and lipids with solubilizing detergents. *Biochim Biophys Acta,* 1508**,** 86-111.

LEITH, C. P., KOPECKY, K. J., CHEN, I. M., EIJDEMS, L., SLOVAK, M. L., MCCONNELL, T. S., HEAD, D. R., WEICK, J., GREVER, M. R., APPELBAUM, F. R. & WILLMAN, C. L. 1999. Frequency and clinical significance of the expression of the multidrug resistance proteins MDR1/P-glycoprotein, MRP1, and LRP in acute myeloid leukemia: a Southwest Oncology Group Study. *Blood,* 94**,** 1086-99.

LEV, S., BEN HALEVY, D., PERETTI, D. & DAHAN, N. 2008. The VAP protein family: from cellular functions to motor neuron disease. *Trends Cell Biol,* 18**,** 282-90.

LEVY, D. E. & DARNELL, J. E., JR. 2002. Stats: transcriptional control and biological impact. *Nat Rev Mol Cell Biol,* 3**,** 651-62.

LI, C., RAMJEESINGH, M., REYES, E., JENSEN, T., CHANG, X., ROMMENS, J. M. & BEAR, C. E. 1993. The cystic fibrosis mutation (delta F508) does not influence the chloride channel activity of CFTR. *Nat Genet,* 3**,** 311-6.

LI, T., CHANG, C. Y., JIN, D. Y., LIN, P. J., KHVOROVA, A. & STAFFORD, D. W. 2004. Identification of the gene for vitamin K epoxide reductase. *Nature,* 427**,** 541-4.

LI, Z. S., SZCZYPKA, M., LU, Y. P., THIELE, D. J. & REA, P. A. 1996. The yeast cadmium factor protein (YCF1) is a vacuolar glutathione S-conjugate pump. *J Biol Chem,* 271**,** 6509-17.

LIEDTKE, C. M., YUN, C. H., KYLE, N. & WANG, D. 2002. Protein kinase C epsilon-dependent regulation of cystic fibrosis transmembrane regulator involves binding to a receptor for activated C kinase (RACK1) and RACK1 binding to Na+/H+ exchange regulatory factor. *J Biol Chem,* 277**,** 22925-33.

LINCKE, C. R., SMIT, J. J., VAN DER VELDE-KOERTS, T. & BORST, P. 1991. Structure of the human MDR3 gene and physical mapping of the human MDR locus. *J Biol Chem,* 266**,** 5303-10.

LINTON, K. J. & HOLLAND, I. B. 2011. *The ABC Transporters of Human Physiology and Disease: Genetics and Biochemistry of Atp Binding Cassette Transporters*, World Scientific Publishing Company Incorporated.

LOCHER, K. P., LEE, A. T. & REES, D. C. 2002. The E. coli BtuCD structure: a framework for ABC transporter architecture and mechanism. *Science,* 296**,** 1091-8.

LOO, T. W. & CLARKE, D. M. 1994. Prolonged association of temperature-sensitive mutants of human P-glycoprotein with calnexin during biogenesis. *J Biol Chem,* 269**,** 28683-9.

LOO, T. W. & CLARKE, D. M. 1995a. Membrane topology of a cysteine-less mutant of human P-glycoprotein. *J Biol Chem,* 270**,** 843-8.

LOO, T. W. & CLARKE, D. M. 1995b. P-glycoprotein. Associations between domains and between domains and molecular chaperones. *J Biol Chem,* 270**,** 21839-44.

LOO, T. W. & CLARKE, D. M. 1997. Correction of defective protein kinesis of human P-glycoprotein mutants by substrates and modulators. *J Biol Chem,* 272**,** 709-12.

LOWRY, O. H., ROSEBROUGH, N. J., FARR, A. L. & RANDALL, R. J. 1951. Protein measurement with the Folin phenol reagent. *J Biol Chem,* 193**,** 265-75.

LU, T. T., MAKISHIMA, M., REPA, J. J., SCHOONJANS, K., KERR, T. A., AUWERX, J. & MANGELSDORF, D. J. 2000. Molecular basis for feedback regulation of bile acid synthesis by nuclear receptors. *Mol Cell,* 6**,** 507-15.

LUCENA, J. F., HERRERO, J. I., QUIROGA, J., SANGRO, B., GARCIA-FONCILLAS, J., ZABALEGUI, N., SOLA, J., HERRAIZ, M., MEDINA, J. F. & PRIETO, J. 2003. A multidrug resistance 3 gene mutation causing cholelithiasis, cholestasis of pregnancy, and adulthood biliary cirrhosis. *Gastroenterology,* 124**,** 1037-42.

LYKAVIERIS, P., VAN MIL, S., CRESTEIL, D., FABRE, M., HADCHOUEL, M., KLOMP, L., BERNARD, O. & JACQUEMIN, E. 2003. Progressive familial intrahepatic cholestasis type 1 and extrahepatic features: no catch-up of stature growth, exacerbation of diarrhea, and appearance of liver steatosis after liver transplantation. *J Hepatol,* 39**,** 447-52.

MA, L. D., MARQUARDT, D., TAKEMOTO, L. & CENTER, M. S. 1991. Analysis of P-glycoprotein phosphorylation in HL60 cells isolated for resistance to vincristine. *J Biol Chem,* 266**,** 5593-9.

MAKISHIMA, M., OKAMOTO, A. Y., REPA, J. J., TU, H., LEARNED, R. M., LUK, A., HULL, M. V., LUSTIG, K. D., MANGELSDORF, D. J. & SHAN, B. 1999. Identification of a nuclear receptor for bile acids. *Science,* 284**,** 1362-5.

MARTINEZ-FERNANDEZ, P., HIERRO, L., JARA, P. & ALVAREZ, L. 2009. Knockdown of ATP8B1 expression leads to specific downregulation of the bile acid sensor FXR in HepG2 cells: effect of the FXR agonist GW4064. *Am J Physiol Gastrointest Liver Physiol,* 296**,** G1119-29.

MATOBA, N., UNE, M. & HOSHITA, T. 1986. Identification of unconjugated bile acids in human bile. *J Lipid Res,* 27**,** 1154-62.

MEIER, P. J. 1995. Molecular mechanisms of hepatic bile salt transport from sinusoidal blood into bile. *Am J Physiol,* 269**,** G801-12.

MEIER, P. J. & STIEGER, B. 2002. Bile salt transporters. *Annu Rev Physiol,* 64**,** 635-61.

MEIER, Y., PAULI-MAGNUS, C., ZANGER, U. M., KLEIN, K., SCHAEFFELER, E., NUSSLER, A. K., NUSSLER, N., EICHELBAUM, M., MEIER, P. J. & STIEGER, B. 2006. Interindividual variability of canalicular ATP-binding-cassette (ABC)-transporter expression in human liver. *Hepatology,* 44**,** 62-74.

MEIER, Y., ZODAN, T., LANG, C., ZIMMERMANN, R., KULLAK-UBLICK, G. A., MEIER, P. J., STIEGER, B. & PAULI-MAGNUS, C. 2008. Increased susceptibility for intrahepatic cholestasis of pregnancy and contraceptive-induced cholestasis in carriers of the 1331T>C polymorphism in the bile salt export pump. *World J Gastroenterol,* 14**,** 38-45.

MELBY, T. E., CIAMPAGLIO, C. N., BRISCOE, G. & ERICKSON, H. P. 1998. The symmetrical structure of structural maintenance of chromosomes (SMC) and MukB proteins: long, antiparallel coiled coils, folded at a flexible hinge. *J Cell Biol,* 142**,** 1595-604.

MEUSSER, B., HIRSCH, C., JAROSCH, E. & SOMMER, T. 2005. ERAD: the long road to destruction. *Nat Cell Biol,* 7**,** 766-72.

MILLER, J. P., LO, R. S., BEN-HUR, A., DESMARAIS, C., STAGLJAR, I., NOBLE, W. S. & FIELDS, S. 2005. Large-scale identification of yeast integral membrane protein interactions. *Proc Natl Acad Sci U S A,* 102**,** 12123-8.

MIRSKI, S. E., GERLACH, J. H. & COLE, S. P. 1987. Multidrug resistance in a human small cell lung cancer cell line selected in adriamycin. *Cancer Res,* 47**,** 2594-8.

MITRA, V. & METCALF, J. 2009. Metabolic functions of the liver. *Anaesthesia & Intensive Care Medicine,* 10**,** 334-335.

MIYAKE, K., MICKLEY, L., LITMAN, T., ZHAN, Z., ROBEY, R., CRISTENSEN, B., BRANGI, M., GREENBERGER, L., DEAN, M., FOJO, T. & BATES, S. E. 1999.

Molecular cloning of cDNAs which are highly overexpressed in mitoxantrone-resistant cells: demonstration of homology to ABC transport genes. *Cancer Res,* 59**,** 8-13.

MOCHLY-ROSEN, D., KHANER, H. & LOPEZ, J. 1991. Identification of intracellular receptor proteins for activated protein kinase C. *Proc Natl Acad Sci U S A,* 88**,** 3997-4000.

MOLDOVAN, N. I., HELTIANU, C., SIMIONESCU, N. & SIMIONESCU, M. 1995. Ultrastructural evidence of differential solubility in Triton X-100 of endothelial vesicles and plasma membrane. *Exp Cell Res,* 219**,** 309-13.

MOLINARI, A., CALCABRINI, A., MESCHINI, S., STRINGARO, A., DEL BUFALO, D., CIANFRIGLIA, M. & ARANCIA, G. 1998. Detection of P-glycoprotein in the Golgi apparatus of drug-untreated human melanoma cells. *Int J Cancer,* 75**,** 885-93.

MOLINARI, A., CIANFRIGLIA, M., MESCHINI, S., CALCABRINI, A. & ARANCIA, G. 1994. P-glycoprotein expression in the Golgi apparatus of multidrug-resistant cells. *Int J Cancer,* 59**,** 789-95.

MONIER, S., PARTON, R. G., VOGEL, F., BEHLKE, J., HENSKE, A. & KURZCHALIA, T. V. 1995. VIP21-caveolin, a membrane protein constituent of the caveolar coat, oligomerizes in vivo and in vitro. *Mol Biol Cell,* 6**,** 911-27.

MONTRUCCHIO, G., SAPINO, A., BUSSOLATI, B., GHISOLFI, G., RIZEA-SAVU, S., SILVESTRO, L., LUPIA, E. & CAMUSSI, G. 1998. Potential angiogenic role of platelet-activating factor in human breast cancer. *Am J Pathol,* 153**,** 1589-96.

MORELLO, J. P., PETAJA-REPO, U. E., BICHET, D. G. & BOUVIER, M. 2000. Pharmacological chaperones: a new twist on receptor folding. *Trends Pharmacol Sci,* 21**,** 466-9.

MORITA, S. Y., KOBAYASHI, A., TAKANEZAWA, Y., KIOKA, N., HANDA, T., ARAI, H., MATSUO, M. & UEDA, K. 2007. Bile salt-dependent efflux of cellular phospholipids mediated by ATP binding cassette protein B4. *Hepatology,* 46**,** 188-99.

MOROTTI, R. A., SUCHY, F. J. & MAGID, M. S. 2011. Progressive familial intrahepatic cholestasis (PFIC) type 1, 2, and 3: a review of the liver pathology findings. *Semin Liver Dis,* 31**,** 3-10.

MULLENBACH, R., BENNETT, A., TETLOW, N., PATEL, N., HAMILTON, G., CHENG, F., CHAMBERS, J., HOWARD, R., TAYLOR-ROBINSON, S. D. & WILLIAMSON, C. 2005. ATP8B1 mutations in British cases with intrahepatic cholestasis of pregnancy. *Gut,* 54**,** 829-34.

MULLENBACH, R., LINTON, K. J., WILTSHIRE, S., WEERASEKERA, N., CHAMBERS, J., ELIAS, E., HIGGINS, C. F., JOHNSTON, D. G., MCCARTHY, M. I. & WILLIAMSON, C. 2003. ABCB4 gene sequence variation in women with intrahepatic cholestasis of pregnancy. *J Med Genet,* 40**,** e70.

MULLER, M., ISHIKAWA, T., BERGER, U., KLUNEMANN, C., LUCKA, L., SCHREYER, A., KANNICHT, C., REUTTER, W., KURZ, G. & KEPPLER, D. 1991. ATP-dependent transport of taurocholate across the hepatocyte canalicular membrane mediated by a 110-kDa glycoprotein binding ATP and bile salt. *J Biol Chem,* 266**,** 18920-6.

MURATA, M., PERANEN, J., SCHREINER, R., WIELAND, F., KURZCHALIA, T. V. & SIMONS, K. 1995. VIP21/caveolin is a cholesterol-binding protein. *Proc Natl Acad Sci U S A,* 92**,** 10339-43.

MUSRATI, R. A., KOLLAROVA, M., MERNIK, N. & MIKULASOVA, D. 1998. Malate dehydrogenase: distribution, function and properties. *Gen Physiol Biophys,* 17**,** 193-210.

NAKAGAWA, H., WAKABAYASHI-NAKAO, K., TAMURA, A., TOYODA, Y., KOSHIBA, S. & ISHIKAWA, T. 2009. Disruption of N-linked glycosylation enhances ubiquitin-mediated proteasomal degradation of the human ATP-binding cassette transporter ABCG2. *FEBS J,* 276**,** 7237-52.

NAKKEN, K. E., LABORI, K. J., RODNINGEN, O. K., NAKKEN, S., BERGE, K. E., EIKLID, K. & RAEDER, M. G. 2009. ABCB4 sequence variations in young adults with cholesterol gallstone disease. *Liver Int,* 29**,** 743-7.

NG, T., SHIMA, D., SQUIRE, A., BASTIAENS, P. I., GSCHMEISSNER, S., HUMPHRIES, M. J. & PARKER, P. J. 1999. PKCalpha regulates beta1 integrin-dependent cell motility through association and control of integrin traffic. *EMBO J,* 18**,** 3909-23.

NICHOLS, C. G. 2006. KATP channels as molecular sensors of cellular metabolism. *Nature,* 440**,** 470-6.

NICOLAOU, M., ANDRESS, E. J., ZOLNERCIKS, J. K., DIXON, P. H., WILLIAMSON, C. & LINTON, K. J. 2012. Canalicular ABC transporters and liver disease. *J Pathol,* 226**,** 300-15.

NISHIDA, T., GATMAITAN, Z., CHE, M. & ARIAS, I. M. 1991. Rat liver canalicular membrane vesicles contain an ATP-dependent bile acid transport system. *Proc Natl Acad Sci U S A,* 88**,** 6590-4.

NISHIMURA, Y., HAYASHI, M., INADA, H. & TANAKA, T. 1999. Molecular cloning and characterization of mammalian homologues of vesicle-associated membrane protein-associated (VAMP-associated) proteins. *Biochem Biophys Res Commun,* 254**,** 21-6.

NISHIZUKA, Y. 1995. Protein kinase C and lipid signaling for sustained cellular responses. *FASEB J,* 9**,** 484-96.

NOE, J., KULLAK-UBLICK, G. A., JOCHUM, W., STIEGER, B., KERB, R., HABERL, M., MULLHAUPT, B., MEIER, P. J. & PAULI-MAGNUS, C. 2005. Impaired expression and function of the bile salt export pump due to three novel ABCB11 mutations in intrahepatic cholestasis. *J Hepatol,* 43**,** 536-43.

NOE, J., STIEGER, B. & MEIER, P. J. 2002. Functional expression of the canalicular bile salt export pump of human liver. *Gastroenterology,* 123**,** 1659-66.

OBMOLOVA, G., BAN, C., HSIEH, P. & YANG, W. 2000. Crystal structures of mismatch repair protein MutS and its complex with a substrate DNA. *Nature,* 407**,** 703-10.

ORNSTEIN, L. 1964. Disc Electrophoresis. I. Background and Theory. *Ann N Y Acad Sci,* 121**,** 321-49.

ORR, G. A., HAN, E. K., BROWNE, P. C., NIEVES, E., O'CONNOR, B. M., YANG, C. P. & HORWITZ, S. B. 1993. Identification of the major phosphorylation domain of murine mdr1b P-glycoprotein. Analysis of the protein kinase A and protein kinase C phosphorylation sites. *J Biol Chem,* 268**,** 25054-62.

ORTIZ, D. F., MOSELEY, J., CALDERON, G., SWIFT, A. L., LI, S. & ARIAS, I. M. 2004. Identification of HAX-1 as a protein that binds bile salt export protein and regulates its abundance in the apical membrane of Madin-Darby canine kidney cells. *J Biol Chem,* 279**,** 32761-70.

OUDE ELFERINK, R. P. & GROEN, A. K. 2002. Genetic defects in hepatobiliary transport. *Biochim Biophys Acta,* 1586**,** 129-45.

OUDE ELFERINK, R. P. & PAULUSMA, C. C. 2007. Function and pathophysiological importance of ABCB4 (MDR3 P-glycoprotein). *Pflugers Arch,* 453**,** 601-10.

PADHAN, K., TANWAR, C., HUSSAIN, A., HUI, P. Y., LEE, M. Y., CHEUNG, C. Y., PEIRIS, J. S. & JAMEEL, S. 2007. Severe acute respiratory syndrome coronavirus Orf3a protein interacts with caveolin. *J Gen Virol,* 88**,** 3067-77.

PAINTER, J. N., SAVANDER, M., ROPPONEN, A., NUPPONEN, N., RIIKONEN, S., YLIKORKALA, O., LEHESJOKI, A. E. & AITTOMAKI, K. 2005. Sequence variation in the ATP8B1 gene and intrahepatic cholestasis of pregnancy. *Eur J Hum Genet,* 13**,** 435-9.

PANG, A., AU, W. Y. & KWONG, Y. L. 2004. Caveolin-1 gene is coordinately regulated with the multidrug resistance 1 gene in normal and leukemic bone marrow. *Leuk Res,* 28**,** 973-7.

PARISSENTI, A. M. & RIEDEL, H. 2003. Yeast as a host to screen for modulators and regulatory regions of mammalian protein kinase C isoforms. *Methods Mol Biol,* 233**,** 491-516.

PAULI-MAGNUS, C., KERB, R., FATTINGER, K., LANG, T., ANWALD, B., KULLAK-UBLICK, G. A., BEUERS, U. & MEIER, P. J. 2004a. BSEP and MDR3 haplotype structure in healthy Caucasians, primary biliary cirrhosis and primary sclerosing cholangitis. *Hepatology,* 39**,** 779-91.

PAULI-MAGNUS, C., LANG, T., MEIER, Y., ZODAN-MARIN, T., JUNG, D., BREYMANN, C., ZIMMERMANN, R., KENNGOTT, S., BEUERS, U., REICHEL, C., KERB, R., PENGER, A., MEIER, P. J. & KULLAK-UBLICK, G. A. 2004b. Sequence analysis of bile salt export pump (ABCB11) and multidrug resistance p-glycoprotein 3 (ABCB4, MDR3) in patients with intrahepatic cholestasis of pregnancy. *Pharmacogenetics,* 14**,** 91-102.

PAULI-MAGNUS, C., STIEGER, B., MEIER, Y., KULLAK-UBLICK, G. A. & MEIER, P. J. 2005. Enterohepatic transport of bile salts and genetics of cholestasis. *J Hepatol,* 43**,** 342-57.

PAULUSMA, C. C., FOLMER, D. E., HO-MOK, K. S., DE WAART, D. R., HILARIUS, P. M., VERHOEVEN, A. J. & OUDE ELFERINK, R. P. 2008. ATP8B1 requires an accessory protein for endoplasmic reticulum exit and plasma membrane lipid flippase activity. *Hepatology,* 47**,** 268-78.

PAULUSMA, C. C., GROEN, A., KUNNE, C., HO-MOK, K. S., SPIJKERBOER, A. L., RUDI DE WAART, D., HOEK, F. J., VREELING, H., HOEBEN, K. A., VAN MARLE, J., PAWLIKOWSKA, L., BULL, L. N., HOFMANN, A. F., KNISELY, A. S. & OUDE ELFERINK, R. P. 2006. Atp8b1 deficiency in mice reduces resistance of the canalicular membrane to hydrophobic bile salts and impairs bile salt transport. *Hepatology,* 44**,** 195-204.

PAULUSMA, C. C., KOOL, M., BOSMA, P. J., SCHEFFER, G. L., TER BORG, F., SCHEPER, R. J., TYTGAT, G. N., BORST, P., BAAS, F. & OUDE ELFERINK, R. P. 1997. A mutation in the human canalicular multispecific organic anion transporter gene causes the Dubin-Johnson syndrome. *Hepatology,* 25**,** 1539-42.

PAUMI, C. M., MENENDEZ, J., ARNOLDO, A., ENGELS, K., IYER, K. R., THAMINY, S., GEORGIEV, O., BARRAL, Y., MICHAELIS, S. & STAGLJAR, I. 2007. Mapping protein-protein interactions for the yeast ABC transporter Ycf1p by integrated split-ubiquitin membrane yeast two-hybrid analysis. *Mol Cell,* 26**,** 15-25.

PEET, D. J., JANOWSKI, B. A. & MANGELSDORF, D. J. 1998. The LXRs: a new class of oxysterol receptors. *Curr Opin Genet Dev,* 8**,** 571-5.

PELECH, S. L., PRITCHARD, P. H., BRINDLEY, D. N. & VANCE, D. E. 1983. Fatty acids promote translocation of CTP:phosphocholine cytidylyltransferase to the endoplasmic reticulum and stimulate rat hepatic phosphatidylcholine synthesis. *J Biol Chem,* 258**,** 6782-8.

PETRIZ, J., GOTTESMAN, M. M. & ARAN, J. M. 2004. An MDR-EGFP gene fusion allows for direct cellular localization, function and stability assessment of P-glycoprotein. *Curr Drug Deliv,* 1**,** 43-56.

PHIZICKY, E. M. & FIELDS, S. 1995. Protein-protein interactions: methods for detection and analysis. *Microbiol Rev,* 59**,** 94-123.

PLASS, J. R., MOL, O., HEEGSMA, J., GEUKEN, M., DE BRUIN, J., ELLING, G., MULLER, M., FABER, K. N. & JANSEN, P. L. 2004. A progressive familial intrahepatic cholestasis type 2 mutation causes an unstable, temperature-sensitive bile salt export pump. *J Hepatol,* 40**,** 24-30.

PLATTE, H. D., HONSCHA, W., SCHUH, K. & PETZINGER, E. 1996. Functional characterization of the hepatic sodium-dependent taurocholate transporter stably transfected into an immortalized liver-derived cell line and V79 fibroblasts. *Eur J Cell Biol,* 70**,** 54-60.

POUPON, R., BARBU, V., CHAMOUARD, P., WENDUM, D., ROSMORDUC, O. & HOUSSET, C. 2010. Combined features of low phospholipid-associated cholelithiasis and progressive familial intrahepatic cholestasis 3. *Liver Int,* 30**,** 327-31.

PRESCOTT, S. M., ZIMMERMAN, G. A., STAFFORINI, D. M. & MCINTYRE, T. M. 2000. Platelet-activating factor and related lipid mediators. *Annu Rev Biochem,* 69**,** 419-45.

PREVOSTEL, C., ALICE, V., JOUBERT, D. & PARKER, P. J. 2000. Protein kinase C(alpha) actively downregulates through caveolae-dependent traffic to an endosomal compartment. *J Cell Sci,* 113 (Pt 14)**,** 2575-84.

PUSL, T. & BEUERS, U. 2007. Intrahepatic cholestasis of pregnancy. *Orphanet J Rare Dis,* 2**,** 26.

RAGGERS, R. J., VOGELS, I. & VAN MEER, G. 2001. Multidrug-resistance P-glycoprotein (MDR1) secretes platelet-activating factor. *Biochem J,* 357**,** 859-65.

RAPPAPORT, A. M., BOROWY, Z. J., LOUGHEED, W. M. & LOTTO, W. N. 1954. Subdivision of hexagonal liver lobules into a structural and functional unit; role in hepatic physiology and pathology. *Anat Rec,* 119**,** 11-33.

RAYMOND, M., RUETZ, S., THOMAS, D. Y. & GROS, P. 1994. Functional expression of P-glycoprotein in Saccharomyces cerevisiae confers cellular resistance to the immunosuppressive and antifungal agent FK520. *Mol Cell Biol,* 14**,** 277-86.

RAZANI, B., RUBIN, C. S. & LISANTI, M. P. 1999. Regulation of cAMP-mediated signal transduction via interaction of caveolins with the catalytic subunit of protein kinase A. *J Biol Chem,* 274**,** 26353-60.

RAZANI, B., WOODMAN, S. E. & LISANTI, M. P. 2002. Caveolae: from cell biology to animal physiology. *Pharmacol Rev,* 54**,** 431-67.

REDDY, J. K. & MANNAERTS, G. P. 1994. Peroxisomal lipid metabolism. *Annu Rev Nutr,* 14**,** 343-70.

REES, D. C., JOHNSON, E. & LEWINSON, O. 2009. ABC transporters: the power to change. *Nat Rev Mol Cell Biol,* 10**,** 218-27.

REYES, H. & SIMON, F. R. 1993. Intrahepatic cholestasis of pregnancy: an estrogen-related disease. *Semin Liver Dis,* 13**,** 289-301.

RICHERT, N. D., ALDWIN, L., NITECKI, D., GOTTESMAN, M. M. & PASTAN, I. 1988. Stability and covalent modification of P-glycoprotein in multidrug-resistant KB cells. *Biochemistry,* 27**,** 7607-13.

RIETVELD, A. & SIMONS, K. 1998. The differential miscibility of lipids as the basis for the formation of functional membrane rafts. *Biochim Biophys Acta,* 1376**,** 467-79.

RIORDAN, J. R. & LING, V. 1979. Purification of P-glycoprotein from plasma membrane vesicles of Chinese hamster ovary cell mutants with reduced colchicine permeability. *J Biol Chem,* 254**,** 12701-5.

RIORDAN, J. R., ROMMENS, J. M., KEREM, B., ALON, N., ROZMAHEL, R., GRZELCZAK, Z., ZIELENSKI, J., LOK, S., PLAVSIC, N., CHOU, J. L. & ET AL. 1989. Identification of the cystic fibrosis gene: cloning and characterization of complementary DNA. *Science,* 245**,** 1066-73.

ROMAN, H. 1956. Studies of gene mutation in Saccharomyces. *Cold Spring Harb Symp Quant Biol,* 21**,** 175-85.

ROMSICKI, Y. & SHAROM, F. J. 2001. Phospholipid flippase activity of the reconstituted P-glycoprotein multidrug transporter. *Biochemistry,* 40**,** 6937-47.

ROSMORDUC, O., HERMELIN, B., BOELLE, P. Y., PARC, R., TABOURY, J. & POUPON, R. 2003. ABCB4 gene mutation-associated cholelithiasis in adults. *Gastroenterology,* 125**,** 452-9.

ROSMORDUC, O., HERMELIN, B. & POUPON, R. 2001. MDR3 gene defect in adults with symptomatic intrahepatic and gallbladder cholesterol cholelithiasis. *Gastroenterology,* 120**,** 1459-67.

ROSMORDUC, O. & POUPON, R. 2007. Low phospholipid associated cholelithiasis: association with mutation in the MDR3/ABCB4 gene. *Orphanet J Rare Dis,* 2**,** 29.

ROST, S., FREGIN, A., IVASKEVICIUS, V., CONZELMANN, E., HORTNAGEL, K., PELZ, H. J., LAPPEGARD, K., SEIFRIED, E., SCHARRER, I., TUDDENHAM, E. G., MULLER, C. R., STROM, T. M. & OLDENBURG, J. 2004. Mutations in VKORC1 cause warfarin resistance and multiple coagulation factor deficiency type 2. *Nature,* 427**,** 537-41.

ROTHBERG, K. G., HEUSER, J. E., DONZELL, W. C., YING, Y. S., GLENNEY, J. R. & ANDERSON, R. G. 1992. Caveolin, a protein component of caveolae membrane coats. *Cell,* 68**,** 673-82.

RUBENSTEIN, R. C., EGAN, M. E. & ZEITLIN, P. L. 1997. In vitro pharmacologic restoration of CFTR-mediated chloride transport with sodium 4-phenylbutyrate in cystic fibrosis epithelial cells containing delta F508-CFTR. *J Clin Invest,* 100**,** 2457-65.

RUMSBY, M. G., DREW, L. & WARR, J. R. 1998. Protein kinases and multidrug resistance. *Cytotechnology,* 27**,** 203-24.

RUSSELL, D. W. 2003. The enzymes, regulation, and genetics of bile acid synthesis. *Annu Rev Biochem,* 72**,** 137-74.

RUSSELL, D. W. & SETCHELL, K. D. 1992. Bile acid biosynthesis. *Biochemistry,* 31**,** 4737-49.

SAEKI, T., UEDA, K., TANIGAWARA, Y., HORI, R. & KOMANO, T. 1993. Human P-glycoprotein transports cyclosporin A and FK506. *J Biol Chem,* 268**,** 6077-80.

SARDINI, A., MINTENIG, G. M., VALVERDE, M. A., SEPULVEDA, F. V., GILL, D. R., HYDE, S. C., HIGGINS, C. F. & MCNAUGHTON, P. A. 1994. Drug efflux mediated by the human multidrug resistance P-glycoprotein is inhibited by cell swelling. *J Cell Sci,* 107 (Pt 12)**,** 3281-90.

SAUNA, Z. E., MULLER, M., PENG, X. H. & AMBUDKAR, S. V. 2002. Importance of the conserved Walker B glutamate residues, 556 and 1201, for the completion of the catalytic cycle of ATP hydrolysis by human P-glycoprotein (ABCB1). *Biochemistry,* 41**,** 13989-4000.

SCHEFFER, G. L., KOOL, M., HEIJN, M., DE HAAS, M., PIJNENBORG, A. C., WIJNHOLDS, J., VAN HELVOORT, A., DE JONG, M. C., HOOIJBERG, J. H., MOL, C. A., VAN DER LINDEN, M., DE VREE, J. M., VAN DER VALK, P., ELFERINK, R. P., BORST, P. & SCHEPER, R. J. 2000. Specific detection of multidrug resistance proteins MRP1, MRP2, MRP3, MRP5, and MDR3 P-glycoprotein with a panel of monoclonal antibodies. *Cancer Res,* 60**,** 5269-77.

SCHEPER, W., THAMINY, S., KAIS, S., STAGLJAR, I. & ROMISCH, K. 2003. Coordination of N-glycosylation and protein translocation across the endoplasmic reticulum membrane by Sss1 protein. *J Biol Chem,* 278**,** 37998-8003.

SCHINKEL, A. H. 1999. P-Glycoprotein, a gatekeeper in the blood-brain barrier. *Adv Drug Deliv Rev,* 36**,** 179-194.

SCHINKEL, A. H., KEMP, S., DOLLE, M., RUDENKO, G. & WAGENAAR, E. 1993. N-glycosylation and deletion mutants of the human MDR1 P-glycoprotein. *J Biol Chem,* 268**,** 7474-81.

SCHINKEL, A. H., MAYER, U., WAGENAAR, E., MOL, C. A., VAN DEEMTER, L., SMIT, J. J., VAN DER VALK, M. A., VOORDOUW, A. C., SPITS, H., VAN TELLINGEN, O., ZIJLMANS, J. M., FIBBE, W. E. & BORST, P. 1997. Normal viability and altered pharmacokinetics in mice lacking mdr1-type (drug-transporting) P-glycoproteins. *Proc Natl Acad Sci U S A,* 94**,** 4028-33.

SCHINKEL, A. H., SMIT, J. J., VAN TELLINGEN, O., BEIJNEN, J. H., WAGENAAR, E., VAN DEEMTER, L., MOL, C. A., VAN DER VALK, M. A., ROBANUS-MAANDAG, E. C., TE RIELE, H. P. & ET AL. 1994. Disruption of the mouse mdr1a P-glycoprotein gene leads to a deficiency in the blood-brain barrier and to increased sensitivity to drugs. *Cell,* 77**,** 491-502.

SCHMELZLE, T., HELLIWELL, S. B. & HALL, M. N. 2002. Yeast protein kinases and the RHO1 exchange factor TUS1 are novel components of the cell integrity pathway in yeast. *Mol Cell Biol,* 22**,** 1329-39.

SCHMIDT, E. V., CHRISTOPH, G., ZELLER, R. & LEDER, P. 1990. The cytomegalovirus enhancer: a pan-active control element in transgenic mice. *Mol Cell Biol,* 10**,** 4406-11.

SCHMITT, L., BENABDELHAK, H., BLIGHT, M. A., HOLLAND, I. B. & STUBBS, M. T. 2003. Crystal structure of the nucleotide-binding domain of the ABC-transporter haemolysin B: identification of a variable region within ABC helical domains. *J Mol Biol,* 330**,** 333-42.

SCHROEDER, A., ECKHARDT, U., STIEGER, B., TYNES, R., SCHTEINGART, C. D., HOFMANN, A. F., MEIER, P. J. & HAGENBUCH, B. 1998. Substrate specificity of the rat liver Na(+)-bile salt cotransporter in Xenopus laevis oocytes and in CHO cells. *Am J Physiol,* 274**,** G370-5.

SEWARD, D. J., KOH, A. S., BOYER, J. L. & BALLATORI, N. 2003. Functional complementation between a novel mammalian polygenic transport complex and an evolutionarily ancient organic solute transporter, OSTalpha-OSTbeta. *J Biol Chem,* 278**,** 27473-82.

SHAPIRO, A. B. & LING, V. 1994. ATPase activity of purified and reconstituted P-glycoprotein from Chinese hamster ovary cells. *J Biol Chem,* 269**,** 3745-54.

SHAROM, F. J. 2011. The P-glycoprotein multidrug transporter. *Essays Biochem,* 50**,** 161-78.

SHAROM, F. J., YU, X. & DOIGE, C. A. 1993. Functional reconstitution of drug transport and ATPase activity in proteoliposomes containing partially purified P-glycoprotein. *J Biol Chem,* 268**,** 24197-202.

SHAROM, F. J., YU, X., LU, P., LIU, R., CHU, J. W., SZABO, K., MULLER, M., HOSE, C. D., MONKS, A., VARADI, A., SEPRODI, J. & SARKADI, B. 1999. Interaction of the P-glycoprotein multidrug transporter (MDR1) with high affinity peptide chemosensitizers in isolated membranes, reconstituted systems, and intact cells. *Biochem Pharmacol,* 58**,** 571-86.

SIMONS, K. & IKONEN, E. 1997. Functional rafts in cell membranes. *Nature,* 387**,** 569-72.

SIMONS, K. & TOOMRE, D. 2000. Lipid rafts and signal transduction. *Nat Rev Mol Cell Biol,* 1**,** 31-9.

SINGER, S. J., MAHER, P. A. & YAFFE, M. P. 1987. On the transfer of integral proteins into membranes. *Proc Natl Acad Sci U S A,* 84**,** 1960-4.

SINGER, S. J. & NICOLSON, G. L. 1972. The fluid mosaic model of the structure of cell membranes. *Science,* 175**,** 720-31.

SKOVSGAARD, T. 1978. Mechanisms of resistance to daunorubicin in Ehrlich ascites tumor cells. *Cancer Res,* 38**,** 1785-91.

SMIT, J. J., SCHINKEL, A. H., OUDE ELFERINK, R. P., GROEN, A. K., WAGENAAR, E., VAN DEEMTER, L., MOL, C. A., OTTENHOFF, R., VAN DER LUGT, N. M., VAN ROON, M. A. & ET AL. 1993. Homozygous disruption of the murine mdr2 P-glycoprotein gene leads to a complete absence of phospholipid from bile and to liver disease. *Cell,* 75**,** 451-62.

SMITH, A. J., DE VREE, J. M., OTTENHOFF, R., OUDE ELFERINK, R. P., SCHINKEL, A. H. & BORST, P. 1998. Hepatocyte-specific expression of the human MDR3 P-glycoprotein gene restores the biliary phosphatidylcholine excretion absent in Mdr2 (-/-) mice. *Hepatology,* 28**,** 530-6.

SMITH, A. J., TIMMERMANS-HEREIJGERS, J. L., ROELOFSEN, B., WIRTZ, K. W., VAN BLITTERSWIJK, W. J., SMIT, J. J., SCHINKEL, A. H. & BORST, P. 1994. The human MDR3 P-glycoprotein promotes translocation of phosphatidylcholine through the plasma membrane of fibroblasts from transgenic mice. *FEBS Lett,* 354**,** 263-6.

SMITH, A. J., VAN HELVOORT, A., VAN MEER, G., SZABO, K., WELKER, E., SZAKACS, G., VARADI, A., SARKADI, B. & BORST, P. 2000. MDR3 P-glycoprotein, a phosphatidylcholine translocase, transports several cytotoxic drugs and directly interacts with drugs as judged by interference with nucleotide trapping. *J Biol Chem,* 275**,** 23530-9.

SMITH, P. C., KARPOWICH, N., MILLEN, L., MOODY, J. E., ROSEN, J., THOMAS, P. J. & HUNT, J. F. 2002. ATP binding to the motor domain from an ABC transporter drives formation of a nucleotide sandwich dimer. *Mol Cell,* 10**,** 139-49.

SOBOLEWSKI, A., RUDARAKANCHANA, N., UPTON, P. D., YANG, J., CRILLEY, T. K., TREMBATH, R. C. & MORRELL, N. W. 2008. Failure of bone morphogenetic protein receptor trafficking in pulmonary arterial hypertension: potential for rescue. *Hum Mol Genet,* 17**,** 3180-90.

SOROKA, C. J., BALLATORI, N. & BOYER, J. L. 2010. Organic solute transporter, OSTalpha-OSTbeta: its role in bile acid transport and cholestasis. *Semin Liver Dis,* 30**,** 178-85.

SPELLMAN, S. J., SHAFFER, E. A. & ROSENTHALL, L. 1979. Gallbladder emptying in response to cholecystokinin. A cholescintigraphic study. *Gastroenterology,* 77**,** 115-20.

STAGLJAR, I. & FIELDS, S. 2002. Analysis of membrane protein interactions using yeast-based technologies. *Trends Biochem Sci,* 27**,** 559-63.

STAGLJAR, I., KOROSTENSKY, C., JOHNSSON, N. & TE HEESEN, S. 1998. A genetic system based on split-ubiquitin for the analysis of interactions between membrane proteins in vivo. *Proc Natl Acad Sci U S A,* 95**,** 5187-92.

STAPELBROEK, J. M., PETERS, T. A., VAN BEURDEN, D. H., CURFS, J. H., JOOSTEN, A., BEYNON, A. J., VAN LEEUWEN, B. M., VAN DER VELDEN, L. M., BULL, L., OUDE ELFERINK, R. P., VAN ZANTEN, B. A., KLOMP, L. W. & HOUWEN, R. H. 2009. ATP8B1 is essential for maintaining normal hearing. *Proc Natl Acad Sci U S A,* 106**,** 9709-14.

STEINER, J. W. & CARRUTHERS, J. S. 1961. Studies on the Fine Structure of the Terminal Branches of the Biliary Tree: I. The Morphology of Normal Bile Canaliculi, Bile Pre-ductules (Ducts of Hering) and Bile Ductules. *Am J Pathol,* 38**,** 639-61.

STELLAARD, F., KLEIN, P. D., HOFMANN, A. F. & LACHIN, J. M. 1985. Mass spectrometry identification of biliary bile acids in bile from patients with gallstones before and during treatment with chenodeoxycholic acid. An ancillary study of the National Cooperative Gallstone Study. *J Lab Clin Med,* 105**,** 504-13.

STEVENS, A. & LOWE, J. S. 2005. *Human histology*, Elsevier/Mosby.

STIEGER, B., FATTINGER, K., MADON, J., KULLAK-UBLICK, G. A. & MEIER, P. J. 2000. Drug- and estrogen-induced cholestasis through inhibition of the hepatocellular bile salt export pump (Bsep) of rat liver. *Gastroenterology,* 118**,** 422-30.

STIEGER, B., O'NEILL, B. & MEIER, P. J. 1992. ATP-dependent bile-salt transport in canalicular rat liver plasma-membrane vesicles. *Biochem J,* 284 (Pt 1)**,** 67-74.

STOTZ, A., MULLER, P. P. & LINDER, P. 1993. Regulation of the ADE2 gene from Saccharomyces cerevisiae. *Curr Genet,* 24**,** 472-80.

STRAUTNIEKS, S. S., BULL, L. N., KNISELY, A. S., KOCOSHIS, S. A., DAHL, N., ARNELL, H., SOKAL, E., DAHAN, K., CHILDS, S., LING, V., TANNER, M. S., KAGALWALLA, A. F., NEMETH, A., PAWLOWSKA, J., BAKER, A., MIELI-VERGANI, G., FREIMER, N. B., GARDINER, R. M. & THOMPSON, R. J. 1998. A gene encoding a liver-specific ABC transporter is mutated in progressive familial intrahepatic cholestasis. *Nat Genet,* 20**,** 233-8.

STRAUTNIEKS, S. S., BYRNE, J. A., PAWLIKOWSKA, L., CEBECAUEROVA, D., RAYNER, A., DUTTON, L., MEIER, Y., ANTONIOU, A., STIEGER, B., ARNELL, H., OZCAY, F., AL-HUSSAINI, H. F., BASSAS, A. F., VERKADE, H. J., FISCHLER, B., NEMETH, A., KOTALOVA, R., SHNEIDER, B. L., CIELECKA-KUSZYK, J., MCCLEAN, P., WHITINGTON, P. F., SOKAL, E., JIRSA, M., WALI, S. H., JANKOWSKA, I., PAWLOWSKA, J., MIELI-VERGANI, G., KNISELY, A. S., BULL, L. N. & THOMPSON, R. J. 2008. Severe bile salt export pump deficiency: 82 different ABCB11 mutations in 109 families. *Gastroenterology,* 134**,** 1203-14.

STRAZZABOSCO, M. 1997. Transport systems in cholangiocytes: their role in bile formation and cholestasis. *Yale J Biol Med,* 70**,** 427-34.

SUNDLER, R. & AKESSON, B. 1975. Regulation of phospholipid biosynthesis in isolated rat hepatocytes. Effect of different substrates. *J Biol Chem,* 250**,** 3359-67.

SZABO, K., BAKOS, E., WELKER, E., MULLER, M., GOODFELLOW, H. R., HIGGINS, C. F., VARADI, A. & SARKADI, B. 1997. Phosphorylation site mutations in the human multidrug transporter modulate its drug-stimulated ATPase activity. *J Biol Chem,* 272**,** 23165-71.

SZCZYPKA, M. S., WEMMIE, J. A., MOYE-ROWLEY, W. S. & THIELE, D. J. 1994. A yeast metal resistance protein similar to human cystic fibrosis transmembrane conductance regulator (CFTR) and multidrug resistance-associated protein. *J Biol Chem,* 269**,** 22853-7.

TAMAI, I. & SAFA, A. R. 1990. Competitive interaction of cyclosporins with the Vinca alkaloid-binding site of P-glycoprotein in multidrug-resistant cells. *J Biol Chem,* 265**,** 16509-13.

THAMINY, S., AUERBACH, D., ARNOLDO, A. & STAGLJAR, I. 2003. Identification of novel ErbB3-interacting factors using the split-ubiquitin membrane yeast two-hybrid system. *Genome Res,* 13**,** 1744-53.

THIEBAUT, F., TSURUO, T., HAMADA, H., GOTTESMAN, M. M., PASTAN, I. & WILLINGHAM, M. C. 1987. Cellular localization of the multidrug-resistance gene product P-glycoprotein in normal human tissues. *Proc Natl Acad Sci U S A,* 84**,** 7735-8.

THIEBAUT, F., TSURUO, T., HAMADA, H., GOTTESMAN, M. M., PASTAN, I. & WILLINGHAM, M. C. 1989. Immunohistochemical localization in normal tissues of different epitopes in the multidrug transport protein P170: evidence for localization in brain capillaries and crossreactivity of one antibody with a muscle protein. *J Histochem Cytochem,* 37**,** 159-64.

THORISSON, G. A., MUILU, J. & BROOKES, A. J. 2009. Genotype-phenotype databases: challenges and solutions for the post-genomic era. *Nat Rev Genet,* 10**,** 9-18.

THORNE, R. F., MELDRUM, C. J., HARRIS, S. J., DORAHY, D. J., SHAFREN, D. R., BERNDT, M. C., BURNS, G. F. & GIBSON, P. G. 1997. CD36 forms covalently associated dimers and multimers in platelets and transfected COS-7 cells. *Biochem Biophys Res Commun,* 240**,** 812-8.

TOMMASINI, R., EVERS, R., VOGT, E., MORNET, C., ZAMAN, G. J., SCHINKEL, A. H., BORST, P. & MARTINOIA, E. 1996. The human multidrug resistance-associated protein functionally complements the yeast cadmium resistance factor 1. *Proc Natl Acad Sci U S A,* 93**,** 6743-8.

TOUGERON, D., FOTSING, G., BARBU, V. & BEAUCHANT, M. 2012. ABCB4/MDR3 gene mutations and cholangiocarcinomas. *J Hepatol,* 57**,** 467-8.

TOWBIN, H., STAEHELIN, T. & GORDON, J. 1979. Electrophoretic transfer of proteins from polyacrylamide gels to nitrocellulose sheets: procedure and some applications. *Proc Natl Acad Sci U S A,* 76**,** 4350-4.

TRAUNER, M. & BOYER, J. L. 2003. Bile salt transporters: molecular characterization, function, and regulation. *Physiol Rev,* 83**,** 633-71.

TUSNADY, G. E., SARKADI, B., SIMON, I. & VARADI, A. 2006. Membrane topology of human ABC proteins. *FEBS Lett,* 580**,** 1017-22.

TVETEN, K., HOLLA, O. L., RANHEIM, T., BERGE, K. E., LEREN, T. P. & KULSETH, M. A. 2007. 4-Phenylbutyrate restores the functionality of a misfolded mutant low-density lipoprotein receptor. *FEBS J,* 274**,** 1881-93.

TYGSTRUP, N., STEIG, B. A., JUIJN, J. A., BULL, L. N. & HOUWEN, R. H. 1999. Recurrent familial intrahepatic cholestasis in the Faeroe Islands. Phenotypic heterogeneity but genetic homogeneity. *Hepatology,* 29**,** 506-8.

UEDA, K., CARDARELLI, C., GOTTESMAN, M. M. & PASTAN, I. 1987. Expression of a full-length cDNA for the human "MDR1" gene confers resistance to colchicine, doxorubicin, and vinblastine. *Proc Natl Acad Sci U S A,* 84**,** 3004-8.

UETZ, P., GIOT, L., CAGNEY, G., MANSFIELD, T. A., JUDSON, R. S., KNIGHT, J. R., LOCKSHON, D., NARAYAN, V., SRINIVASAN, M., POCHART, P., QURESHI-EMILI, A., LI, Y., GODWIN, B., CONOVER, D., KALBFLEISCH, T., VIJAYADAMODAR, G., YANG, M., JOHNSTON, M., FIELDS, S. & ROTHBERG, J. M. 2000. A comprehensive analysis of protein-protein interactions in Saccharomyces cerevisiae. *Nature,* 403**,** 623-7.

UJHAZY, P., ORTIZ, D., MISRA, S., LI, S., MOSELEY, J., JONES, H. & ARIAS, I. M. 2001. Familial intrahepatic cholestasis 1: studies of localization and function. *Hepatology,* 34**,** 768-75.

ULLOA-AGUIRRE, A., JANOVICK, J. A., BROTHERS, S. P. & CONN, P. M. 2004. Pharmacologic rescue of conformationally-defective proteins: implications for the treatment of human disease. *Traffic,* 5**,** 821-37.

VALLEJO, M., BRIZ, O., SERRANO, M. A., MONTE, M. J. & MARIN, J. J. 2006. Potential role of trans-inhibition of the bile salt export pump by progesterone metabolites in the etiopathogenesis of intrahepatic cholestasis of pregnancy. *J Hepatol,* 44**,** 1150-7.

VALVERDE, M. A., DIAZ, M., SEPULVEDA, F. V., GILL, D. R., HYDE, S. C. & HIGGINS, C. F. 1992. Volume-regulated chloride channels associated with the human multidrug-resistance P-glycoprotein. *Nature,* 355**,** 830-3.

VAN ASPEREN, J., VAN TELLINGEN, O. & BEIJNEN, J. H. 2000. The role of mdr1a P-glycoprotein in the biliary and intestinal secretion of doxorubicin and vinblastine in mice. *Drug Metab Dispos,* 28**,** 264-7.

VAN DER BLIEK, A. M., BAAS, F., TEN HOUTE DE LANGE, T., KOOIMAN, P. M., VAN DER VELDE-KOERTS, T. & BORST, P. 1987. The human mdr3 gene encodes a novel P-glycoprotein homologue and gives rise to alternatively spliced mRNAs in liver. *EMBO J,* 6**,** 3325-31.

VAN HELVOORT, A., SMITH, A. J., SPRONG, H., FRITZSCHE, I., SCHINKEL, A. H., BORST, P. & VAN MEER, G. 1996. MDR1 P-glycoprotein is a lipid translocase of broad specificity, while MDR3 P-glycoprotein specifically translocates phosphatidylcholine. *Cell,* 87**,** 507-17.

VAN MEER, G., VOELKER, D. R. & FEIGENSON, G. W. 2008. Membrane lipids: where they are and how they behave. *Nat Rev Mol Cell Biol,* 9**,** 112-24.

VAN MIL, S. W., HOUWEN, R. H. & KLOMP, L. W. 2005. Genetics of familial intrahepatic cholestasis syndromes. *J Med Genet,* 42**,** 449-63.

VAN MIL, S. W., VAN DER WOERD, W. L., VAN DER BRUGGE, G., STURM, E., JANSEN, P. L., BULL, L. N., VAN DEN BERG, I. E., BERGER, R., HOUWEN, R. H. & KLOMP, L. W. 2004. Benign recurrent intrahepatic cholestasis type 2 is caused by mutations in ABCB11. *Gastroenterology,* 127**,** 379-84.

VANCE, D. E., VANCE, J. E., DENNIS, E. V. & JEAN, E. V. 2008. Chapter 8 - Phospholipid biosynthesis in eukaryotes. *Biochemistry of Lipids, Lipoproteins and Membranes (Fifth Edition).* San Diego: Elsevier.

VANKEERBERGHEN, A., CUPPENS, H. & CASSIMAN, J. J. 2002. The cystic fibrosis transmembrane conductance regulator: an intriguing protein with pleiotropic functions. *J Cyst Fibros,* 1**,** 13-29.

VANOYE, C. G., CASTRO, A. F., POURCHER, T., REUSS, L. & ALTENBERG, G. A. 1999. Phosphorylation of P-glycoprotein by PKA and PKC modulates swelling-activated Cl- currents. *Am J Physiol,* 276**,** C370-8.

VEMBAR, S. S. & BRODSKY, J. L. 2008. One step at a time: endoplasmic reticulum-associated degradation. *Nat Rev Mol Cell Biol,* 9**,** 944-57.

VERDON, G., ALBERS, S. V., DIJKSTRA, B. W., DRIESSEN, A. J. & THUNNISSEN, A. M. 2003. Crystal structures of the ATPase subunit of the glucose ABC transporter from Sulfolobus solfataricus: nucleotide-free and nucleotide-bound conformations. *J Mol Biol,* 330**,** 343-58.

VERHULST, P. M., VAN DER VELDEN, L. M., OORSCHOT, V., VAN FAASSEN, E. E., KLUMPERMAN, J., HOUWEN, R. H., POMORSKI, T. G., HOLTHUIS, J. C. & KLOMP, L. W. 2010. A flippase-independent function of ATP8B1, the protein affected in familial intrahepatic cholestasis type 1, is required for apical protein expression and microvillus formation in polarized epithelial cells. *Hepatology,* 51**,** 2049-60.

VIKIS, H. G. & GUAN, K. L. 2004. Glutathione-S-transferase-fusion based assays for studying protein-protein interactions. *Methods Mol Biol,* 261**,** 175-86.

VOLONTE, D., GALBIATI, F. & LISANTI, M. P. 1999. Visualization of caveolin-1, a caveolar marker protein, in living cells using green fluorescent protein (GFP) chimeras. The subcellular distribution of caveolin-1 is modulated by cell-cell contact. *FEBS Lett,* 445**,** 431-9.

WAKABAYASHI, Y., DUTT, P., LIPPINCOTT-SCHWARTZ, J. & ARIAS, I. M. 2005. Rab11a and myosin Vb are required for bile canalicular formation in WIF-B9 cells. *Proc Natl Acad Sci U S A,* 102**,** 15087-92.

WANG, G. S. & COOPER, T. A. 2007. Splicing in disease: disruption of the splicing code and the decoding machinery. *Nat Rev Genet,* 8**,** 749-61.

WANG, L., SOROKA, C. J. & BOYER, J. L. 2002. The role of bile salt export pump mutations in progressive familial intrahepatic cholestasis type II. *J Clin Invest,* 110**,** 965-72.

WANG, R., SALEM, M., YOUSEF, I. M., TUCHWEBER, B., LAM, P., CHILDS, S. J., HELGASON, C. D., ACKERLEY, C., PHILLIPS, M. J. & LING, V. 2001. Targeted inactivation of sister of P-glycoprotein gene (spgp) in mice results in nonprogressive but persistent intrahepatic cholestasis. *Proc Natl Acad Sci U S A,* 98**,** 2011-6.

WANG, X., VENABLE, J., LAPOINTE, P., HUTT, D. M., KOULOV, A. V., COPPINGER, J., GURKAN, C., KELLNER, W., MATTESON, J., PLUTNER, H., RIORDAN, J. R., KELLY, J. W., YATES, J. R., 3RD & BALCH, W. E. 2006. Hsp90 cochaperone Aha1 downregulation rescues misfolding of CFTR in cystic fibrosis. *Cell,* 127**,** 803-15.

WARD, A., REYES, C. L., YU, J., ROTH, C. B. & CHANG, G. 2007. Flexibility in the ABC transporter MsbA: Alternating access with a twist. *Proc Natl Acad Sci U S A,* 104**,** 19005-10.

WELCH, W. J. 2004. Role of quality control pathways in human diseases involving protein misfolding. *Semin Cell Dev Biol,* 15**,** 31-8.

WILEY, J. W., O'DORISIO, T. M. & OWYANG, C. 1988. Vasoactive intestinal polypeptide mediates cholecystokinin-induced relaxation of the sphincter of Oddi. *J Clin Invest,* 81**,** 1920-4.

WITTKE, S., LEWKE, N., MULLER, S. & JOHNSSON, N. 1999. Probing the molecular environment of membrane proteins in vivo. *Mol Biol Cell,* 10**,** 2519-30.

YAMAGUCHI, A., HORI, O., STERN, D. M., HARTMANN, E., OGAWA, S. & TOHYAMA, M. 1999a. Stress-associated endoplasmic reticulum protein 1 (SERP1)/Ribosome-associated membrane protein 4 (RAMP4) stabilizes membrane proteins during stress and facilitates subsequent glycosylation. *J Cell Biol,* 147**,** 1195-204.

YAMAGUCHI, Y., KASANO, M., TERADA, T., SATO, R. & MAEDA, M. 1999b. An ABC transporter homologous to TAP proteins. *FEBS Lett,* 457**,** 231-6.

YANG, C. P., GALBIATI, F., VOLONTE, D., HORWITZ, S. B. & LISANTI, M. P. 1998. Upregulation of caveolin-1 and caveolae organelles in Taxol-resistant A549 cells. *FEBS Lett,* 439**,** 368-72.

YANG, J. M., CHIN, K. V. & HAIT, W. N. 1996. Interaction of P-glycoprotein with protein kinase C in human multidrug resistant carcinoma cells. *Cancer Res,* 56**,** 3490-4.

YU, G., AHMAD, S., AQUINO, A., FAIRCHILD, C. R., TREPEL, J. B., OHNO, S., SUZUKI, K., TSURUO, T., COWAN, K. H. & GLAZER, R. I. 1991. Transfection with protein kinase C alpha confers increased multidrug resistance to MCF-7 cells expressing P-glycoprotein. *Cancer Commun,* 3**,** 181-9.

ZAITSEVA, J., OSWALD, C., JUMPERTZ, T., JENEWEIN, S., WIEDENMANN, A., HOLLAND, I. B. & SCHMITT, L. 2006. A structural analysis of asymmetry required for catalytic activity of an ABC-ATPase domain dimer. *EMBO J,* 25**,** 3432-43.

ZHANG, F., ZHANG, W., LIU, L., FISHER, C. L., HUI, D., CHILDS, S., DOROVINI-ZIS, K. & LING, V. 2000. Characterization of ABCB9, an ATP binding cassette protein associated with lysosomes. *J Biol Chem,* 275**,** 23287-94.

ZHANG, Z., WU, J. Y., HAIT, W. N. & YANG, J. M. 2004. Regulation of the stability of P-glycoprotein by ubiquitination. *Mol Pharmacol,* 66**,** 395-403.

ZIMMER, V., MULLENBACH, R., SIMON, E., BARTZ, C., MATERN, S. & LAMMERT, F. 2009. Combined functional variants of hepatobiliary transporters and FXR aggravate intrahepatic cholestasis of pregnancy. *Liver Int,* 29**,** 1286-8.

ZIMMERMANN, A. & MATSCHINER, J. T. 1974. Biochemical basis of hereditary resistance to warfarin in the rat. *Biochem Pharmacol,* 23**,** 1033-40.

ZOLNERCIKS, J. K., ANDRESS, E. J., NICOLAOU, M. & LINTON, K. J. 2011. Structure of ABC transporters. *Essays Biochem,* 50**,** 43-61.

ZOLNERCIKS, J. K., WOODING, C. & LINTON, K. J. 2007. Evidence for a Sav1866-like architecture for the human multidrug transporter P-glycoprotein. *FASEB J,* 21**,** 3937-48.

ZUTZ, A., GOMPF, S., SCHAGGER, H. & TAMPE, R. 2009. Mitochondrial ABC proteins in health and disease. *Biochim Biophys Acta,* 1787**,** 681-90.

Appendix

Appendix I. Primary sequence alignment of ABCB4, Abcb1a and Sav1866.

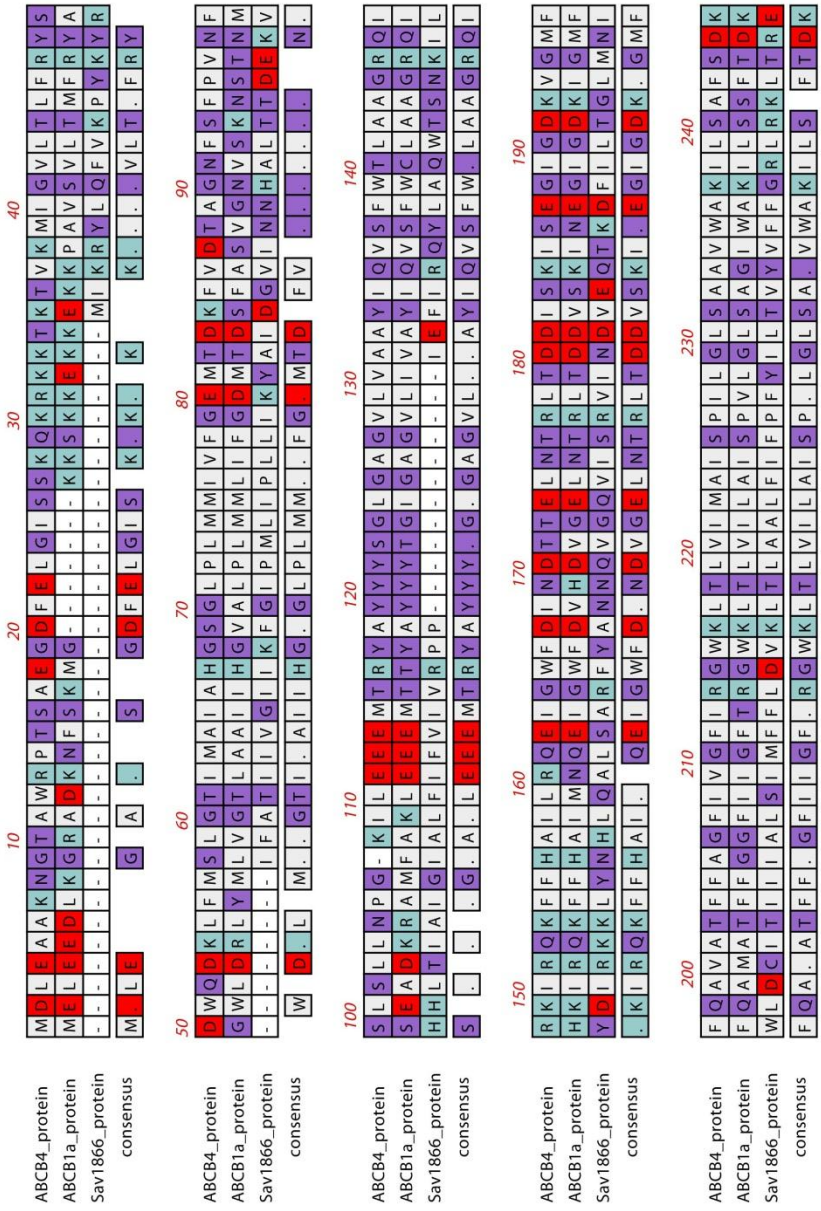

Appendix I. Primary sequence alignment of ABCB4, Abcb1a and Sav1866. Red, acidic; cyan, basic; white, hydrophobic; purple, hydrophilic.

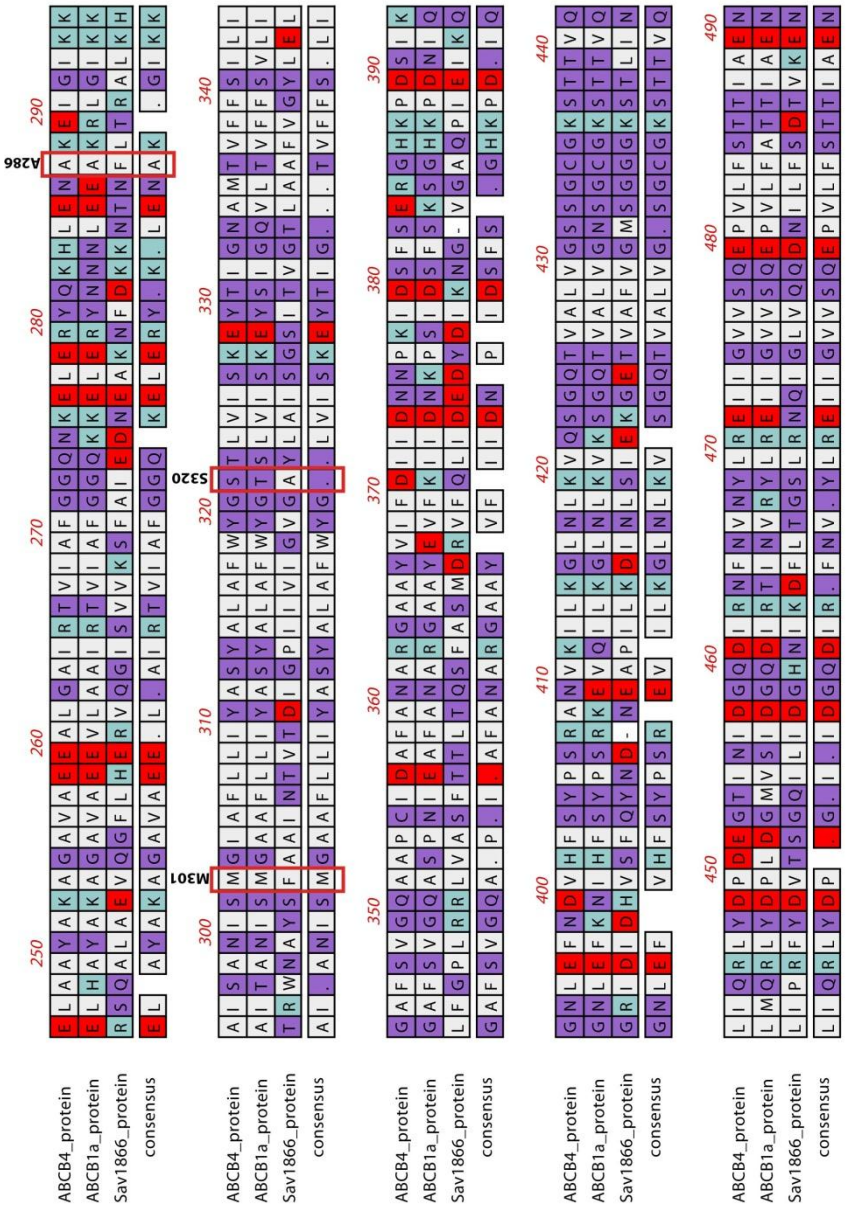

Appendix I. Primary sequence alignment of ABCB4, Abcb1a and Sav1866. Red, acidic; cyan, basic; white, hydrophobic; purple, hydrophilic.

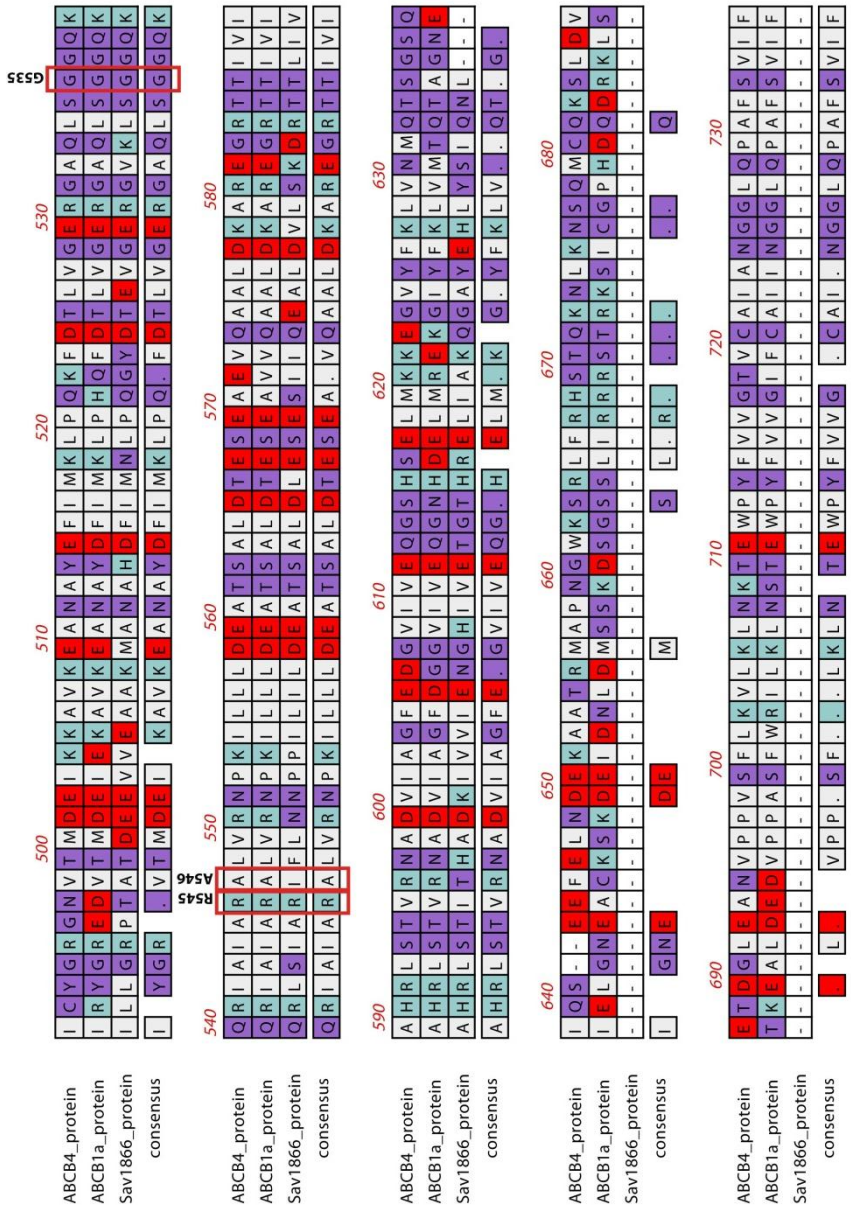

Appendix I. Primary sequence alignment of ABCB4, Abcb1a and Sav1866. Red, acidic; cyan, basic; white, hydrophobic; purple, hydrophilic.

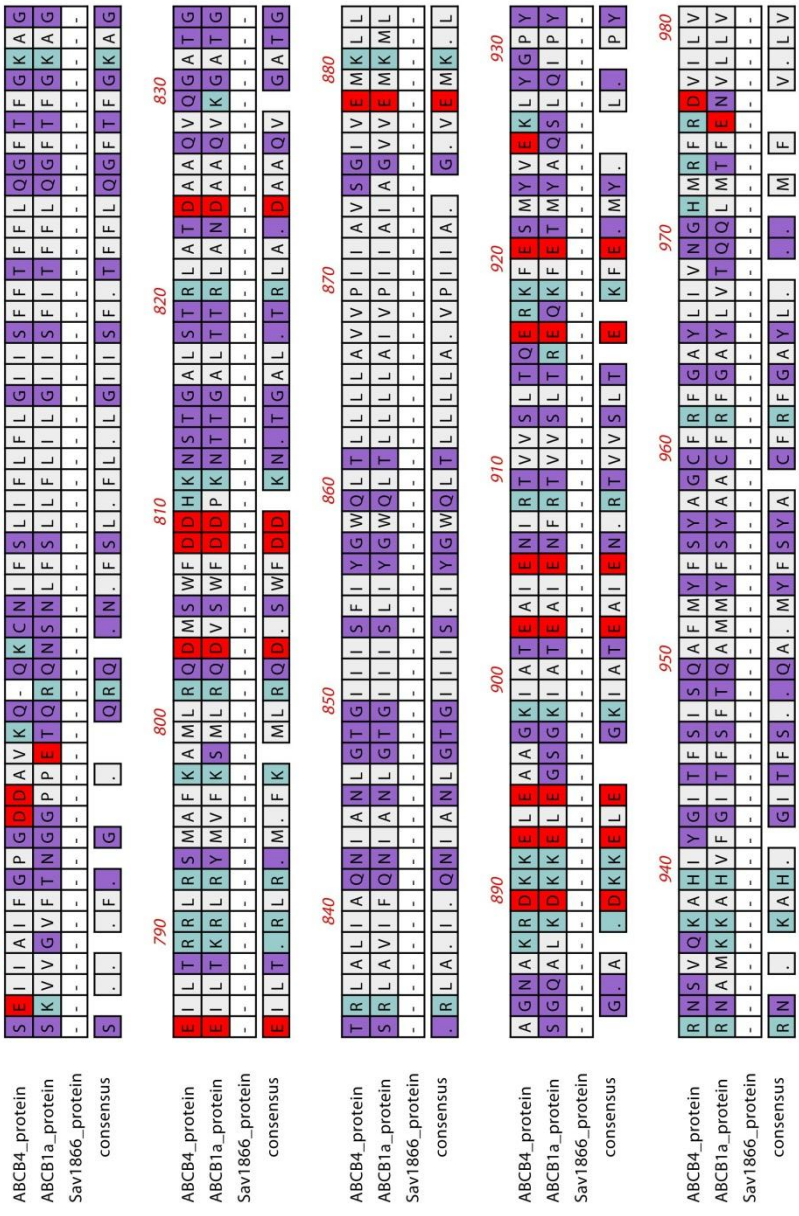

Appendix I. Primary sequence alignment of ABCB4, Abcb1a and Sav1866. Red, acidic; cyan, basic; white, hydrophobic; purple, hydrophilic.

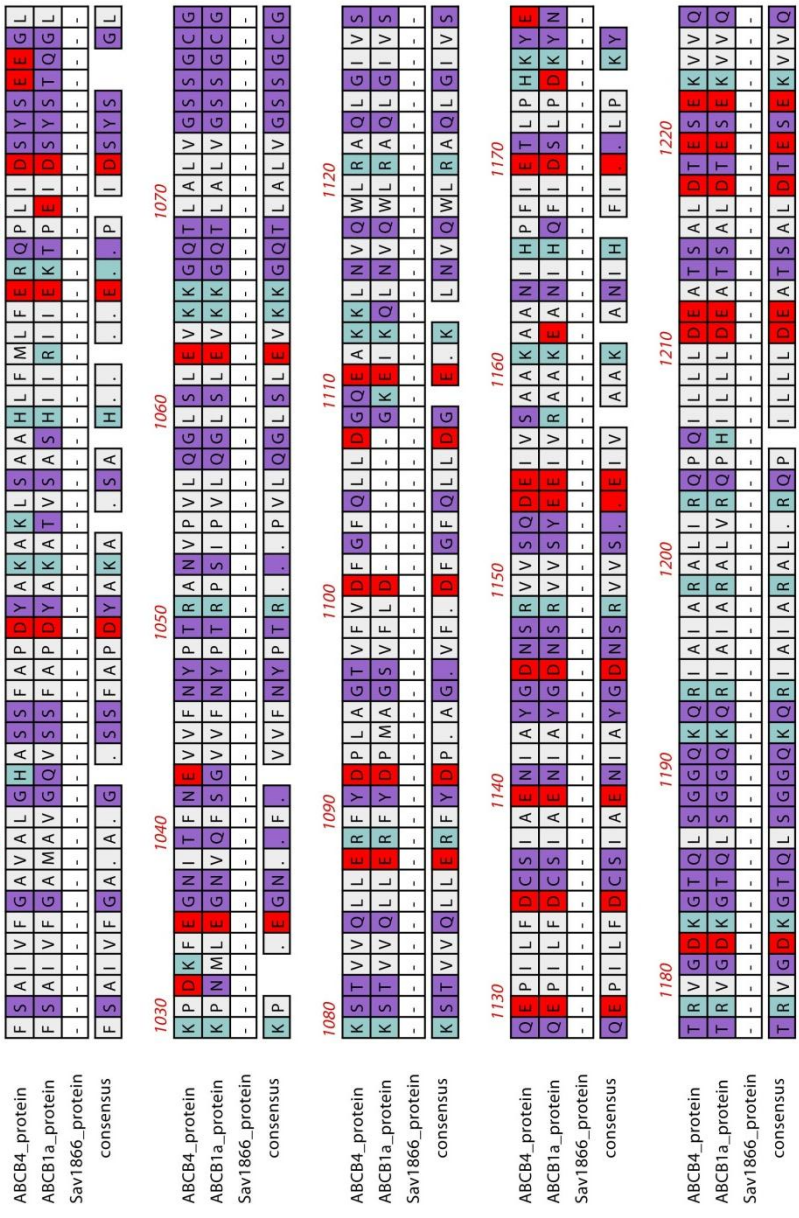

Appendix I. Primary sequence alignment of ABCB4, Abcb1a and Sav1866. Red, acidic; cyan, basic; white, hydrophobic; purple, hydrophilic.

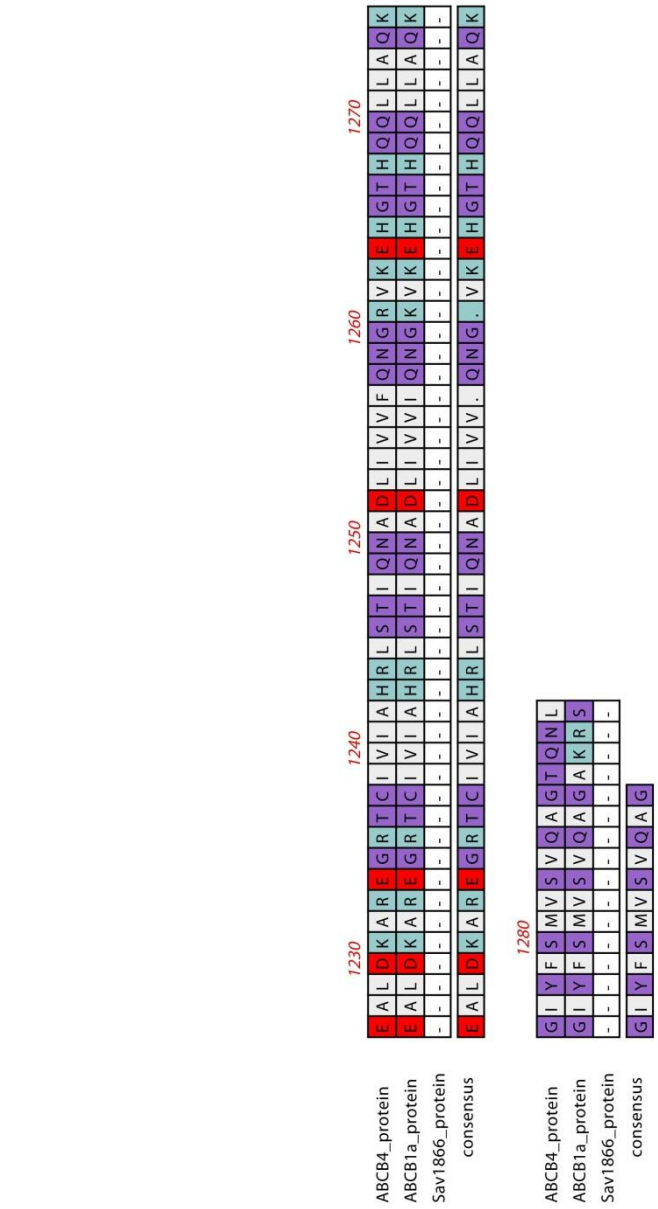

Appendix I. Primary sequence alignment of ABCB4, Abcb1a and Sav1866. Red, acidic; cyan, basic; white, hydrophobic; purple, hydrophilic.